SSC-395

SHIP MAINTENANCE PROJECT

Phases II and III- Volume 5

Fitness for Purpose Evaluation of Critical Structual Details in Tankers

SHIP STRUCTURE COMMITTEE

1997

SHIP STRUCTURE COMMITTEE

The SHIP STRUCTURE COMMITTEE is constituted to prosecute a research program to improve the hull structures of ships and other marine structures by an extension of knowledge pertaining to design, materials and methods of construction.

RADM J. C. Card, USCG (Chairman)
Chief, Office of Marine Safety, Security
and Environmental Protection
U. S. Coast Guard

Mr. John Grinstead
Director, Policy and Legislation
Marine Regulatory Directorate
Transport Canada

Mr. Edwin B. Schimler
Associate Administrator for Ship
Building and Technology Development
Maritime Administration

Dr. Donald Liu
Senior Vice President
American Bureau of Shipping

Mr. Robert McCarthy
Director, Survivability and Structural
Integrity Group (SEA 03P)
Naval Sea Systems Command

Mr. Thomas Connors
Acting Director of Engineering (N7)
Military Sealift Command

Dr. Ross Grahm
Head, Hydronautics Section
Defence Research Establishment-Atlantic

EXECUTIVE DIRECTOR

CDR Stephen E. Sharpe, USCG
U. S. Coast Guard

CONTRACTING OFFICER TECHNICAL REPRESENTATIVE

Mr. William J. Siekierka
Naval Sea Systems Command

SHIP STRUCTURE SUBCOMMITTEE

The SHIP STRUCTURE SUBCOMMITTEE acts for the Ship Structure Committee on technical matters by providing technical coordination for determinating the goals and objectives of the program and by evaluating and interpreting the results in terms of structural design, construction and operation.

MILITARY SEALIFT COMMAND

Mr. Robert E. Van Jones (Chairman)
Mr. Rickard A. Anderson
Mr. Michael W. Touma
Mr. Jeffrey E. Beach

MARITIME ADMINISTRATION

Mr. Frederick Seibold
Mr. Richard P. Voelker
Mr. Chao H. Lin
Dr. Walter M. Maclean

U. S. COAST GUARD

Capt. George Wright
Mr. Walter Lincoln
Mr. Rubin Sheinberg

AMERICAN BUREAU OF SHIPPING

Mr. Glenn Ashe
Mr. John F. Conlon
Dr. Phillip G. Rynn
Mr. William Hanzalek

NAVAL SEA SYSTEMS COMMAND

Mr. W. Thomas Packard
Mr. Charles L. Null
Mr. Edward Kadala
Mr. Allen H. Engle

TRANSPORT CANADA

Mr. Peter Timonin
Mr. Felix Connolly
Mr. Francois Lamanque

DEFENCE RESEARCH ESTABLISHMENT ATLANTIC

Dr. Neil Pegg
LCDR Stephen Gibson
Dr. Roger Hollingshead
Mr. John Porter

SHIP STRUCTURE SUBCOMMITTEE LIAISON MEMBERS

Ship Structure Committee

An Interagency Advisory Committee

SSC-395
SR-1360
SR-1371

February 27, 1997

SHIP MAINTENANCE PROJECT
Phases II and III

This report presents the results of the second and third phases of the subject project of which phase one was first presented in our four volume set -- SSC-386. These studies investigated the development of engineering technology that could lead improvements in structural maintenance for new and existing tankers. These projects built further upon the work started in phase I specifically focusing on critical structural details and corrosion limits.

The report has been divided into five volumes, each of which may stand alone. Volume one opens with a summary of all three phases by Professor Robert G. Bea, the coordinating investigator for the program and follows with a report on corrosion limits for tankers. The second and fifth volumes look into evaluation of cracked critical structural details in tankers. The third volume presents theory and user instructions for software to manage repair of critical structural details. The fourth volume applies to fatigue classification of critical structural details. The software developed in the project will be available on the next Ship Structure Committee CD Rom release, which is anticipated to be released in the next year. The industry is encouraged to contact Professor Bea at the University of California, Berkeley to discuss further possibilities in application of the work undertaken here in the industry.

C. CARD
Rear Admiral, U.S. Coast Guard
Chairman, Ship Structure Committee

DTIC QUALITY INSPECTED 3

Technical Report Documentation Page

1. Report No. SSC-395-5	2. Government Accession No. PB97-142863	3. Recipient's Catalog No.
4. Title and Subtitle Ship Maintenance Project Phases II and III Volume 5 Fitness for Purpose Evaluation of Critical Structural Details in Tankers		5. Report Date 1997
		6. Performing Organization Code
		8. Performing Organization Report No.
7. Author(s) Robert Bea, Tao Xu		
9. Performing Agency Name and Address University of California at Berkeley Department of Naval Architecture and Ocean Engineering Berkeley, CA 94720		10. Work Unit No. (TRAIS)
		11. Contract or Grant No.
		13. Type of Report and Period Covered
12. Sponsoring Agency Name and Address Ship Structure Committee U. S. Coast Guard (G-MSE/SSC) 2100 Second St. S.W. Washington, DC 21\0593-0001		Final
		14. Sponsoring Agency Code G-M

15. Supplementary Notes

Sponsored by the Ship Structure Committee. Jointly funded by other organizations as a joint industry project. See inside the report for futher details on sponsors.

16. Abstract

This report presents the results of the second and third phases of the subject project of which phase one was first presented in our four volume set - SSC-386. These studies investigated the development of engineering technology that could lead to improvements in structural maintenance for new and existing tankers. These projects built further upon the work started in phase I specifically focusing on critical structural details and corrosion limits.

The report has been divided into five volumes, each of which may stand alone. Volume one opens with a summary of all three phases by Professor Robert G. Bea, the coordinating investigator for the program, and follows with a report on corrosion limits for tankers. The second and fifth volumes look into evaluation of cracked critical structural details in tankers. The third volume presents theory and user instructions for software to manage repair of critical structural details. The fourth volume applies to fatigue classification of critical structural details. The software developed in the project will be available on the next Ship Structure Committee CD Rom release which is anticipated to be released in the next year. The industry is encouraged to contact Professor Bea at the University of California, Berkeley to discuss further possibilities in application of the work undertaken here in the industry.

17. Key Words fatigue, critical structural details, tanker structures, repairs, fatigue classification		18. Distribution Statement Distribution unlimited, available from: National Technical Information Service U.S. Department of Commerce Springfield, VA 22151 (703)487-4690	
19. Security Classif. (of this report) Unclassified	20. SECURITY CLASSIF. (of this page) Unclassified	21. No. of Pages 286	22. Price

Form DOT F 1700.7 (8/72)   Reproduction of form and completed page is authorized.

METRIC CONVERSION CARD

Approximate Conversions to Metric Measures

Symbol	When You Know	Multiply by	To Find	Symbol
	LENGTH			
in	inches	2.5	centimeters	cm
ft	feet	30	centimeters	cm
yd	yards	0.9	meters	m
mi	miles	1.6	kilometers	km
	AREA			
in^2	square inches	6.5	square centimeters	cm^2
ft^2	square feet	0.09	square meters	m^2
yd^2	square yards	0.8	square meters	m^2
mi^2	square miles	2.6	square kilometers	km^2
	acres	0.4	hectares	ha
	MASS (weight)			
oz	ounces	28	grams	g
lb	pounds	0.45	kilograms	kg
	short tons (2000 lb)	0.9	metric ton	t
	VOLUME			
tsp	teaspoons	5	milliliters	mL
Tbsp	tablespoons	15	milliliters	mL
in^3	cubic inches	16	milliliters	mL
fl oz	fluid ounces	30	milliliters	mL
c	cups	0.24	liters	L
pt	pints	0.47	liters	L
qt	quarts	0.95	liters	L
gal	gallons	3.8	liters	L
ft^3	cubic feet	0.03	cubic meters	m^3
yd^3	cubic yards	0.76	cubic meters	m^3
	TEMPERATURE (exact)			
°F	degrees Fahrenheit	subtract 32, multiply by 5/9	degrees Celsius	°C
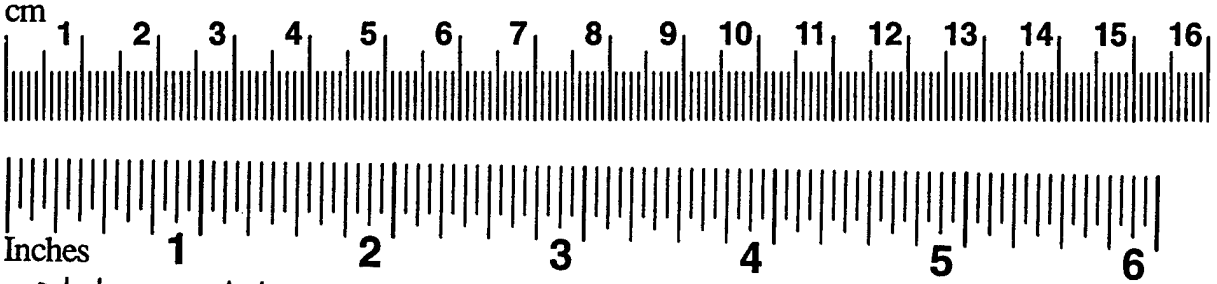
Approximate Conversions from Metric Measures

Symbol	When You Know	Multiply by	To Find	Symbol
	LENGTH			
mm	millimeters	0.04	inches	in
cm	centimeters	0.4	inches	in
m	meters	3.3	feet	ft
m	meters	1.1	yards	yd.
km	kilometers	0.6	miles	mi
	AREA			
cm^2	square centimeters	0.16	square inches	in^2
m^2	square meters	1.2	square yards	yd^2
km^2	square kilometers	0.4	square miles	mi^2
ha	hectares (10,000 m^2)	2.5	acres	
	MASS (weight)			
g	grams	0.035	ounces	oz
kg	kilograms	2.2	pounds	lb
t	metric ton (1,000 kg)	1.1	short tons	
	VOLUME			
mL	milliliters	0.03	fluid ounces	fl oz
mL	milliliters	0.06	cubic inches	in^3
L	liters	2.1	pints	pt
L	liters	1.06	quarts	qt
L	liters	0.26	gallons	gal
m^3	cubic meters	35	cubic feet	ft^3
m^3	cubic meters	1.3	cubic yards	yd^3
	TEMPERATURE (exact)			
°C	degrees Celsius	multiply by 9/5, add 32	degrees Fahrenheit	°F

°C: -40 -20 0 32 20 37 60 80 98.6 100 212 °F
-40 0 32 80 160 212

water freezes — body temperature — water boils
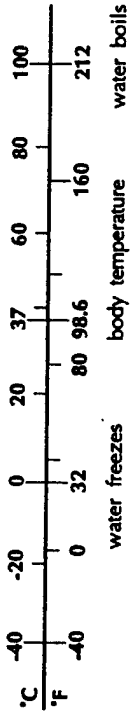
Ship Structural Maintenance Projects II and III
Cross Reference Listing

SSC Vol	SMP #	Title	Authors	Date	NTIS Number
	II				
2	-1	Fatigue Analysis of CSD in a 150K DWT Double-Hull Tanker	Xu, Bea	10/93	PB97-142830
2	-2	Fatigue Analysis of CSD in a 190K DWT Double-Hull Tanker	Xu, Bea	10/93	PB97-142830
2	-3	CSD Library and Finite Element Stress Contours	Xu, Bea	10/93	PB97-142830
1	-4	Development of a Rational Basis for Defining Corrosion Limits in Tankers	Mayoss, Bea	12/93	PB97-142822
3	-4a	RMS for CSD in Ships – User Manual	Ma, Bea	9/93	PB97-142848
3	-4b	RMS for CSD in Ships – Theory	Ma, Bea	9/93	PB97-142848
4		Fatigue Classification of CSD in Tankers	Schulte-Strathaus, Bea	1/94	PB97-142855
	III				
3	-1-1	RMS for Fatigue Cracks in Ship CSDs	Ma, Bea	10/94	PB97-142848
5	-2-1	Fitness for Purpose Analysis Procedure of Cracked CSDs in Tankers	Xu, Bea	1/95	PB97-142863
5	-2-2	A Load Shedding Model of Fracture Mechanics Analysis of Cracked SCDs in Tankers	Xu, Bea	1/95	PB97-142863
5	-2-3	FRACTURE- A Computer Code for Fracture Mechanics Analysis of Crack Growth of Cracked CSD in Tankers	Xu, Bea	1/95	PB97-142863
5	-5	Pro-IMR: A Computer Code for Probability-Based Inspection Planning	Xu, Bea	10/94	PB97-142863

Fitness for Purpose Evaluation of Critical Structural Details in Tankers

Fitness for Purpose Analysis Procedure of Cracked Critical Structural Details in Tankers

Tao Xu
and
Professor Robert G. Bea

Department of Naval Architecture and Offshore Engineering
University of California, Berkeley

Preface

The one year Joint Industry Research Project **"Fitness for Purpose Evaluation of Cracked Critical Structural Details (CSD) in Tankers"** was initiated in 1993 by the Department of Naval Architecture & Offshore Engineering, University of California at Berkeley as an extension of the projects **"Structural Maintenance for New and Existing Ships"** and **"Ship Structural Maintenance"**. The objective of this project is to develop engineering guidelines and procedures to help ship repair engineers, port superintendents and surveyors make evaluations of the fitness for purpose of cracked Critical Structural Details (CSD) in tankers.

This project was made possible by the following sponsoring organizations:

- **American Bureau of Shipping**
- **Chevron Shipping Cooperation**
- **Mitsubishi Heavy Industries**
- **Newport News Shipbuilding & Dry Dock Co.**
- **Ship Structure Committee**

This report documents a load shedding model for fracture mechanics analysis of cracked critical structural details (CSD) in tankers.

Table of Contents

List of Figures

List of Tables

Chapter 1

Introduction

1.1 Objective

The objective of this study was to calibrate a load shedding model for fracture mechanics analysis of cracked Critical Structural Details (CSD) in tankers.

This study was intended to establish empirical formula to describe the effects of load shedding in the propagation of cracks in cracked CSD in tankers.
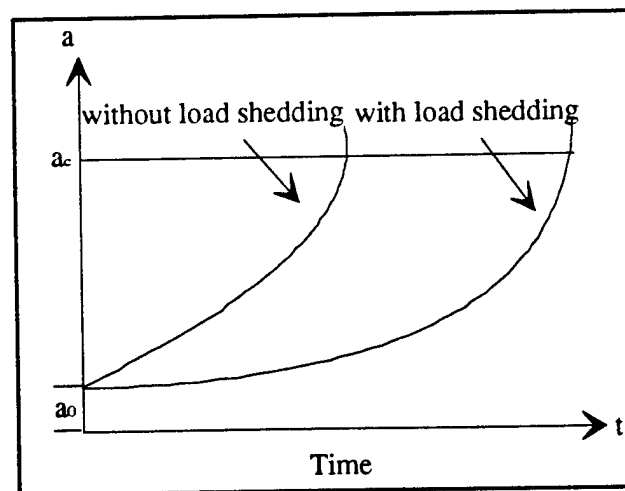
Fig 1.1 Description of Load Shedding Effects

Fig. 1.1 shows the typical load shedding effects in the propagation of cracks in cracked CSD in tankers. Here, a is the crack size. a_o is the initial crack size. a_c is the critical crack size.

1.2 Scope

This report documents the sources of load shedding in cracked CSD, the development and verification of empirical formula to characterize load shedding and applies the load shedding effects in general fracture mechanics analysis.

This report addresses the following questions :

What is load shedding and how does it effect crack propagation ?

How can we analyze and model load shedding and its effects ?

How can we verify and calibrate a load shedding model ?

During the this study, a literature survey was conducted which focused on load shedding models for tubular joints in offshore structures. Based on results from the literature survey, a theoretical and numerical study for load shedding was conducted and verified with experimental data. A general formula for load shedding was proposed based on this verification. This formula was applied to several CSD in tankers.

1.3 Background

Load shedding is a stress redistribution for cracked structures due to the boundary conditions and adjacent elements during the crack propagation.

The two edge cracked plates in Fig 1.2 are subjected to cyclic tensile loadings. The magnitudes of the two loadings are such that the crack opening stresses are identical. The crack in plate A propagates at an increasing rate until the critical crack length is reached

(Fig 1.1 : without load shedding curve). The crack in plate B propagates at a slower rate because as the crack gets larger, a portion of the loading is transferred to the support provided at the right vertical edge (Fig 1.1 : with load shedding curve).
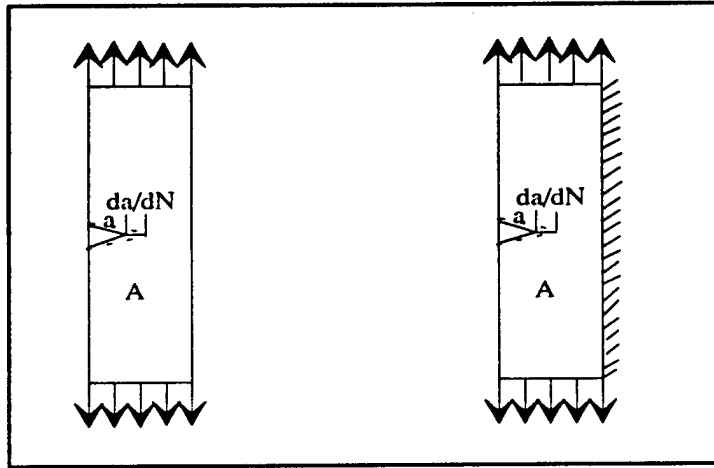
Fig 1.2 Description of the Load Shedding due to Boundary Conditions.

A comparable mechanism of load shedding is illustrated in Fig 1.3. As the crack in plate B propagates to the vertical stiffener, the stiffener will act to absorb the loading. The crack propagation rate will be reduced.
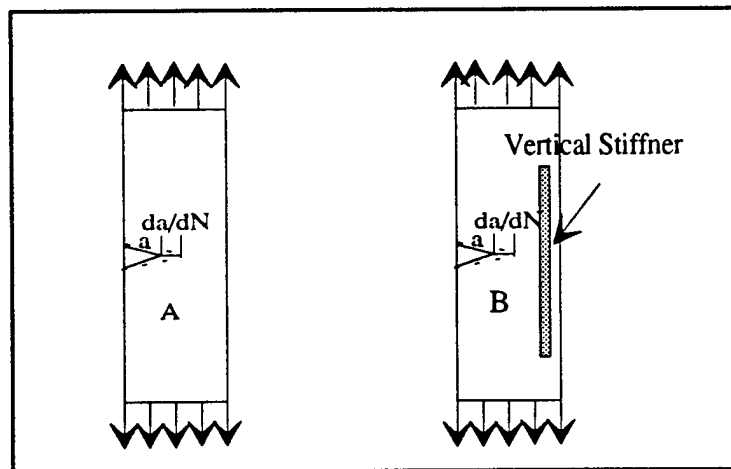
Fig 1.3 Description of Load shedding due to adjacent structures

Thus, load shedding is the process in which crack-section loading is re-distributed to other adjacent elements and components.

1.4 Previous Research

Previous research on load shedding effects has been focused mainly on the stress redistribution of offshore tubular joints. In this case, the stress flow through a tubular joint is strongly affected by the presence of a crack. As a crack is growing through the tubular joints' high stress region, the load is redistributed to less stressed parts of the joint. This load shedding effect is important for fracture mechanics modeling e.g. Fig 1.4
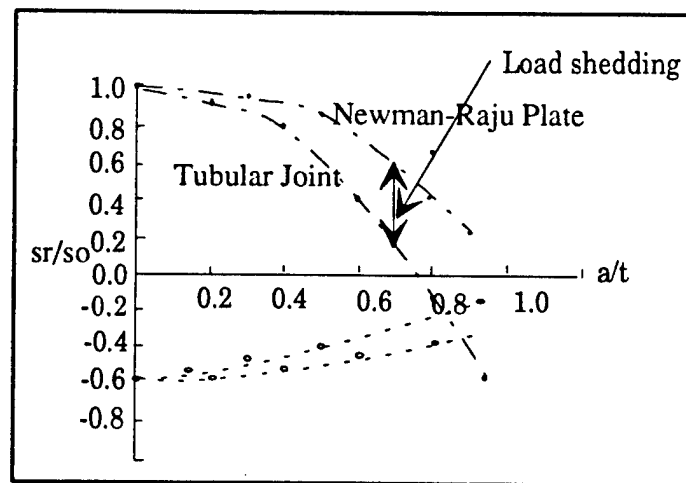
Fig 1.4 Load Shedding Study in Offshore Tubular Joints.

In Fig 1.4, a/t is the ratio of the crack depth and plate thickness. so is the hot spot stress on crack initiation site. sr is the crack opening stress on the crack tip when the crack propagates. One curve is the stress ratio (crack opening stress/hot spot stress) which is computed by finite element analysis (FEA) for Newman-Raju plate[1]. Another curve is the real crack opening stress for tubular joints. This curve is computed by FEA for different

* Newman-Raju plate is a flat plate with a central crack. The stress intensity factor for this case is called Newman-Raju solution. It is widely applied in computation of stress intensity factors of tubular joints

crack depth, a/t . The difference between these two curves is due to the redistribution of the stress. In this figure, the dashed line is the stress on the top of the plate, and the dotted is line the stress on the bottom of the plate. The crack propagates from top to bottom.

The previous research on load shedding for offshore tubular joints is summarized as follows :

Forbes [1992] proposed a model for tubular joints where experimental data for the stress relaxation is applied to a flat plate with specific boundary conditions to simulate the stiffness of a cylindrical shell. Good correspondence with test data was obtained.

Haswell [1992] explored load shedding using finite element analysis (FEA) methods. Computed values for the stress intensity factor at discrete values a/t (crack depth to plate thickness ratio) was correlated with a "Degree of Bending" parameter (DoB). DoB is the ratio S_b/S_{HS}. where S_b S_{HS} are the bending stress and hotspot stress respectively. A linear model for the Newman-Raju solution was assumed where A and B are regression coefficients derived for selected values of a/t. Analysis showed that the stress intensity factor depends not only on DoB parameter, but is substantially influenced by the structural geometry of the joint.

Aaghaakouchak, et al. [1989] proposed a simplified load shedding model for tubular joints where the hot spot stress was separated into a membrane and a bending component. The membrane stress, σ_m, was assumed to be unaffected by the crack. The bending component was allowed to decrease linearly with crack length, This model was shown to give stress intensity factors in good correspondence with experimental values derived from crack growth rates in tubular joints. But the analysis were only limited to one value of the aspect ratio, (ratio of crack depth to crack width) which was a/2c=0.1.

1.5 Approach

This study was organized into the following six tasks:

Task 1 - Perform a literature review

Task 2 - Perform a numerical study of stress intensity factors for general cracked problem.

Task 3 - Perform a theoretical study of stress intensity factors for general cracked problems

Task 4 - Calibrate a general load shedding model for use in the computation of stress intensity factors based on the results from the theoretical study, numerical study, and existing experimental data

Task 5 - Apply the load shedding model to the computation of the stress intensity factors for the cracked structural details.

Task 6 - Develop and summarize empirical load shedding analytical expression for different CSD.

1.6 Summary

The following summarizes the answers to the key questions posed at the beginning of this study.

What is Load Shedding and how does it affect crack propagation?

Crack growth through the plate thickness in a plane weld is illustrated in Fig. 1.5 where a is the crack length and N is the number of cycles to fatigue failure (Note the extremely rapid acceleration of growth after the crack has reached a certain length). This

is typical for crack growth in plane unstiffened structures, where cracks will tend to advance with a straight crack front (small aspect ratio). The acceleration of crack growth then reflects the Paris' power-law. The similar behavior is seen for cracks growing from cut-outs in unstiffened structures Fig. 1.6 and1.7.
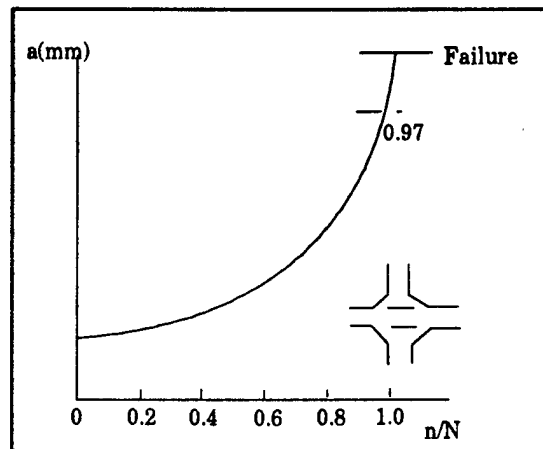
Fig 1.5 Fatigue Crack Growth from a Cruciform Joint
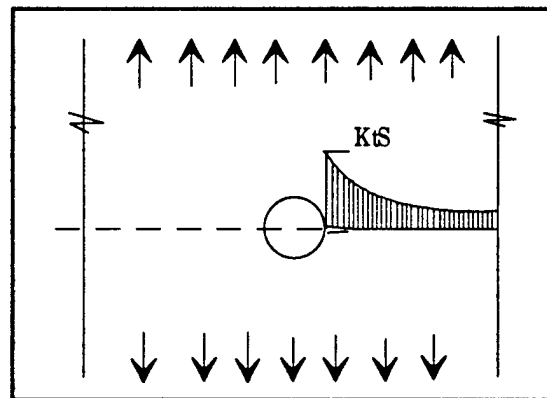
Fig 1.6 : Stress distribution for a crack initiated from a cut-out

For cracks growing from a cut-out, a short crack will sense the hotspot stress at the cut-out as a homogeneous field. A long crack will sense the average stress, but with the cut-out as a part of the crack, leading to an accelerated crack growth rate. (Fig 1.7)

7
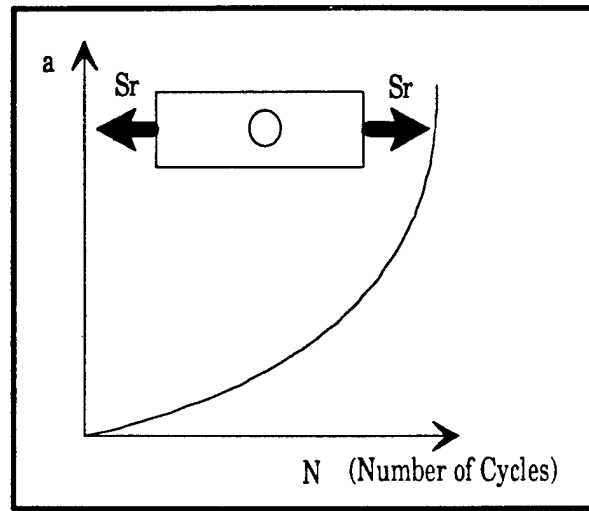
Fig 1.7: Crack growth from a circular cut-out in a plate

A consequence of this is that for the geometries in Fig 1.6 and 1.7, any significant size weld defect will have a very detrimental effect on fatigue life. Moreover, the time to failure after the crack reaches a detectable size may be too short for inspections to be reliable. Therefore, the potential for a sudden loss of load carrying capacity of single members should be considered in design.

For stiffened members in tankers, the progress of crack growth is somewhat different. Fig 1.8 shows a typical crack growing in a stiffened plate. In this case, redistribution of stresses to the stiffeners and other adjacent members will take place during crack growth. the stiffeners may arrest the crack growth entirely. The net effect is a reduction in stress intensity (Fig 1.8b), and a retardation of growth rate when the crack tip approaches a stiffener (Fig 1.8c). This general effect of stiffening and load shedding is one reason why fatigue cracks can be tolerated to some extent in tanker structures (Fig 1.8d).

8
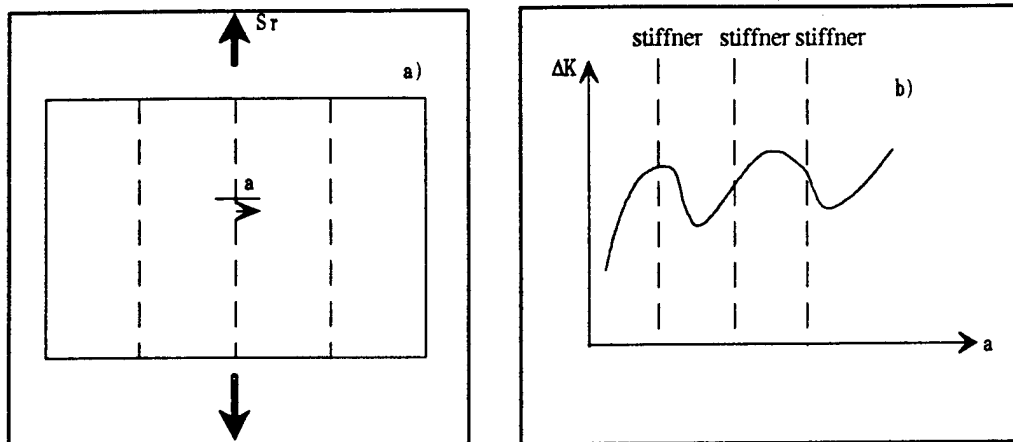
Fig 1.8 Fatigue Loaded Stiffened Plate

a) Crack Growing Perpendicular to the Stiffeners.

b) Stress Intensity factor for a crack growing perpendicular to the stiffeners in the

stiffened panel
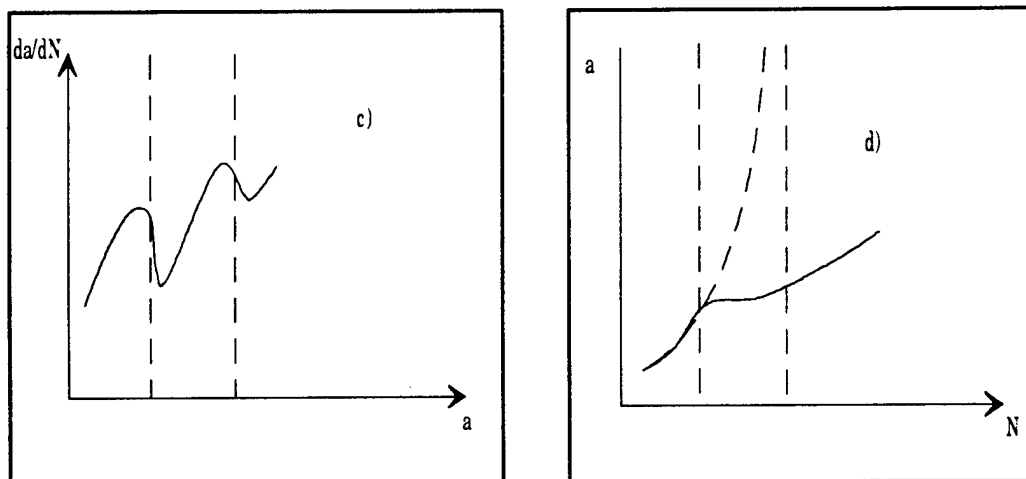
Fig 1.8 Fatigue Loaded Stiffened Plate

Fig 1.8 c) Crack growth rate for stiffened panel

d) Crack growth for an unstiffened plate and stiffened plate

In Fig 1.8d, the dashed line is for unstiffened plate, and the plain line is for stiffened plate. The difference between these two lines is due to load shedding

The difference between unstiffened plates which are studied extensively in general fracture mechanics and stiffened plates which are used in tanker structures is :

1)These plates between the stiffeners are redundantly restrained by stiffeners, and

2)There are stress concentrations for crack initiations due to stiffeners.

From the previous discussions, we can define load shedding precisely as :

Load shedding is the stress redistribution for statically indeterminate cracked structures due to the redundant boundary conditions and adjacent elements when cracks grow under the arbitrary stress field.

This definition implies that load shedding is the stress redistribution under three restrictions. They are :

1 - Statically indeterminate cracked structures,

2 - Redundant boundary conditions, and

3 - Arbitrary stress fields.

How can we analysis and model load shedding and its effects ?

From the precise definition of load shedding, It can be concluded that a methodology or solution for stress intensity factors should be included two factors which contribute to load shedding. One is the stress redistribution due to the redundant boundary conditions. The other is the stress gradient due to an arbitrary stress field. The arbitrary

stress field is caused by local stress concentrations. That is to say that the stress gradient factor is the factor which represents the local stress concentration effects.

How can we calibrate and verify a load shedding model ?

The calibration was based on a numerical study, a theoretical study, and an experimental study.

The load shedding model was calibrated through two factors which contributed to the stress intensity factor's computation. That is stress redistribution factor and stress gradient factor.

The stress redistribution factor was calibrated based on the results from FEA and experimental tests.

The stress gradient factor was calibrated using the Green function method[*], FEA and experimental data.

The calibration and verification will be addressed in detail in subsequent chapters.

How can we develop the empirical formula for load shedding ?

The empirical stress gradient factors for different details were derived based on results from a parameteric study of different details with different dimensions.

---

[*] Green function method is a general numerical method to compute stress intensity factors for cracked structures

The empirical stress redistribution factors for different details were derived from theoretical study and experiment data for general cracked structures.

1.7 Report

This report is divided into six additional chapters. Chapter 2 discusses the FEA for cracked CSD. Chapter 3 summarizes the Newman Raju equation for the stress intensity factors for surface cracks. Chapter 4 discusses the calibration of the load shedding model for surface cracks. Chapter 5 develops a load shedding calibration for through thickness cracks. Chapter 6 proposes empirical formula for load shedding effects in different CSD. Chapter 7 is the application of the load shedding model in a cracked CSD in a 165,000 DWT tanker. Chapter 8 is a summary and conclusion.

Chapter 2

Finite Element Analysis

2.1 Introduction

Finite element analysis (FEA) is one of the most applicable numerical methods in the study of the crack problems. In order to develop and calibrate a load shedding model, several finite element approaches were employed. The following presents a displacement approach with non-singular elements and a stress approach with non-singular elements. These two approaches were employed in this development.

2.2 Displacement approach

The displacement method with non-singular elements involves a correlation of the finite element nodal point displacement with the well known crack-tip displacement equations. For mode-I crack*, the displacement equations can be given as :

$$u_i = \frac{K_1}{G} \sqrt{\frac{r}{2\pi}} f_i(\theta, v) \tag{2.1}$$

---

* Mode-I crack is the crack due to tensile loads

where K_I is a function of the geometry of the body containing the crack and of the applied loading conditions. The term $f_i(\theta, v)$ is:

$$f_i = \begin{bmatrix} \cos\dfrac{\theta}{2}(1-2v+\sin^2\dfrac{\theta}{2}) \\ \sin\dfrac{\theta}{2}(2-2v-\cos^2\dfrac{\theta}{2}) \end{bmatrix} \qquad \text{for plane strain} \qquad (2.2)$$

$$f_i = \begin{bmatrix} \cos\dfrac{\theta}{2}(\dfrac{1-v}{1+v}+\sin^2\dfrac{\theta}{2}) \\ \sin\dfrac{\theta}{2}(\dfrac{2}{1+v}-\cos^2\dfrac{\theta}{2}) \end{bmatrix} \qquad \text{for plane stress} \qquad (2.3)$$

Rearranging the above equation, and substituting nodal displacements, u_i^*, at some point (r,θ) close to the crack tip (Fig 2.1), a quantity K_I^* can be computed :

$$K_I^* = \sqrt{\dfrac{2\pi}{r}}G[f_i(\theta, v)]u_i^* \qquad (2.4)$$

From plots of K_I^* as a function of r for fixed values of θ and a particular displacement component (u^* or v^*), an estimate of K_I can be made by extrapolating back to r-> 0. At this stage, one must observe that nodal displacements are rather inaccurate at an infinitesimal distance from the crack. This limitation can be overcome by refining the mesh near the crack-tip. With a suitably refined mesh, it is possible to use tangent extrapolation to estimate the stress intensity factor. (Fig. 2.2)

2.3 Stress Approach

The stress approach with non-singular elements involves a correlation of the finite element nodal or Gauss point stresses with the crack-tip stress equations, as follows:

$$\sigma_{ij} = \dfrac{K_M}{\sqrt{2\pi r}}f_{ij}(\theta) \qquad (2.5)$$

14
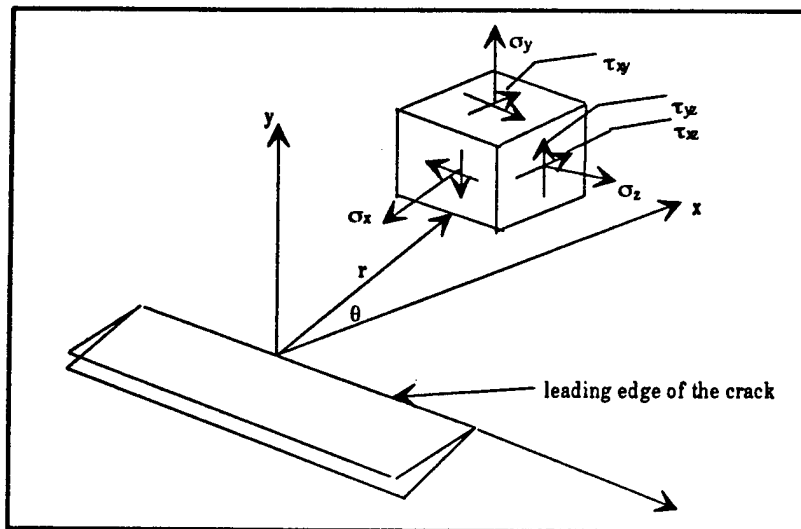
Fig 2.1 Crack-tip coordinates and stress state
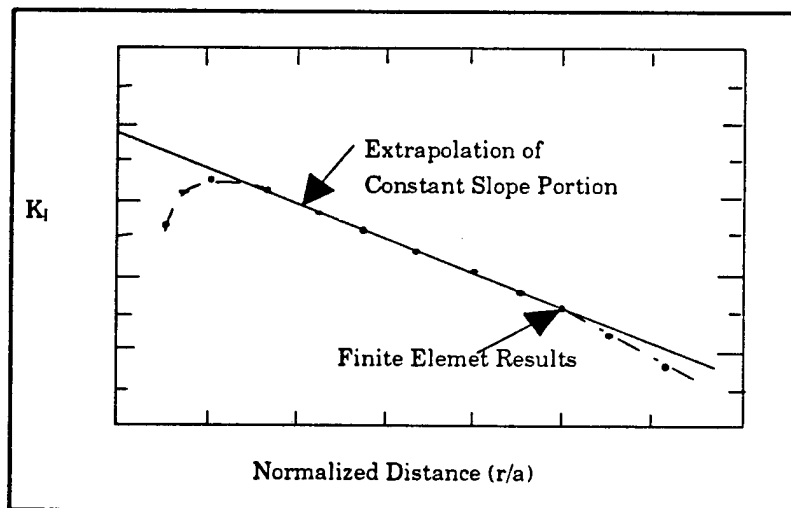
Fig 2.2 Variation of K_I^* with r/a for a finite crack in a plate.

Rearranging the above equation gives:

$$K_M = \frac{\sqrt{2\pi r}}{f_{ij}(\theta)} \sigma_{ij}$$

(2.6)

with M=I,II,or III depending upon the examined mode.

Nodal point stress $\sigma_{ij}*$ in the vicinity of the crack-tip can be substituted in equation 2.5 and 2.6 so that values of $K_M^\bullet$ can be obtained. Again, from plots of $K_M^\bullet$ as a function of r near the crack-tip for fixed θ and a particular stress component, an estimate of K_M can be made. In view of the inability of the conventional constant strain elements to represent the stress singularity condition at the crack-tip, the $K_M^\bullet$ curves for r > 0 must again be extrapolated back to r=0.

2.4 Example

In order to illustrate the finite element analysis for crack problems. A series study for a cracked plate is conducted. Fig 2.3 shows the geometry, dimension.

Length	200
width	100
thickness	14

unit : mm

P=100 KN
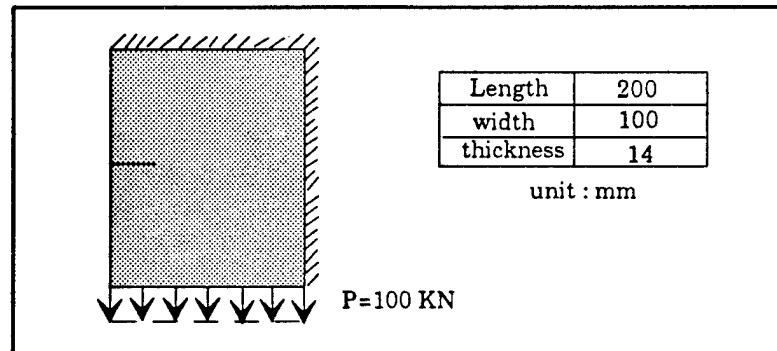
Fig 2.4 Finite Element Analysis for a Cracked Plate

The finite element analysis was carried out for two boundary conditions and two load cases (see Fig 2.5)
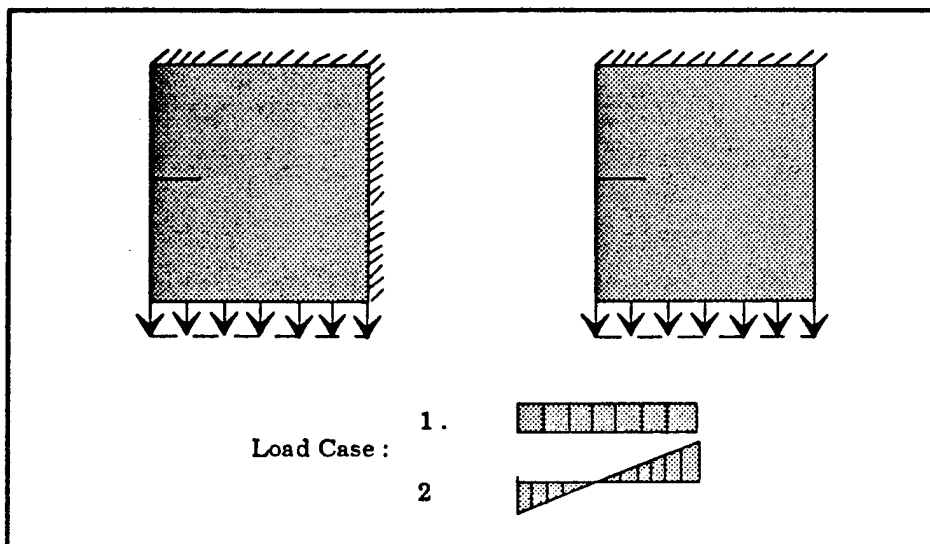
Fig 2.5 Boundary conditions and load cases for proposed cracked plate
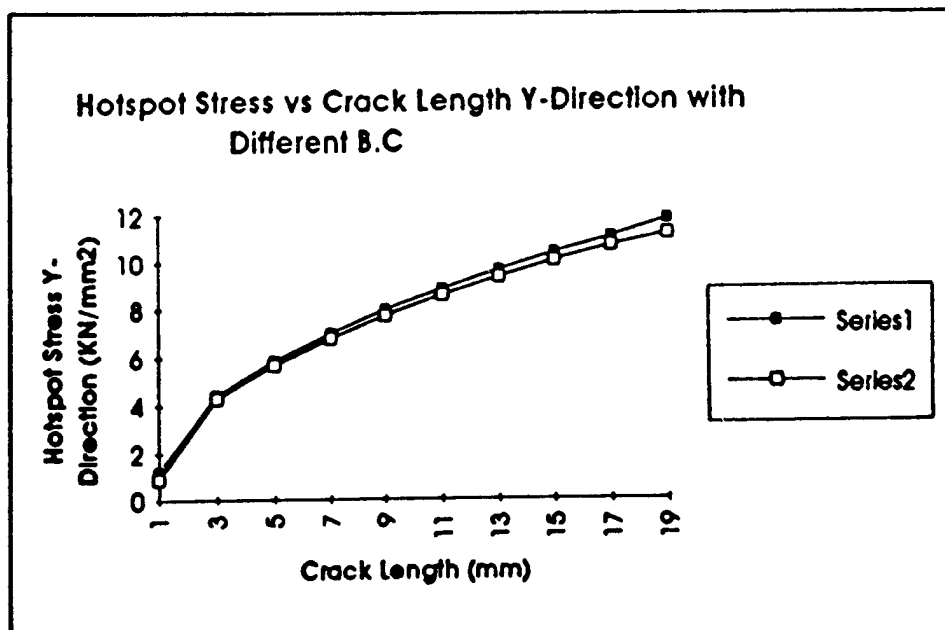
Fig 2.6 Hot spot stress vs Crack Length for different Boundary Conditions
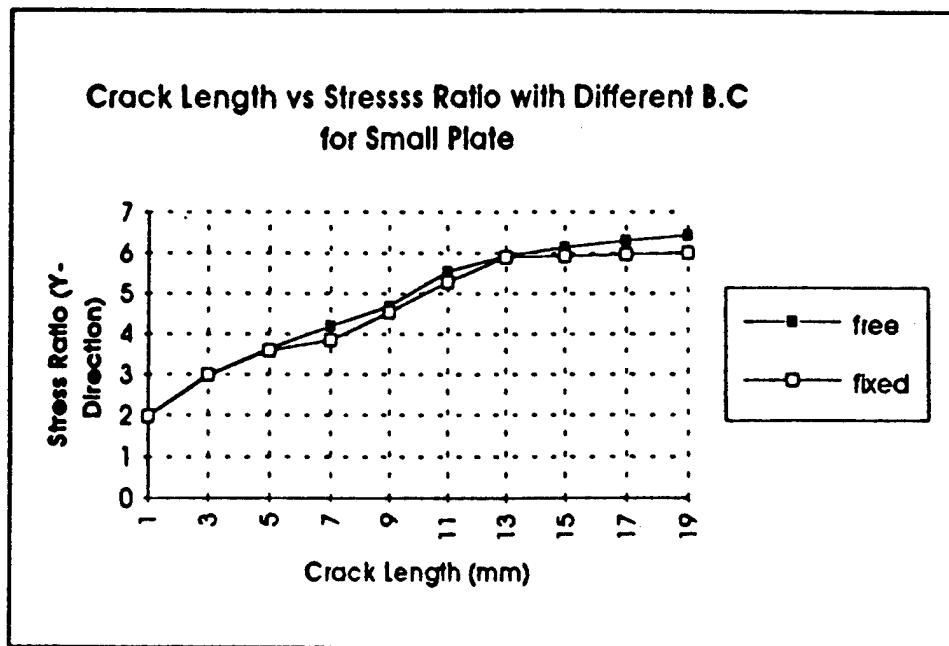
Fig 2.7 Hot spot stress vs Crack Length for Linear Bending Stress
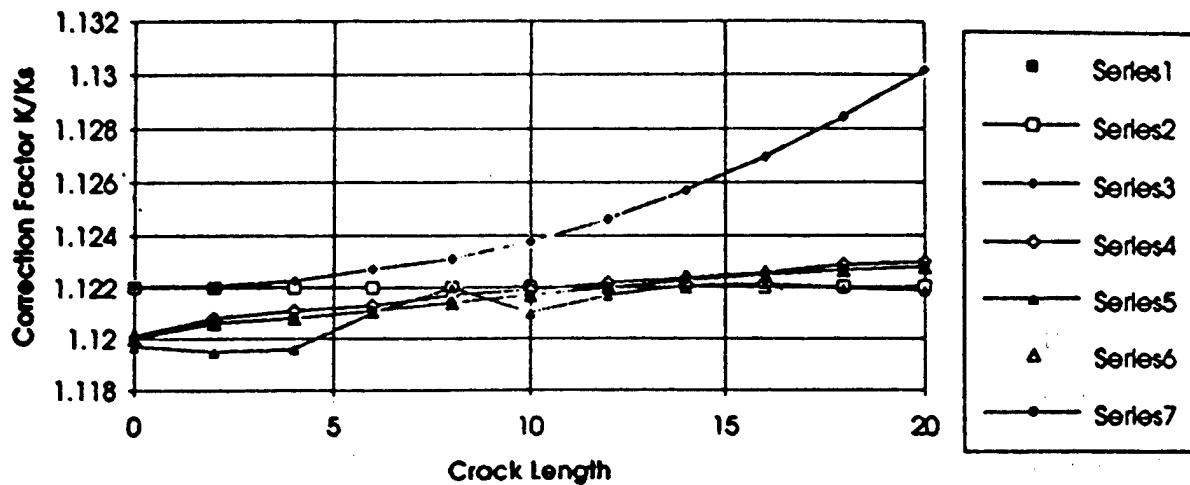
Fig 2.8 Stress Intensity Factor (SIF) comparison for uniform tension stress

Existing analytical solution and Finite Element Solution

18

In this analysis, 3-D solid element is used to model the plate. The analysis is carried out under different boundary conditions and load cases.

In Fig 2.6, the effects of boundary conditions for crack opening stress for the plate under uniform tension is displayed. This effects is not significant in the figure. The reason may be as follows:

1 - The crack is far away from the boundary conditions. The ratio of crack length to plate width (a/w) is very small. The fixed right side of plate does not absorb more loading during the crack propagation.

2 - The crack is propagated under the uniform tension. For the load case of uniform tension, the stress redistribution effects is not significant.

In Fig 2.7, the crack opening stress under load case 2 is displayed. One line is the crack opening stress for the cracked plate with a fixed side. The other line is the crack opening stress for the cracked plate with the free side. There is a trend for relatively large difference between these two lines. This difference is due to the load shedding factor. The reason that the difference is small in this faigue is that the ratio of the crack length to plate width (a/b) is small for this case (a/b=0.05).

In Fig 2.8, The comparison of the SIF from analytical results (Newman-Raju Equation) and from numerical results (FEA) is displayed. The data on series 1 is the SIF for a small cracked plate with a free boundary side from FEA. The data on series 2 is the SIF from analytical solution. The data on series 3 is the SIF for a small cracked plate with a fixed boundary side from FEA. The data on series 4 is the SIF for a large cracked plate with a free boundary side. The data on series 5 is the SIF for a large cracked plate with a fixed boundary side from FEA. The data on series 6 is the SIF for a small cracked plate

with a simply-supported boundary side from FEA. The data on series 7 is the SIF for a large cracked plate with a simply-supported boundary side from FEA.

It has been shown from Fig 2.8 that all these SIF are nearly the same. The reason may be :

1 - The crack is subjected to a uniform stress field. There is no stress gradient along the crack.

2 - The ratio of the crack length to plate width is small. For example, in a small cracked plate, $a/b < 0.1$ (a is the crack length, b is the plate width). Thus, the boundary side is far away from the crack. The load shedding can be neglected.

3 - The crack is subjected to pure tension. The stress redistribution under tension is not as important as that under bending.

2.5 Summary

Finite element analysis (FEA) is one of the most applicable numerical methods in the study of the crack problems. In order to develop and calibrate a load shedding model, several finite element approaches were employed in this project. This chapter presents a displacement approach with non-singular elements and a stress approach with non-singular elements which were employed in the load shedding development.

A numerical example was carried out to compare the analytical results and FEA results. It has been found that these two approaches can provide the same results (Fig 2.8). Based on the analysis in this chapter, experience has been gained to be used in the further development of load shedding model in Chapter 4 and 5.

Chapter 3

Newman-Raju Equation

3.1 Introduction

In the past ten years, various semi-analytical models for the computation of stress intensity factors (SIF) have been proposed. Newman-Raju equation is the one which is widely used in the computation of surface cracks. Newman-Raju equation is a semi-analytical model for a cracked plate with finite width. (Fig 3.1)
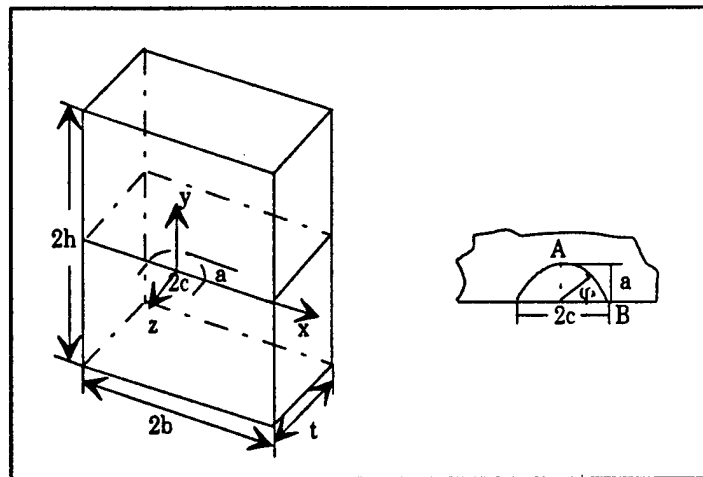
Fig 3.1 Surface Crack in a Finite Plate

3.2 Newman-Raju Equation

Newman-Raju [1981] proposed a semi-empirical equation for the SIF for a surface crack (part-through crack e.g. Fig 3.1) in a finite plate subjected to tension and bending loads. The stress-intensity factor equation for combined tension and bending loads is :

$$K = (\sigma_t + H\sigma_b) \sqrt{\frac{\pi a}{Q}} \, F(a/t, a/c, c/b, \varphi) \tag{3.1}$$

with

σ_t = remote uniform-tension stress (Fig 3.2a)

σ_b = remote uniform outer-fiber bending stress (Fig 3.2b)

H = function, depend on φ, a/t, a/c

a = depth of surface crack

Q = shape factor for elliptical crack

F = stress intensity boundary-correction factor

t = plate thickness

c = half-length of surface crack

b = half-width of cracked plate

φ = parametric angle of the ellipse

The factor Q takes into account the effect of crack front curvature, i.e. crack shape. A useful approximation for Q has been developed by Rawe (J.G.Merkle et. 1973):

$$Q = 1 + 1.464(a/c)^{1.65} \qquad a/c < 1 \tag{3.2}$$

The functions F and H are defined so that the boundary correction factor for tension is equal to F and the correction factor for bending is equal to the product of F and H.

The function F was obtained from a systematic curve-fitting procedure by using double-series polynomials in terms of a/c,a/t, and angular functions of φ. The function F was taken to be :

$$F = [M_1 + M_2(a/t)^2 + M_3(a/t)^4]f_\varphi g f_w \qquad (3.3)$$

where :

$$M_1 = 1.13 - 0.09(a/t) \qquad (3.3a)$$

$$M_2 = -0.54 + \frac{0.89}{0.2 + (a/c)} \qquad (3.3b)$$

$$M_3 = 0.5 - \frac{1.0}{0.65 + (a/c)} + 1.4(1.0 - \frac{a}{c}) \qquad (3.3c)$$

$$g = 1 + [0.1 + 0.35(\frac{a}{t})^2](1 - \sin\varphi)^2 \qquad (=1 \text{ for } \varphi = \pi/2) \qquad (3.3d)$$

The function f_φ an angular function from the embedded elliptical-crack solution is :

$$f_\varphi = [(\frac{a}{t})^2\cos^2\varphi + \sin^2\varphi]^{1/4} \qquad (=1 \text{ for } \varphi = \pi/2) \qquad (3.4)$$

The function f_w, a finite width correction factor is :

$$f_w = [\sec(\frac{\pi c \alpha}{2 b t})]^{1/2} \qquad (3.5)$$

The function H is of the form :

$$H = H_1 + (H_2 - H_1) \sin^p\varphi \qquad (= H_2 \text{ for } \varphi = \pi/2) \qquad (3.6)$$

where :

$$p = 0.2 + \frac{a}{c} + 0.6 \frac{a}{t} \qquad (3.6a)$$

$$H_1 = 1 - 0.34\frac{a}{t} - 0.11\frac{a}{c}(\frac{a}{t}) \qquad (3.6b)$$

23

$$H_2 = 1 + G_1(\frac{a}{t}) + G_2(\frac{a}{t})^2 \qquad (3.6c)$$

In this equation for H_2:

$$G_1 = -1.22 - 0.12\frac{a}{c} \qquad (3.6d)$$

$$G_2 = 0.55 - 1.05(\frac{a}{c})^{0.75} + 0.47(\frac{a}{c})^{1.5} \qquad (3.6e)$$

The remote bending stress, σ_b, and tension stress, σ_t, in the equation for the stress intensity factor refer to the pure bending or tension stress.
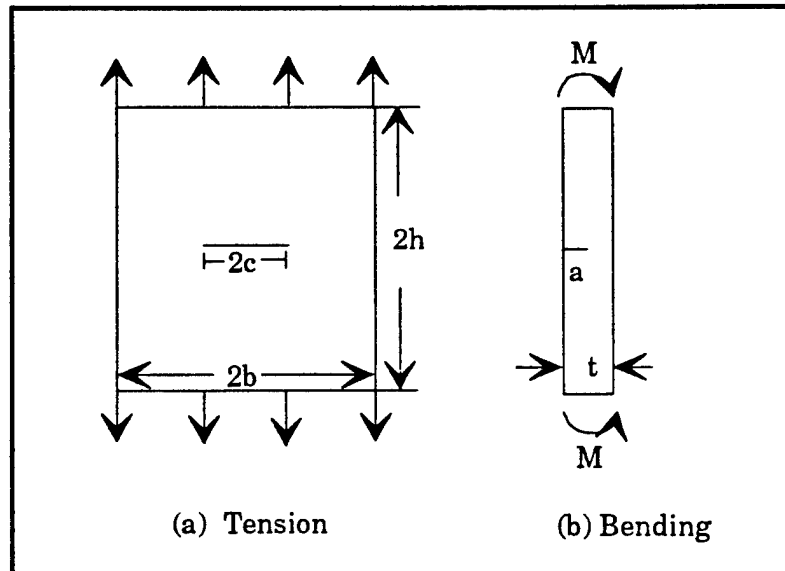
(a) Tension   (b) Bending

Fig 3.2 Surface-Cracked Plate Subjected to Tension or Bending Loads

3.3 Summary

The Newman-Raju equation has been summarized. It should be noted that the Newman-Raju equation can only be applied in the statically determinate cases although there is a boundary correction factor in this equation. The application of the Newman-Raju

equation to CSD in tankers which is statically indeterminate can be a problem. In this case, as a crack grows, the portion of the loadings of the cracked section is likely to vary due to the possibility of multiple-load paths. This results in a stress redistribution due to redundant boundary effects. Another problem is that the Newman-Raju equation is only valid for pure tension, linear bending or the tension and bending combination. It is different from the real stress field in cracked CSD where the stress field is arbitrary due to the local stress concentrations.

Chapter 4

Calibration for Surface Crack

4.1 Introduction

In the past ten years, various semi-analytical models for the computation of SIF have been proposed. Newman-Raju equation is the one for the computation of **surface cracks or part-through thickness cracks**. The Newman-Raju solution is only valid for finite plate with free ends. When the equation is applied for cracked CSD in tankers, the load shedding effects which are due to stress gradient from the local geometry and redistribution from the structural redundancy should be included. **It's the objective of this chapter to define and calibrate a load shedding model for application in tanker CSD.**

The FEA procedure for crack problem is discussed in chapter 2. The Newman-Raju equation is presented at in chapter 3. Based on the Newman-Raju equation and FEA, a calibrated load shedding model is proposed and verified in this chapter.

When the Newman-Raju equation is applied to ship CSD, two factors should be considered. One is the stress gradient accounting for the real stress field which is different

from uniform tension or pure bending. The other is the boundary effects which accounts for the degree of structural redundancy.

4.2 Calibration for Boundary Effects

Newman-Raju equation has been derived from the case of cracks in bodies where the loading is applied at three free ends or the statically determinate structure. If some degrees of redundancy are introduced in a structure, the local stiffness of cracked section changes as the crack grows. In general the decrease of local stiffness reduces the force and moments in the cracked section which results in a reduction in SIF.

To study the effects of the boundary conditions, a series of flat plates containing an edge crack were analyzed under different boundary conditions. Extremely fine meshes were used around the crack tip to simulate the crack tip singularity and the results of stresses were used to calculate the SIF by Equation 2.5. Fig 4.1 shows an example of the FE mesh used for analysis of the edge cracked plate under different boundary conditions.

The finite analysis was conducted under several load cases. Fig 4.2 shows the typical load cases.

This plate was analyzed under four different boundary conditions shown in Fig 4.1 and Fig 4.2. In configuration (1) only one end of the plate was fixed. Two types of loading were applied to the free end of this configuration. They were pure axial force and pure bending moment. In configuration (2), both ends of the plate were simply supported. In configuration (3), one end of the plate was fixed and the other end was restrained against vertical transition. Finally, in configuration (4), one end was fixed and the other end was restrained against rotation and vertical translation.
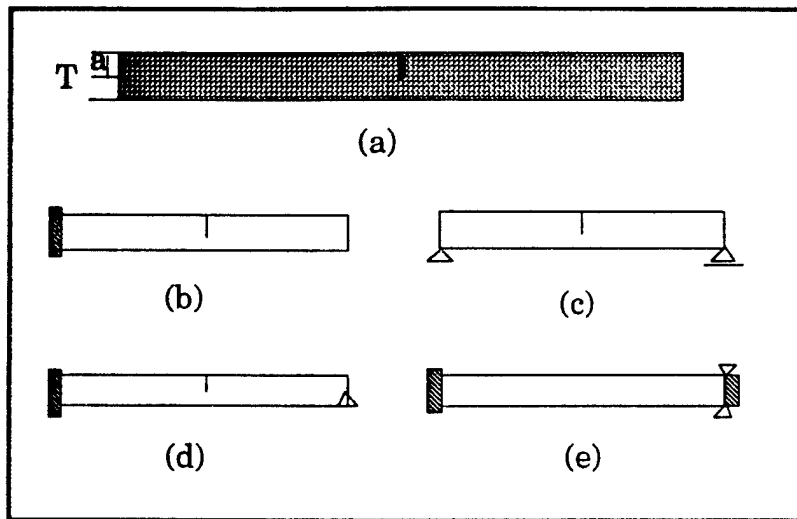
Fig 4.1 Edge cracked plate under different boundary conditions

a) FEA Mesh

b) Boundary condition 1, one end fixed

c) Boundary condition 2, both ends simply supported

e) Boundary condition 3, one end fixed and other end simply supported

f) Boundary condition 4, one fixed and other end restrained against

rotation and vertical displacement.
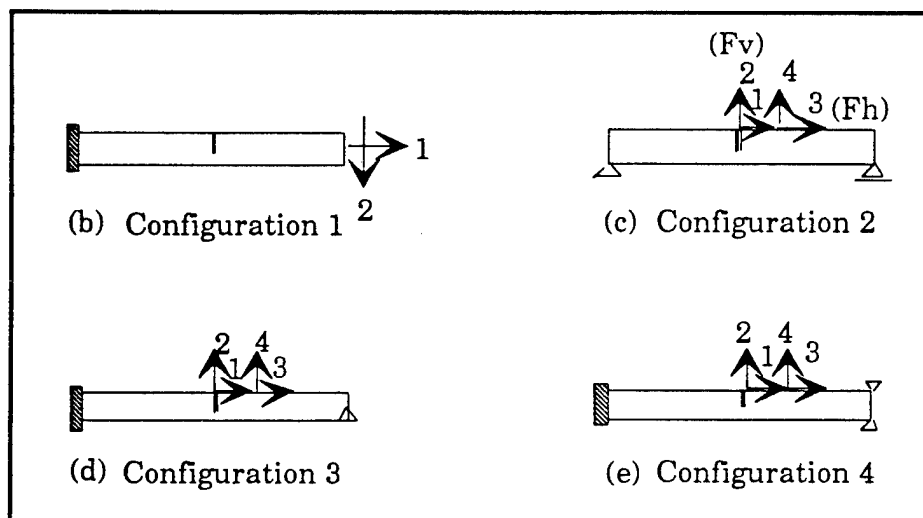
Fig 4.2 Edge Crack Plate under Four Different Load Cases

28

Four types of loading were applied to configuration (2), (3) and (4) as shown in Fig 4.2. For each load case only one point load were applied, which was either parallel or normal to the plate axis, was applied to the structure. Load cases (3) and (4) were identical to load cases (1) and (2), but in the former cases the point loads were applied two elements away from the crack to eliminate numerical error due to the application loads close to the crack. Load cases (1) and (3) produced a combination of axial force and bending moment at the crack section of the uncracked body. Load cases (2) and (4) produced a bending moment only.

Analyses of different configurations was carried out for the non-dimensionalized crack sizes, a/T. The results of crack displacement were used to calculate the mode I stress intensity factors, K. In order to make a comparison between the variation of SIF under different configurations as the crack length increased, they were normalized by dividing the SIF for any crack length (K) to the SIF for the standard crack length, which was 1/3 of plate width ($K_{1/3}$), for the same configuration.

Fig 4.3 shows the variation of stress intensity factors as a function of crack length in configuration (1), in Fig 4.2, when the plate is subjected to pure tension and bending.

Fig 4.4 shows the variations for different load cases in configuration (2). For load cases (1) and (2) which produce pure tension or bending at the crack section, the SIFs in both configurations are almost the same. Load case (3) which produces slightly different bending and tension at the crack section, compared to load case (1), closely follows the variation due to load case (1). Load case (4), which also produces only a bending moment at the crack section, follows exactly the variation due to load case (2) and shows that the application of the load to the crack face, has not caused significant numerical error for load case (2)
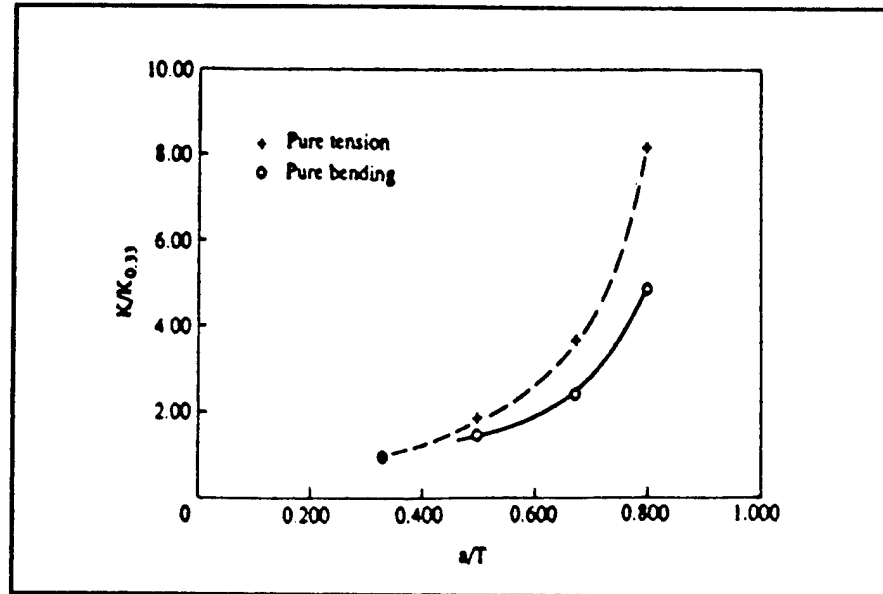
Fig 4.3 Variation of SIFs for the Edge Cracked Plate, Configuration (1)
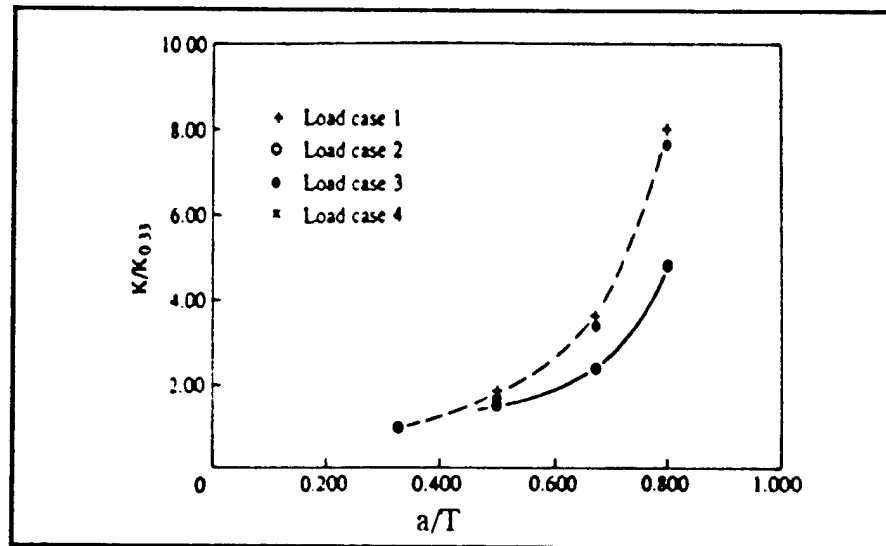
Fig 4.4 Variation of SIFs for the Edge Cracked Plate Configuration (2)

The SIF variation for the various load cases for the edge-cracked plate, in configuration (3), is shown in Fig. 4.5. This figure shows that the presence of a degree of

30

redundancy has significantly decreased the rate of SIF increase as a function of relative depth a/t. The variation of SIF for load case (2) which produces only a bending moment at the crack section, is directly comparable with similar load cases in configurations (1) and (2) which show a substantial reduction in the rate of SIF increase.
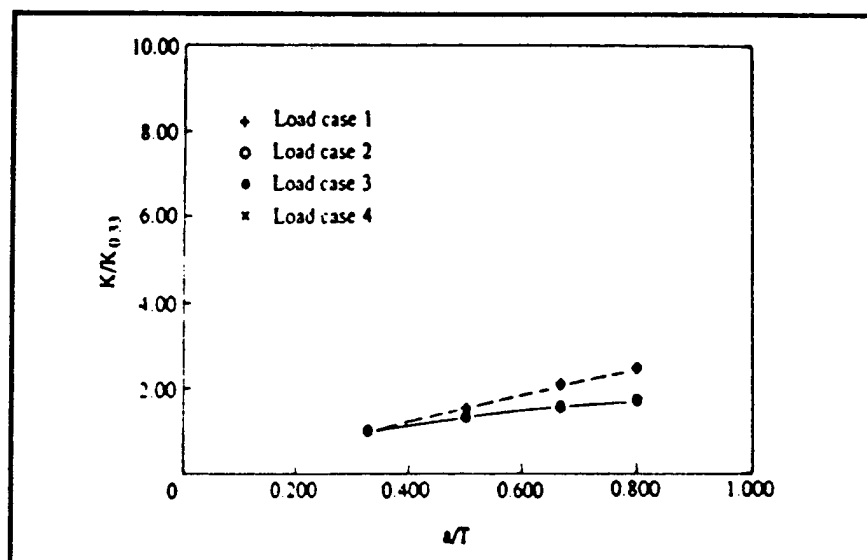
Fig 4.5 Variation of SIFs for the Edge Cracked Plate, Configuration (3)

Fig 4.6 shows the same set of results for configuration (4), which shows a further reduction in the rate of SIF increase, compared to configuration (3).

For load case (2) which produced only a bending moment at the cracked section for all the configurations, the stress intensity calibration factors, Y were calculated using the equation:

$$Y = \frac{K}{\sigma\sqrt{\pi a}}$$ (4.1)

where σ is the maximum bending stress at crack section in the uncracked body.

The variation of Y factors vs the crack size for all configurations are shown in Fig 4.7. The figure shows that the results for the first two configurations, which are **statically determinate**, are almost identical. However, for the other two **statically indeterminate** configurations they are substantially lower, especially for larger cracks.
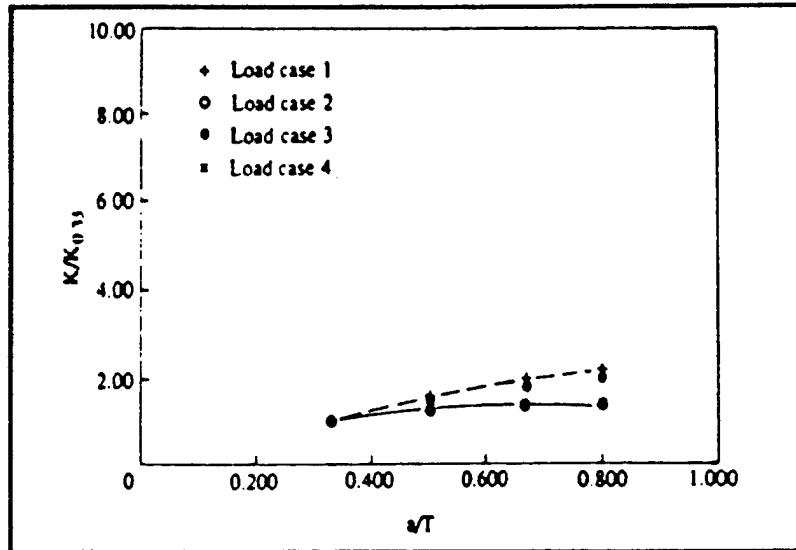
Fig 4.6 Variation of SIFs for the Edge Cracked Plate, Configuration (4)

Examination of the deformed shapes and the reductions in the cracked structures suggests that as the crack length increases, the behavior of the cracked section in configurations (3) and (4) approaches that of a hinge reducing the bending moment transferred through the section to zero.

Fig 4.8 compares the deformed shapes of the uncracked body and also the cracked body of configuration (4) when the crack length is 80% of the plate width for the second load case.
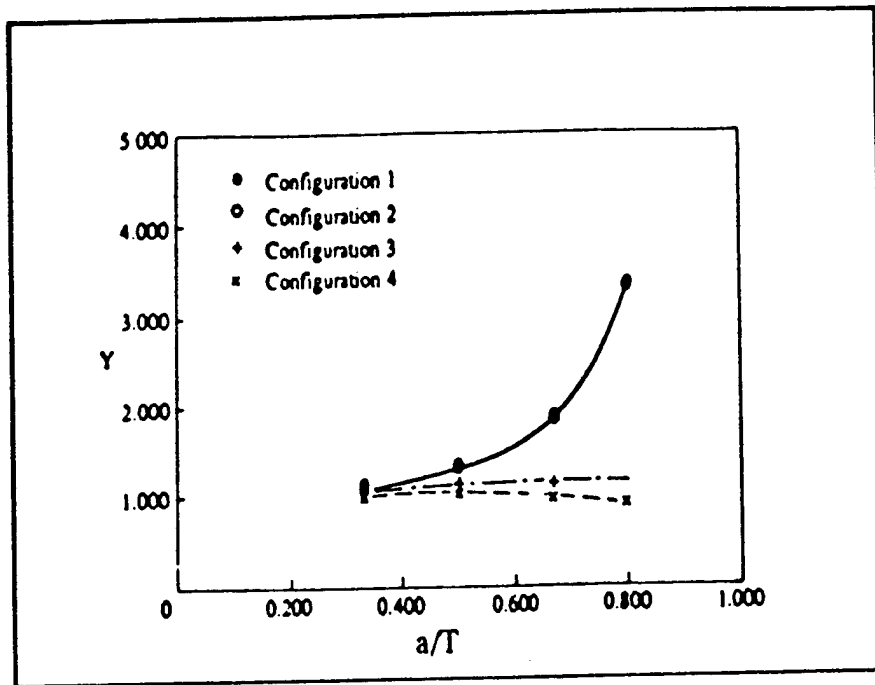
Fig 4.7 Correction Factor Y for the Edge Crack Subjected to the Bending

under Different Boundary Condition

(a) Uncracked body

(b) Cracked body
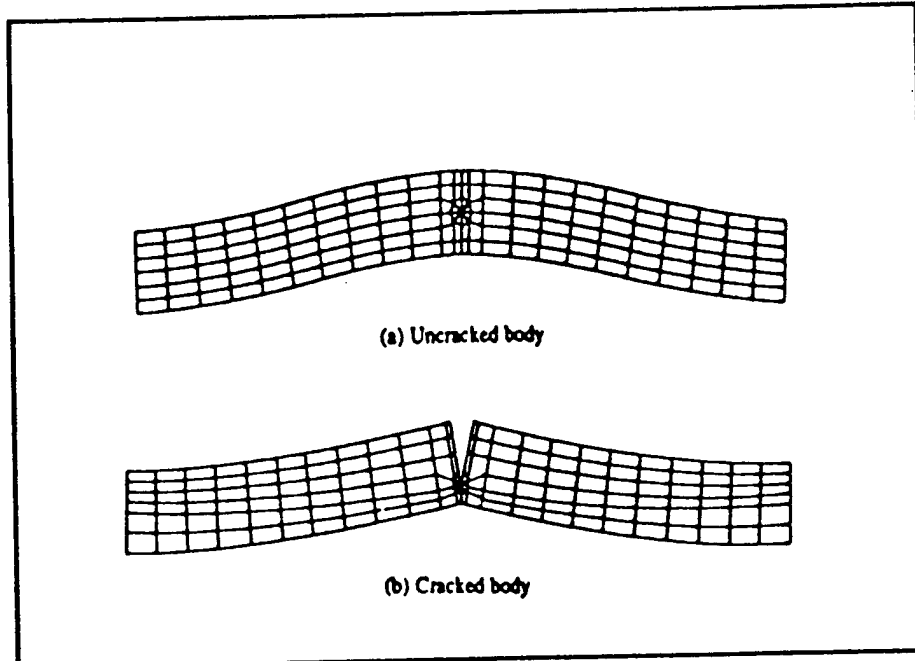
Fig 4.8 Deformed Shapes of the Plate with Fixed Ends Subjected to Bending

33

The results of the reactions at supports, obtained from FEA, showed that as the crack size increased, the moment at the fixed end of the plates in configurations (3) and (4) increased. In these cases, the bending moments carried across the cracked section were calculated using the support reactions and equilibrium equations. The results showed that the bending moment carried across the cracked section decreased as the crack size increased.

The ratio of fixed end bending moment to the initial value of uncracked section is plotted in Fig 4.9. This ratio shows that as the crack size increases, the local flexibility of the cracked section increases and the section behavior approaches that of a hinge.

The ratio of bending moment carried across the cracked section, M, to the bending moment in the uncracked body, Mo, is plotted in Fig 4.10. The figure shows a continuos reduction in the bending moment transmitted across this section as the crack length increases.

Based on Fig 4.10, a general moment release model was proposed :

For a/t < 0.25 $F_r = 0$ (4.2)

For a/t > 0.25 $F_r = 1 - \left(\dfrac{a}{t}\right)^r$ (4.3)

For r = 1, it's a linear moment release model. For r=2, it is a parabolic moment release model.
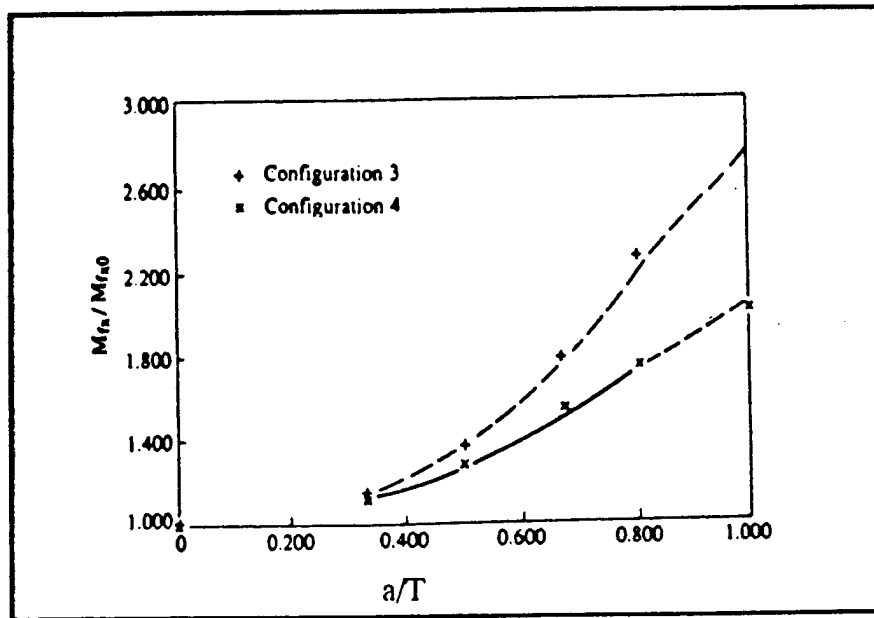
Fig 4.9 Variation of the Fixed End Bending Moment for the Edge-Cracked Plate
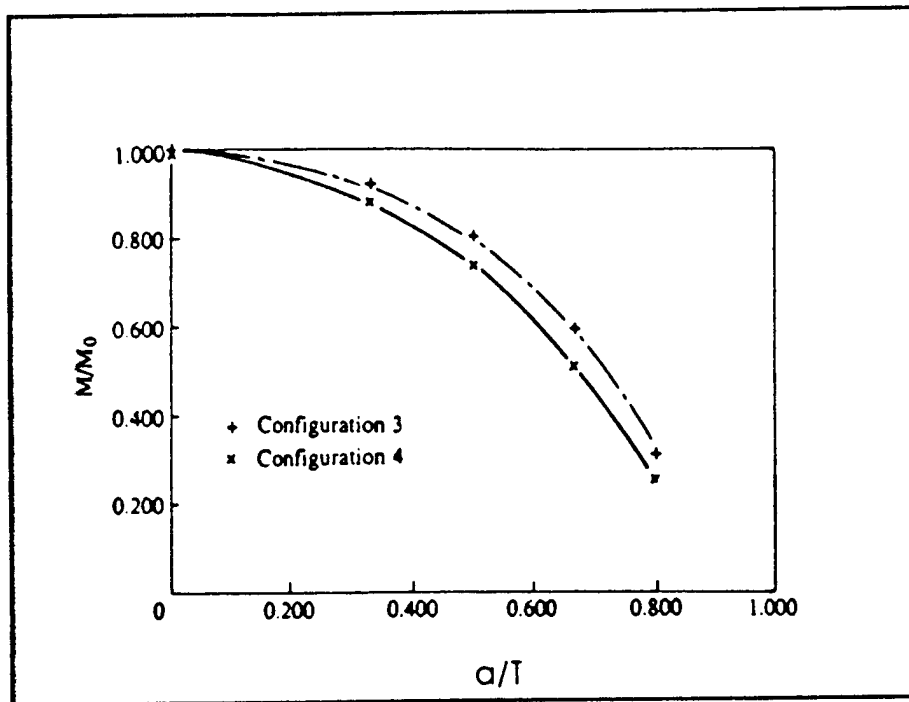
Fig 4.10 Ratio of the Bending Moment at Cracked Section to the Bending moment at

Uncracked Sections for the Edge-Cracked Plate

4.3 Calibration for Stress Gradient Effects

As we discussed about Newman-Raju equation early, the correction with regard to the actual stress gradients has to be made in order to account arbitrary stress distribution.

The stress gradient correction factor F_G can be derived from known solutions for K. This solution of a crack stress field problem can be visualized as a two step process.

Step 1. The stress distribution problem is solved in a manner satisfying the boundary conditions (displacements, stresses) but with the crack considered absent.

Step 2. To this stress field is superposed another stress field which cancels any stresses acting directly across the crack along the line of the crack.

Step 1 is a non-singular elasticity problem and can be solved by a FEM analysis. As the addition of a non-singular stress field ($\sigma(x)$, Step 1) does not affect the value of K (caused by $-\sigma(x)$, Step 2) the resulting K will be identical with that obtained from Step 2.

To evaluate K from Step 2, an influence (Green's) function method is employed. An influence function can be defined as :

$$G_I(b,a) = \frac{1}{P}K_{IP}(b,a)$$

(4.4)

where K_{IP} = due to a load P at x = b

P = load per unit sheet thickness / width

Hence, $G_I(b,a)$ is the K_I value arising from a unit force (per unit thickness/width) applied at abscissa $x = b$. $G_I(b,a)$ is independent of loading and depends merely on all the geometry parameters of the cracked body. If a solution for the stress intensity factor is known for any particular load system, then this information is sufficient to determine the stress intensity factor for any other load system.

A pressure $p(x)$ applied on an infinitesimal surface t (or W) dx results in an infinitesimal stress factor :

$$dK_I(x,a) = G_I(x,a)p(x)dx \qquad (4.5)$$

Thus, the K_I resulting from the total crack surface loading is :

$$K_I = \int_0^a G_I(x,a)p(x)dx \qquad (4.6)$$

In a part- through crack case the computation of the stress gradient corrector F_G maight be based on the following solution of the problem shown in Fig.4.11 :

$$K_I = \frac{2P}{\sqrt{\pi a}} \frac{1}{\sqrt{1-(b/a)^2}}F(b/a) \qquad (4.7)$$

Therefore the influence function in this case is :

$$G_I = \frac{2}{\sqrt{\pi a}} \frac{1}{\sqrt{1-(b/a)^2}} F(b/a) \qquad (4.8)$$

With the condition of $p(x) = \sigma(x)$, yields (Fig 4.12) :

$$K_I = \frac{2}{\pi}\sqrt{\pi a} \int_0^a \sigma(x) F(x/a)dx \qquad (4.9)$$

where $\sigma(x)$ can be obtained from a FEA.

37

$$K_1 = \frac{2p}{\sqrt{\pi a}} \cdot \frac{a}{\sqrt{a^2 - b^2}} \cdot F(b/a)$$
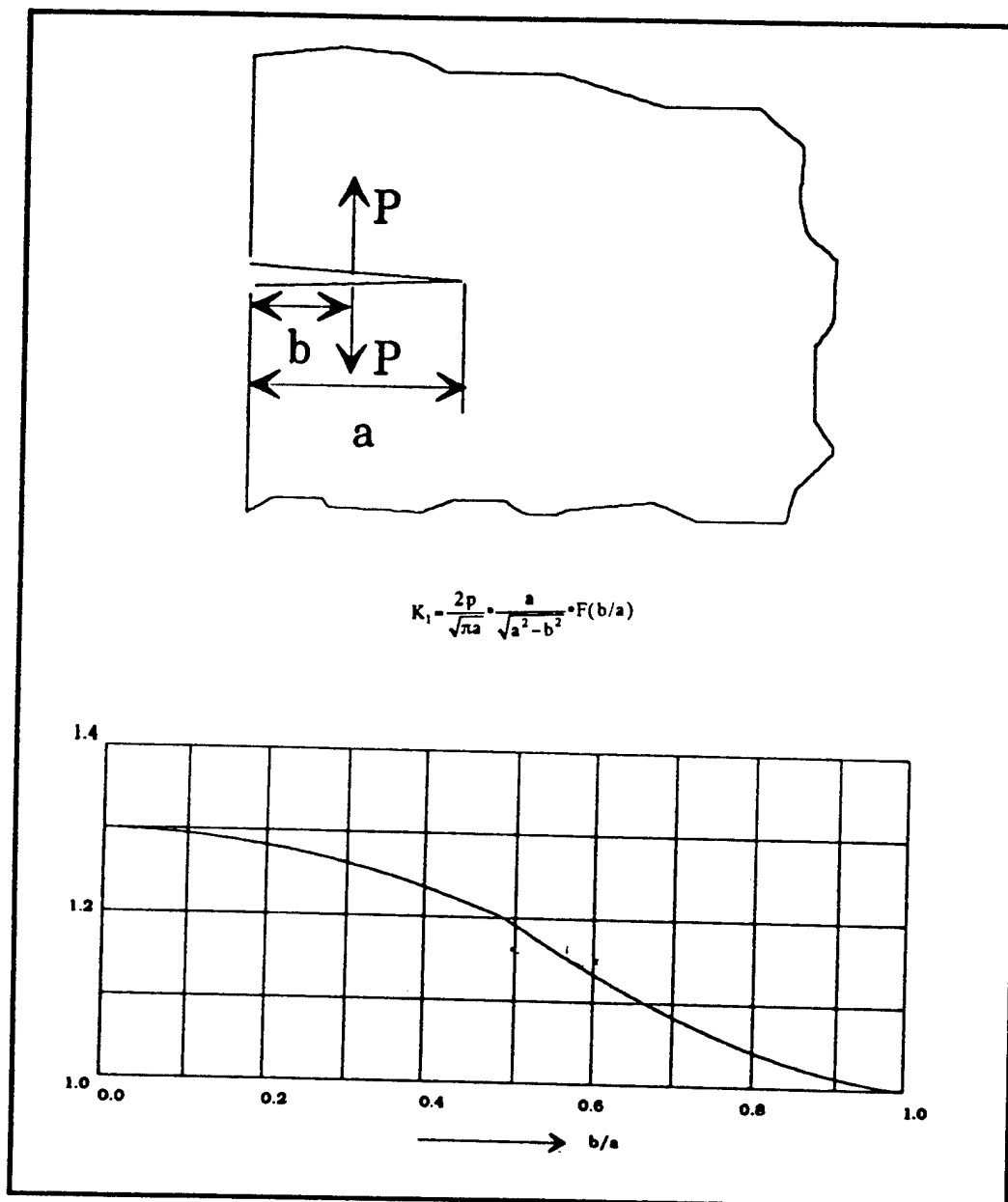
Fig 4.11 Calculation of K-Value by a Pair of Splitting Forces applied to the Crack Surface
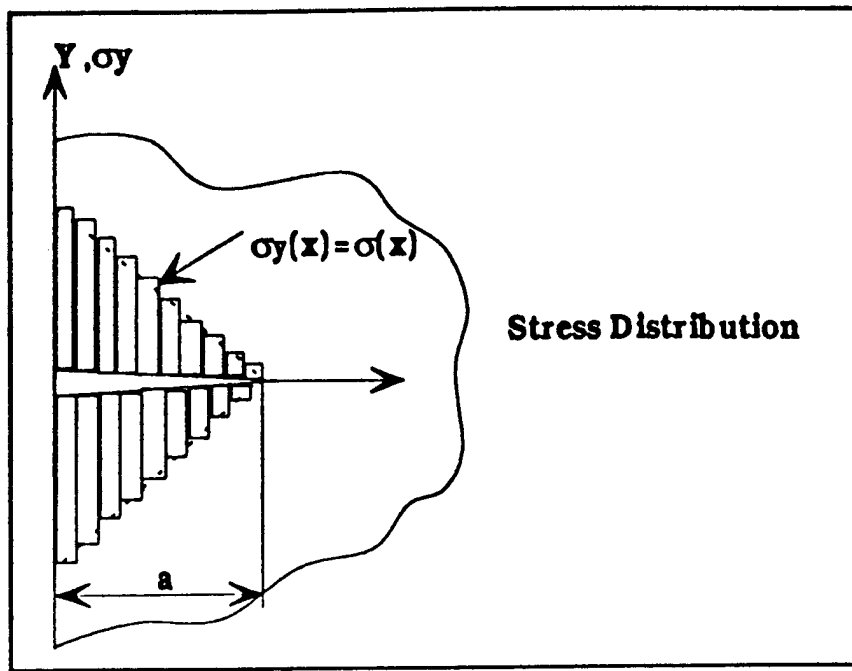
Fig 4.12 Stress Distribution along a crack

The stress distribution could be represented by a polynomial expression and could be intergrated analytically. Consider a single edge crack in a finite width plate; the crack is subjected to various polynomial stress distribution represented by :

$$\frac{\sigma(x)}{\sigma} = \sum_{n=0}^{N} S_n \cdot X^n \qquad (4.10)$$

The stress intensity factor for such a stress distribution can be easily determined by superposition of the basic stress intensity factor solutions due to power stress distributions with a unified form :

$$K = F\sigma\sqrt{\pi a} \qquad (4.11)$$

the non-dimensional stress intensity factor F can be determined by :

$$F = \sum_{n=0}^{N} S_n \cdot F_n \qquad (4.12)$$

where Sn are the stress polynomial coefficients and Fn is the factor determined by power stress series.

39

The stress intensity factor for power stress series was computed by Eq. 4.9 and Table 4.1 summarizes the results.

For the case of an edge crack described here the effect of the stress gradient on the stress surface correction factor Fs can be included in FG in the following way.

$$F_G = \frac{F}{1.122}$$ (4.13)

That is :

$$F_G = \frac{1}{1.122} \sum_{n=0}^{N} S_n \cdot F_n$$ (4.14)

Table 4.1 Stress intensity factor **Fn** for a single edge crack in a finite width plate with crack face power loading : $\sigma(x)/\sigma = x^n$

α	n						
	0	1	2	3	4	5	6
0.01	1.1226	6.82E-03	5.25E-05	4.40E-07	3.86E-09	3.48E-11	3.19E-13
0.05	1.1402	3.45E-02	1.32E-03	5.54E-05	2.42E-06	1.09E-07	5.00E-09
0.1	1.189	7.09E-02	5.40E-03	4.50E-04	3.93E-05	3.53E-06	3.23E-07
0.2	1.3672	1.56E-01	2.32E-02	3.81E-03	6.60E-04	1.18E-04	2.14E-05
0.3	1.6602	2.68E-01	5.78E-02	1.40E-02	3.58E-03	9.50E-04	2.58E-04
0.4	2.1113	4.25E-01	1.18E-01	3.71E-02	1.25E-02	4.34E-03	1.56E-03
0.5	2.8241	6.63E-01	2.20E-01	8.40E-02	3.45E-02	1.48E-02	6.55E-03
0.6	4.0333	1.06E+00	4.01E-01	1.78E-01	8.52E-02	4.30E-02	2.24E-02
0.7	6.3558	1.81E+00	7.59E-01	3.75E-01	2.03E-01	1.17E-01	6.94E-02
0.75	8.4537	2.49E+00	1.09E+00	5.61E-01	3.92E-01	1.93E-01	1.22E-01
0.8	11.9548	3.62E+00	1.63E+00	8.77E-01	5.21E-01	3.30E-01	2.18E-01
0.85	18.6264	5.78E+00	2.68E+00	1.49E+00	9.15E-01	6.01E-01	4.14E-01
0.9	34.6348	1.10E+01	5.20E+00	2.96E+00	1.87E+00	1.27E+00	9.03E-01

where;

$\alpha = a/t$, and

t : plate width

In order to apply Newman - Raju's empirical stress intensity factor equation in the case of an arbitrary stress field the following transformations have to be made.

For tension stresses   - F is replaced by F^*F_G,at

For bending stresses   - F is replaced by F^*F_G,ab

- H is replaced by $H/F_G,nb$

F_G,at and F_G,ab are correction factors, which account for the difference between a uniform and a non-uniform tension or bending stress distribution in the crack growth plane. These factors are calculated using the above equation with the actual through thickness stress distributions (tension for F_G,at and bending for F_G,ab). A calculation for pure bending provided the extraction on the effect of this distribution and gave F_G,nb.

4.4 Xu-Bea (X-B) Modification

Two correction factors have been developed for the Newman-Raju equation. One is the stress redistribution factor, Fr, which accounts for the boundary effects on stress redistribution. Another is the stress gradient factor, F_G. which accounts for the real stress distribution. It is assumed that these two factors are not correlated.

The modified Newman-Raju equation taking the load shedding into account (X-B modification) is as follows :

For tension stresses, F is replaced by FF_G,at, the modified Newman-Raju equation is:

$$K = \sigma_t \sqrt{\frac{\pi a}{Q}} F(a/t, a/c, c/b, \varphi) F_{G,at} \tag{4.15}$$

F_G,at is the correction factor which accounts for the difference between a uniform and a non-uniform tension stress distribution.

For bending stresses, F is replaced by FF_G,ab and H is replaced by HF_r/F_G,nb. F_G,ab are bending stress gradient correction factor which accounts for the difference between a uniform and a non-uniform bending stress distribution in the crack growth plane. A linear bending stress distribution (pure bending) provided the extraction of the effect of this distribution and gave F_G,nb. Fr is the stress redistribution correction factor due to boundary effects :

$$K = HF_r \sigma_b \sqrt{\frac{\pi a}{Q}} F(a/t, a/c, c/b, \varphi) F_{G,ab} / F_{G,nb} \tag{4.16}$$

For the bending and tension combination, the following general expression is proposed as the modification of Newman-Raju equation : .

$$K = [F_{G,at} \sigma_t + \left(\frac{F_{G,ab}}{F_{G,nb}} \right) \cdot HF_r \sigma_b] \sqrt{\frac{\pi a}{Q}} F(a/t, a/c, c/b, \varphi) \tag{4.17}$$

4.5 Verification

The proposed X-B model has been verified from the existing literature and experimental data. Due to the lack of the experimental data for ship CSD, the experimental data on the load shedding of tubular joints has been utilized. The experimental data is from the published references. [Forbes, et. 1992]

The experimental stress intensity factors were determined on the basis of measured fatigue growth rates in tubular welded specimen. The geometry and dimensions of the specimens are shown in Fig 4.12. The experiments reported are two specimens. One is

under cyclic axial loading and one under cyclic in-plane bending. The stress ratio, R, for the axially loaded specimen was 0.16 and the R-ratio for the in-plane bending specimen was 0.05.

The specimens were tested under constant amplitude at a frequency of 2.5 to 3 Hz. Fatigue cracks were measured periodically using the Direct Current Potential Drop technique and the Alternating Current Potential Drop technique at Memorial University in St. John's, Newfoundland while the in-plane bending specimen was tested at the University of Waterloo.

Fatigue cracks 0.5mm deep were detected early of the crown position in the in plane bending specimen. In the axially loaded specimen, the crack initiated and grew at the saddle. All the fatigue cracks initiated along the weld toe and then propagated through the chord wall material.

The periodic crack measurements made it possible to measure both the crack depth, a, and the crack length, 2c, as a function of the number of load cycles, N. The results were used to derive an experimental relation between the crack depth, a, and crack growth rate, da/dN.

The corresponding stress intensity factor values were determined from the Paris equation.

$$\Delta K = \left[\frac{1}{C} \times \frac{da}{dN} \right]^{\frac{1}{m}}$$

(4.18)

The Paris equation constants were $C = 6.2 \times 10^{-12}$ and $m = 3$. The final results were given in terms of the geometrical stress intensity correction factor Y :

43
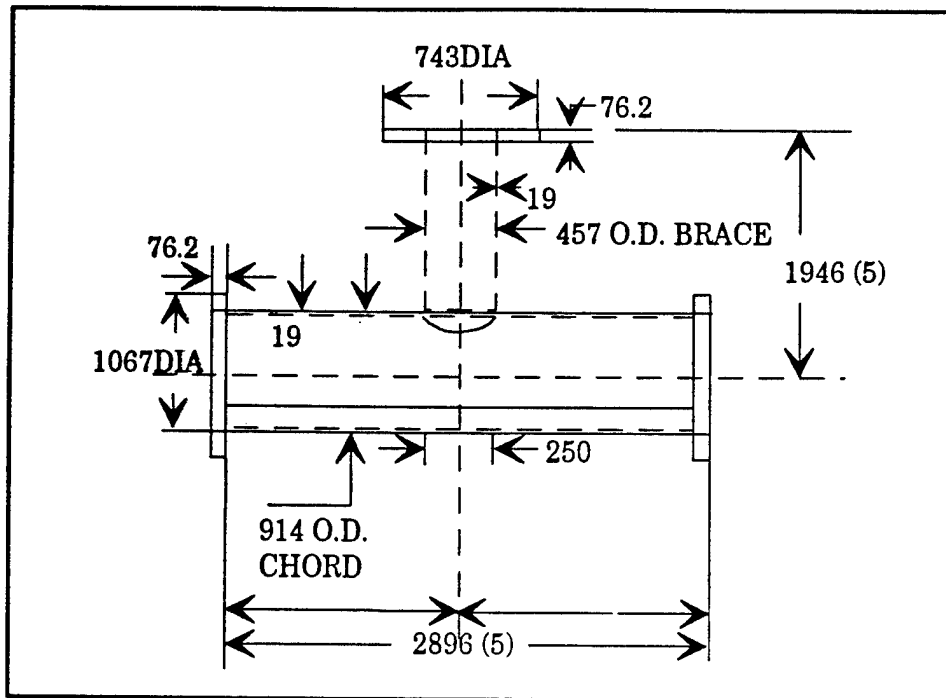
Fig 4.12 Geometry and Dimension of Tested Tubular Joint (Unit mm)
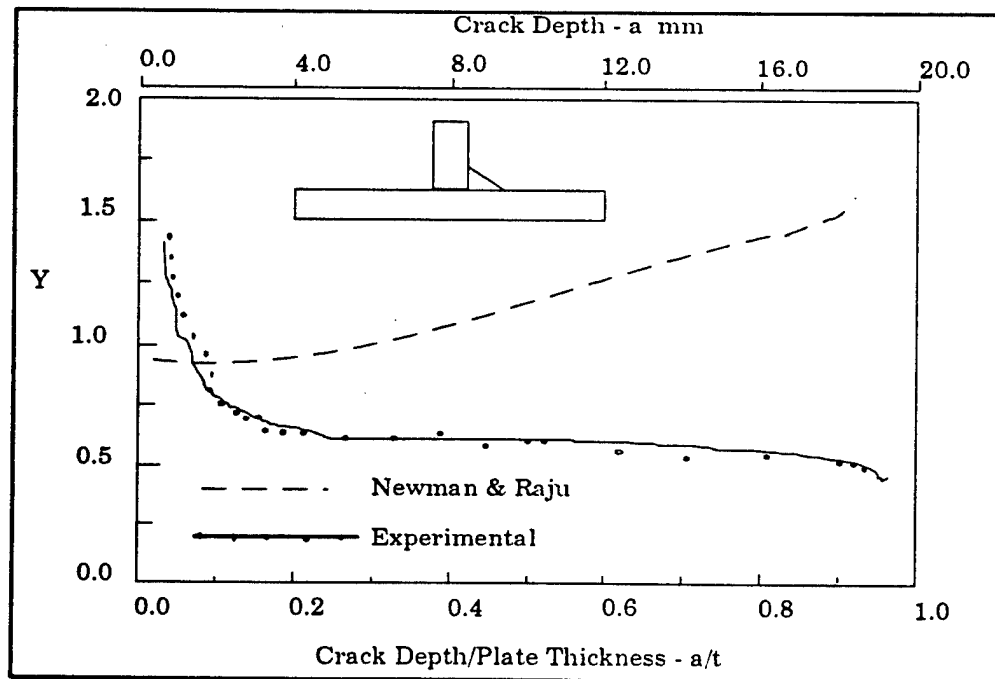
Fig 4.13 Comparision between Experimental Results and Newman-Raju Solution

for Tubular Joint under Axial Loading
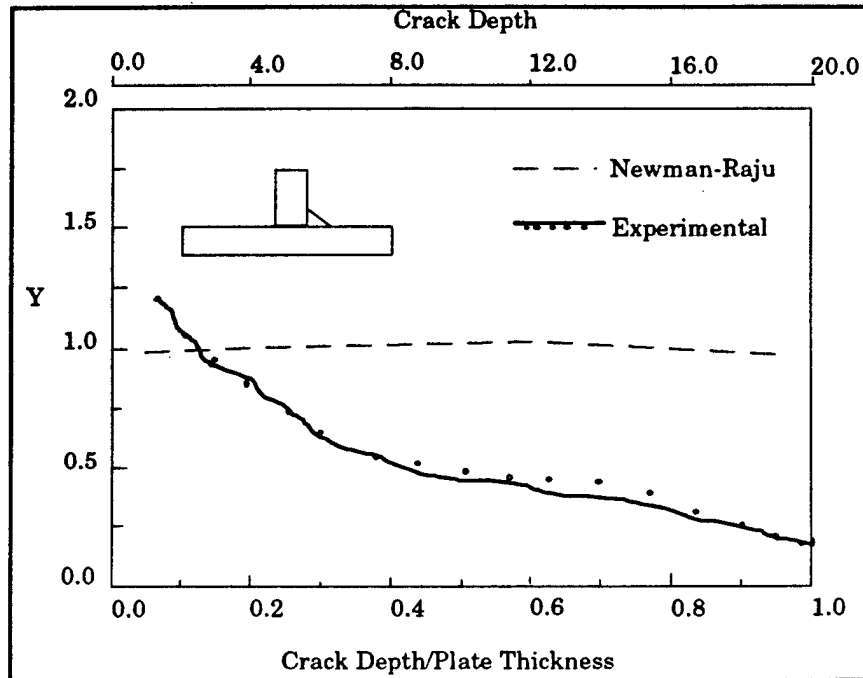
Fig 4.14 Comparision between Experimental Results and Newman-raju Solution

for Tubular Joint under Pure Bending

$$Y = \frac{\Delta K}{\Delta \sigma_{HS} \sqrt{\pi a}} \qquad (4.19)$$

The variation of the geometrical Y factor as a function of the crack depth is shown

in Fig 4.13-4.14. The experimental data is compared with Newman-Raju solution. It has

been shown that there is a considerable difference between experimental results and

Newman solution. It was found that it under-estimated the stress intensity factor for

tension in $0< a/t < 0.3$. However, high over-estimation of the stress intensity factor based

on the Newman-Raju solution occurred for $0.3 < a/t < 1.0$.

As discussed early, the major differences between a crack in a flat plate and similar

cracks in a tubular joint / critical structural detail are due to stress redistribution factor

which is from different boundary conditions and stress gradient factor which is from real

45

stress distribution. Newman-Raju Equation was derived from statically determinate flat plate configurations where the same moments and nominal loads were transferred through the cracked section regardless of the crack size and the stiffness of the cracked section under the tension and bending combination. In the case of tubular joints / critical structural detail, first the crown/saddle bending moments and the stresses driving the crack growth depend on the cracked section stiffness and as consequence they are depend on the crack size, second the real stress distribution is different from tension and bending combination. Therefore, the input of the initial linear combination of tension and bending stress is over-estimated. (See Fig 4.13-4.14). This is the load shedding defined in Chapter 1.

Based on X-B load shedding model, the stress intensity factors were recomputed from Equations 4.15 and 4.16.

Stress Gradient Correction

The stress intensity factor considering the stress gradient factor was computed by Equation 4.13. The Newman-Raju stress field and real stress field was shown in Fig 4.15. Sr is the stress distribution along the crack depth. sn is the nominal stress. The comparison between the experimental results, Newman-Raju solution and X-B model considering the stress gradient factor only is plotted in Figs 4.16 and 4.17.

In Fig 4.16 4.17, The results from X-B model with stress gradient factor fitted the experimental data extremely well for $0 < a/t < 0.3$. This could be concluded that stress gradient effect is much more important for small crack . For $0.3 < a/t < 1.0$, the results from X-B model with stress gradient factor didn't fitted well with the experimental data. It could be explained as follows:

The stress gradient factor represented the effects of local stress concentration factor. This effect can be neglected for deep crack (0.3 < a/t < 1.0) since the crack tip was far away from the local notch.
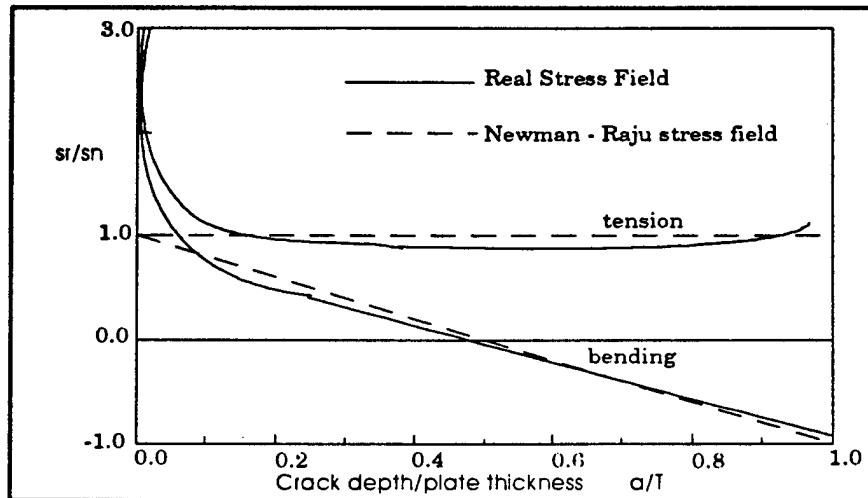
Fig 4.15 Nondimensional Stress Distribution for Stress Gradient factor calculation
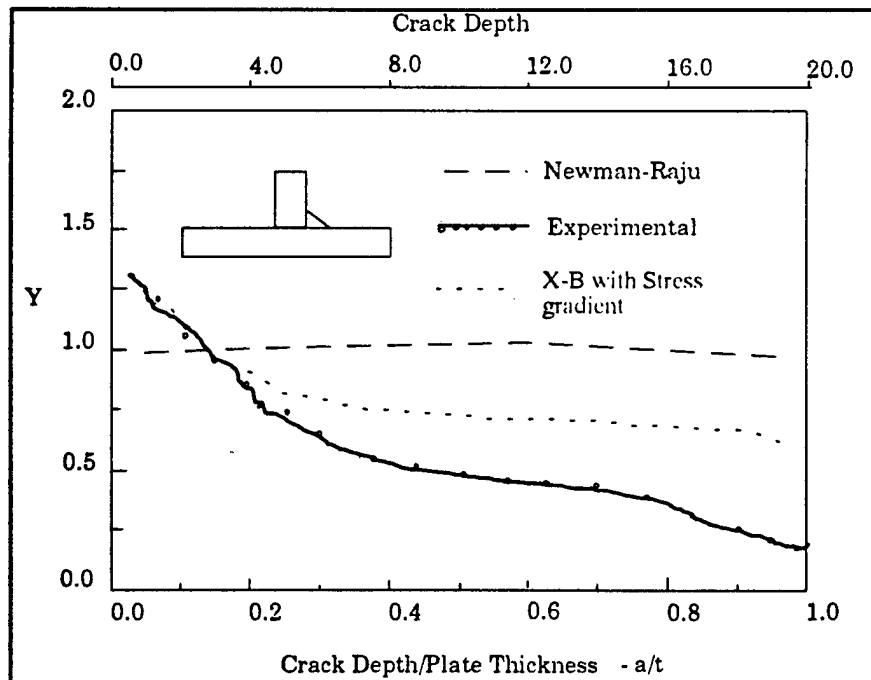
Fig 4.16 Experimental and Theortical calibration of Y for T-Joint under Tension

47
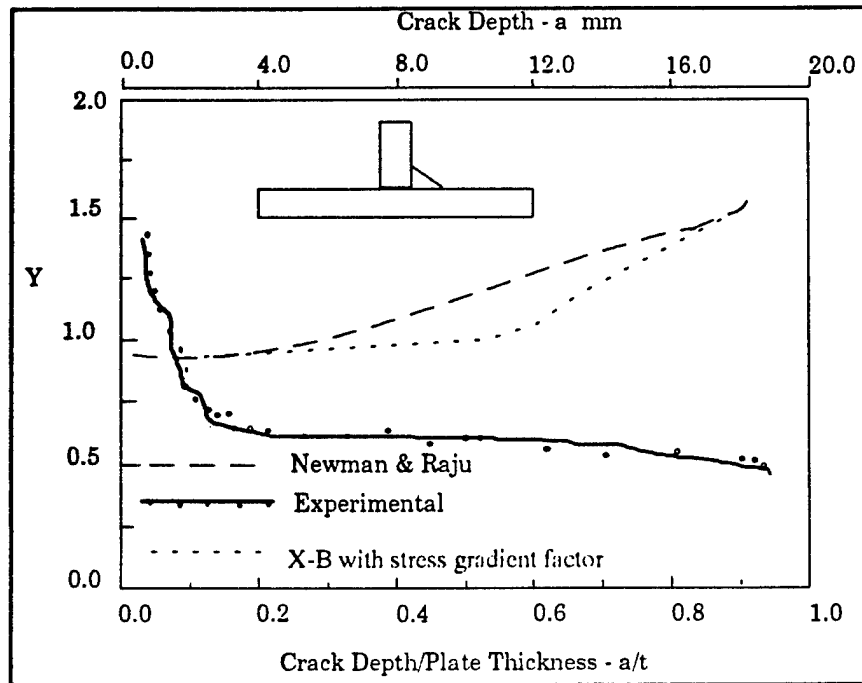
Fig 4.17 Experimental and Theoretical Calibration of Y for T-Joint under Bending

Stress Redistribution Correction

Two stress redistribution model were used. One is the parabolic moment release model, the other is the linear moment release model.

The parabolic model is :

$$F_r = 1 - \left(\frac{a}{t}\right)^2 \tag{4.20}$$

The linear model is

$$F_r = 1 - \left(\frac{a}{t}\right) \tag{4.21}$$

For these two stress redistribution models, the stress intensity factor considering the stress gradient and stress redistribution was computed and plotted in Fig 4.18 for T-Joint under bending.
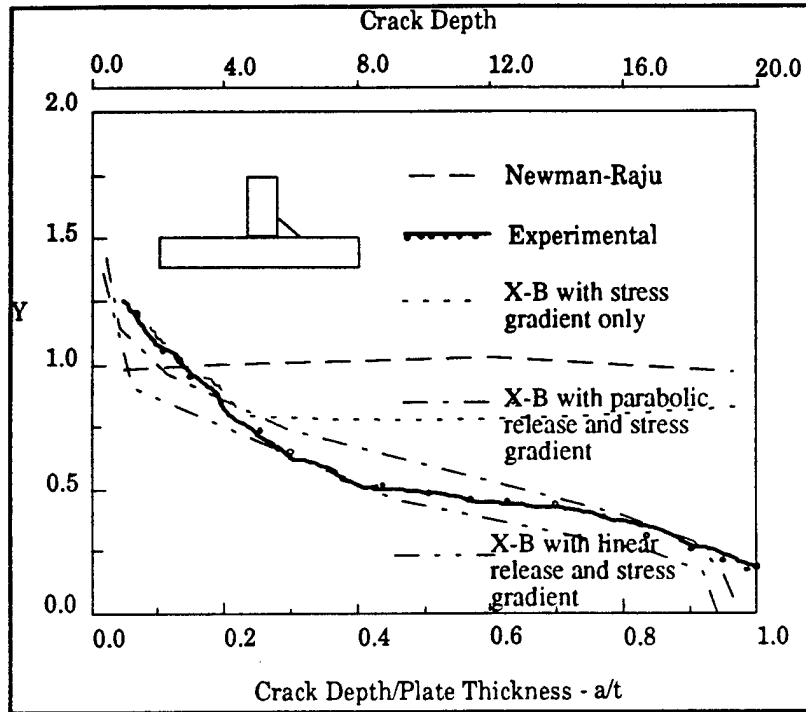
Fig 4.18 Experimental and modified Theoretical Results for T-Joint under Bending

In Fig 4.18, The results of X-B model with stress gradient fitted the experimental data for 0 < a/t < 0.25. But they didn't fit the experimental data for 0.25 < a/t < 1.0. With the additional correction factor, stress redistribution factor, the results of X-B model fitted the experimental data for 0.3 < a/t < 0.8. Thus, we could conclude a load shedding model as follows :

For 0 < a/t < 0.3, the stress gradient factor should be included in Newman-Raju equation while the stress redistribution factor can be neglected because the local nonlinear notch stress factor is important for small cracks while the stress redistribution is small for small cracks.

49

For $0.3 < a/t < 0.9$, the stress redistribution factor and stress gradient factor should be included together in Newman-Raju equation because the stress redistribution is important for large cracks.

4.6 Summary

The application of plate model predictions of SIF should take two additional factors into account. One is the stress gradient factor which is due to real stress distribution in ship CSD. The other is the stress redistribution factor which is due to applied boundary conditions or adjacent elements.

This chapter presented a modified Newman-Raju equation (X-B model) for SIF computation in cracked CSD in tankers. The model was calibrated by numerical analysis and verified by the experimental data. Several empirical formula for stress gradient factors and stress redistribution factors was proposed for several welded joints for application to cracked CSD in the next chapters.

The proposed load shedding model is relatively simple. Several other factors should be addressed. These factors will be discussed briefly in appendix B.

Chapter 5

Calibration for Through Crack

5.1 Introduction

Chapter 4 developed and verified a load shedding model for Newman-Raju Equation which is valid for surface cracks. But, through - thickness cracks are another fatigue cracking problem for Ship CSD. The Newman-Raju equation can not applied in through crack cases. Thus, a Hybrid method [7] has been applied to compute the stress intensity factors for through thickness crack. The load shedding model based on Hybrid method is developed and verified in this chapter.

5.2 Hybrid Method

The problem of estimating the SIF, K, for the case of a through thickness crack can be solved by using the hybrid method. This development has taken the stress gradient correction factor F_G into account. It is therefore necessary to apply stress redistribution factor only in Hybrid method. Based on Hybrid method, the SIF can be written as:

$$K = \sigma\sqrt{\pi a}F \qquad (5.1)$$

50 B

Here, F is a function of the stress gradient correction factor, F_G, and the finite width correction factor, F_W, only :

$$K = \sigma\sqrt{\pi a}\ F_G\,F_W \tag{5.2}$$

The computation of F_G in the case of a through crack might be based on a solution of the problem shown in Fig. 5.1

As described in Chapter 4, the stress gradient correction factor can be determined by using a superposition method combined with an influence (Green's) function method. The following solution for the stress intensity factor for a crack in an infinite sheet subjected to a pair of splitting forces, which do not have to be at the center of the crack has been used.

$$K_{l+a} = \frac{P}{\sqrt{\pi a}} \bullet \sqrt{\frac{a+b}{a-b}} \qquad \text{or} \qquad K_{l-a} = \frac{P}{\sqrt{\pi a}} \bullet \sqrt{\frac{a-b}{a+b}} \tag{5.3}$$

This yields the following expression of F_G :

$$F_G = \frac{1}{\pi} \bullet \sum_{i=1}^{n} \left\{ \frac{\sigma_{bi}}{\sigma} \left[\arcsin\frac{b_{i+1}}{a} - \arcsin\frac{b_i}{a} - \sqrt{1-\left(\frac{b_{i+1}}{a}\right)^2} - \sqrt{1-\left(\frac{b_i}{a}\right)^2} \right] \right\} \qquad \text{or}$$

$$F_G = \frac{1}{\pi} \bullet \sum_{i=1}^{n} \left\{ \frac{\sigma_{bi}}{\sigma} \left[\arcsin\frac{b_{i+1}}{a} - \arcsin\frac{b_i}{a} + \sqrt{1-\left(\frac{b_{i+1}}{a}\right)^2} + \sqrt{1-\left(\frac{b_i}{a}\right)^2} \right] \right\} \tag{5.4}$$

where b in (-a, +a)

F_G can be determined by polynomial stress series which is presented in Chapter 4.

The finite width correction factor F_W can be calculated using the general methods defined in Reference [7].

5.3 Calibration Model

The load shedding model for through-cracks is based on that for surface cracks. It includes the stress redistribution factor in Equation 5.1 to take the boundary effects into account. The proposed model is :

51

$$K = (\sigma_m + F_r \sigma_b)\sqrt{\pi a} \cdot F_w \cdot F_G \qquad (5.5)$$

where $F_G = 1-ka$ the stress redistribution factor,

      k is the linear release model parameter,

      σ_m is the membrane stress, and

      σ_b is the bending stress.

The linear release model parameter k can be determined from FEA which is presented in Section 4.2. Based on the experience in this project, k value can be selected from (0.85-1.15) for $0.3 < a/b < 0.9$ (Fig 5.2).

5.4 Summary

This chapter discusses the load shedding in through crack cases. The hybrid method for stress intensity factors of through thickness cracks is presented at first. The load shedding model is proposed based on the experience from surface cracks. The calibrated model only considers stress redistribution factor since the stress gradient factors is already included in Hybrid method.

$$(K_I)_{\pm a} = \frac{P}{\sqrt{\pi a}} \sqrt{\frac{a \pm b}{a \mp b}}$$
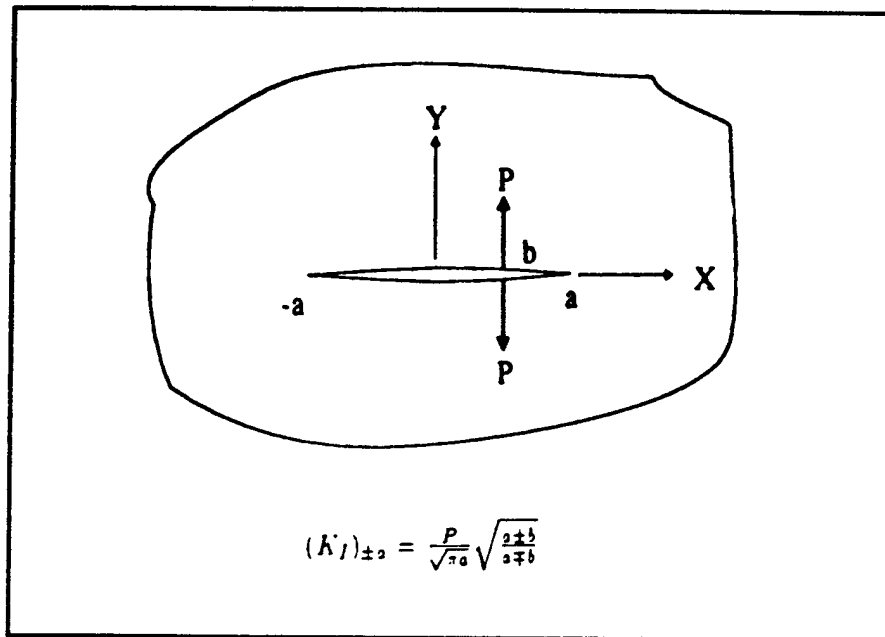
Fig 5.1 One Pair of Splitting Forces on a Through Crack in an Infinite Sheet

boundary conditions
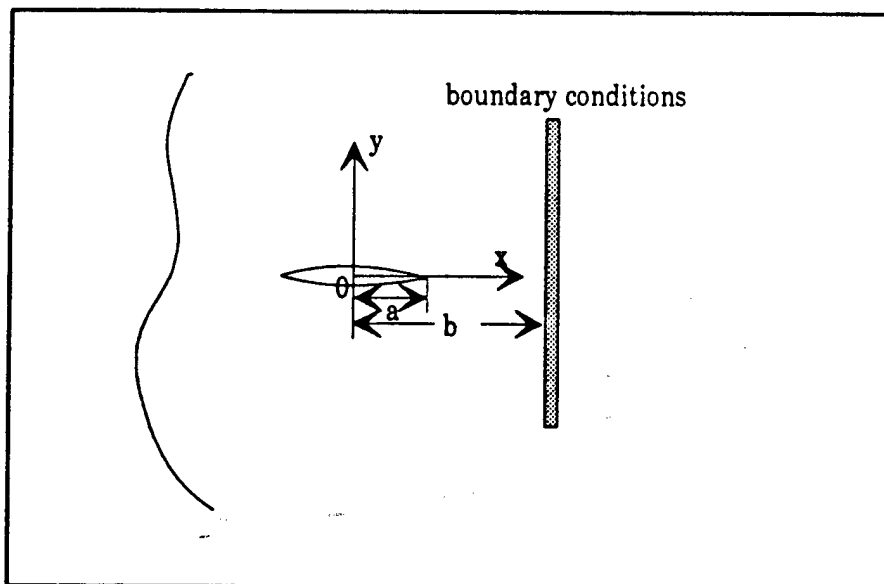
Fig 5.2 Load Shedding for through crack case

Chapter 6

Calibrated Empirical Formula

6.1 Introduction

A load shedding model was presented and verified in previous chapters. Based on the proposed model, a stress redistribution factor and a stress gradient factor are two new factors in this model. This chapter proposes several empirical formulas of these two factors for welded joints. The following have been considered in this chapter : **plates with welded-on flat side gussets, non-load carrying transverse and longitudinal attachments, and lap joints with fillet welds.** Parametric formulae have been established for stress gradient factors, F_G, and stress redistribution factor, F_r.

When the proposed calibrated model is applied in the SIF computation of welded joints, the typical through thickness stress distribution in welded joints can be classified into three components. (Fig 6.1) The total stress is separated into three parts: membrane stress, σ_m, the shell bending stress, σ_b, which is linearly distributed, and the nonlinear peak stress, $\sigma_p(x)$, which is due to the local notch.

For a given stress distribution, $\sigma(x)$, for $x=0$ at one surface and $x=t$ at through thickness, an analytical separation can be developed :

$$\sigma_m = \frac{1}{t} \cdot \int_{x=0}^{x=t} \sigma(x) \cdot dx$$

(6.1a)

$$\sigma_b = \frac{6}{t} \cdot \int_{x=0}^{x=t} \sigma(x) \cdot (\frac{t}{2} - x) \cdot dx$$

(6.1b)

$$\sigma_p(x) = \sigma(x) - \sigma_m - \sigma_b(x)$$

(6.1c)
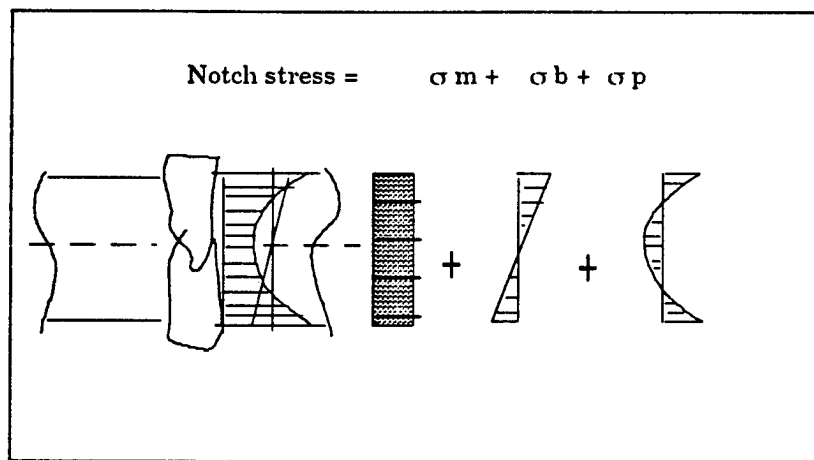
Fig 6.1 Stres components in welded joint

Based on the above stress distribution, the stress intensity factor for welded joints has been computed and compared with available experimental data.

6.2 Plates with welded-on Flat Side Gussets

The first study was performed for the structural detail and crack configuration of a plate with a welded-on flat gusset. The cracks emanate as usually experienced, from the weld toe (Fig 6.2)

55
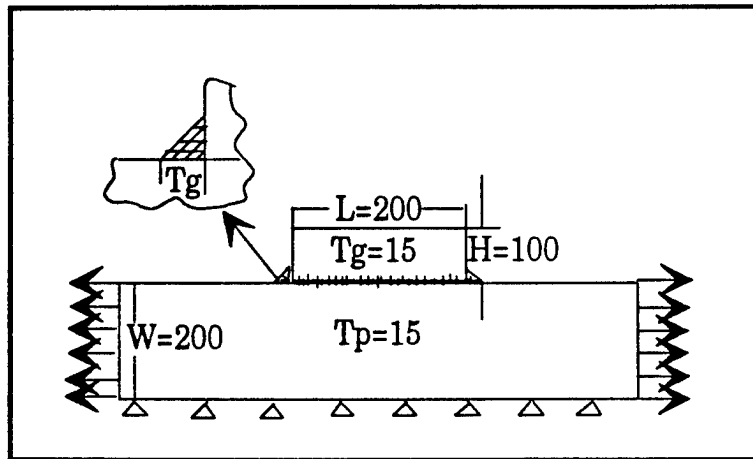
Fig 6.2 Plate under tension with welded-on lateral flat gusset

For the finite element modeling of the specimen, two dimensional plane quadrilateral isoparametric elements were used. The analysis was carried out for plane stress because of the limited thickness range used in welds of this detail.

The welds at the end of the gussets were assumed to have a leg length equal to the gusset thickness and a weld profile angle of 45 degree. (Fig 6.2)

Stress Concentration   Reference Configuration
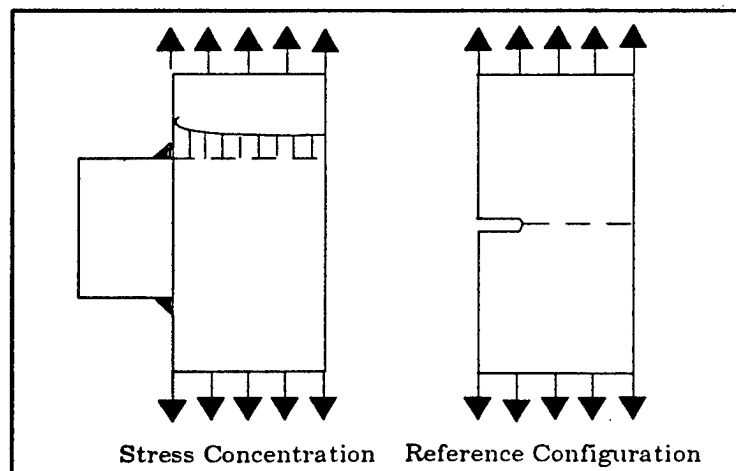
Fig 6.3 Real Structure and Reference Structure

In order to study this detail, the stress distribution at the uncracked specimen was first determined and then, using the reference crack configuration, the new stress intensity factors was calculated based on the stress distribution with load shedding model. The attraction of this method is that for the calculation of numerous stress intensity factors along the crack path, only a single finite element analysis is required.

Stress Gradient Factor

In this detail, the welded-on gusset introduces an additional eccentricity which creates a nonlinear stress by which the stresses in the weld transition are reduced. By reasons of conservatism, the bending action was suppressed by zeroing the displacements of the plate opposite to the gusset in the direction transverse to the load.

The objective of this study was to conduct the numerical simulation of the gusset effects on stress intensity factors. The numerical example is designed as a plate with width of 200mm, a gusset length of 200mm and a gusset height of 100 mm. The length of the gusset was varied from 10 to 800 mm and the height from 15 to 200mm.

Based on Equations in Chapter 4, the F_G is computed and plotted in Fig 6.4 for different gusset height and Fig 6.5 for different gusset length. The effects of the gusset height and length can determined from these figures.

The effect of length of the gusset for the stress gradient factor is displayed in Fig 6.4. At short gussets, the curves tend to a limit. At very long gussets, this is obvious also the case. No significant high value for F_G beyond the curve for 800 mm are expected. The effect of gusset height (Fig 6.5) results in a different situation. The F_G values at 100 and at

200 mm are close together. At higher gussets, no higher F_G values are expected. On the other hand, the effect of the gusset vanishes with the reduction of height of gusset. The effect of wall thickness of gusset is that F_G values diminish at smaller thickness. With the reduction of thickness, the effects of length and height decrease.

Based on the above analysis, the following formulae is proposed as:

$$F_G = C \cdot \left(\frac{a}{T}\right)^k \qquad (6.2)$$

where :

$$\log_{(10)}C = -0.2979 + 0.04406*(L/W) - 0.005056*(L/W)^2$$
$$+ 0.2084*(H/W) - 0.1291*(H/W)^2 \qquad (6.3)$$
$$k = 0.2643 + 0.02848*(H/W) \qquad (6.4)$$
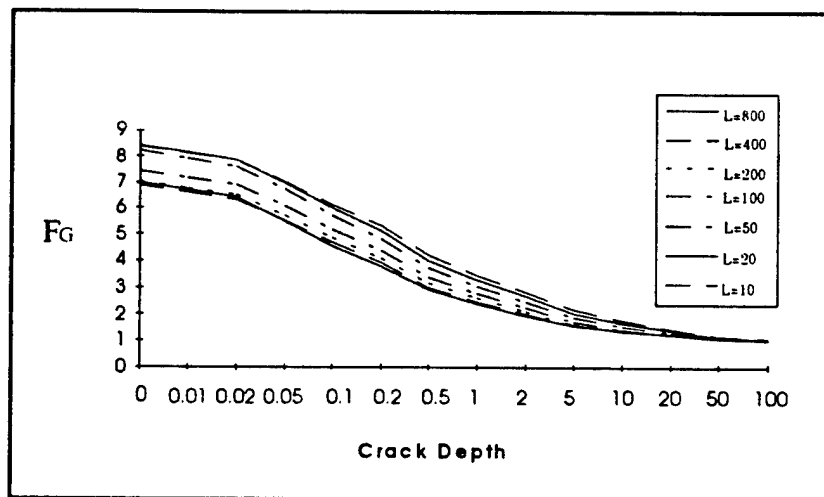
Fig 6.4 Stress Gradient Factor Vs Gusset Length for Plate with Welded on Gusset Plate
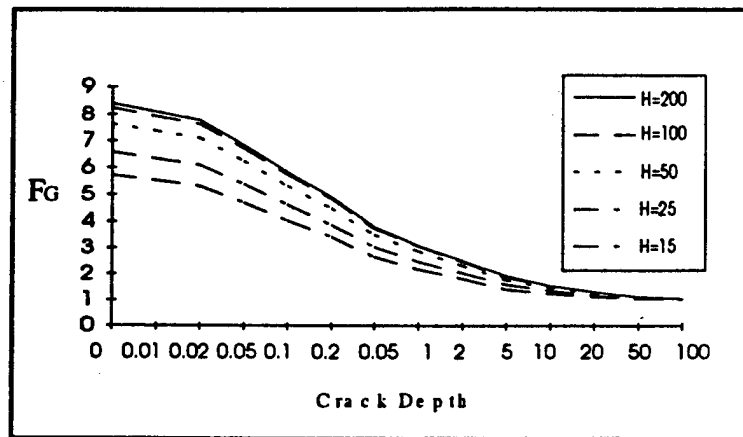
Fig 6.5 Stress Gradient Factor Vs Gusset Height for Plate with Welded on Gusset Plate

This equation does not cover the effects of the thickness ratio of gusset and plate. In the real applications, they aregenerally approximately equal thickness. If there are thinner gussets, this formulation will be conservative.

Stress Redistribution Factor

The stress redistribution model is derived based on the reference configuration (Fig 6.3). Based on the analysis in Chapter 4, the stress redistribution factor is proposed as :

$$Fr=0 \qquad \text{for } a/t < 0.25$$
$$Fr=1-(a/t)^r \qquad \text{for } a/t > 0.25$$
$$r =1, \text{ or } 2 \tag{6.5}$$

6.3 Transverse Non-load carrying Attachment

Fig 6.6 shows the typical transverse non-loadcarrying attachment while Table 6.1 is the variation of dimensions and validity range (transv. att.). The stress gradient factor is computed by the equations in Chapter 4

59

Dimension	Min	Max
H/T	0.2	1
W/T	0.2	1
theta	15	60
A/T	0.175	0.72
t/T	0.125	2(4)

Table 6.1 Variation of Dimensions for Transverse Non-Loading Carrying Attachment
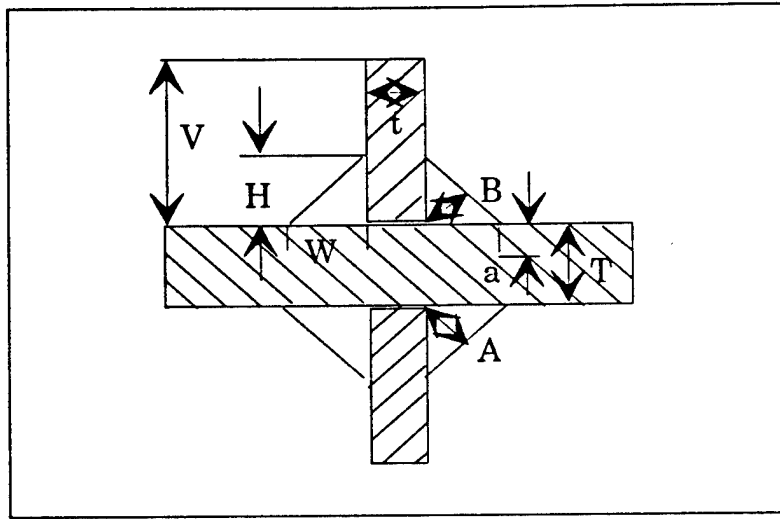
Fig 6.7 Transverse non-load carrying attachment

The stress Gradient Factor was defined as:

$$F_G = C \bullet \left(\frac{a}{T}\right)^k$$

$$C = 0.8068 - 0.1554(H/T) + 0.0429(H/T)^2 + 0.0794(W/T)$$

$$k = -0.1993 - 0.1839(H/T) + 0.0495(H/T)^2 + 0.0815(W/T) \quad (6.6)$$

The stress redistribution factor was defined as:

$$F_r = 0 \qquad \text{for } a/t < 0.25$$

$$F_r = 1 - (a/t)^2 \qquad \text{for } a/t > 0.25 \qquad (6.7)$$

60

6.4 Longitudinal Non-load carrying attachment

Fig 6.8 shows the geometry of the typical longitudinal non-load carrying attachment. Table 6.2 is the variation of dimensions and validity range. The stress gradient factor is computed by equations in Chapter 4 and plotted in Fig 6.9. The empirical stress gradient factor was defined as:

$$F_G = C \cdot \left(\frac{a}{T}\right)^k$$

$$C = 0.9089 - 0.2357(t/T) + 0.0249(L/T) + 0.00038(L/T)^2$$

$$+ 0.0186(B/T) - 1.1414(\theta/T)$$

$$k = -0.02285 + 0.0167(t/T) - 0.3863(4\theta/\pi) + 0.123(4\theta/\pi)^2 \quad (6.8)$$

The stress redistribution factor was calibrated as:

$$Fr = 1 - (a/t)^2 \quad \text{for } a/t < 0.25$$

$$Fr = 1 - a/t \quad \text{for } a/t > 0.25 \quad (6.9)$$
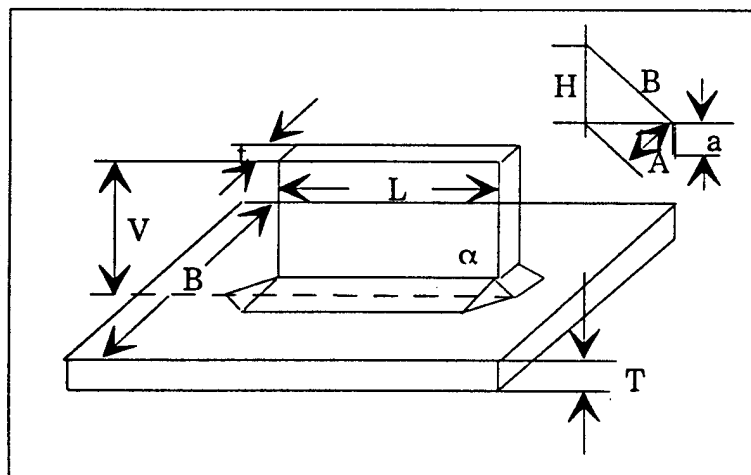
Fig 6.7 Longitudinal non-load carrying attachment

61

Table 6.2 Variation of Dimensions and Validity Range (Long. Att.)

Dimensions	Min	Max
L/T	5	40
B/T	2.5	40
t/T	0.25	2
4θ/π	0.670	1.33
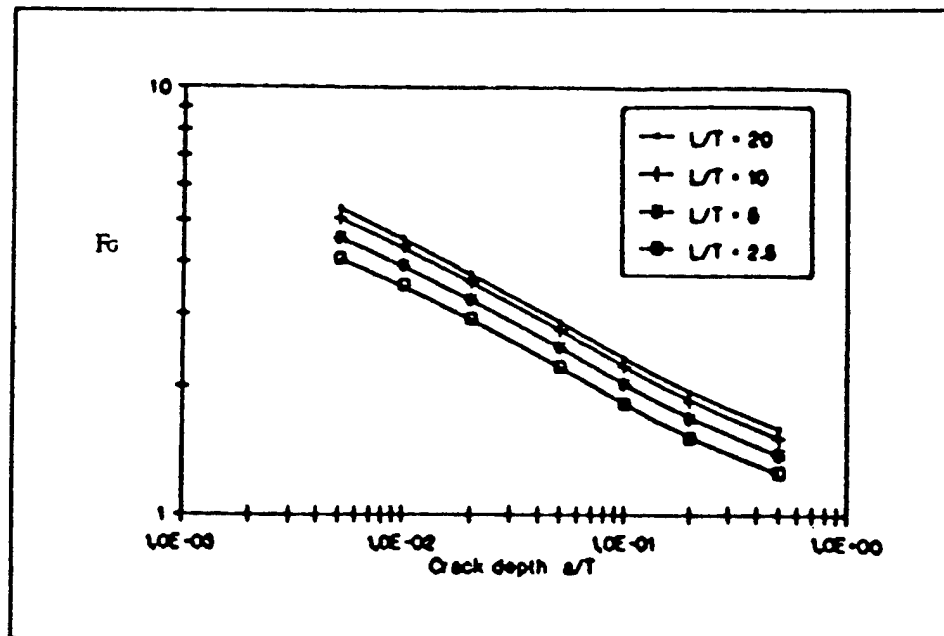
Fig 6.8a Long. attach : Effect of att. Length L/T

In Fig 6.8, it is clear that the variation of the ratio of the wall thickness t/T has a clear effect (Fig 6.8a). The thicker the attachment, the higher the stress gradient factor. The effect of the attachment length also appears from the results. From a length L/T =

2.5 the stress gradient factor rises constant, but at 10-20 an asymptotic effect is encountered.

The variation of the plate with B/T shows a significant effect (Fig 6.8c). The wider the plate, the more local and sharp the stress concentration. The higher stress gradient factor. The extreme will be reached at an infinitely wide plate. Whether or not there is asymptotic effect near a width of B/T = 10 can not be decided from the current analysis. At the other side, at small widths the joint type more and more approaches that of a thick transverse attachment with a low stress concentration and a lower stress gradient factor. This gives an indication that at longitudinal attachments near the plate edge or at flat side gussets, the larger distance to the plate edge might be decisive parameter.
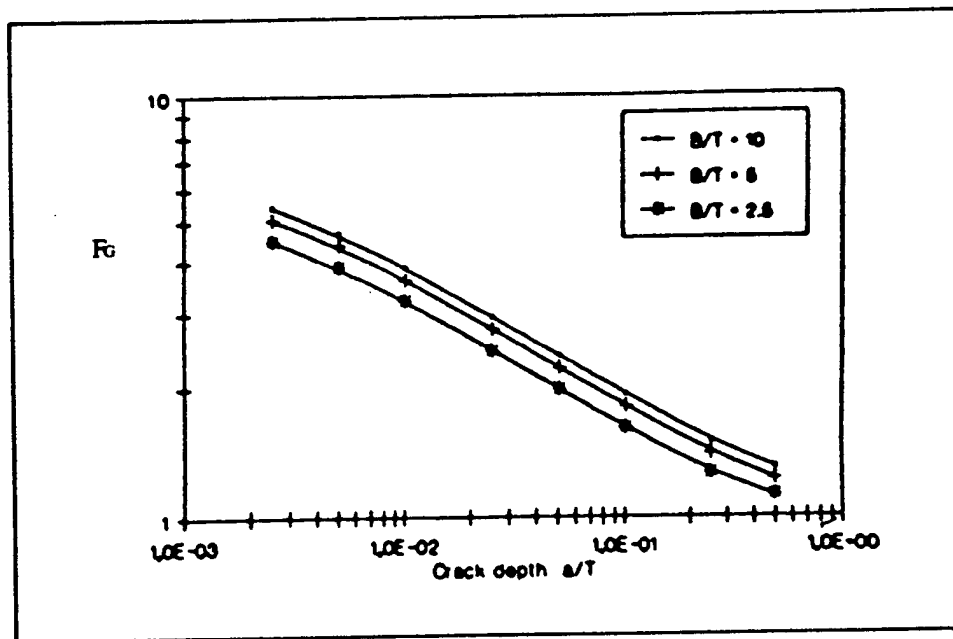
Fig 6.8b Long. att : Effect of Plate Width B/T
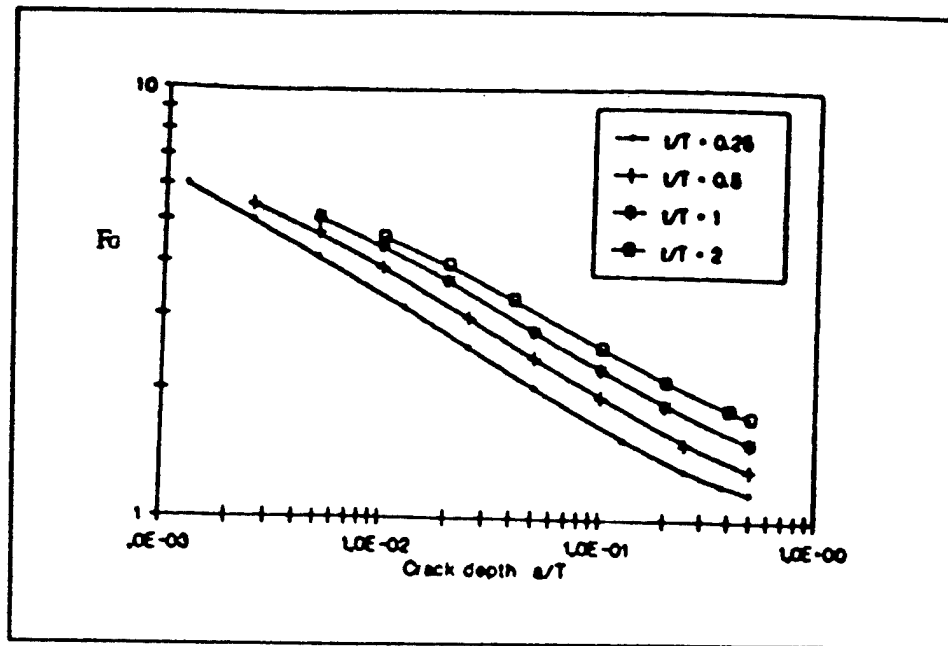
Fig 6.8c Long. attach Effects of Plate Width B/T
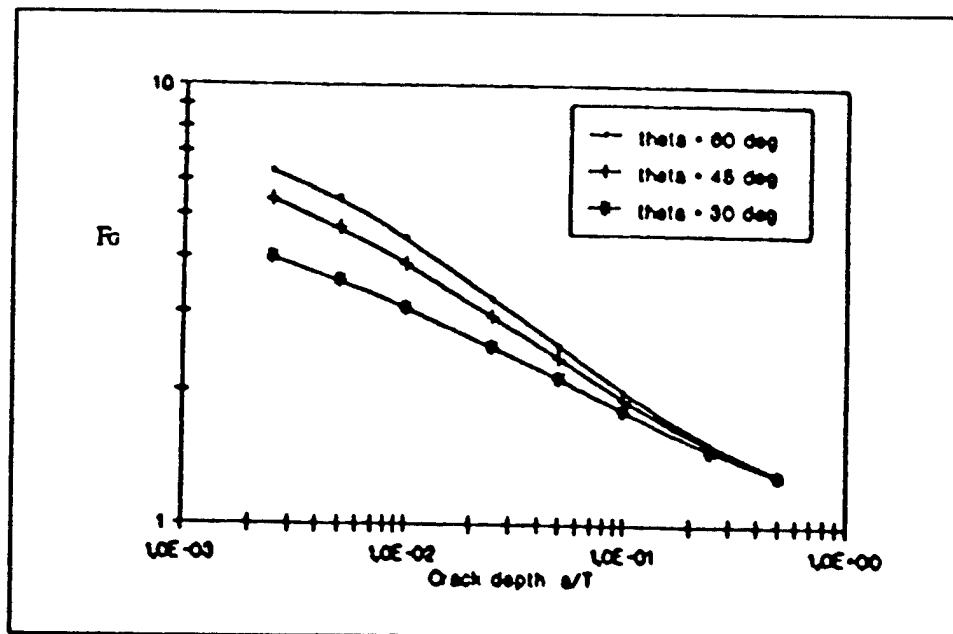
Fig 6.8d Long. attach : Effect of Welded Angle Theta

Fig 6.8 Effect of Dimensional Parameters at Non-Load Carrying Longitudinal
Attachment.

6.5 Lap Joints with Fillet Welds

Fig 6.9 shows a typical lap joint. The variation of the dimensional parameters suggests an effect of the wall thickness ratio t/T. However, wall thickness can not be varied independently from the weld legs H and W. Small thicknesses at the overlapping plate require small weld legs H and put the variation parameters out of balance.

There is a clear effect of the weld throat (Fig 6.10a). In the proposed formula, it is represented in terms of the weld legs H and W. The same applies to the effect of the weld angle. The overlap length at the main plate gives an additional support to the lap plates and restricts the bending displacement by contact. This is typically effective at a small overlap.

Based on the results from Fig 6.10, the stress gradient factor and stress redistribution factor is defined as:

$$F_G = C \bullet \left(\frac{a}{T} \right)^k \tag{6.10}$$

$$C = 1.021 - 0.3772(H/T) + 0.1844(H/T)^2 - 0.0187(W/T)^2$$
$$-0.1856(U/T) + 0.1362(U/T)^2 \tag{6.11}$$

$$k = -0.4535 - 0.1121(H/T) + 0.3409(W/T) - 0.0824(W/T)^2$$
$$+ 0.0877(U/T) - 0.0417(U/T)^2 \tag{6.12}$$

The stress redistribution factor was calibrated as:

$Fr=1-(a/t)^2$ for a/t < 0.25

$Fr=1-a/t$ for a/t > 0.25   (6.13)
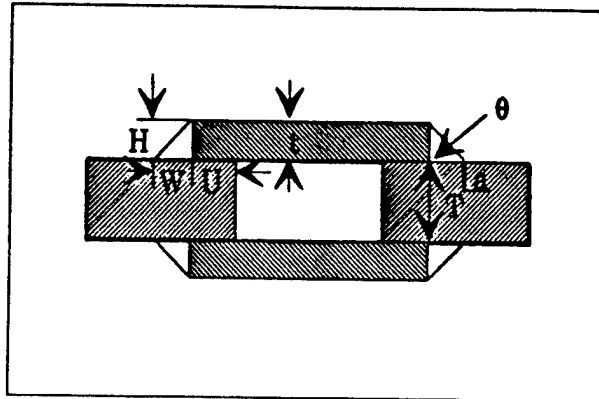
Fig 6.9 Lap Joint
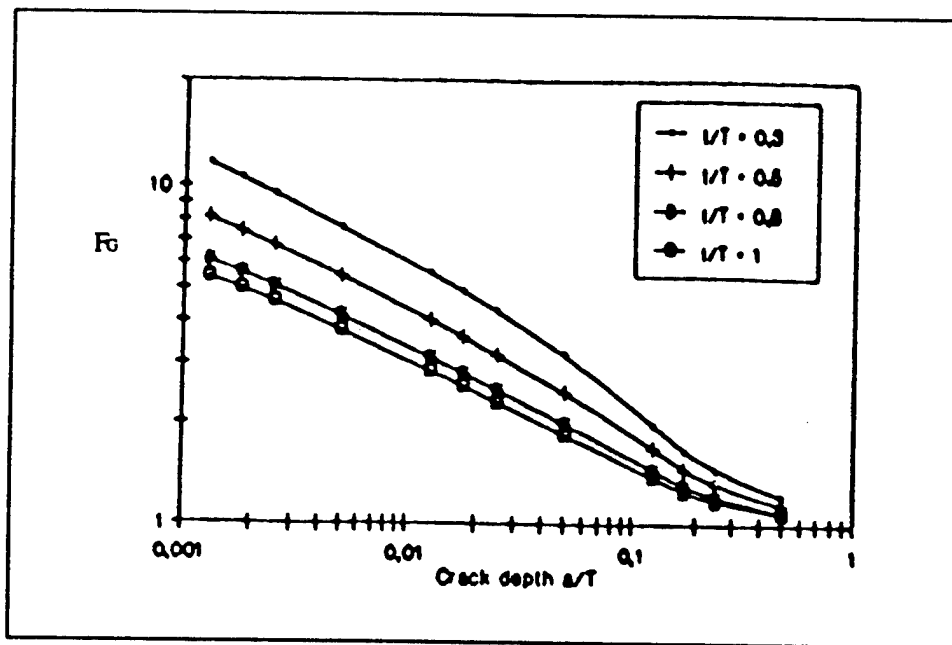
Fig 6.10a Lap Joint : Effect of Wall thickness t/T

66
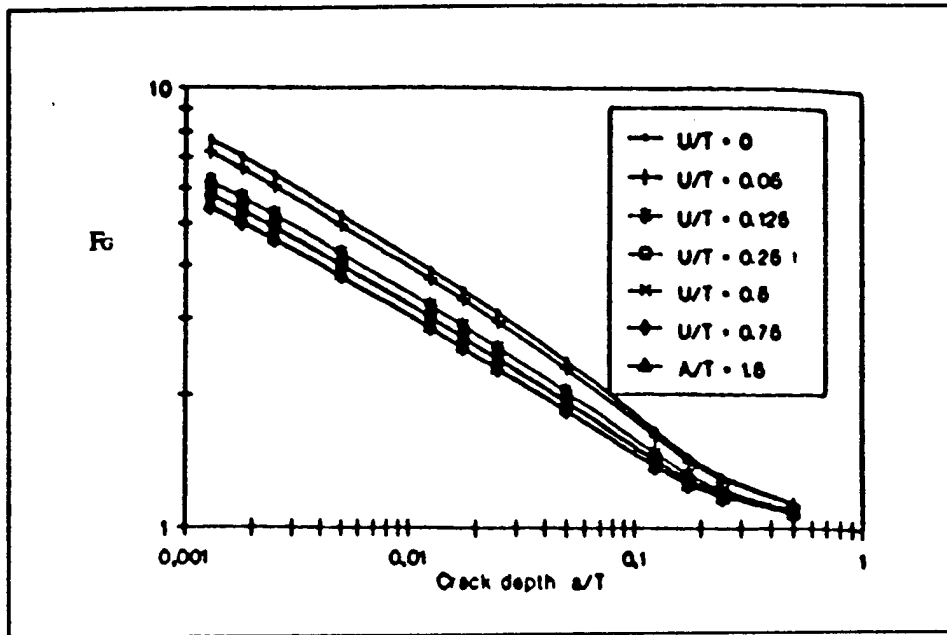
Fig 6.10b Lap Joint : Effect of overlap length U/T
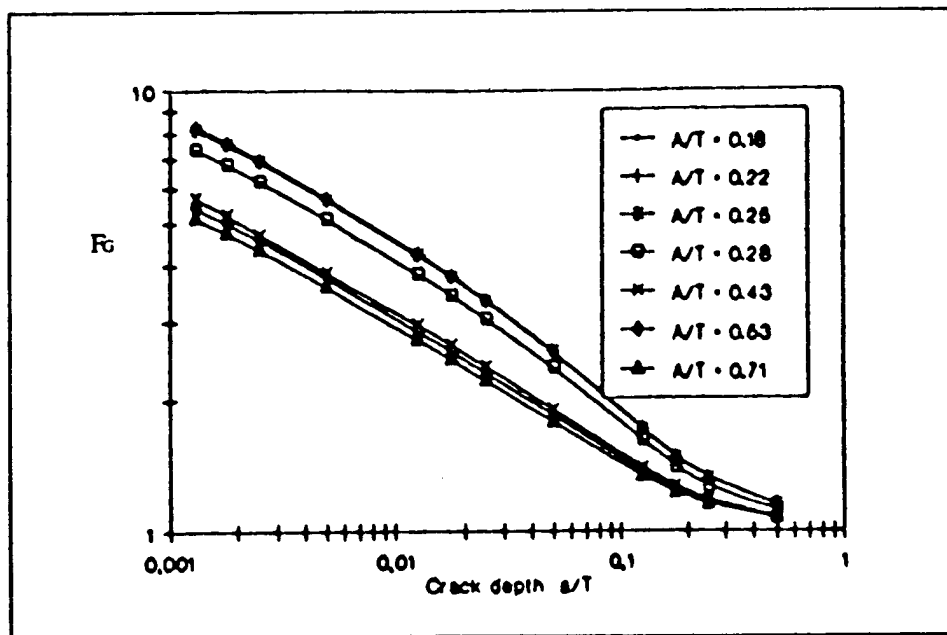
Fig 6.10c Lap Joint : Effect of weld throat A/T
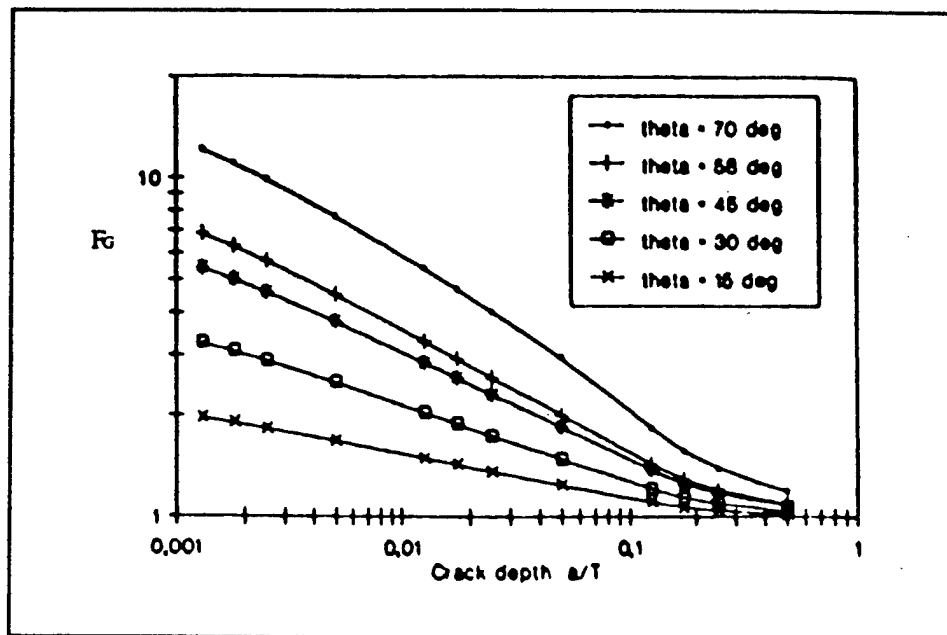
Fig 6.10d Lap Joint : Effect of weld angle theta

Fig 6.10 Effect of dimensional parameters at lap joints

6.6 Summary

This chapter presents empirical formulas for the stress gradient factors and stress redistribution factors associated with ship CSD. It should be pointed out that the formula for stress redistribution factors need be further verified for the lap joint.

These empirical formula will provide a strong tool in fracture mechanics modeling for cracked CSD in tankers.

Chapter 7

Application

7.1 Introduction

In the previous Chapters, a general load shedding formula was calibrated and verified. Some empirical formulas were proposed for different welded joints for CSD in tankers. This Chapter will present the application of these formulas in CSD in a 165,000 DWT tanker.

7.2 165,000 DWT Tanker

The proposed tanker was studied in SMP I [5] and Fitness for Purpose Analysis [7]. The characteristics for this tanker are summarized in Table 7.1. The general arrangement is shown in Fig 7.1, and Fig 7.2 is the midsection.

7.3 Critical Structural Details (CSD)

The proposed CSD was one of the CSDs in SMP I project. It is the sideshell longitudinal 33 on tank 4. The geometry configuration and dimension are shown in Fig 7.3.
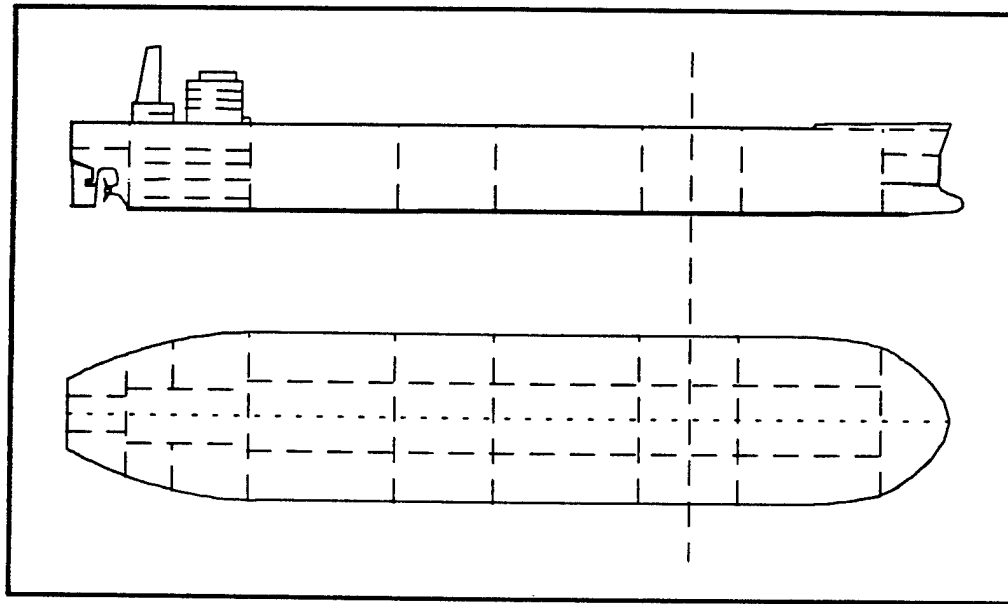
Fig 7.1 General arrangement for a 165,000 DWT tanker.

DWT	165,000
LOA	274.2m
LBP	262.1m
Breadth	52.7m
Depth	22.9m
Draft	17.4m
Construction	Single Hull

Table 7.1 Overall Dimensions for the 165,000 DWT Tanker

7.4 Previous Studies

A detailed fatigue analysis based on S-N curves was conducted during SMP I for this CSD [5]. During this project, the fitness for purpose analysis for this cracked CSD was performed based on the equivalent S-N approach [7]. Following summarized some results from fitness for purpose analysis.

70
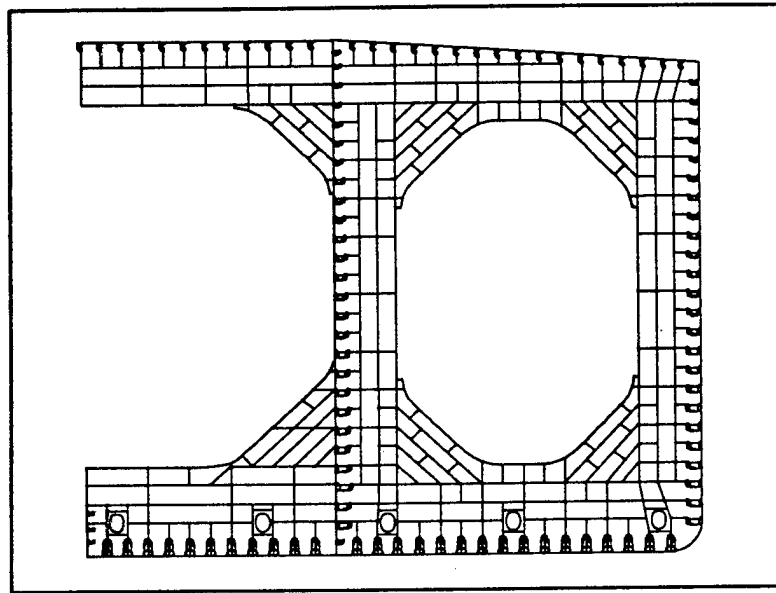
Fig 7.2 Midsection for a 165,000 DWT tanker

The proposed fitness for purpose analysis was conducted based on the following steps.

1 - Definition of structural detail and crack location.

2 - Computation of the transfer function for the ship. The transfer functions are computed for the two load cases. Full load and Ballast and for several wave headings and speeds based on the proposed travel routines and sea environment.

3 - Determination of the stress vectors at the Hotspots from finite element analysis. Estimation of the long-term distribution of the stress range σ at a hotspot. This estimation is based on a specified travel routine for given Madsen zones and specified maneuvering philosophy.

4 - Determination of the initial crack size for given hotshot

5 - Determination of the critical crack size for given hot-spot based on material toughness or durability requirement.

6 - Determination of the stress intensity factors for given hot-spots at the specified CSD

7 - Construction of the equivalent S-N curves for the hot-spot in given CSD.

8 - Determination of the remaining fatigue life based on the long-term extreme stress range and constructed equivalent S-N curves.

Frame Spacing	5120 mm
Longitudinal Spacing	890 mm

Fig 7.3 Configuration for Detail in Sideshell 32- 36.

The development of equivalent S-N curves is one of the key step in this procedure. Based on the procedure in Reference 7, the equivalent S-N curve for two hot spot had been constructed (Fig 7.4). Fig 7.5 shows the results for hot spot B.
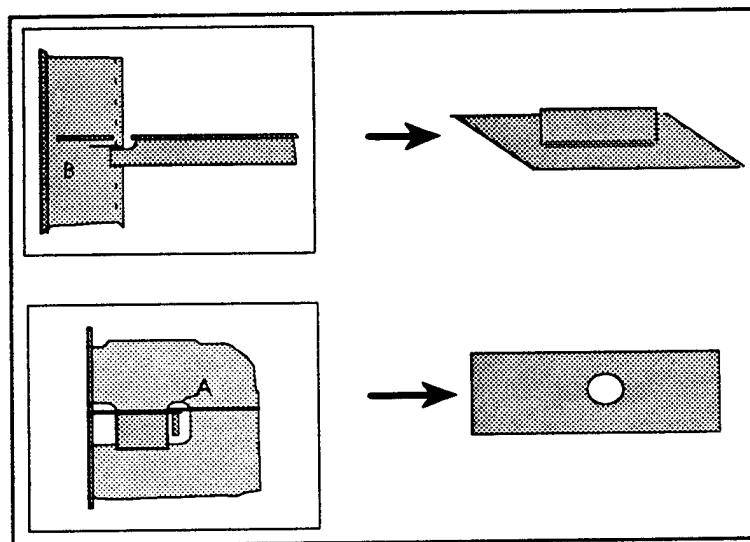
Fig 7.5 CSD Hot spots and Corresponding Specimens
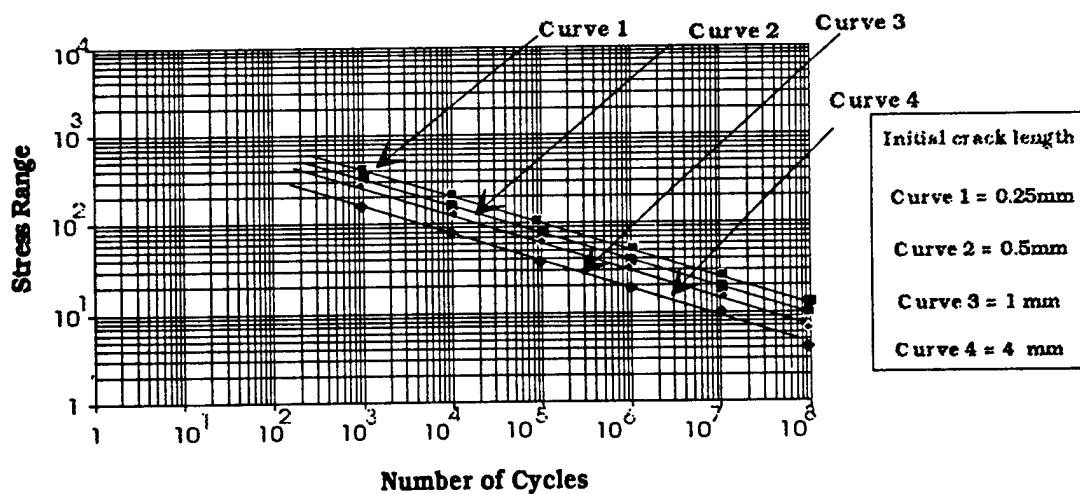
Fig 7.5 Equivalent S-N curves for Hotspot B

73

The probability of failure for the remaining 10 year service is displayed in Fig 7.6.
The uncertainty is this analysis is shown in Table 7.2.

Fabrication and Assembly	1.2	0.2
SeaState Characterization	1.1	0.3
Wave Loads	0.8	0.2
Determination of Loads	0.9	0.3
SCF	1.0	0.3
	Median Bias	Cov Bias
Total	0.95	0.63

Table 7.2 Uncertainty Modeling in Fitness for Purpose Analysis
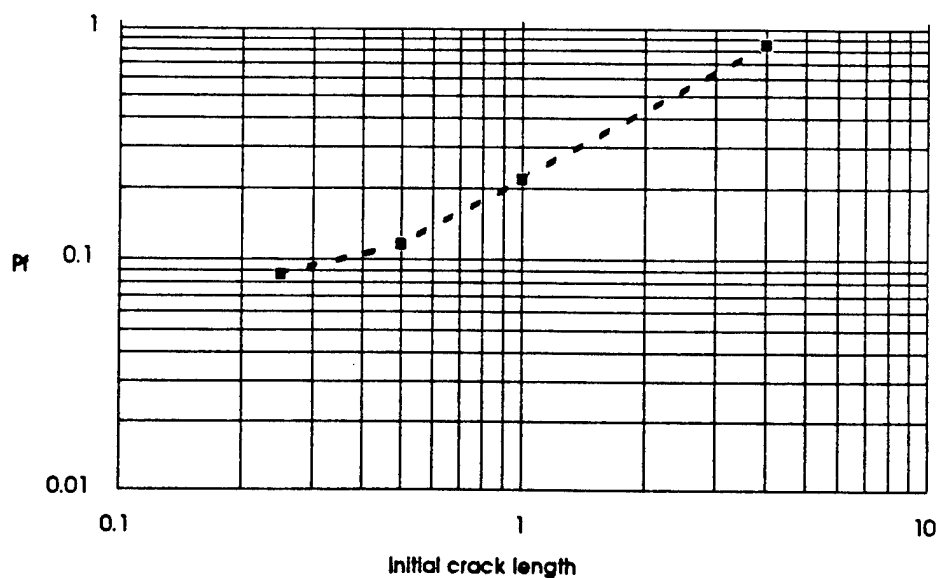
Fig 7.6 Probability of Failure during the Remaining 10 Years Serive Life

in Fitness for Purpose Analysis. (Load Shedding is not included)

74

The results here did not take load shedding effects in to account.

7.4 Load Shedding Effects

When the load shedding effects is taken into account, the equivalent S-N curves has to be re-constructed. The following is the mathematical formulation.

Based on the Paris equation, the crack growth da/dN can be calculated as:

$$\frac{da}{dN} = C(\Delta K)^m$$

(7.1)

Here C and m are material constants, and ΔK is the range of stress intensity factor.

It is known that the part-through crack was considered in hot spot B [7]. Based on the general formula for stress intensity factors with X-B model, ΔK can be expressed as :

$$K = \left[F_{G,at} \sigma_t + (F_{G,ab} / F_{G,nb}) \bullet HF_r \right] \sqrt{\frac{\pi a}{Q}} F(a/t, a/c, c/b, \varphi)$$

(7.2)

The ratio of the Newman-Raju SIF to the X-B SIF can be derived approximately as :

$$\frac{K_{X-B}}{K_{N-B}} = \frac{F_{X-B}}{F_{N-R}} = [1 - (1 - F_r) \bullet DoB] \bullet F_G$$

(7.3)

where :

Fr :   Stress redistribution factor

FG :   Stress gradient factor

DoB   Degree of Bending which is the ratio of the bending stress to hot spot   stress.

From equations (7.1), (7.2) and (7.3), the equivalent S-N curves with load shedding effects is derived for constant stress range as :

$$N_{res} = \int_{a_i}^{a_f} \frac{da}{da/dN} = \frac{1}{C \bullet (\Delta\sigma)^m} \int_{a_i}^{a_f} \frac{da}{(\frac{\Delta K}{\Delta\sigma})^m}$$

(7.4)

or :

$$N_{res} = \int_{a_i}^{a_f} \frac{da}{da/dN} = \frac{I}{C \bullet (\Delta\sigma)^m}$$

(7.5)

where :

$$I = \int_{a_i}^{a_f} \frac{da}{(\frac{\Delta K}{\Delta\sigma})^m} = \frac{1}{\pi^{m/2}} \bullet \int_{a_0}^{a_f} \frac{da}{a^{m/2} \bullet F^m}$$

(7.6)

Thus, Based on equation (7.3), the modified S-N curves with X-B load shedding model can be derived as :

$$N_{res} = \int_{a_i}^{a_f} \frac{da}{da/dN} = \frac{I_{X-B}}{C \bullet (\Delta\sigma)^m}$$

(7.7)

where :

$$I_{X-B} = \frac{1}{\pi^{m/2}} \bullet \int_{a_i}^{a_f} \frac{da}{a^{m/2} \bullet \left[F_{N-R} \bullet (1-(1-F_r) \bullet DoB)F_G\right]^m}$$

(7.8)

while the original equivalent S-N curves development is expressed as :

$$N_{res} = \int_{a_i}^{a_f} \frac{da}{da/dN} = \frac{I_{N-R}}{C \bullet (\Delta\sigma)^m}$$

(7.9)

$$I_{N-R} = \frac{1}{\pi^{m/2}} \bullet \int_{a_i}^{a_f} \frac{da}{a^{m/2} \bullet \left[F_{N-R}\right]^m}$$

(7.10)

The load shedding effects can be expressed as :

$$\frac{N_{N-R}(\Delta\sigma)^m}{N_{X-B}(\Delta\sigma)^m} = \frac{I_{N-R}}{I_{X-B}} = \frac{N_{N-R}}{N_{X-B}} \qquad (7.11)$$

The equations 7.7, 7.8 is hard to derive an close form solution. The numerical analysis is being implemented in the computer program FRACTURE. Here, a simplified study about the load shedding effects on equivalent S-N curve development is performed.

7.5 Effects of Fr

Suppose we only consider Fr effects, and F_{N-R}, F_G are separated variables during the crack propagation, the mean effects of Fr can be defined as $\overline{F}_r^{S-N}$ and approximated as

$$\frac{N_{X-B}}{N_{N-B}} = \frac{I_{X-B}}{I_{N-R}} \approx \overline{F}_r^{S-N} = \frac{1}{a_f - a_i} \cdot \int_{a_i}^{a_f} \frac{da}{[1 - (1-F_r)\cdot DoB]^m} \qquad (7.12)$$

The mean effects is supposed to be the effect of the stress distribution on fatigue life. Thus, for linear moment release model and m=3, The $\overline{F}_r^{S-N}$ is derived as :

$$\overline{F}_r^{S-N} = (1.3 - DoB) \cdot \left[\frac{2 - DoB}{2(1 - DoB)} \right]$$

This effects is displayed in Fig 7.7.

In Fig 7.7, the x-axis is the DoB which is the ratio of the bending stress to hot spot stress. the y-axis is the ratio of the fatigue life with load shedding to that without the load shedding. That is N_{X-B}/N_{N-R}. It is clear that Fr has strong effects on fatigue life when the

DoB is larger. For the CSD in the proposed 165,000 DWT tanker, DoB is approximated as 0.6 in previous analysis [5], thus, fatigue residual life is increased about 60 %.
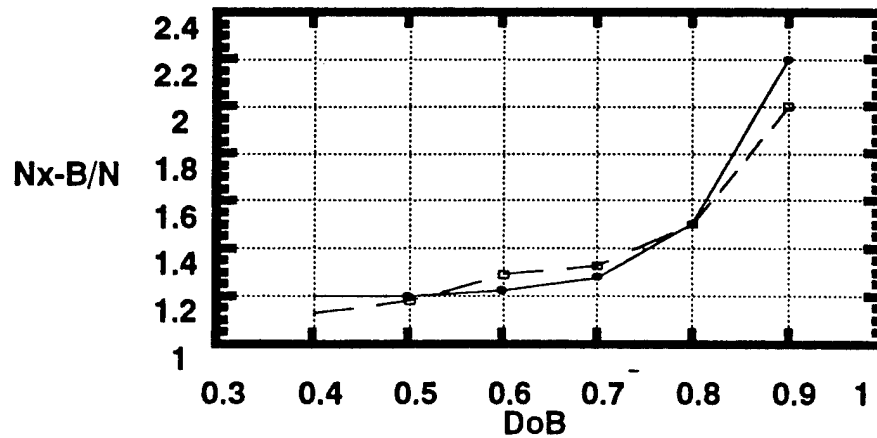
Fig 7.7 Effects of Fr on Fatigue Life

Thus, the probability of failure during the next 10 years can be approximated in Fig 7.9 with this simple stress redistribution effects. The probability of failure is significantly reduced as the result of load shedding, and the results seem to be more rational.
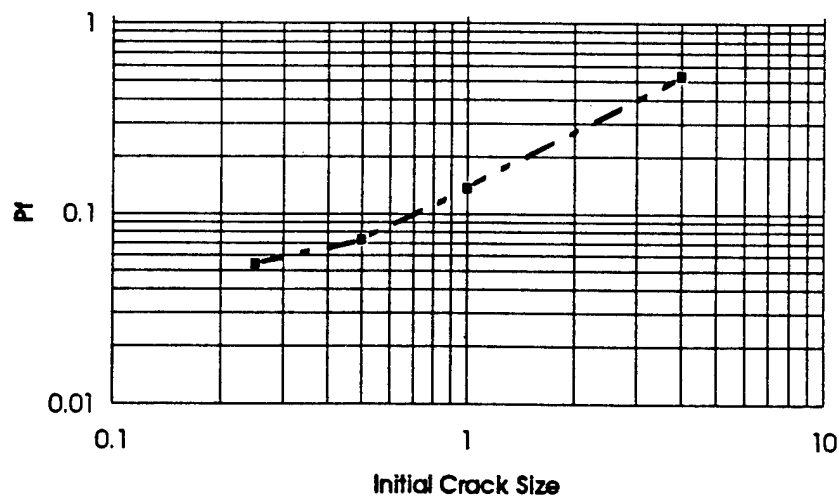
Fig 7.8 Probability of failure during 10 years Remaining Service for initial Crack size ai=0.25mm,0.5mm,1mm,4mm. (With Stress Redistribution at DoB=0.6)

78

7.6 Effects of F_G

Suppose we only consider effects of F_G, and F_{N-R}, F_r are separated variables during crack propagation. The mean effects of F_G during the crack propagation can be defined $\overline{F}_G^{S-N}$ and approximated as :

$$\frac{I_{N-R}}{I_{X-B}} = \frac{N_{N-R}}{N_{X-B}} = \overline{F}_G^{S-N} \tag{7.14}$$

This mean effects is supposed to the effects of the stress gradient factor on fatigue life. Thus, we can derived as :

$$\overline{F}_G^{S-N} = \frac{1}{a_f - a_i} \bullet \int_{a_i}^{a_f} \frac{da}{F_G^m} \tag{7.15}$$

where :

$$F_G = p \bullet \left(\frac{a}{t}\right)^q \tag{7.16}$$

p, q : empirical parameters

$m=3$

Thus, we have :

$$\overline{F}_G^{S-N} = \frac{1}{p^m} \bullet \frac{1}{(1-q)} \tag{7.17}$$

Since the development of equivalent S-N curves for cracked CSD in the proposed 165,000 DWT tanker is based on the Hybrid method where F_G has already been taken into account, the equation (7.17) need not be applied to the cracked CSD in the proposed tanker.

7.7 Summary

A general load shedding formula is applied to the study of the fatigue life of a cracked CSD in a 165,000 DWT tanker. This model is applied to the general development of equivalent S-N curves for cracked CSD in tankers. The effects of stress redistribution factor and stress gradient factor on fatigue life has been studied. A simplified method for these effects is proposed together with the complex method. The load shedding effects on the fatigue life of proposed CSD has been conducted in the simplified approach. The results has shown that load shedding may increase fatigue life more than 60%.

Chapter 8

Conclusions and Future Studies

8.1 Conclusion

It can be concluded from this study that **load shedding is the stress redistribution for statically indeterminate cracked structure due to redundant boundary conditions or adjacent elements when a crack grows under an arbitrary stress field.**

There are two additional factors which should be included in Newman-Raju equation for surface cracks. They are :

1) stress redistribution due to redundant boundary conditions, and

2) stress gradient factor due to the local stress concentration.

The general formula for these two factors were developed, calibrated and verified as:

$$F_G = C \bullet \left(\frac{a}{T}\right)^k$$

$$(8.1)$$

$$F_r = 1 - \left(\frac{a}{T}\right)^r$$

where :

F_G	stress gradient factor,
C,k	empirical parameters,
a	crack depth,
T	thickness,
F_r	stress redistribution factor,
r	parameter based on linear or parabolic moment release model.

One additional factor, a stress redistribution factor should be included in Hybrid method for through cracks. The general formulae developed and calibrated was :

$$F_r = 1 - ka$$

where:

F_r	stress redistribution factor,
k	empirical parameter, and
a	crack depth

Several empirical formulas for stress redistribution factors and stress gradient factors were proposed for different welded details for application to analysis of ship CSD. It need be further calibrated based on more experimental data.

8.2 Future Studies

It should be pointed out that the topic in this report is only about a single crack in a detail under redundant conditions. If one considers interactions with adjacent structures

or cracks, several other factors influence load shedding. For example, multiple crack effects, stiffener effects (broken or unbroken). These need be further studied. Background on some of these aspects is provided in appendix.

The following future studies are suggested based on results from this project.

Extension and verification of the load shedding formulae for through thickness cracks. A fatigue crack propagation test for ship CSD is recommended for this study. Based on analytical study, numerical study and experimental study, the load shedding formulae for through thick crack can be verified.

Appendix A

References

1. Newman, J.C. and Raju, I.C, "An empirical stress intensity factor equation for the surface crack", Engineering Fracture Mechanics, vol. 15, 1981, pp. 185-192

2. J.Forbes, G.Glinka, and D.J.Burns, "Fracture Mechanics Analysis of Fatigue Cracks and Load Shedding in Tubular Welded Joints", Proceedings of 11th International Conference on Offshore Mechanics and Arctic Engineering, Vol. 2, 1992, pp307-313

3. A. Aaghaakouchak, G.Glinka, and S.Dharmavasan, "A Load Shedding Model for Fracture Mechanics Analysis of Fatigue Cracks in Tubular Joints", Proceedings of 8th International Conference on Offshore Mechanics and Arctic Engineering, Vol. 2, 1989, pp159-165

4. J.V.Haswell, "A General Fracture Mechanics Model for a Cracked Tubular Joint Derived from the Results of a Finite Element Parametric Study", Proceedings of 11th International Conference on Offshore Mechanics and Arctic Engineering, Vol. 2, 1992, pp267-274

5 Tao Xu and Robert, G Bea, "Fitness for Purpose Analysis Procedure for Cracked Critical Structural Details (CSD) in Tankers", Report SMP III 2-1 Ship Structural Maintenance Project, 1994. Dept. of Naval Architecture & Offshore Engineering, University of California at Berkeley, Berkeley, CA 94720

6. Tao Xu and Robert,G Bea, **"FRACTURE - A Computer Code for Crack Growth Analysis of Cracked Critical Structural Details (CSD) in Tankers"**, Report SMP III 2-3 Ship Structural Maintenance Project, 1994. Dept. of Naval Architecture & Offshore Engineering, University of California at Berkeley, Berkeley, CA 94720

7. S.A.Meguid, **"Engineering Fracture Mechanics"**, Elsevier Applied Science, 1989

8. D.J.Cartwright and D.P. Rooke, **"Approximate Stress Intensity Factors Compounded from Known Solutions"**, Engineering Fracture Mechanics, Vol. 6 563-571, 1974

9. H.Neuber, **"Theory of Notch Stresses"**, Springer, Berlin (1958). Translation series AEC-tr-4547, U.S. Atomic Energy Commission.

10. Niu X and Glinka G, **"Stress Intensity Factors for Semi-Elliptical Surface Cracks in Welded Joints"**, International Journal of Fracture, 1988

Appendix B

The following notes are about the multiple crack effects and stiffener effects which are the load shedding contribution in tanker panel structure. The methodology which is primarily developed here is different from the previous approaches for local structural details. The further development about the relation between these methodology is recommended.

Appendix B

B-1 - Multiple Cracks

There are a number of situations where multiple cracks occur. For example, cracks arise at the cutouts. Only a few solutions are available for stress intensity factors for multiply-cracked finite bodies. Accurate mathematical analyses are complex and time-consuming to apply to such cases. However, if high accuracy is not required for a given application, a simple approach based on the concept of "**Load Relief**" may be adequate.

It is known that under certain loading conditions the stress concentration effect of multiple **parallel** notches is less than that of a single notch [Neuber 1974]. In fact, a design procedure in which additional notches are provided primarily to effect a redistribution of the stresses is called "load-relieving notches". Neuber investigated this effect and suggested a concept that he referred to as the coefficient of "load relief" for notches. A similar concept to be called the "load relief factor" may be appropriate to opening mode stress intensity factors for multiple cracks in stress bodies. This "**Load Relief**" factor can be included in the load shedding formulae.

The load relief factor F can generally be defined as the stress intensity factor of multiple-cracked, infinite body $(K_I)_{m,\infty}$ divided by the stress intensity factor of a single cracked body $(K_I)_{s,\infty}$ of the same geometry and loading conditions. Hence for the Mode I stress intensity factors the load relief factor is given by :

$$F = (K_I)_{m,\infty} / (K_I)_{s,\infty} \qquad \text{(B-1)}$$

where F is known for an infinite (or semi-infinite) body it is then assumed that the same value of F applies to a finite cracked body with similar geometry and loading conditions, i.e :

$$(K_I)_{m,f} = F_x (K_I)_{s,f} \qquad \text{(B-2)}$$

where $(K_I)_{s,f}$ is the stress intensity factor for a single-cracked finite body of the same loading conditions as that included in the determination of F and $(K_I)_{m,f}$ is the required solution for the same finite body with multiple cracks. (Fig B-1)
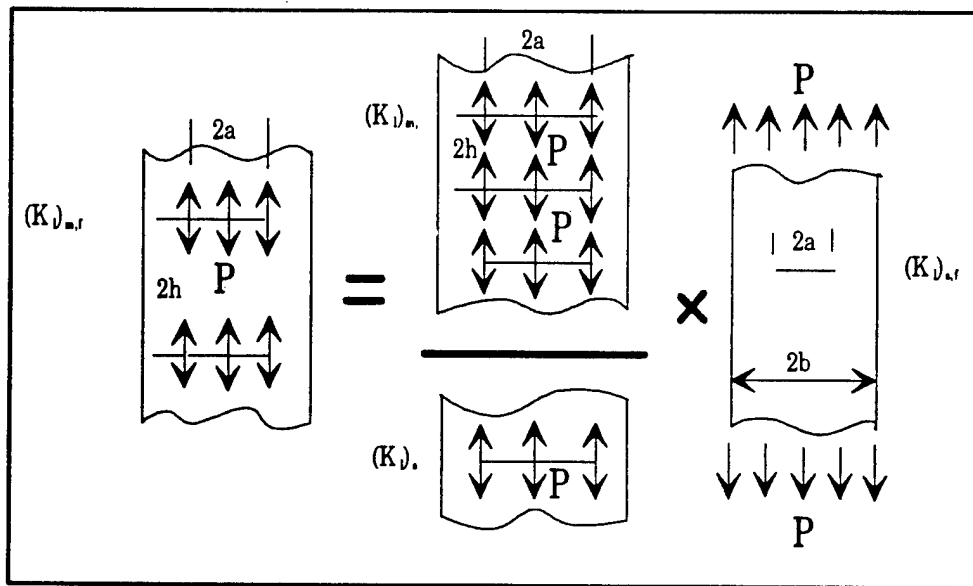
Fig B-1 Schematic showing method of obtaining stress intensity factor for an infinite array of internally-pressurized central parallel cracks in an infinitely long strip of finite width

The substitution of eqn [B-1] into eqn [B-2] gives

$$(K_1)_{m,f} = \frac{(K_1)_{m,\infty}}{(K_1)_{s,\infty}}(K_1)_{s,f}$$
(B-3)

This factor can be included in Newman-Raju equation or Hybrid method by simply multiplying F.

Although the formulae is easy, the computation of $(K_1)_{m,f}$ is difficult due to the difficulty in the calculation of $(K_1)_{m,\infty}$.

B-2 - Stiffener Effects

Stiffener are frequently attached to plates used in tanker stucture to improve the strength and the stability and to provide a means of slowing down or arresting the growth of cracks in plate. The opening mode stress intensity factor is less in the vicinity of an intact stiffener because the load is concentrated in the stiffener and hence the stress is lower in the plate. However, if the stiffener breaks under the load, the stress inensity factor increase dramatically.

Stress intensity factor for simple CSD / joints was presented in previous reports. But they are not directly applicable to the stiffener panels of typical tanker structures. The compounding method described here is a versatile and quick way of extending these solutions for the CSD / joints to other, more complex configurations for which the stress intensity factors are not known.

If a cracked structural has several boundaries, (e.g. holes) other cracks or edges; the computation for stress intensity factors is more complex since all these will influence the stress intensity factor at the tip of the crack under the study. The main principle of the comatponding model is to obtain the solution by separating the complex configuration into a number of simpler ancilary configurations which have known solutions. Each ancillary configuration will usually, contain only one boundary which interacts with the crack. The contributions from each ancillary configuration are compounded according to the following formula:

$$K_r = \overline{K} + \sum_{\substack{all \\ n}} (K_n - \overline{K}) + K_e \qquad \text{(B-4)}$$

where Kr is the resultant stress intensity factor with all the boundaries present, Kn is the stress intensity factor with only the nth boundary present, $\overline{K}$ is the stress intensity factor in the absence of all boundaries and Ke is the contribution which may be present due to boundary-boundaru interaction. It is convient to express the compounding formula in terms of normalized stress intensity factors $Q(=K/\overline{K})$ since many of the known ancillary solutions are given in this form. Then

$$Q_r = 1 + \sum_{\substack{all \\ n}} (Q_n - 1) + Q_e \qquad \text{(B-5)}$$

The difficulty in the compounding technique is the evaluation of Qe which is the term of the boundary-boundary interaction effects. This effect is different from the boundary effects for load shedding. Such effects are not included in the modified Newman-Raju equation or Hybrid-method. Thus, previous method is a special case of the compounding when boundary -boundary interaction effects are negligible.

The evaluation of Qe can be in terms of the residual stress fields at the boundaries by using Schwarz alternating technique. [Schwarz 1974]. The residaul stresses were originially ignored in the derivation of fracture mechanics equations which is based on the principle of superposition. For many problems Qe is small and can be ignored. For problems which is important, approximate method have been developed for evaluating it.

The magintude of the boundary-boundary interactions can be estimated by calculating the stress intensity factors from known equation from which the alternative solutions are available [Cartwright 1982]. The magnitude of Qe was found to be depend on the number and type of boundaries; it increased as the number of boundaries increases and as the crack approached a boundary. Straight boundaries had more effect than curved boundaries such as holes, and other cracks had a smaller effect than holes.

The simple compounding procedure of adding together the effects of the individual boundaries needs to be modified if the crack crosses one of the boundaries or a crack beneath a stiffener. Before the effect of other boundaries can be considered, the crack plus the boundary it crosses must be replaced by an equivalent crack which then interacts with the other boundaries. If the stress intensity factor Ko when only the boundary the crack crosses is present, then the equivalent crack length a' is given by

$$a' = \left(\frac{K_0}{\overline{K}}\right)^2 a = Q_0^2 a \qquad (B-6)$$

The effects of the other boundaries on the original crack plus boundary is now considered to be the same as the effects on the equivalent crack. In order to calculate the effects, the distances of the other boundaries from the equivalent crack must be determined. These distances are determined subjected to the condition that each boundary must be the same distance from the nearer tip of the equivalent crack in each ancillary configuration as it was in the original configuration. The compounding formula is then modified to :

$$K_r = K_0 + \sum_{n \neq 0}(K_n' - K_0) + K_e \qquad (B-7)$$

where Kn' is the stress intensity factor for the equivalent crack in the presence of the nth boundary condition only. The above equation can be written in terms of the normalized stress intensity factors and becomes :

$$Q_r = Q_0[1 + \sum_{n \neq 0}(Q_n' - 1) + Q_e] \qquad (B-8)$$

where $Q_n' = K_n' / K_0$. With these modifed formulae the stress intensity factor can be calcualted for stiffener panels. Based on the previous studies, the boundary-boundary interaction is small.

In some case, bounary-boundary interactions can not be neglected, for instance a crack at the edge of a hole which is near another boundary. A measure of the interaction may be obtained from the difference in the stress concentration factor Kt at the edge of the hole in the uncracked configuartion with and without other boundaries. If the change in Kt is significant then the boundary-boundary inetraction Qe in the cracked configuration will also be significant.

In the following the principles of compounding are applied to determine the stress intensity factor for a periodically stiffened, loaded panel with a series of collinear, equal-length cracks centred on each of the stiffeners. This is typically shown in Fig B-2.

The problem considered contains an infinite series of cracks, of length 2a centred on and perpendicular to stiffeners that are a distance b apart. The panel is subjected to a uniform stress σ remote from the crack; the stresses in the stiffeners, in order to maintain strain compatibility, is (Es/E)σ where E and Es are the Young's modulus of the panle and stiffener respectively. The ancillary configurations required, in general, are :

(1) a crack centred about a stiffener which may be broken or unbroken, .

(2) a crack near to an unbroken stiffener, and

(3) three collinear cracks in a uniformly stressed panel.

If tip A of the crack at stiffener So in Fig 1 is the tip under consideration and stiffeners to the right of A are labelled with positive integers and stiffeners to the left with negative integers, then eqn [B-3] has been shown to become

$$K_r = K_0 + \sum_{n \neq 0} (K'_{s,n} - K_0) + \sum_{n > 0} (K'_{c,\pm n} - K_0) \qquad \text{(B-9)}$$

The stress intensity factors K_0, $K_{s,n}'$ and $K'_{c,\pm n}$ are defined as follows:

K_0 is for a crack of length 2a in ancillary configuration (1);

$K_{s,n}'$ is for a crack of length $2a_0'(=2Q_0^2a)$ whose centre is a distance $bv_{0,n}'$ from the nth stiffener as in ancillary configuration (2);

and $K_{c,\pm n}'$ is a crack of length $2a_0'$ located symmetrically between two cracks of length $2a_n'(=2Q_n^2a)$ as in ancillary configuration (3).

The equivalent cracks of length 2an' are obtained by replacing each crack/stiffener pair by a crack with the same stress intensity factor; the length an' is given in terms of an by eqn [1] with Qn replacing Q₀ and the distance between crack centres do,n is given by :

$$d_{0,n} - a_0' - a_n' = b - 2a \qquad \text{(B-10)}$$

Qn is the normalized stress intensity factor for a crack of length 2an centred on stiffener Sn in a panel with no other stiffeners or cracks present. In this periodic configuration an=a for all n. If all the stiffeners are unbroken then Qn=Q₀ for all n, but if So is broken then all the Qns are equal for n ≠ 0 and Q₀ > Qn.

Because of the periodicity of the stiffeners eqn [1] can be simplified since

$$K_0 + \sum_{n \neq 0} (K_{s,n}' - K_0) = K_p \qquad \text{(B-11)}$$

where Kp the stress intensity factor for a crack centred about one of the stiffeners in a periodic set.

All these K values can be found from previous studies or hybrid method, thus the Kp can be determined.
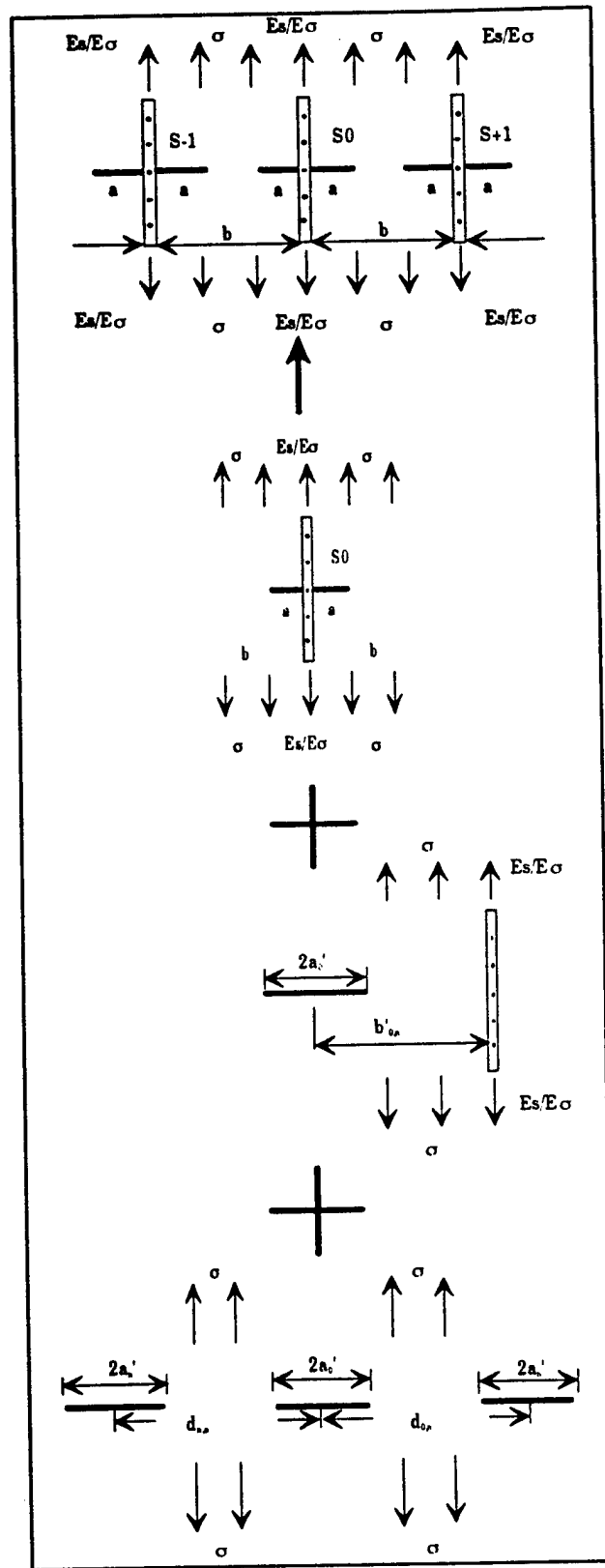
Fig 1 Ancillary configuration for collinear cracks in a periodically stiffened panel

Fitness for Purpose Evaluation of Critical Structural Details in Tankers

A Load Shedding Model of Fracture Mechanics Analysis of Cracked Critical Structural Details in Tankers

Tao Xu
and
Professor Robert G. Bea

Department of Naval Architecture and Offshore Engineering
University of California, Berkeley

Preface

The one year Joint Industry Research Project **"Fitness for Purpose Evaluation of Cracked Critical Structural Details (CSD) in Tankers"** was initiated in 1993 by the Department of Naval Architecture & Offshore Engineering, University of California at Berkeley as an extension of the projects **"Structural Maintenance for New and Existing Ships"** and **"Ship Structural Maintenance"**. The objective of this project is to develop engineering guidelines and procedures to help ship repair engineers, port superintendents and surveyors make evaluations of the fitness for purpose of cracked Critical Structural Details (CSD) in tankers.

This project was made possible by the following sponsoring organizations:

- **American Bureau of Shipping**   **-Chevron Shipping Cooperation**
- **Mitsubishi Heavy Industries**   **-Newport News Shipbuilding & Dry Dock Co.**
- **Ship Structure Committee**

This report documents a fitness for purpose analysis procedure of cracked critical structural details (CSD) in tankers.

Table of Contents

List of Figures

List of Tables   **Page No.**

Summary

Objective

The objective of this project is to develop engineering guidelines and procedures to help ship repair engineers, port superintendents, and surveyors make evaluations of the fitness for purpose of cracked critical structural details (CSD) in tankers.

This project is the the third phase of the Joint Industry Research Project "Structural Maintenance for New and Existing Ships"(SMP) which has been conducted by Department of Naval Architecture & Offshore Engineering, University of California at Berkeley.

A general fatigue analysis procedure was developed and updated during SMPI and SMPII. This provided the naval architect with the necessary information to reduce the chances of experiencing unexpected fatigue damage in CSD in tankers. The SMP fatigue analysis should not be expected to result in a **perfectly crack free tanker**. The uncertainties and variabilities associated with the fatigue analysis and economics associated with the cyclic stress reduction will not allow a perfectly crack free tanker to be practical. **Sufficient durability** for the **cracked** critical structural details (CSD) in tankers and its associated maintenance are the principle objective of this **fitness for purpose** analysis.

Fitness for Purpose Procedure

A general fitness for purpose evaluation for cracked CSD in tankers has been developed during this project. The procedure can be summarized as follows:

1) Identification of the specific critical structural details (CSD) where cracks occur based on previous experience, inspections or the SMP fatigue analyses based on traditional S-N curves.

2) Inspection of these details to define the initial crack size (a_0) to be used in the remaining life analysis.

3) Determination of the fracture toughness value of the steel plate used in the CSD to derive the final critical crack length. The final critical crack length is the length that a crack must reach before the crack can propagate in a brittle fracture mode.

4) Development of equivalent S-N curves for cracked CSD based on the initial crack length and final critical crack length.

5) Based on the long term fatigue loading and equivalent S-N curves, the residual fatigue life for cracked CSD can be evaluated.

6) Based on the estimated residual life, the inspection and repair program can be established for extended safe and reliable service.

The application of the proposed procedure has been illustration with evaluation of cracked CSD in a 165,000 DWT single hull tanker.

Scope

The fitness for purpose procedure developed during this project is based on fracture mechanics. This report documents in detail the linear fracture mechanics based methods used to derive the fitness for purpose procedure. The report is divided into seven chapters.

Chapter 1 introduces fatigue cracking in tankers with the overview of the previous projects.

Chapter 2 summarizes the linear fracture mechanics methods. The general theory and principles of the crack growth are briefly described. The models for crack growth calculation of large CSD are described. The procedure for evaluating fatigue life due to constant and random loading are outlined.

Chapter 3 addresses the computation of Stress Intensity Factors (SIF). It presents the hybrid method for evaluation of SIF. The hybrid method is a combination of an influence function method and a superposition methods. It employs available solutions for two- and three dimensional crack problems. From these, the influence of different factors affecting the stress intensity factor, K are separated and used to " compose" an estimation of K in actual structural details.

Chapter 4 documents the numerical methodology for the S-N curve development. This method includes the local notch approach for the estimation of the crack initiation phase and the fracture mechanics approach for the crack propagation phase. The cracked CSD S-N curves are developed based on fracture mechanics in the crack propagation phase.

Chapter 5 contains a discussion about the long-term fatigue loading. A new analytical formula for a wide banded loading process is derived. The load sequence is

briefly discussed. A damage model is presented to enable aan evaluation of sequence fatigue damage.

Chapter 6 presents a fitness for purpose analysis of a cracked CSD in a 165,000 DWT single hull tanker. It is shown that fitness for purpose procedure can provide a rational procedure to help engineers make repair and maintenance decision for cracked CSD in tankers.

Chapter 7 summarizes results from this study and makes recommendations for future work.

Chapter 1

Introduction

1.1 Background

In the present generation of very large crude carriers (VLCC), fatigue related cracks in critical structural details (CSD) constitute one of the single largest maintenance problems associated with these ships. The fundamental reason for fatigue cracking is excessive high cyclic stresses in CSD. There are two fundamental ways to reduce fatigue cracking: (1) reduce the numbers of cyclic loads and (2) reduce the magnitude of cyclic stresses. In general, there are not too many ways to reduce the number of high cyclic loads although slowing the ship down avoiding the bad weather, and choosing headings in severe seas can minimize the cyclic loads. The most effective way to reduce fatigue cracking is to reduce the stress levels in the CSD. This can be accomplished by a variety of structural strategies such as increasing the scantlings of the steel sections, providing gradual changes in stiffness of intersections, providing balanced stiffness and strength in connections to eliminate "secondary stresses", improving weld profiles (to provide gradual changes in stiffness), reducing fabrication misalignments and more effective and efficient detail design. These approaches were addressed in detail in previous SMP I and SMP II projects. [1.1-1.2]

A general fatigue analysis procedure was developed and updated in SMP I and SMP II project to provide the marine engineer with the necessary information to reduce the chances of experiencing unexpected fatigue cracking and provide an acceptable degree of "durability" in the CSD. But the fatigue analysis should not be expected to result in a perfectly crack free tankers. The uncertainties and variabilities associated with the fatigue analysis and economics associated with cyclic stress reductions will not allow a perfectly crack free tanker to be practically realized. Sufficient durability for the cracked CSD and its associated maintenance planning are the principle objective of this SMP III project.

The Joint Industry Project **"Fitness for Purpose Evaluation for Cracked Critical Structural Details (CSD) in Tankers"** is the extension of the research of the fatigue damage evaluation in SMP I and SMP II project. **The objective of this project is to develop engineering guidelines and procedures to help ship repair engineers, port superintendents, and surveyors make evaluations of the fitness for purpose of cracked CSD in tankers. The main focus is on the residual life of the cracked CSD in tankers[1.3].**

1.2 Fatigue Cracks in Tanker Structures

Based on the results from the previous SMP I & II projects, Something of the order of 40% to 50% of cracks in the class of VLCC studied were located in the connection between side shell longitudinal and transverse frames[1.1]. A typical example of crack locations is shown in Fig. 1.1.

2
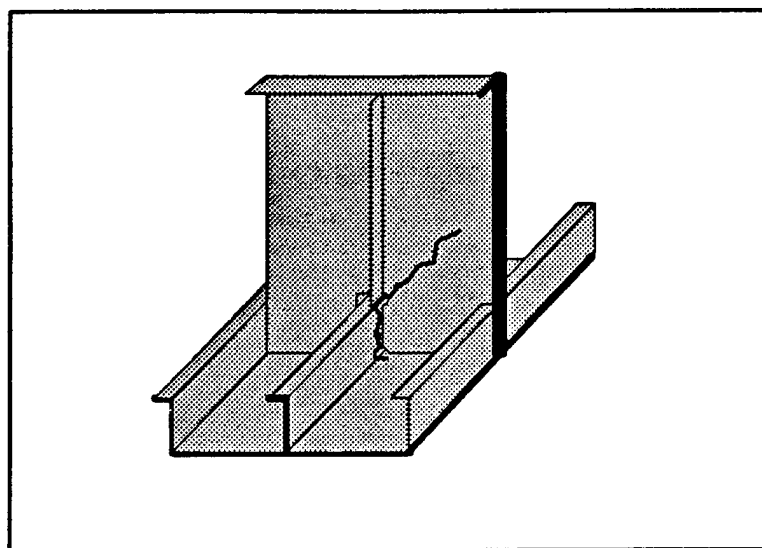
Fig 1.1 Cracks in Sideshell Longitudinal CSD

Most of the fatigue cracks of side longitudinal occur in the region between fully loaded water line and ballast water line. This region is basically the highly cyclic and dynamic loading area. This is due to the high fluctuating hydrostatic and hydrodynamic pressure on sideshell waterline (Fig. 1.2).
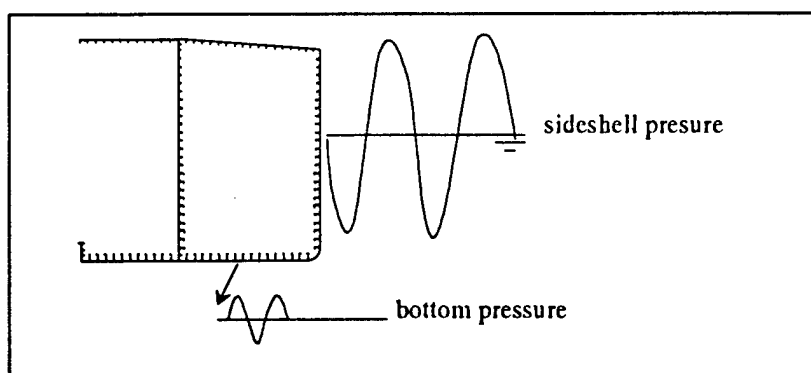
Fig. 1.2 Schematical pressure load on bottom or sideshell

The cracks normally start at welded connections between side shell longitudinal and supporting stiffeners or brackets. Cracks most frequently initiate in the weld heat affected zone or poor fabricated sections, poor welded sections and poor aligned sections. Fig. 1.3 is typical illustration of the fatigue crack initiation and growth of CSD in tankers.
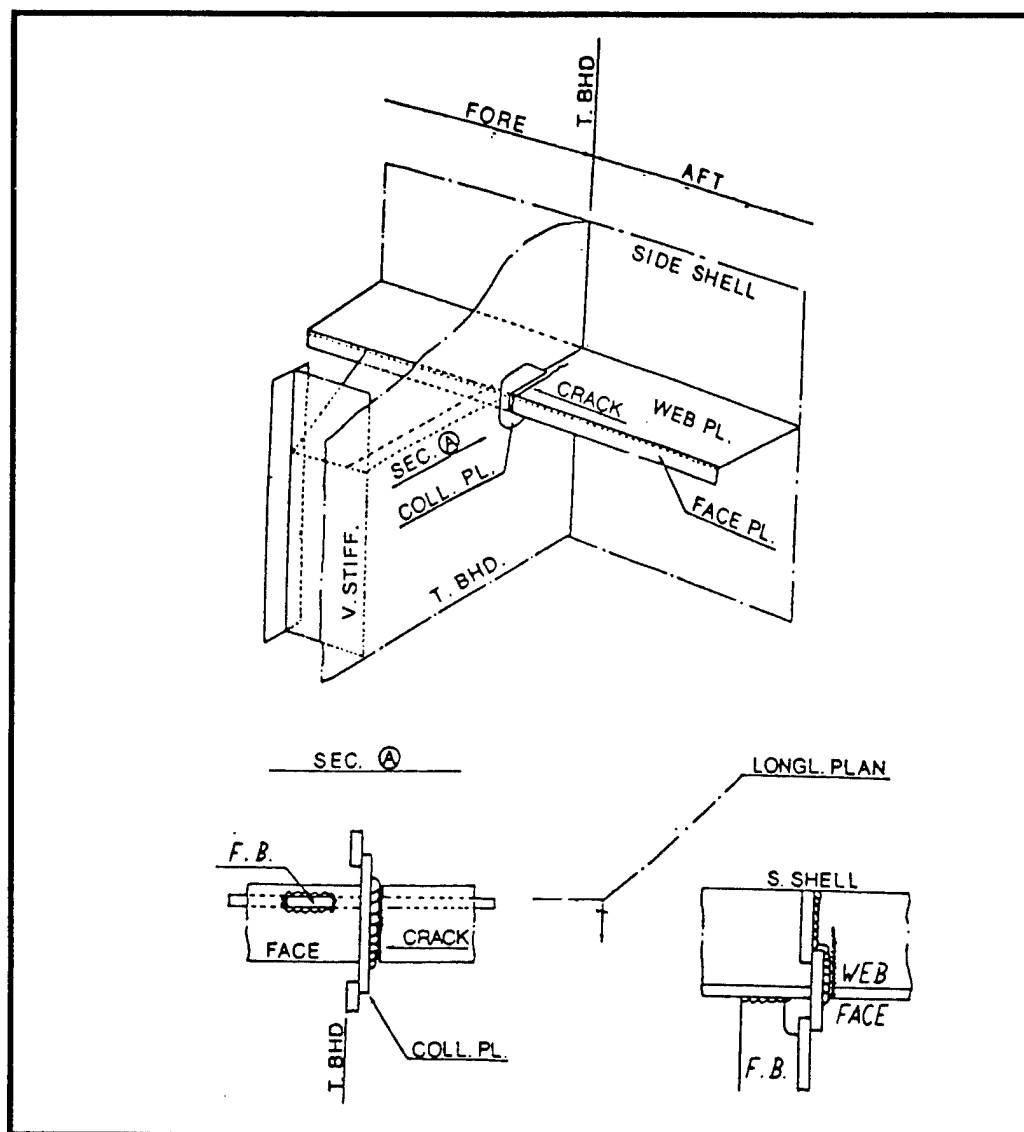
Fig 1.3 Crack initiation and Growth of CSD in Tankers

1.3 Fitness for Purpose Evaluation Procedure

The general **fitness for purpose** procedure developed during this project can be summarized as follows:

1) Identification of the specific critical structural details (CSD) where cracks occur based on previous experience, inspections or the SMP fatigue analyses based on traditional S-N curves.

2) Inspection of these details to define the initial crack size (a0) to be used in the remaining life analysis.

3) Determination of the fracture toughness value of the steel plate used in the CSD to derive the final critical crack length. The final critical crack length is the length that a crack must reach before the crack can propagate in a brittle fracture mode.

4) Development of equivalent S-N curves for cracked CSD based on the initial crack length and final critical crack length.

5) Based on the long term fatigue loading and equivalent S-N curves, the residual fatigue life for cracked CSD can be evaluated.

6) Based on the estimated residual life, the inspection and repair program can be established for extended safe and reliable service.

Many factors related to the fatigue crack growth process are variable, indefinite, or unknown, leading to large uncertainties. As the result of the uncertainties, the safety of the considered tanker against fatigue failure should be evaluated in a probabilistic sense. An advanced reliability analysis for fatigue cracks and its maintenance would be

addressed in the subsequent reports. In this report, a deterministic linear fracture mechanics procedure is developed as the basis for the probabilistic development.

This report is divided into seven chapters. Chapter 1 is the introduction. Chapter 2 describes the linear fracture mechanics method. Chapter 3 discusses the evaluation of stress intensity factor. Chapter 4 documents the development of the equivalent S-N curves based on the linear fracture mechanics. Chapter 5 addresses the long-term fatigue loading. Chapter 6 applies the detailed fitness for purpose evaluation procedure for cracked CSD in 165,000 DWT tanker. Chapter 6 summarizes the results from this study and recommends future on this topic.

1.4 Reference

1.1 Structural maintenance for New and Existing Ships, Research Report SMP 1-1 through SMP 5-2. Dept. of Naval Architecture & Offshore Engineering, University of California at Berkeley, Berkeley, CA 94720. October, 1992

1.2 Ship Structural Maintenance Project, Research Report SMP II-1 through SMP II-3. Dept. of Naval Architecture & Offshore Engineering. October, 1993

1.3 Tao Xu & Robert, G Bea. Proposal for Joint Government-Industry Project **Evaluation of Fitness for Purpose of Cracked CSD in Tankers.** May 1993

Chapter 2

Linear Fracture Mechanics

2.1 Introduction

During cyclic loading, a crack can propagate at stress levels well below the static fracture stress. This fatigue problem is usually treated by use of a fatigue analysis based on Cyclic Stress Range - Number of Cycles to Failure (S-N) and the well known Miner-Palmgren hypothesis. However, this problem may be treated in a more versatile way through the use of fracture mechanics. In this chapter, fracture mechanics models will be described and developed for the estimation of crack growth and fatigue life of ship CSD.

First, the general theory and principles of crack growth are described. Second, actual models for crack growth calculations of large scale CSD are described. Third, methods and procedures for estimating fatigue life due to constant and random loading are outlined.

2.2 Crack Growth and Fatigue Life

2.2.1 Crack Growth

A brief review of the procedures for calculating crack growth will be discussed in this

section, however, only aspects which are related to this work will be addressed in detail.

2.2.2 Crack Mechanisms

On the basis of a re-analysis of crack propagation data obtained by several investigators, Paris and Erdogan [2.1] suggested that the most relevant parameter to describe the fatigue crack growth was the range of stress intensity factor, ΔK, where:

$$\Delta K = K \max - K \min \qquad (2.1)$$

Kmax and Kmin are the value of stress intensity factor, K, at the upper and lower limit stresses of cyclic loading.

As discussed in chapter 3, the stress intensity factor, K, is a single term parameter which describes the stress condition adjacent to the crack tip. In most fatigue crack propagation situations, cracking will occur under linear elastic and quasi-elastic conditions, and the size of any plastic zone at the crack tip will be small compared to the crack length and the actual plate thickness. Under such circumstances, the stresses and strain condition at the crack tip can be described by the stress intensity parameter.

However, it is not generally applicable to define the cyclic stress intensity factor (ΔK) by use of the upper and lower limit stresses, because the crack growth rate is dependent on some other factors such as mean stress level, residual stress and environments (e.g. corrosion). Problems associated with these factors will be considered later in this chapter while the stress intensity factor evaluation is addressed in Chapter 3.

On the macroscopic scale, at which cracks are treated in this study, fatigue fracture surfaces are generally flat and smooth in appearance. They tend to grow as model-I (Fig 2.1) cracks irrespective of initial orientation, so attention is mainly confined

to this mode. Other modes (Fig 2.1) can occur when a crack follows a plane of weakness or is initiated at a notch with large shear stresses and/or in a biaxial stress field. Such cracks can be treated as if they were mode-I cracks, where the opening mode-I stresses are taken as the maximum principal applied stresses. This simplification is justified by the fact that a crack subjected to different crack opening modes is found to propagate perpendicular to the direction of the maximum principal stress [2-2]. But the maximum stress can not be defined as fatigue stress for real CSD in tankers due to its complex stress fields in such details. Generally, fatigue stress for CSD is defined as the stress which is normal to the crack direction. [2-1].

mode I Opening Mode   mode II Sliding mode   mode III tearing mode
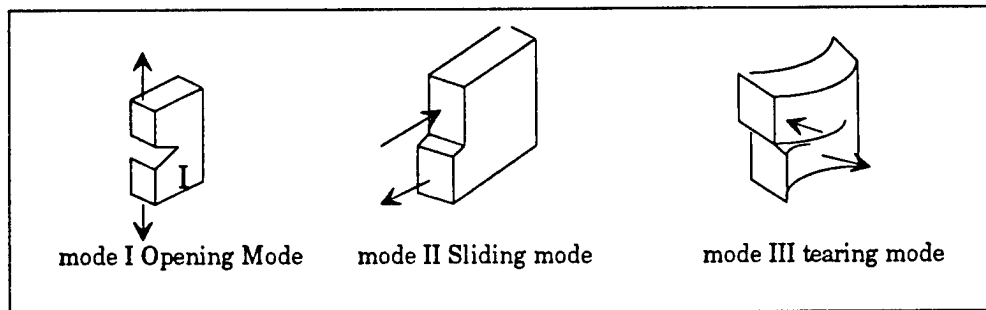
Fig 2.1 Three Cracking Mode

In Fig. 2.2 a schematic crack growth rate curve is shown. Three distinct regions are indicated : the well-known threshold region (crack initiation), intermediate region (stable growth) and the failure region (unstable growth).
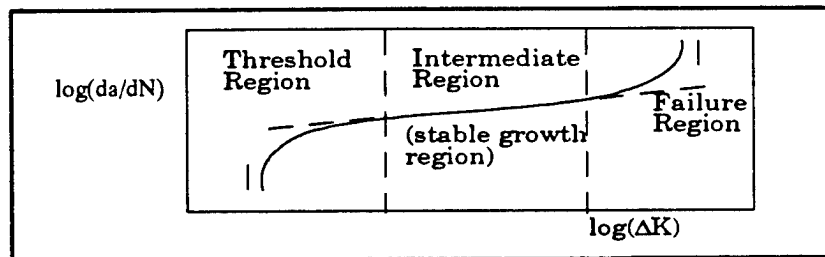
Fig. 2.2 Schematic crack growth rate curve showing the variation of crack propagation rate (da/dN) with cyclic stress intensity factors

The variation of da/dN with ΔK is rather complicated, being sigmoidal in form (log-log plot) and bounded at extremes by values of ΔK_{th} and ΔK_c, (ie the threshold value and the critical value) of ΔK respectively.

The different regions are associated with the following crack growth stages.

- crack initiation
- stable crack growth
- final fracture (unstable crack growth)

At sufficiently low stress intensity range, there is no crack growth. The corresponding value of stress intensity factor is called the threshold stress intensity factor range (ΔK_{th}).

At intermediate values of K, there is an approximate linear relationship between crack growth rate and ΔK on a log-log scale.

As the stress intensity factor approaches the fracture toughness of the material, the growth rate increases sharply, and becomes an asymptotic value of (ΔK) for an infinite crack growth rate, i.e. an instable crack length is reached.

2.2.3 Crack Propagation Laws

A large number of crack propagation laws have been developed [2.2-2.5], the majority can be described in the form:

$$da / dN = K(\Delta K, \Delta K_{th}, Kc)H(a, R) \qquad (2.2)$$

11

where

ΔK - range of cyclic stress intensity factor

ΔK_{th} - threshold stress intensity range

R   - stress ratio

a   - crack length

F,H   - are usually power functions

Most of the proposed relations are attempting to model one or more of the crack propagation regions, hence they might include effects of threshold values - and critical values of the stress intensity factor.

In general the crack growth rate will also be dependent on :

- stress ratio,

- material strength,

- material type,

- environments,

- load type and nature of loads, and

- frequency of loading,

Crack propagation is dependent on a variety of different parameters. Many relations for predicting the growth rate have been developed. The majority include empirical crack growth parameters, which must be evaluated for the actual material and circumstances.

Many attempts have been made to derive a theoretical law for fatigue crack growth, but none of the proposed expression have a general application. For engineering

problems, the simple knowledge that (da/dN) is a function of (ΔK) will often be sufficient. Therefore, the crack propagation relationship is more often deduced from test data.

Semi-empirical laws have been derived from empirical data, and each one is valid for certain scope which can be represented from these data. The scatter for crack propagation test data is very large. It can be concluded [2-2] that there is little basis for arguments about the usefulness of different proposed empirical laws. Many of them have certain merits in a limited region or for a particular set of test data. Therefore no one proposed empirical law for (da/dN) versus (ΔK) can be taken to have significant advantage over the others.

Paris and Erdogan [2-2] suggested the following simple relation:

$$da / dN = C(\Delta K)^m \qquad\qquad (2.3)$$

where C and m are material parameters for a given material and environment. This expression becomes a straight line in a log-log graph, (Fig. 2.1), The slope of the line represents the material parameter m, and the intersection with the ordinate-axis represents the parameter C. This equation is found to provide an adequate description of the behavior for the mid-range of growth rates. However, the equation has been found to have wide practical application for analyzing cracks in as-welded steel structures, where small initial cracks always are present in or nearby welds. Under such circumstances, the crack initiation stage is negligible, and the major part of the total fatigue life is occupied by the crack growth stage, i.e. the mid region, which is adequately described by Paris-Erdogan relation. The failure region will be very short for almost all practical calculations. Hence it can be negligible due to the rapid increasing growth rate.

2.2.4 Parameters m and C

As discussed early, the parameters C and m are not strictly material constants, since they depend on factors as the stress conditions and the environments. The value of C and m, for any particular material and set of conditions, have to be defined experimentally. Many attempts have been made to obtain an empirical relationship between C and m. In general the proposed relations are of the kind

$$C = A \bullet B^{-m} \tag{2.4}$$

where A and B are constants for a particular type of material and set of conditions. Experimental results on steels tested in air at R=0, indicates that log(C) is linearly related to m. Based on the re analysis of several published crack propagation test results of structural steels, Gurney [2-3] obtained the following relation:

$$C = (1.315 \text{x} 10^{-4}) / (895.4)^m \tag{2.5}$$

By inserting this into Eq. (2.3),

$$da / dN = 1.315 \text{x} 10^{-4} (\Delta K / 895.4)^m \tag{2.6}$$

which implies that all (da/dN - ΔK) relations for all steels pass through the point da/dN =1.315 x 10^{-4} -mm/cycle at Δk=895.4 N/mm$^{3/2}$. At present it is not known what defines the value of m and C for any particular material. For structural steels m usually lies in the range 2.4 to 3.6 [2.4]. The value m=3 is the one that is frequently assumed for design purposes.

Generally, one may state that when ΔK is less than 895.4 N/mm$^{3/2}$, smaller rate for propagation is obtained by an increasing m. As most of the life of a crack is spent at short cracks, a larger m will be beneficial at low ΔK.

2.2.5 Mean Stress and Residual Stress

The effect of mean stress level on fatigue crack propagation can be studied by using the stress ratio parameter R, where R is equal to $\sigma_{min}/\sigma_{max}$, σ_{min} and σ_{max} are the minimum and maximum values of the fluctuating stress.

Several investigations have been conducted to study the effect of mean stress, (see e.g. [2-4,2-5]). Many models have been proposed, both theoretical and empirical [2-4,2-5], but none of them are generally valid.

The general effect of mean stress level is shown in Fig. 2.3.
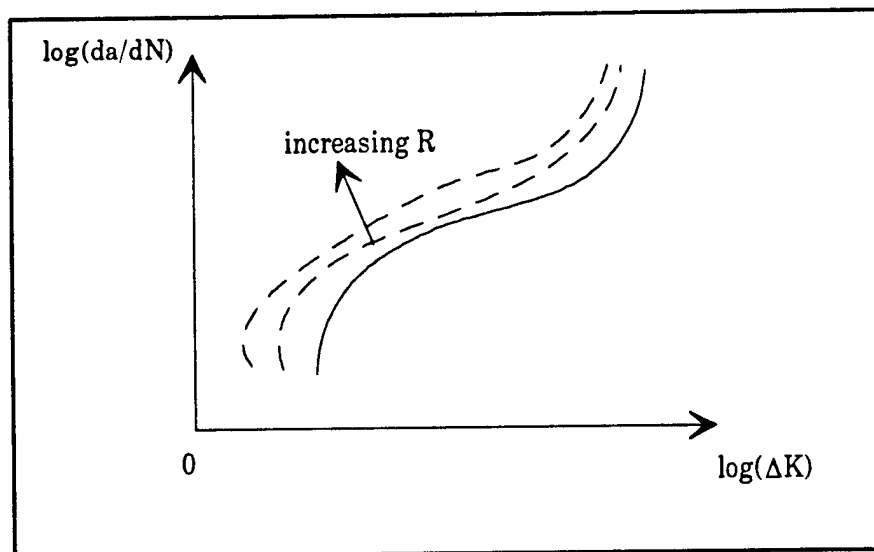
Fig. 2.3 Effect of Stress Ratio on Crack Growth Rates

High stress ratios tend to reduce the threshold value and to increase the crack growth rate at a given value of the stress intensity range. Tanker structures may experience both negative and positive mean stress levels. In the case of partly negative stresses, the growth rates seem to follow the range of the positive part of the cycle.

$$\Delta K_{eff} = K_{max} = \frac{\Delta K}{1-R} = \frac{\Delta \sigma}{1-R}\sqrt{\pi a}\,F \qquad (2.7)$$

This indicates that the negative part of a load cycle is non-damaging. It is generally assumed that crack closure is responsible for this effect.

However, it might be concluded the effect of mean stress level becomes insignificant due to residual stresses [2-5,2-6].

Residual stresses in structures may be categorized into two types

- short range stresses, and
- long range stresses

Short range stresses or welding residual stresses exists only in and close to welds, and are self-balanced over the cross section of the member. The stresses are caused by the heat input during welding, and thermal contraction of part of the cross section under restraint from cooler portions. Such short range stress are always associated with small member end displacements.

Long-range stresses are associated with large deflections and rotations , and are self-balancing within the detail and its adjacent details. These stresses are usually induced during fabrication process, whereby welding shrinkage, local heating, mechanical restraint, and brute forces (e.g. to imposed align misaligned sections) are main sources.

Very little is known about residual stresses, but measurements show that short range stresses are usually of yield magnitude with large through thickness gradients, see e.g. [2-6], while long range stresses can be assumed approximately equal to 25% of the

yield stress[2-6]. Short range stresses may easily be reduced by heat treatment, while long-term stresses which are associated with large strain energy due to large deflections and rotations are not easily reduced by heat treatment or other residual stress reducing techniques. As a consequence, residual stresses will always be present in tanker structures, and can never thought to be be taken lower than 25% of yield magnitude[2-6].

Residual stresses will significantly affect the mean stress level in welded steel structures. The level will almost always be at yield stress tension in and near by welds, where fatigue cracks in as-welded structures are most likely to occur. The stress range will pulsate downwards from yield stress tension, i.e. at a high stress ratio. As a consequence, the effect of mean stress level due to static applied loads becomes insignificant in crack growth calculation for as-welded structures.

On this basis, the so-called stress range approach has been adopted in realistic fatigue crack growth calculations, implying that the whole stress range or stress intensity factor range is taken as effective. The effects of mean stress level and residual stresses are implicitly taken care of by adopting crack growth parameters (C,m) obtained experimentally at high stress ratios and/or at high stress levels.

2.3 Fatigue Crack Growth Modeling

2.3.1 Surface Crack Growth Stage

Crack growth in most types of welded steel materials can be adequately characterized by the well-known Paris-Erdogan relationship. The growth modeled by this relation is a strong function of the cyclic stress intensity factor (ΔK). This factor depends on geometry and load configurations and has to be determined for the actual case.

17

Of special interest in fatigue crack growth problems are part through-surface cracks, which usually are initiated from crack like defects at the weld toe or nearby the welds and weld affected zone. Such cracks are often found to grow with a semi-elliptical crack front, hence such cracks become of special interest in crack growth problems. Unfortunately no closed form analytical stress intensity solution is available for this case. Nevertheless, approximate solutions can be obtained by adding basic solutions [2.7-2.9]. Complex configurations are considered to be a combination of a number of separate simple configurations with separate boundary conditions which have known stress intensity factors. The stress intensity factors for the simple configurations are then added to obtain the required solution. Using this technique, and the well known superposition principle [2.5], stress intensity factor estimates at the deepest point of a semi-elliptical crack can be obtained from empirical stress intensity factor equations and the closed form edge crack influence results.

Using this method, problems with complex stress gradients in the plate-depth direction can be solved. This method has successfully been applied in earlier works e.g. [2.10-2.11].

However, the method is only capable of handling a single degree of freedom crack growth. Hence, it becomes dependent on empirical relations of crack shapes (aspect ratio -a/c; crack depth a to crack width c) for deriving reliable and accurate crack growth results. The empirical relations are usually obtained from lab test of small specimens with a certain local and global geometry. As a result, the applicability of each set of data becomes an important limitation when it comes to large scale structural problems. In particular, one must count on large limitations in performing generalized analyses, due to limited availability of data and large resources required to derive such data.

In order to overcome these limitations in performing generalized analyses of large scale problems, a two degrees of freedom crack growth model must be developed, which can account for complex crack surface loading.

Semi-elliptical cracks requires two length dimensions for their characterization, a and c, (Fig. 2.5). In reality, as indicated above, cracks can change shape as they grow, [2-12] that is, as a and c increases, the value of b=a/c, changes. The manner in which b changes will depend on the initial crack shape, the geometry and the applied stress distribution. In all cases, it appears that the aspect ratio, b, will tend toward the value that produces a constant stress intensity range ΔK along the crack periphery. However, this equilibrium value of b will depend on the nature of the applied stress. Hence it may vary during the crack growth process [2-12,2-13].

The rate at which b extends will depend on the cyclic value of k along the crack front, as well as the fatigue crack growth characteristics of the material, i.e. values of C and m in Paris equation [2-12,2-13].

The stress intensity factor to be employed must be carefully defined, because K varies along the crack front. Considerations of local growth rate controlled by the local value of K along the crack front would be analytical prohibitive and probably unrealistic [2-9,2-12]. Semi-elliptical cracks would not necessarily remain semi-elliptical, and stress intensity factor solutions for non-elliptical cracks would be required, Therefore, it will be assumed that the growth of a and C need only to be considered, with appropriate selection of the controlling stress intensity factors.

A two degrees of freedom crack growth model for semi-elliptical cracks may be utilized using two different stress intensity approaches:

i)   The growth in the depth direction is controlled by the cyclic value of K at the point of maximum crack penetration, and the growth of C is controlled by the cyclic K at the surface. This is called the local K approach.

ii)   The growth in the two directions are controlled separately by some average stress intensities along the crack front.

Suggested average values are the "RMS-average" associated with each degree of freedom a and C. This seems to be a more realistic assumption than the use of simply local values. Therefore, these "RMS-average" values will be assumed to govern the rate of growth of a and C.

The suitability of using RMS-average stress intensity factors can be judged from experimental evidence. Cruse, et. all. [2-11,2-14] provide comparisons of theoretical and experimental results which suggestes that such values are reasonable.

Further discussions concerning this approach can be found in [2-11,2-13]. An advantage of this formulation is that the RMS-average values can be evaluated for arbitrary stresses on the crack plane by the use of influence functions [2-11,2-13,2-15]. These functions can be evaluated from information on the opening displacements on the crack surface for an arbitrary state of stress, solutions for basic problems are given in the literature, Basically, the RMS-average values are denoted by a "bar" over the K, and are defined as follows:

$$\overline{K}_a{}^2 = \frac{1}{\Delta A_a} \int_0^{\frac{\pi}{2}} K^2(\varphi) d\left[\Delta A_a(\varphi)\right] \qquad (2.8)$$

$$\overline{K}_c{}^2 = \frac{1}{\Delta A_c} \int_0^{\frac{\pi}{2}} K^2(\varphi) d\left[\Delta A_c(\varphi)\right] \qquad (2.9)$$

These equations will be discussed in detail in Chapter 3 and coded in computer program FRACTURE [2-10].

The use of local values of K would require considerably more numerical stress analyses for each crack length and stress system of interest, due to the fact that these values can not be evaluated by the simple use of influence function (or similar approaches) which can be integrated over the cracked surface to give the stress intensity in question.

One basic question arises; whether a local or average stress intensity factor should be used for prediction of fatigue crack growth. The same question yields the prediction of unstable fracture. This question will not be discussed in detail in this work. It is only noted that the two different values of the stress intensity factor are very much alike and does not differ significantly [2-12].

In accordance with the foregoing considerations, a two degree of freedom model of crack growth can be established by the use of Paris equation, and the crack growth can be taken to be governed by the following equations(Fig. 2.4) :

$$da / dN = C_a \Delta \overline{K}_a^m \qquad\qquad (2.10)$$

$$dc / dN = C_c \Delta \overline{K}_c^m \qquad\qquad (2.11)$$

where subscript a and c denotes the depth and width direction respectively. Ca and Cc are assumed to be equal.

For each crack increment in the depth direction a corresponding increment in the width direction can be estimated:

$$\Delta c = \frac{Cc}{Ca} (\frac{\Delta K_c}{\Delta K_a})^m \Delta a \qquad\qquad (2.12)$$

Applying this procedure, the crack shape development can be predicted in analytical terms.

As discussed, Ka and Kc depend on the aspect ratio a/c (among other things) so that the growth in the depth and length dimension are still coupled. This model is coded in FRACTURE [2-10].

Alternative approaches for predicting the crack growth are suggested in the literature, e.g. [2-12,2-13]. One approach that has been proposed is to use a different crack growth "law" for growth along the surface versus growth in the depth direction. Discussions concerning this approach can be found in [2-12,2-17].
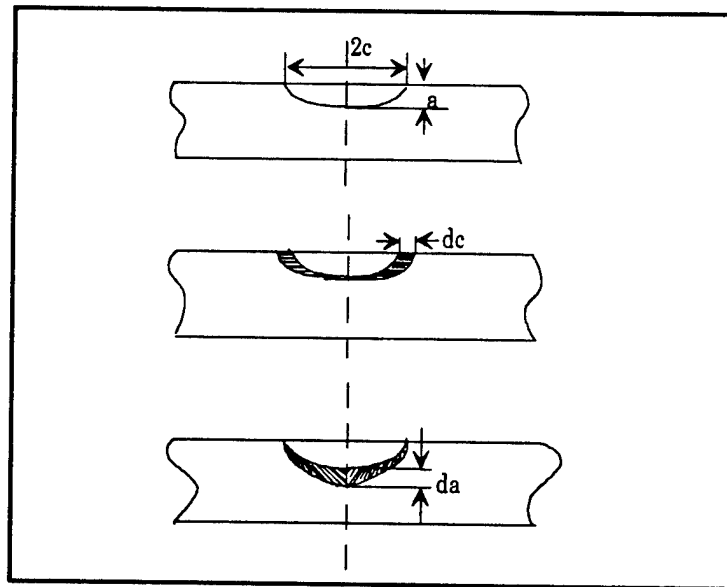
Fig. 2.5 Semi-elliptical Surface Crack with Two Degrees of Freedom

2.3.2 Through Thickness Crack Growth Stage

Fatigue crack growth for grow stage are also modeled by use of Paris equation. For the simple case of a symmetric crack surface loading, (Fig. 2.5), the stress intensity factor range becomes equal at both crack tips. This problem may be modeled with a single degree of freedom; only growth in one length dimension needs to be considered.

$$\Delta a = C(\Delta K)^m \Delta N \qquad\qquad (2.13)$$

The total crack length advance becomes $2\Delta a$.
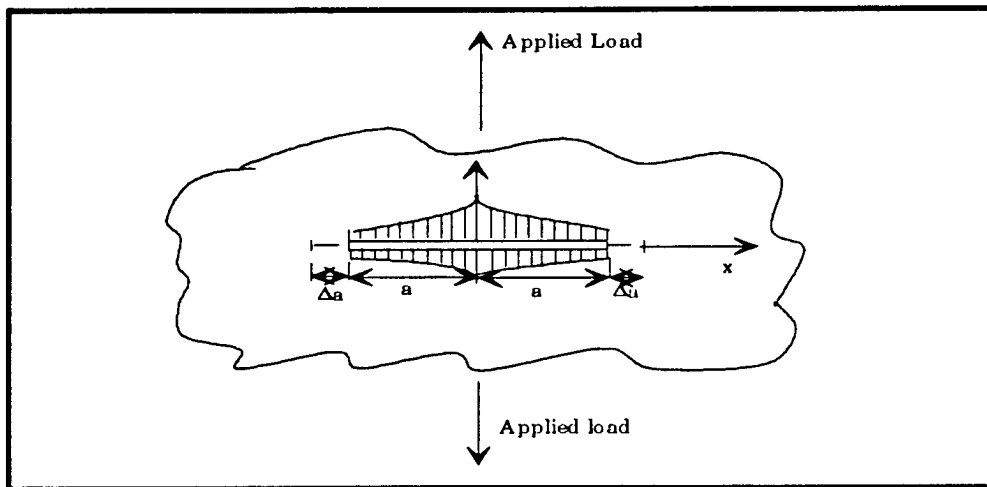
Fig 2.6 Through Thickness Crack with Symmetric Crack Surface Loading

In the case of an unsymmetric or arbitrary state of stress, the stress intensity factor range will be different at the two crack tips (Fig. 2.7). The growth then becomes unsymmetric: a different crack advance at the two crack tips. The center line of the crack will not remain at the initial position; it will now move towards the crack side with largest crack growth. See Fig. 2.7 where this growth behavior is illustrated.
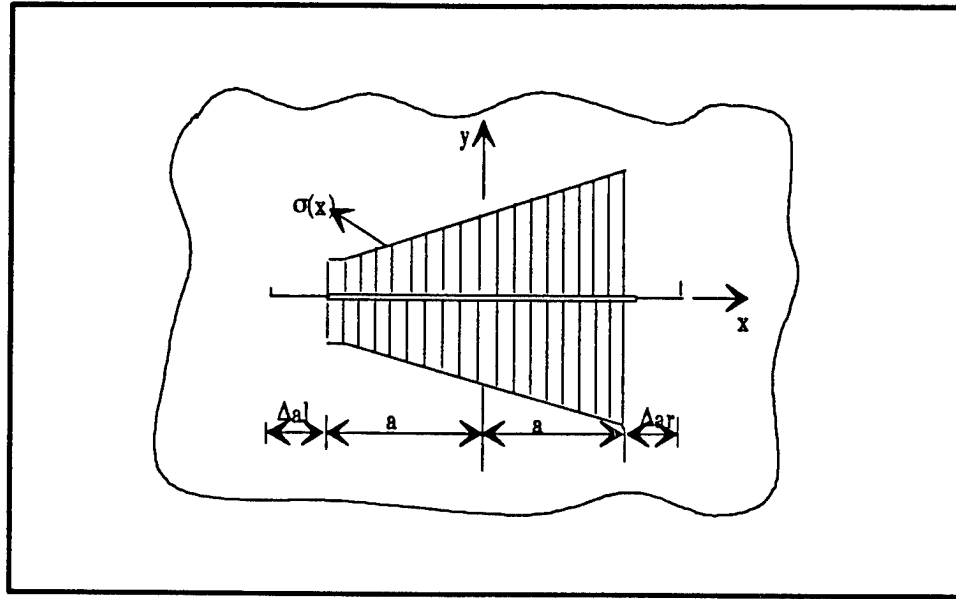
Fig. 2.7 Through Thickness Crack with Arbitrary State of Stress Characterized by a Two

Degree of Freedom Model

This crack growth process requires a two degrees of freedom model for its characterization. A similar procedure as indicated for the surface crack can be utilized. However, the calculation method becomes different because of the unsymmetric growth. The stress intensity factor, hence also the crack growth increments must be estimated by use of an alternative procedure. The following expressions yield for an arbitrary crack increment:

$$\Delta a_R^i = C(\Delta K_R(a_0 + 0,5\Delta a_R^{i-1} + 0,5\Delta a_L^{i-1}, \Delta s^{i-1}))^m . \Delta N \qquad (2.14)$$

$$\Delta a_L^i = C(\Delta K_L(a_0 + 0,5\Delta a_R^{i-1} + 0,5\Delta a_L^{i-1}, \Delta s^{i-1}))^m . \Delta N \qquad (2.15)$$

$$\Delta a_L^i = (\frac{\Delta K_L(a_0 + 0,5\Delta a_R^{i-1} + 0,5\Delta a_L^{i-1}, \Delta s^{i-1})}{\Delta K_R(a_0 + 0,5\Delta a_R^{i-1} + 0,5\Delta a_L^{i-1}, \Delta s^{i-1})})^m \Delta a_R^i \qquad (2.16)$$

$$\Delta s^i = \frac{\Delta a_R^i - \Delta a_L^i}{2} \qquad (2.17)$$

24

$$a_i = a_0 + \frac{\Delta a_R^i + \Delta a_L^i}{2} \tag{2.18}$$

where subscript i denotes iteration number, subscript R and L denotes right-an left crack tip respectively, and $\Delta\sigma$ is the incremental movement of the central line, e.g. Fig. 1.6.

The iteration is stopped when the following considerations are satisfied;
- For $\Delta a_R^i > \Delta a_L^i$

$\Delta a_R = \Delta a_R^i$ when $|\Delta a_R^i - \Delta a_R^{i-1}| < e_t$

$\Delta a_L = \Delta a_L^i$

- For $\Delta a_R^i < \Delta a_L^i$

$\Delta a_R = \Delta a_R^i$

$\Delta a_L = \Delta a_L^i$ when $|\Delta a_L^i - \Delta a_L^{i-1}| < e_t$

- $\Delta a_R > 0$ $\Delta a_L > 0$

where e_t is an infinitesimal test value. The iteration must start with the crack length a_0 and incremental value of N.

Through thickness cracks may propagate away from the welding zone associated with large residual welding stresses. As a result, the effect of mean stress level or residual stress may change, and complicate the calculations. Thus, an equivalent stress intensity range must be determined by use of the stress ratio parameter R.

Material parameters (C and m) derived experimentally at the actual stressed condition must then be used.

A further complication is that more than one crack mode may be involved. This type of problem will not be considered in this project. This study is limited to problems involving a dominant mode-I crack opening configuration.

This problem may be solved by an equivalent stress intensity approach involving the derivation of stress intensity factors for all the crack deformation modes acting. This will also include the derivation of the path of crack. This problem has been a topic of extensive research for the last years, and basic theory can be found in textbooks[2-9].

2.4 Fatigue Life

One might subdivide the entire fatigue life in a crack initiation period (Ni), a crack growth period (Np) and a final fracture period (N_f), i.e.

$$NT = Ni + Np + N_f \qquad (2.19)$$

as was discussed in previous, the crack initiation period in as-welded structures usually occupies a small part of the total life, hence it can be neglected. So also for the final fracture period. Neglecting the contribution from these regions will for most cases lead to small errors, in the conservative direction.

This method is usually called the engineering approach, and crack growth behavior is simplified as shown in Fig. 2.8. The entire crack growth is assumed to follow the Paris-Erdogan relation in all the three distinct regions.

The value of the parameters C and m are chosen in accordance with the condition of each application. Under constant amplitude loading one may introduce a certain threshold value. At stress intensity factor ranges below this value there will be no crack growth. A distinct cut off level can hardly be justified under random amplitude loading. Some (ΔK) value will be above, and some below the threshold for the initial crack. A certain crack growth will take place.

2.4.1 Constant Amplitude Loading :

Having established the crack growth relation and corresponding parameters one may estimate the time or number of cycles required to grow a crack from one size to another.

$$dN_{1-2} = \int_{a_1}^{a_2} \frac{da_{1-2}}{[da/dN]_A} \qquad (2.20)$$

where (dN_{1-2}) is number of cycles, (da_{1-2}) the actual crack increment and where subscript (A) indicates the actual crack growth relation.
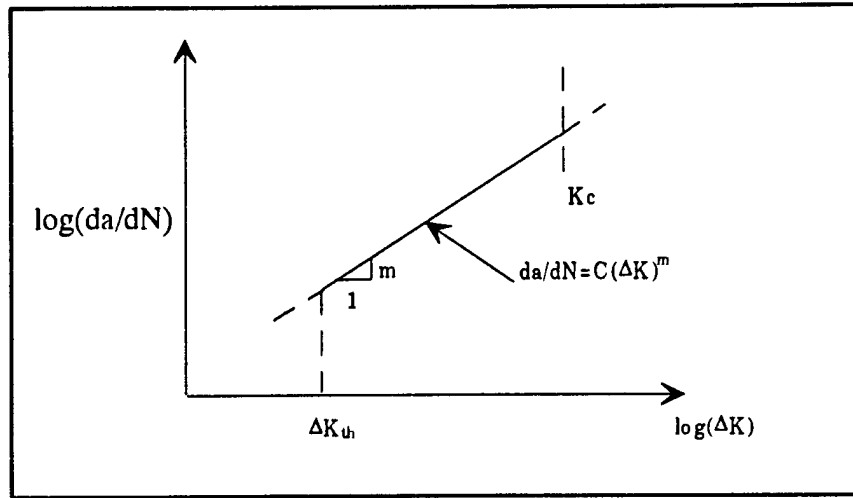
Fig. 2.8 Engineering Approximation of Crack Growth Ratess in as Welded Steels

Applying the Paris-Erdogan relation and integrating over the entire crack propagation stage :

$$N_T = \int_{a_i}^{a_f} \frac{da}{C(\Delta K)^m} \qquad (2.20)$$

where (N_T) is the total life, (a_i) the initial crack length and (a_f) the final crack length.

In the case of a very simple analytic expression of (ΔK), one may obtain a closed form solution, but generally the integration must be performed numerically. The stress intensity factor is a complex parameter, which is dependent on a large number of parameters, and must usually be evaluated by numerical methods; hence, also the crack growth.

2.4.2 Random Amplitude Loading :

Most structures are subjected to varying amplitude loads, this complicates the predication of fatigue life and crack growth of structural problems. The complexity associated with random loading are the definition of load cycle, the cycle counting and interaction effects.

Random loads may be subdivided into two broad classes: -1) narrow banded, and 2) wide banded random loading.

Methods for random process theory [2-14,2-15] must be used for the characterization of such load histories. These in general assumes a stationary process, that is, the statistical characteristics do not alter with time. The narrow-band random loading is the simplest. Under such loading, a cycle does not differ much from its predecessor. The definition of load cycle and the counting of them becomes easy by use of the theory of an stationary and Gaussian stochastic process, which is commonly used for the load characterization of marine structures subjected to ocean waves. In addition the effect of interaction become small for this type of loading [2-20]. More information about the random loading will be discussed in Chapter 5.

One common method of predicting crack growth life is to assume that each cycle causes the same amount of growth as if it were applied as part of a sequence of loads of constant amplitude. The Paris - Erdogan relation must be solved for the crack length, rather than number of cycles to failure. This cycle-by-cycle approach is given in terms of crack length (an) after N cycles as follows:

$$a_n = a_i + \sum_{j=1}^{n} \Delta a_j \qquad (2.21)$$

the crack length increment (Δaj) in cycle No j is given as:

$$\Delta a_j = (\frac{da}{dN})_j = C_1[C(\Delta K_j^m)] \qquad (2.22)$$

where ai is the initial crack length and where C_1 is an interaction coefficient. Thus the interaction coefficient modifies the constant amplitude growth rate to account for interaction, i.e. the effect of acceleration or retardation.

It has been found that the most dominant interaction effect is the retardation effect caused by overloads and/or peak loading [2-20]. However, the benefit of including effects of interaction is very uncertain, in general it should be included on the basis of both theoretical and experimental studies of the actual random loading. Hence also sources causing interaction may be included, e.g. stress history irregularity, crack geometry, crack orientation, environment, residual stresses, frequency and material properties and so on.

When the loading can be assumed to be narrow banded, as for ocean wave loading, the effects of interaction are limited, and the concept of the equivalent constant amplitude stress range which will give the same amount of fatigue crack growth on the

average as the random amplitude stress range history it replaces [2-21]. The equivalent

constant amplitude stress range can be expressed as Fig. 2.9:
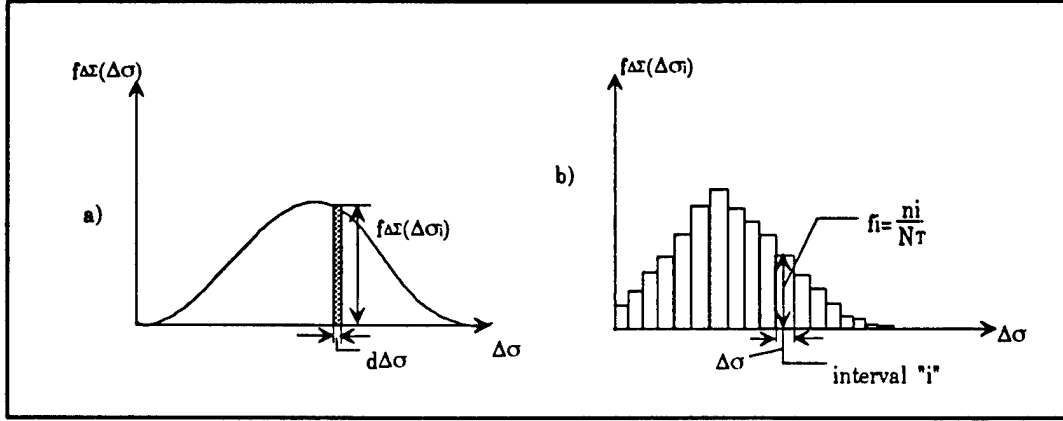
Fig. 2.9 Stress Range Distribution (a) and Histogram (b)

$$\Delta\sigma_{eq} = [\int_0^\infty f_{\Delta\Sigma}(\Delta\sigma) \bullet (\Delta\sigma)^\beta \bullet d\Delta\sigma]^{1/\beta} \qquad (2.23)$$

or as:

$$\Delta\sigma_{eq} = [\sum_{i=1}^k f_{\Delta\Sigma}(\Delta\sigma_i)^\beta]^{1/\beta} \qquad (2.24)$$

where:

$f_{\Delta\Sigma}(\Delta\sigma_i)$ = probability density function of stress range $(\Delta\sigma)$

fi = frequency of occurrence of stress range "i" $(\Delta\sigma_i)$

k = number of histogram class intervals

ni = number of cycles within interval "i"

N_T = total number of cycles

$\Delta\sigma i$ = midpoint of histogram interval "i"

β = empirical or calibration constant

Usually

30

β = 3 RMC (root-mean-cube) stress range

β = 2 RMS (root-mean-square) stress range

The exponent β is the slope of the crack growth curve, i.e. m in the Paris Erdogan relation.

This approach becomes identical to the Miner-Palmgren rule, usually used in the so called "S-N approach" to fatigue. The following conditions must be assumed for the cracked CSD in tankers.

- no fatigue limit

- interaction effects are negligible

- the slope of the crack growth curve is the same as the absolute value of the inverse slope of the S-N curve.

The equivalent stress range approach has been used in many analysis of fatigue crack growth and is found to give good results when applied to welded steel structures[2-12]. This approach will be mainly used in this study while the discussion about its limitation will be addressed in Chapter 5.

2.5 Summary and Conclusion

This chapter presents a brief review of the linear fracture mechanics.

The general theory and principles of crack growth are described at the beginning. The crack mechanism, propagation is discussed here. Residual and mean stress effects are outlined with the discussion about different material parameter.

The actual model for crack growth analysis for critical structural details (CSD) in tankers is addressed later. It describes the computation methodologies for surface crack and through thickness crack. Several models such as 2-D crack growth model, RMS model are discussed and compared.

Finally, the fatigue life prediction based on fracture mechanics is discussed in detail. It focuses on the study of the crack growth under random loading. The methodology about the crack growth under random loading is outlined.

2.6 References

2.1. A. Naess **Fatigue Handbook - Offshore Structures**, TAPIR 1985

2.2 Rolf, S.T. and Barsom, J.M **Fracture and Fatigue Control in Structures**, Prentice-Hall, Inc., New Jersey, 1977

2.3 Paris, P.C. and Erdogan, F **A Critcal Analysis of Crack Propagation Laws**, Journal of Basic Engineering, Trans ASME 1963

2.4 Lawrence, F.V. and Munse. W.H. **Fatigue Crack Propagation in Butt Welds Containing Joint Penetration** Defects. Idem, pp 221-225

2.5 Gurnet, T.R. **Finite Element Analysis of Some Joints with the Welds Transverse to the Direction of Stress**, Welding Research Institue 1976

2.6 Hobbacher A Cumulative **Fatigue by Fracture Mechanics**. International Institute of Welding Doc. IIW-XIII-873-78

2.7 Broke, D. **Elementary Engineering Fracture Mechanics**, Noordhoff International Publisher 1974

2.8 Gurney, T.R. **Fatigue of Welded Structures** Cambridge University Press 1979

2.9 Chang, J.B **Part-Through Crack Fatigue Life Prediction**, ASTM, STP 1979

2.10 Engle, R.M. Jr. **Aspect Ratio Variability in Part-Through Crack Life Analysis** ASTM STP 687

2.11 Newman, Jr. J.C. and Raju, I.S. "**An Empirical Stress-Intensity Factor Equation for the Surface Crack**, Engineering Fracture Mechanics 1981

2.12 Gurney, T.R., and Maddox, S.J., **A Re-analysis of Fatigue Data for Welded Joints in Steel**, Welding Research International, Vol. 3, No.4 1-54 1973

2.13 Fisher, J.W; Nussbaumer, A.C., Keating, P.B. and Yen B.T., **Resistance of Welded Details under Variable Amplitude Long-Life Fatigue Testing**, NCHRP Report 354, 1993

2.14 Alain Nussbaumer **Propagation of Loang Fatigue Cracks in Multi-Cellular Box Beams**, Ph.D Dissertation, Department of Civil Engineering, Lehigh University November 1993

2.15 C.R.Jordan and R.P. Krumpen, Jr. **Design Guide for Ship Structural Details** Report SSC-331 Ship Structure Committee 1990

2.16. **Structural Maintenance for New and Existing Ships**, Reports SMP 1-1 through 5-2, Department of Naval Architecture and Offshore Engineering, University of California at Berkeley, September 1992.

2.17 **Guide for the Fatigue Strength Assessment of Tanker**, American Bureau of Shipping, New York, NY 1992.

2.18 **Definition and Validation of a Practical Rationally-Based Method for the Fatigue Analysis and Design of Ship Hulls.** Society of Naval Architects and Marine Engineers T&R Report No. R-41

2.19 R.G.Bea **Marine Structural Integrity Programs.** Ship Structure Committee Report SSC-365

2.20 Vosikovsky, O. **The Effect of Stress Ratio on Fatigue Crack Growth Rates in Steels**, Engineering Fracture Mechanics 1979

2.21 D.A.Virkler, B.M. Hillberry, and P.K.Goel. **The Statistical Nature of Fatigue Crack Propagation**, Journal of Engineering Materials and Technology. Trans. ASME 1979

2.22 Besuner, P.M. **Fracture Mechanics and Residual Life Fatigue Analysis for Complex Stress Field**, EPRI 217-1, Electric Power Research Institute Technical Report 2 1975

Chapter 3

Stress Intensity Factors

3.1 Introduction

Fracture mechanics analysis and principles forms the basis for predicting the residual strength and fatigue life of a cracked CSD. A prerequisite for any such analysis is the knowledge of the stress intensity factor, K, for the problems under consideration. A large effort has been devoted into the computation of stress intensity factors during the last decades. Commonly used methods are empirical solutions, numerical analysis (e.g. finite element analysis), and superposition and influence-function method (Hybrid method).

This chapter presents the hybrid method for the computation of K for welded joints.

3.2 Stress Intensity Factors for Joints.

The method used in computing the stress intensity factor for joints in CSD is basically a superposition and influence-function method. It employs available solutions for two- and three- dimensional crack problems. From these the influence of different factors affecting K are separated and used to compose an estimate of K [3-1,3-2,3-5,3-8].

3.2.1 General Expression for K

The stress intensity factor can be expressed in a general form as :

$$K = K_B F \tag{3.1}$$

where :

K_B = stress intensity factor pertaining to "standard case".

F = correction factor that modifies K_B to account for the actual

configuration of the local geometry and crack geometry as

compared to the standard case.

The standard case for 2-D is a through crack of length 2a in an infinite plate with a remote uniform tensile stress acting normal to the crack. (Fig. 3.1[1]). The standard K solution is

$$K_{B2} = \sigma \sqrt{\pi a} \tag{3.2}$$

The standard 3-D case is an elliptical crack embedded in an infinite solid subjected to uniform tension (Fig. 3.2). The stress intensity factor along the boundary of the elliptical crack is (Mode I):

$$K_{B3} = \frac{\sigma \sqrt{\pi a}}{\varphi} (\frac{a^2}{c^2} \cos^2 \varphi + \sin^2 \varphi)^{0.25} \tag{3.3}$$

where φ is the complete elliptical integral and is given by:

---

[1]All the figures in chapter 3 are at the end of the chapter

36

$$\phi = \int_0^{\pi/2} \left\{ 1 - (1 - \frac{a^2}{c^2}) \sin^2 \phi \right\}^{0.5} d\phi \qquad (3.4)$$

It is shown that K_{B2} (relating to a straight curve front) differs from K_{B3} (relating to an elliptic, i.e. a curved crack front) by the expression :

$$\frac{1}{\phi} (\frac{a^2}{c^2} \cos^2 \phi + \sin^2 \phi)^{0.25} \qquad (3.5)$$

which accounts for the effect of the crack shape (a/2c) and position (ϕ) on the crack front.

A practical joint case usually differs from a standard case due to

- boundary effects , and

- stress gradients

Boundary- or, finite-dimension-, effects are taken into account through correction factor, as illustrated in Fig. 3.3

The "two dimensional crack" of Fig. 3.3b differs from the standard case of Fig. 3.1, by a finite width, this is taken into account through F_w.

The "two-dimensional crack" case of Fig. 3.3b differs from the standard case of Fig. 3.1 due to finite thickness and the crack emanation from a free surface. These are accounted through factors F_T and F_S respectively.

The "three-dimensional crack" case of Fig. 3.3c differs from the basic case of Fig. 3.2 as the crack emanates from a free surface, and as the body has a finite width and finite thickness. These deviations from the basic case are accounted for through the factors F_S, F_W and F_T.

The "two-dimensional crack" case of Fig. 3.4 differs from the basic case of Fig. 3.1 by the sheet curvature. It's taken into account through Fc.

Stress concentrations are synonymous with stress gradients. This stress condition is an important deviation from a basic case, and must be taken into account through a correction factor F_G.

Fatigue cracks may obtain various shapes (Fig. 3.3), e.g. the crack front may be straight or curved. The curvature (crack shape) is an important parameter influencing K. Thus, it is essential that this effects should be accounted for through a factor F_E. (elliptic shape factor). The solution for the 3-D standard case of Fig. 3.2 includes the effect of crack shape through expression (3.5). A curved crack front (a/2c > 0) specializes to a straight one as a/2c -> 0. The φ (and F_E) -> 1, and accordingly the standard stress intensity factors for the two- and three-dimensional case can be unified through the expression :

$$K_B = \sigma \sqrt{\pi a} F_E \qquad (3.6)$$

The standard solutions are elastic. Local plasticity around the crack tip may occur, however, and is in fact a prerequisite for fatigue cracking to occur. The effect of this plasticity on K is normally insignificant. However, the effect can be generally be taken into account through a plasticity correction factor F_P.

Implementing the above correction factors, F may generally be expressed as

$$F = F_s \bullet F_T \bullet F_W \bullet F_C \bullet F_G \bullet F_P \qquad (3.7)$$

Finally, K may be conveniently expressed as :

$$K = \sigma \sqrt{\pi a} \bullet F \tag{3.8}$$

by including F_E in the factor F, i.e.:

or

$$F = F_B \bullet F_C \bullet F_G \bullet F_P$$

i.e
$$F_B = F_E \bullet F_S \bullet F_T \bullet F_W \tag{3.9}$$

In the above expressions :

F_E = basic crack shape factor,

F_B = boundary correction factor, encompassing the total boundary,

F_S = front face correction factor, accounting for a free surface behind the crack

front,

F_T = back face or finite thickness correction factor, accounting for a free surface

ahead the crack front,

F_W = finite width correction factor, accounting for a free surface ahead of the

crack front,

F_C = cylindrical shell (i.e. curvature) correction factor,

F_G = stress gradient correction factor,

F_P = crack tip plasticity correction factor.

3.2.2 The basic crack shape factor - F_E

This factor takes into account the effect of crack front curvature, i.e., crack shape. It stems from Irwins solution for an elliptical flaw, embedded in an infinite elastic solid subject to uniform tension given in Eq. (3.3). Hence, the resulting F_E for any position along the crack front, describe by angle ϕ to the major axis (Figs 3.2 ,3.5) is :

$$\frac{1}{\varphi}(\frac{a^2}{c^2}\cos^2\varphi + \sin^2\varphi)^{0.25} \qquad (3.10)$$

This equation was derived on the basis of uniform tension across the crack surface. While it may argued that gradients will modify the result, this consideration is taken into account by the F_G correction described later. Likewise, this equation was derived for a crack embedded in an infinite elastic solid. Hence, it may be expected that the free surfaces encountered in practical case (finite body) will influence F_E. Thus, F_E can be interpreted as a factor that accounts for the (elliptical) crack shape without encompassing the complete shape-effect, only the related to the standard case. Parts of the effects are included in the F_S-, F_T- and F_G- estimates, as these are functions of a/2c. Hence, F_E is maintained in its original (i.e. standard case) form for stress intensity estimates. The dependence of F_E on crack shape is shown in Fig. 3.6.

φ is the complete elliptical integral of the second kind, as given in:

$$\varphi = \int_0^{\pi/2}\left\{1-(1-\frac{a^2}{c^2})\sin^2\phi\right\}^{0.5} d\phi \qquad (3.11)$$

A good approximation is obtained through the expression :

$$\varphi = \left\{1 + 4.5945(a/2c)^{1.65}\right\}^{0.5} \qquad (3.12)$$

hence,

$$F_E = \left\{1 + 4.5945(a/2c)^{1.65}\right\}^{-0.5} \qquad (3.13)$$

3.2.3 The Free Front Surface Correction Factor - Fs

This factor accounts for a free surface at the "mouth" of the cracks. (Fig. 3.3). Several expressions are proposed for the crack shape influence on Fs. A reasonable relation provides intermediate values is [3.6]

40

$$F_S = 1.122 - 0.18(a/2c) \qquad\qquad (3.14)$$

while the curved function in Fig. 3.8 provides upper bounds.

3.2.4 The Finite Thickness Correction Factor - F_T

This factor (also called "the back free surface correction factor") accounts for the effect of a finite plate thickness, i.e. a free surface ahead of the crack front (see Fig. 3.3). It depends on :

- crack geometry (size, shape),

- bending conditions (free, restrained) during cracking,

- crack opening stress distribution, and

- position on crack front.

Surface cracks are among the most common flaws in welded CSD. Consequently accurate stress intensity factors for such cracks are needed for reliable prediction of crack growth rates and fracture strengths. However, exact solutions are not available, but several solutions have been obtained by approximate methods. These solutions differ considerably. In reference [3.7] it was shown that the estimates compared varied by 6 per cent when a/2c > 0.3 and a/t < 0.5. Beyond these ranges deviations might exceed 100 per cent. Thus deviations are particularly large for small (a/2c) - ratios.

Two of the closed-form expressions available for uniform tension loading are :

$$F_T = \sqrt{\sec\frac{\pi a}{2t}} \qquad \text{when a/2c =0} \qquad\qquad (3.15a)$$

$$F_T = \sqrt{\frac{2t}{\pi a}\tan\frac{\pi a}{2t}} \qquad \text{when a/2c =0} \qquad\qquad (3.15b)$$

These are the forms most frequently cited in the literature, although in later years very often in modified version, [3.8]. They pertain to the symmetrical crack cases presented in Fig. 3.9, case 1 and 2.

These two expressions are also applicable to non-symmetrical crack configurations where bending is prevented by imposed boundary conditions. Hence, the strips in Fig. 3.9, case 1' and 2', are comparable to those in case 1 and 2. In ship CSD the roller supports might be provided by a web and /or stiffener.

F_T for an edge crack (a/2c =0, see Fig. 3.3) is quite sensitive to whether or not the section is permitted to bend as crack growth occurs. The bending tendency is natural for any strip in which crack growth is not symmetrical with respect to the strip centerline.

Bending amplifies the back surface correction - particularly at high values of a/t where more bending occurs. If the rollers on either strip of Fig. 3.9, case 1' and 2', are removed, the back surface correction must be modified, according to case 3.

It should be noted that the solution for case 3 is valid only when the displacement of the strip is free from constraint. In actual structures, any connected structural member is under constraints imposed by connections. When a crack occurs in a certain component, its compliance increases and load and deformation are redistributed between members. (Load shedding which will be discussed later in this project). Thus, the boundary condition is not displacement-free but displacement-limited.

Other examples of displacement constrained strips with a single edge crack are given in case 4 and 5. The in-plane transverse displacement at infinity is restrained.

In case 4 the local in-plane transverse displacement near the cracked section is not restrained, while it is in case 5.

The F_T - expressions pertaining to the above cases are given as following [3.8,3.9] :

-Case 1;

$$F_T = [1 - 0.025(a/b)^2 + 0.06(a/b)^4] \frac{1}{\sqrt{\cos \frac{\pi a}{2b}}}$$ (3.16)

surface crack : b=t

subsurface crack : b=t/2

-Case 2;

$$F_T = \frac{(1 - 0.122 \cos^4 \frac{\pi a}{2b})}{1.122} \sqrt{\frac{2b}{\pi a} \tan \frac{\pi a}{2b}}$$ (3.17)

Single crack : b=t

Double crack : b=t/2

-Case 3;

$$F_T = \left\{ \frac{0.752 + 2.02(a/b) + 0.37(1 - \sin \frac{\pi a}{2b})^3}{1.122 \cos \frac{\pi a}{2b}} \right\} \sqrt{\frac{2b}{\pi a} \tan \frac{\pi a}{2b}}$$ (3.18)

b=t

-Case 4;

$$F_T = \left\{ \frac{1.122 - 0.561(a/b) + 0.085(a/b)^2 + 0.180(a/b)^3}{1.122\sqrt{1 - a/b}} \right\}$$ (3.19)

b=t

-Case 5;

$$F_T = \sqrt{\frac{2b}{\pi a} \tan \frac{\pi a}{2b}}$$ (3.20)

b=t

43

The above expressions are plotted in Fig. 3.10 which clearly shows the effect of displacement constraint.

Within the computer program FRACTURE [3.9], the user decides which of these cases is closest to the actual case, and has the option to choose the appropriate F_T among the solutions for these cases.

For semi-elliptic surface cracks ($a/2c > 0$), the net ligament on either side of the crack inhibits bending, and significantly limits the crack from sensing the upcoming free surface. Therefore, any amplifications due to bending effects are likely to be small or negligible, as long as the crack is small compared to the cross sectional area of the body. Hence the choice between bending and no bending depends on the structural details as well as how the crack is growing (i.e. the crack shape). Fatigue crack growth at welded cover plates, stiffeners, gusset plates and other common girder attachments in ship structure is rarely symmetrical. Yet, bending is usually limited by virtue of the girder web and/or the attachment itself. Thus, no bending corrections are considered to be most applicable in typical ship structures.

The F_T - estimates adopted here, for semi-elliptic surface cracks are shown in Fig. 3.11 [3.7]. These pertain to the deepest point on the crack front. (i.e. point A in Figure 3.7).

It should be pointed out that all F_T corrections mentioned are strictly valid only in cases of uniform tension stress.

3.2.5 The Finite width Correction Factor - Fw

This correction factor accounts for the effect of finite width on K for a through crack. It is analogous to F_T for a part-through crack when a/2c=0 and, hence, the same expressions are used to estimate Fw by merely replacing t with W (plate width).

3.2.6 The Curvature Correction Factor -Fc

This factor accounts for the effect of the curvature of cylindrical shell upon the flat plate solution for K for a through crack. It may be expressed as [3.10] :

$$F_C = G_m + 2\frac{z}{t}G_b \qquad (3.21)$$

where $\qquad$ G_m = contribution due to membrane stresses

G_b = contribution due to secondary bending stresses (due to the cracking)

z = distance from shell "mid plane"

t = shell thickness

that is,

- On the outer surface : z=+t/2 $\qquad$; Fc = G_m + G_b

- On the inner surface : z=-t/2 $\qquad$; Fc = G_m - G_b

- On the shell mid plane :z =0 $\qquad$; Fc = G_m

G_m and G_b are functions of a / $\sqrt{Rt}$ (Fig. 3.12), where

2a = length of circumferential through crack (perpendicular to the cylinder axis)

R = radius of cylinder (tube)

In the computer program, Fc is set equal to its mean value, i.e. Fc = G_m.

45

3.2.7 The Stress Gradient Correction Factor - F$_G$

This factor (also called " the geometry correction factor") accounts for non-uniform crack opening stresses. i.e. stress field gradients at the crack locus [3.1-3.4,3.7]. The gradients may be due to e.g. non-uniform applied stress (such as bending) or stress concentration caused by detail body. This stress gradient should not be confused with that which occurs at the crack tip. F$_G$ represents a more global condition which is not acknowledged by a strength of materials analysis.

F$_G$ is conveniently derived from known solutions for K in the following manner. The solution of a crack stress field problem can be visualized as a two-step process [3.7,3.8] (Fig. 3.13):

1. The stress distribution problem is solved in a manner satisfying the boundary conditions (displacements, stresses) but with the crack considered absent.

2. To this stress field is superposed another stress field which cancels any stresses acting directly across the crack along the line of the crack.

Step 1 is a non-singular elasticity problem and can be solved by a FEM analysis. As the addition of a non-singular stress field ($\sigma(x)$, Step 1) does not affect the value of K (caused by -$\sigma(x)$, Step 2) the resulting K will be identical with that obtained from Step 2.

To evaluate K from Step 2, an influence (Green's) function method is employed. An influence function can be defined as :

$$G_1(b,a) = \frac{1}{p}K_{IP}(b,a) \qquad\qquad 3.22$$

where K_{IP} = due to a load P at $x = b$, and

P = load per unit sheet thickness / width

Hence, $G_I(b,a)$ is the K_I value arising from a unit force (per unit thickness/width) applied at abscissa $x = b$. $G_I(b,a)$ is independent of loading and depends merely on all the geometry parameters of the cracked body. If a solution for the stress intensity factor is known for any particular load system, then this information is sufficient to determine the stress intensity factor for any other load system.

A pressure $p(x)$ applied on an infinitesimal surface t(or W) dx results in an infinitesimal stress factor :

$$dK_I(x,a) = G_I(x,a) \bullet p(x)dx \qquad\qquad (3.23)$$

Thus, the K_I resulting from the total crack surface loading is

$$K_I = \int_0^a G_I(x,a) \bullet p(x)dx \qquad\qquad (3.24)$$

In the actual case $p(x) = -\sigma(x)$ = crack opening stresses (mode I). Hence, the stress distribution in step 1, although being a non-singular distribution, affects the strength of the singularity through this integral. The most significant general feature of G_I is the inverse square root singularity at the crack tip. This indicates that the stresses near the crack tip exerts a much greater influence on the strength of the singularity than the stresses far from it.

47

Values of K for intermediate crack sizes and the corresponding gradient correction factors can be computed by a simply repeating Step 2 for any desired crack size.

In a part- through crack case the computation of the stress gradient corrector F_G might be based on the following solution of the problem shown in Fig.3.14 [3.8] :

$$K_1 = \frac{2p}{\sqrt{\pi a}} \bullet \frac{1}{\sqrt{1-(b/a)^2}} \bullet F(b/a) \qquad (3.25)$$

Therefore the influence function in this case is :

$$G_1 = \frac{2}{\sqrt{\pi a}} \bullet \frac{1}{\sqrt{1-(b/a)^2}} \bullet F(b/a) \qquad (3.26)$$

With the condition of $p(x) = \sigma(x)$, yields

$$K_1 = \sqrt{\pi a} \bullet \frac{2}{\pi} \int_0^a \frac{\sigma(x)}{\sqrt{a^2 - x^2}} \bullet F(x/a) dx \qquad (3.27)$$

where $\sigma(x)$ can be obtained from a FEM analysis.

The stress distribution could be represented by a polynomial expression and could be integrated analytically. However it is more convenient to use a discretized stress distribution and the above equation then may be reformulated as :

$$K_1 \approx \sqrt{\pi a} \bullet \frac{2}{\pi} \sum_{i=1}^n \sigma_{bi} \bullet F(\overline{b_i}/a) dx \int_{b_i}^{b_{i+1}} \frac{dx}{\sqrt{a^2 - b^2}} \qquad (3.28)$$

where σ_{bi} = stress in block no. "i"

$b_i = 1/2(b_i + b_{i+1})$

The integration is carried out over the block width, and the summation over the number of blocks. After factoring out the nominal stress σ, applied remotely from the crack, integration leads to :

$$K_I = \sigma\sqrt{\pi a} \cdot \{\frac{2}{\pi}\sum_{i=1}^{n}\frac{\sigma_{bi}}{\sigma}\cdot F(\overline{b_i}/a)dx[\arcsin\frac{x}{a}]_{b_i}^{b_{i+1}}\}$$
$$= \sigma\sqrt{\pi a}\cdot\{\frac{2}{\pi}\sum_{i=1}^{n}\frac{\sigma_{bi}}{\sigma}\cdot w_{bi}\}$$
$$= \sigma\sqrt{\pi a}\cdot F \qquad\qquad (3.28)$$

where $\qquad$ wbi = weight of block no. "i".

In the underlying case of Fig. 3.15, i.e. an edge crack is a semi-infinite body, $F_T = F_E = 1.0$ according to the present terminology. Then F corresponds to $F_S \cdot F_G$ ($F_P := 1.0$), and hence, the stress gradient correction factor may isolated as :

$$F_G = \frac{F}{F_S} \qquad\qquad (3.29)$$

F_S depends on the stress distribution, and is equal to 1.122 for the case of uniform stresses acting over the whole area of an edge crack. A non-uniform stress-field with the stress peak at the surface accentuates the free surface effect, as indicated by the weight function in Fig.3.14. Thus, by expressing the gradient factor as :

$$F_G = \frac{F}{1.122} \qquad\qquad (3.30)$$

the stress gradient effect on Fs is included in FG. The resulting expression used in computing FG in the case of an edge crack might then be written as :

$$F_G = \frac{2}{1.122\pi} \sum_{i=1}^{n} \left\{ \frac{\sigma_{bi}}{\sigma} F(\overline{b}_i / a) \bullet [\arcsin \frac{b_{i+1}}{a} - \arcsin \frac{b_i}{a}] \right\} \qquad (3.31)$$

The computation of FG in the case of a through crack might be based on a solution of the problem in Fig. 3.16 [3.8] :

$$K_1 = \frac{2p}{\sqrt{\pi a}} \frac{a}{\sqrt{a^2 - b^2}} \qquad (3.32)$$

which is an exact solution in the case of symmetrically distributed opening stresses. A comparison of this Eqs. and part through thickness Eqs shows that they differ by the factor F(b/a), which thus is a factor accounting for the free surface effect.

FG for this case might be expressed as :

$$F_G = \frac{2}{\pi} \sum_{i=1}^{n} \left\{ \frac{\sigma_{bi}}{\sigma} [\arcsin \frac{b_{i+1}}{a} - \arcsin \frac{b_i}{a}] \right\} \qquad (3.33)$$

with   b ∈ (0, +a)

For more general case in Fig. 3.17 which is not symmetry in the stresses, i.e.

$$K_{1_a} = \frac{p}{\sqrt{\pi a}} \sqrt{\frac{a \pm b}{a \mp b}}$$

This case yields the following expression for FG :

$$(F_G)_{\pm a} = \frac{1}{\pi} \sum_{i=1}^{n} \left\{ \frac{\sigma_{bi}}{\sigma} [\arcsin \frac{b_{i+1}}{a} - \arcsin \frac{b_i}{a} \mp \sqrt{1 - (\frac{b_{i+1}}{a})^2} \pm \sqrt{1 - (\frac{b_i}{a})^2}] \right\} \qquad (3.34)$$

50

where $b \in (-a, +a)$

It should be noted that the F_G - estimate for a part-through crack is conservative when a/2c >0. The conservatism increase as the stress concentration and the crack front curvature increase.

3.2.8 The Plasticity Correction Factor - F_P

This correction factor accounts for the effect of crack tip plasticity on ΔK. Irwin suggested that the effect of small plastic zones corresponding to an apparent increase of the elastic crack length by an increment (r_P) equal to half the plastic zone size (R_P).

The plastic zone size may be written as [3.7] :

$$R_p = \kappa (\frac{\Delta K}{\sigma_y})^2 \tag{3.35}$$

where ΔK = stress intensity factor range

σ_y = monotonic, uniaxial yield stress

κ = coefficient depending on

- type of loading, i.e. monotonic/ cyclic

- stress state , i.e. plane stress/plane strain

Thus, the crack length correction is :

$$r_p = \frac{\kappa}{2} (\frac{\Delta K}{\sigma_y})^2 \tag{3.36}$$

ΔK might be expressed as :

$$\Delta K = \Delta\sigma \sqrt{\pi a} \cdot F_1 \tag{3.37}$$

where F_1 = product of all correction factors except F_P

Taking plasticity into account, the corrected ΔK then is

$$\Delta K^* = \Delta\sigma\sqrt{\pi(a + r_p)} \bullet F_1$$
$$= \Delta\sigma\sqrt{\pi a}\sqrt{1 + \frac{\kappa}{2a}(\frac{\Delta K}{\sigma_y})^2} \bullet F_1 \tag{3.38}$$

Accordingly, the plasticity correction factor might be expressed as :

$$F_p = \sqrt{1 + \frac{\kappa}{2a}(\frac{\Delta K}{\sigma_y})^2} \bullet F_1 \tag{3.39}$$

The plastic zone size coefficient κ is an input parameter to the program. Interesting values for κ are :

$$\kappa = 1/24\pi \qquad \text{; cyclic plane strain}$$

$$\kappa = 1/8\pi \qquad \text{; cyclic plane stress}$$

F_P will usually be close to one for fatigue crack propagation under nominally elastic stresses. It is very often ignored in high-cycle fatigue situations. However, it should be noted that crack tip plasticity affects crack growth (and fatigue life) more than it affects ΔK. This is because ΔK is typically raised to the power 3 in the crack growth equation.

3.3 Stress Intensity Factor for Cutout

Determination of the stress intensity factor for a cutout is relatively complicated. A cavity (pore) model is used to approximate it. stress intensity factor for a penny-shaped

crack (in an infinite solid) with normal stress distribution having circular symmetry [3.9] is

$$K = \frac{2}{\sqrt{\pi a}} \int_0^a \frac{\sigma(r)r}{\sqrt{a^2 - r^2}} dr$$

$$\approx \sqrt{\pi a} \frac{2}{\pi} \frac{1}{a} \sum_{i=1}^n \sigma_{bi} \int_{b_i}^{b_{i+1}} \frac{r}{\sqrt{a^2 - r^2}} dr$$

$$\approx \sqrt{\pi a} \left\{ \frac{2}{\pi} \frac{1}{a} \sum_{i=1}^n \frac{\sigma_{bi}}{\sigma} \left[-\sqrt{a^2 - r^2} \right]_{b_i}^{b_{i+1}} \right\}$$

$$\sqrt{\pi a} \left\{ \frac{2}{\pi} \frac{1}{a} \sum_{i=1}^n \frac{\sigma_{bi}}{\sigma} \left[\sqrt{a^2 - b_i^2} - \sqrt{a^2 - b_{i+1}^2} \right] \right\}$$

$$\approx \sigma \sqrt{\pi a} \bullet F_E \bullet F_G \qquad \text{(no boundaries)} \qquad (3.40)$$

For a Penny-shaped crack   ->   a/2c = 0.5   -> $F_E = 2/\pi$

$$F_G = \frac{1}{a} \sum_{i=1}^n \left\{ \frac{\sigma_{b_i}}{\sigma} (\sqrt{a^2 - b_i^2} - \sqrt{a^2 - b_{i+1}^2}) \right\} \qquad (3.41)$$

The stress intensity factor for a penny-shaped crack emanating from a spherical cavity (pore) :

$$K = \frac{2}{\sqrt{\pi a_e}} \int_R^{a_e} \frac{\sigma(r) \bullet r}{\sqrt{a_e^2 - r^2}} dr \qquad (3.42)$$

where : $2a_e$ = effectively crack length (Fig.3.20)

         $\sigma(r)$ = stress distribution at spherical cavity, i.e. [3.11]

and

$$\sigma(r) = [1 + 0.2237(\frac{R}{r})^3 + 0.8182(\frac{R}{r})^5]\sigma \qquad (3.43)$$

where σ = nominal stress at the cavity

53

Thus the crack-and-pore geometry (Fig3.20a) is treated as a penny-shaped crack with radius a_e (Fig.3.20b) to approximate the crack cutout. Stress concentration effect due to the pore is accounted for employing the above equation in computing the block stresses.

3.4 Summary and Conclusion

This chapter presents the hybrid methodology for the computation of the stress intensity factors. The hybrid method is basically an influence function - and a superposition method. It employs available solutions for two- and three dimensional crack problems. From these the influence of different factors affecting K are separated and used to compose an estimate of K for actual case as :

$$K = \sigma \sqrt{\pi a} \cdot \prod F_i$$

4.44

where Fi are correction factors for different influences

3.5 References

3.1 Structural Maintenance for New and Existing Ships Project. Research Reports SMP1-1 - SMP 5-2. Dept. of Naval Architecture & Offshore Engineering, University of California at Berkeley, Berkeley, CA 94720. October 1992

3.2 Ship Structural Maintenance Project. Research Reports FACTS1-1, SMP II 1-1 - SMP II 1-3, SMP II 2-1, RMS-1. Dept. of Naval Architecture & Offshore Engineering, University of California at Berkeley, Berkeley, CA 94720. October 1993

3.3 Ship Structural Maintenance Project. Research Reports SMP III-1 - SMP III-2, SMP III-3. Dept. of Naval Architecture & Offshore Engineering, University of California at Berkeley, Berkeley, CA 94720. October 1994

3.4 Fatigue Handbook, Offshore Steel Structures. Tapir, 1985 A. Almar-Naess

3.5 Stress Gradient Correction Factor for Stress Intensity at Welded Stiffeners and Cover Plates. Welding Research Supplement, Vol. 56, No. 12, 1977 Zettlempoyer, N. and Fisher, J.W.

3.6 Life - A Computer Program for Fracture Mechanics Analysis of Crack Growth in Welded Structural Components. SINTEF Report 84-44. K. Engesvik, 1984. Trondheim Norway.

3.7 A Review and Assessment of the Stress-Inyensity factors for Surface Cracks. Part-through Crack Fatigue Life Prediction, ASTM STP 687, 179. Newman, Jr. J.C

3.8 Probabilistic Analysis of the Uncertainty in the fatigue Capacity of Welded Joints. Engineering Fracture Mechanics. Vol. 18, No. 4 1983. Engesvik, K.M and Moan, T

3.9 The Stress Analysis of Cracks Handbook. Del Research Corportation, Hellertown, Pennsylvania, 1973. Tada, H., Paris, P.C. and Irwin, G.R

3.10 Compendium of Stress Intensity Factors. London, HMSO, 1976 Rooke, D.P. and Cartwaright, D.J.:

3.11 A Critical Analysis of Crack Propagation Laws. Journal of basic Engineering. Dec 1963. P.Paris and F.Erdogan.

3.12 An Analysis of fatigue Cracks in Fillet Welded Joints. International Journal of Fracture, Vol. 11 No. 2 1975. Maddox, S.J.
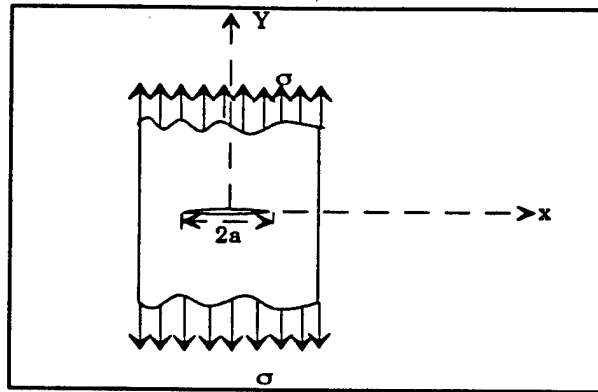
Fig. 3.1 Two-dimensional standard case : Through crack in an infinite

sheet subjected to uniform tension
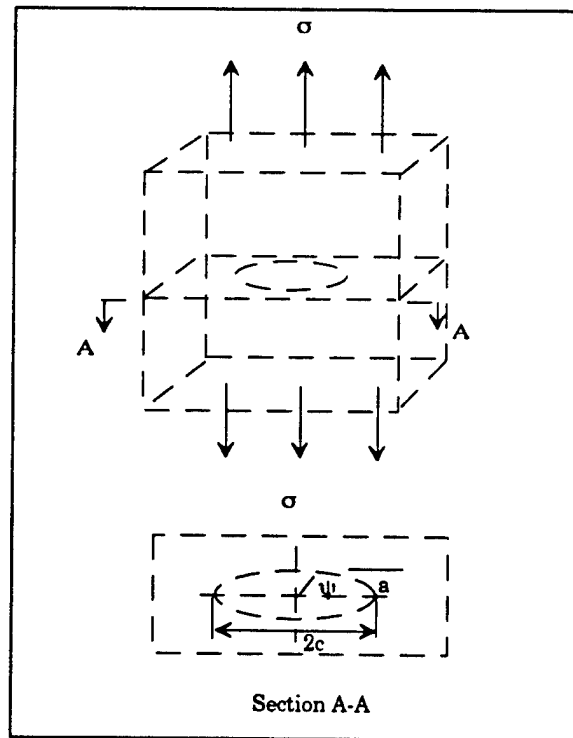
Fig. 3.2 Three-dimensional standard case : Embedded elliptical crack

in an infinite solid subjected to uniform tension.
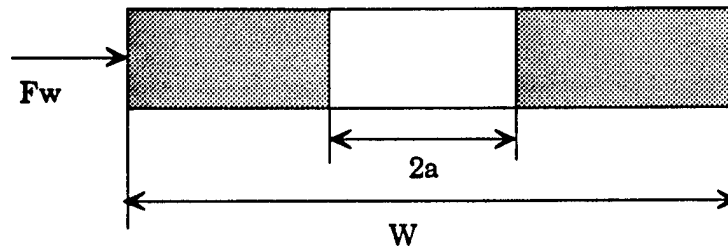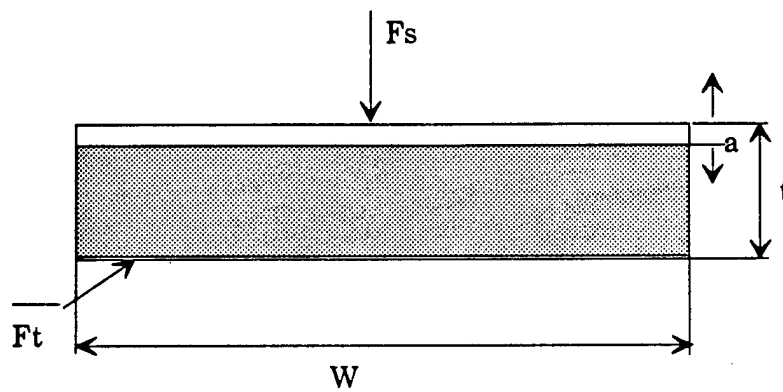
a) "Through" Crack

b) "Edge" Crack
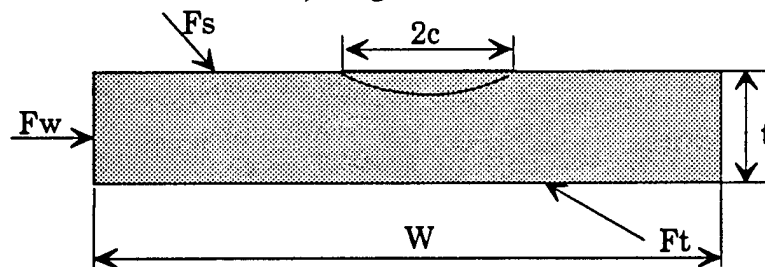
c) "Surface" crack

Fig. 3.3 Plate Cross-Section with various Crack Geometries.

Free Surface and Related Correction Factors
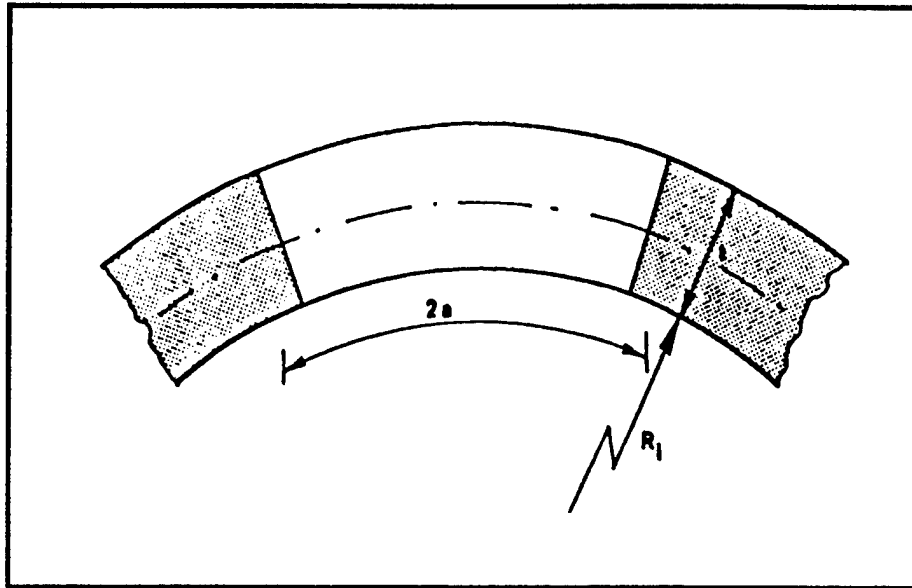
Fig. 3.4 Through Crack in a Curved Sheet
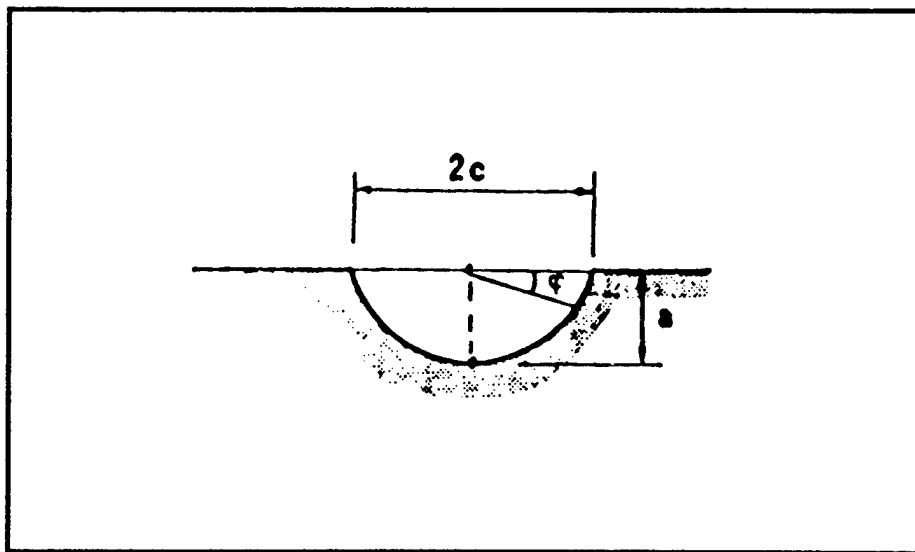
Fig. 3.5 Crack Front as Given by the Angle φ
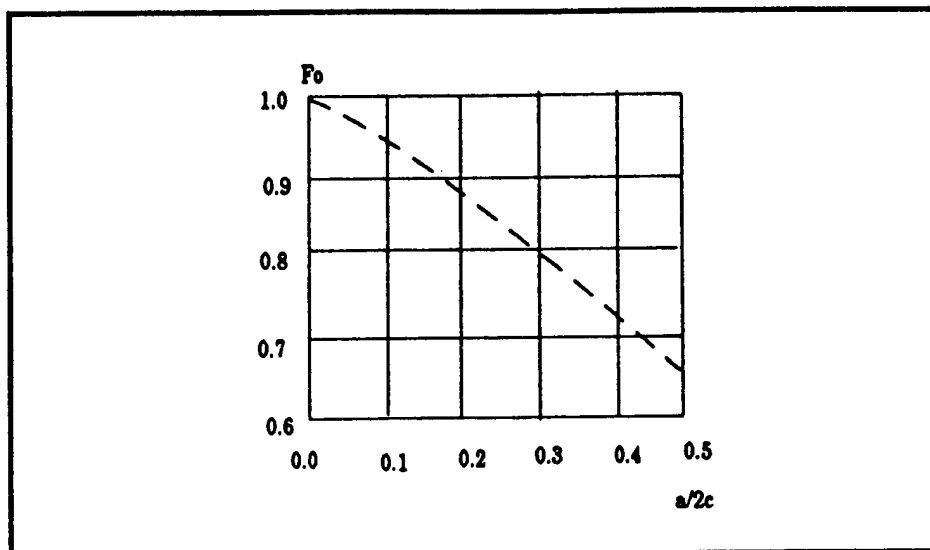
Fig 3.6 The Basic (elliptic) Shape Correction Factor
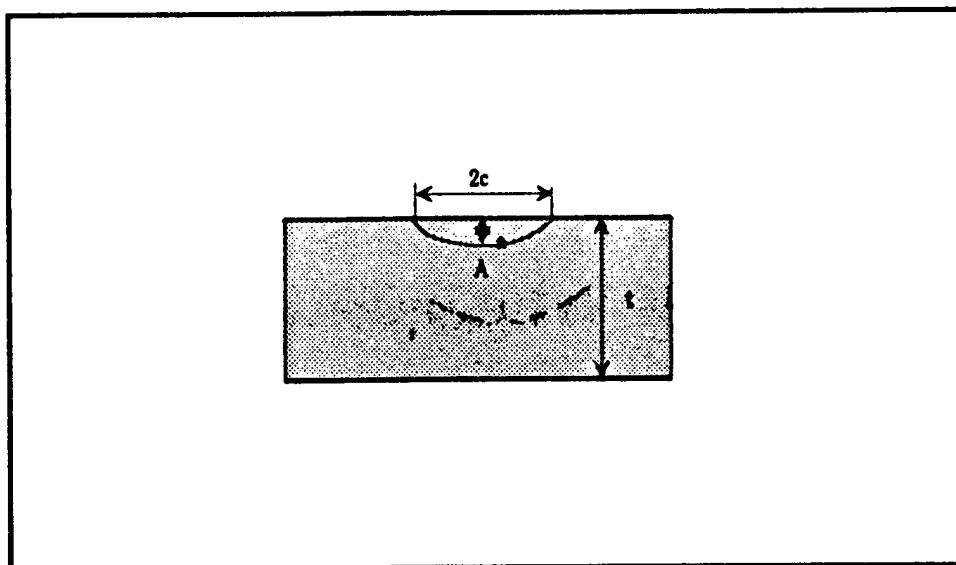
Fig 3.7 Semi-elliptic Surface Crack
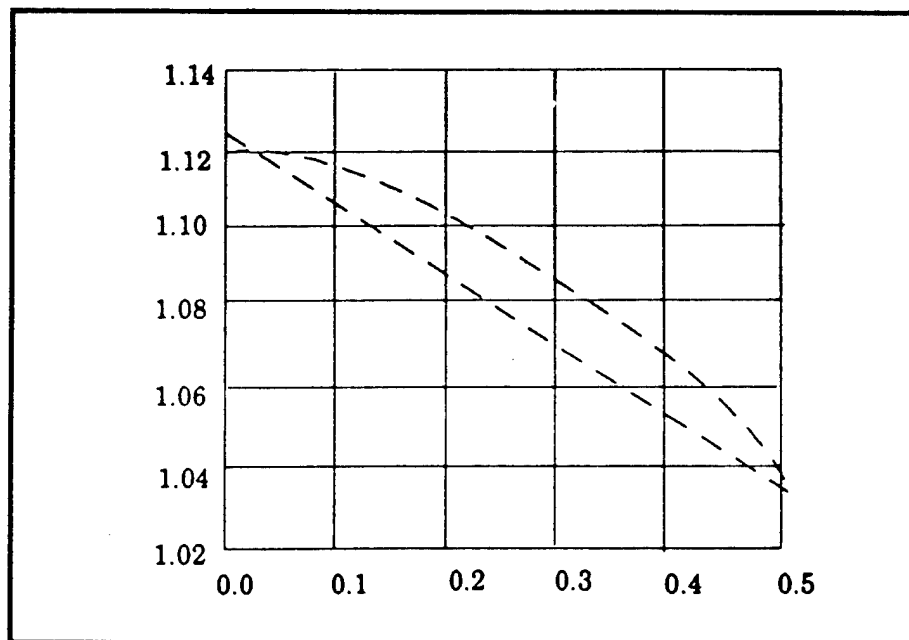
Fig 3.8 The Front Free Surface Correction Factor
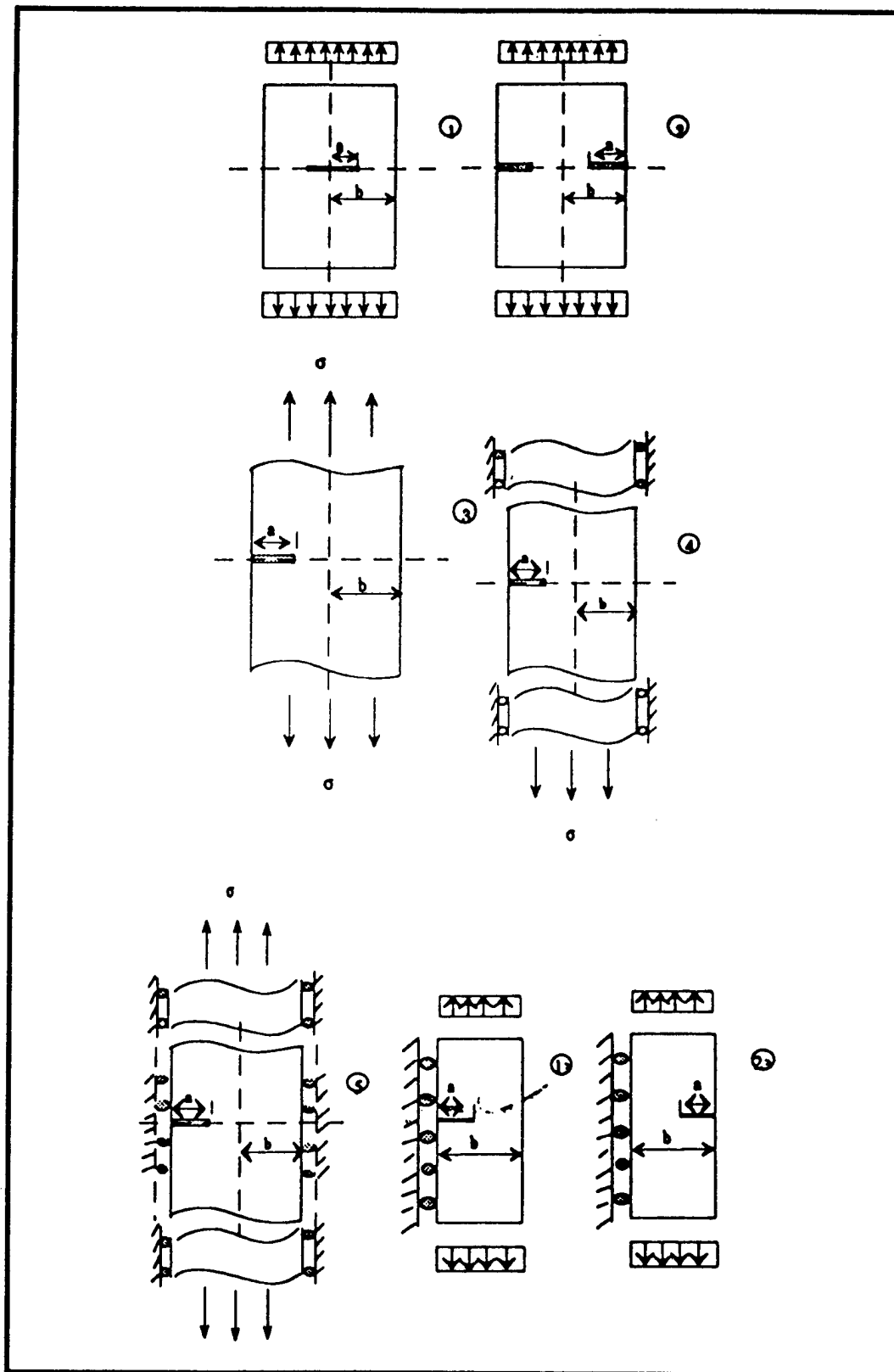
Fig. 3.9 Various Cases of Cracking and Boundary Conditions

61
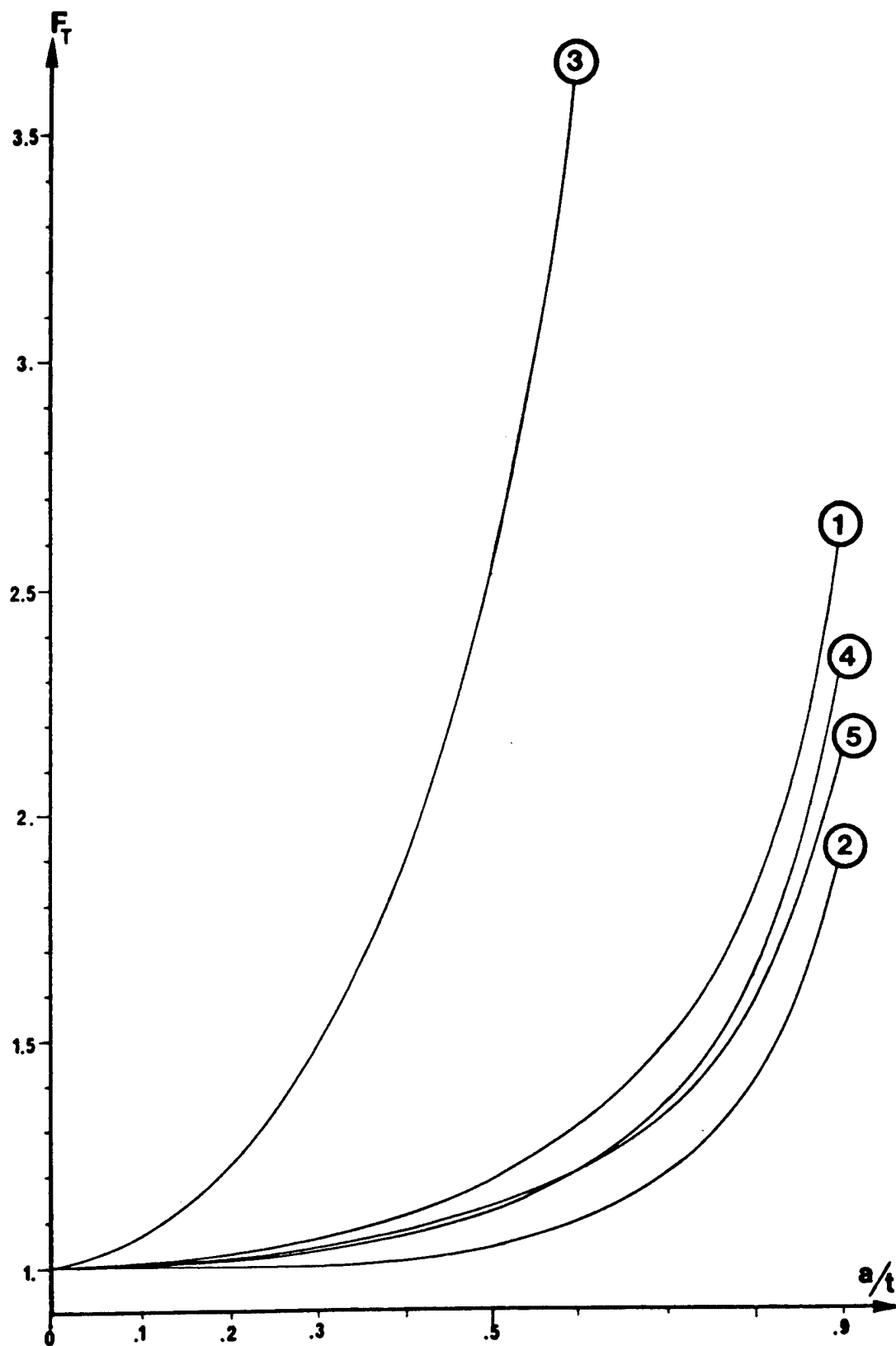
Fig. 3.10 The Finite Thickness Correction Factor Straight Crack Front (a/2c=0)
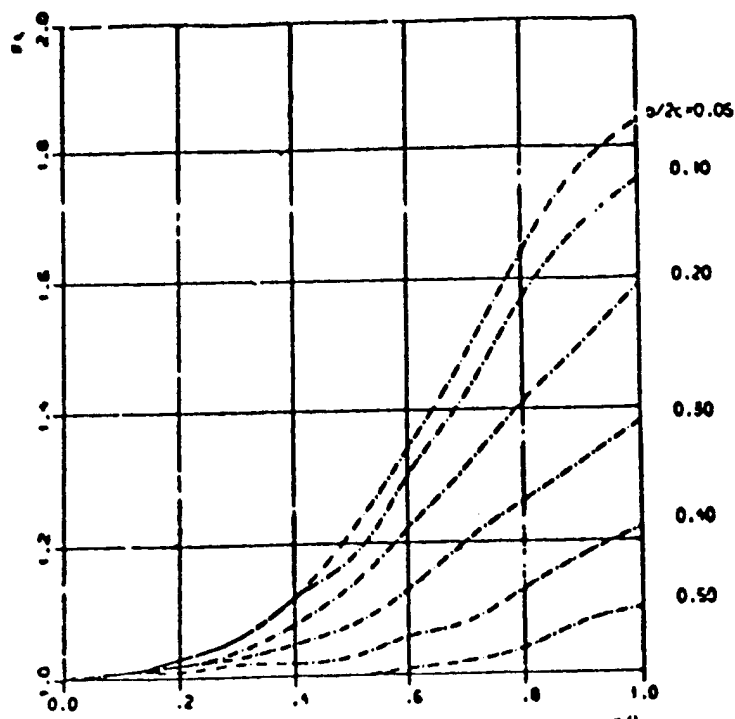
Fig 3.11 The Finite Thickness Correction Factor Curved Crack Front (a/2c >0)
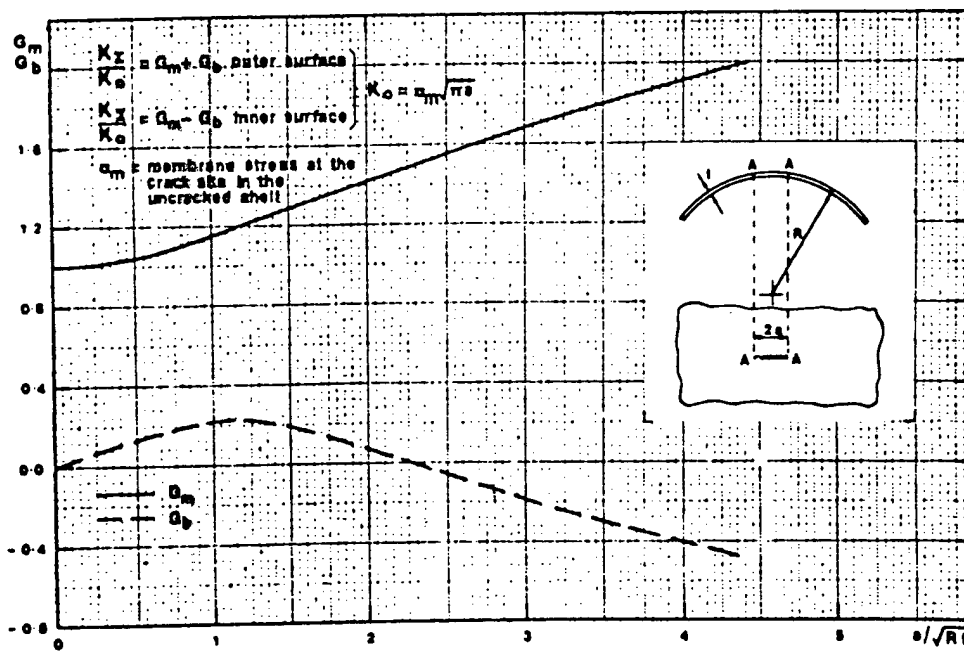
Fig. 3.12 KI for point A of a Circumferential Crack in a Cylindrical Shell Subjected to a

Uniform Membrane Stress [3.10]
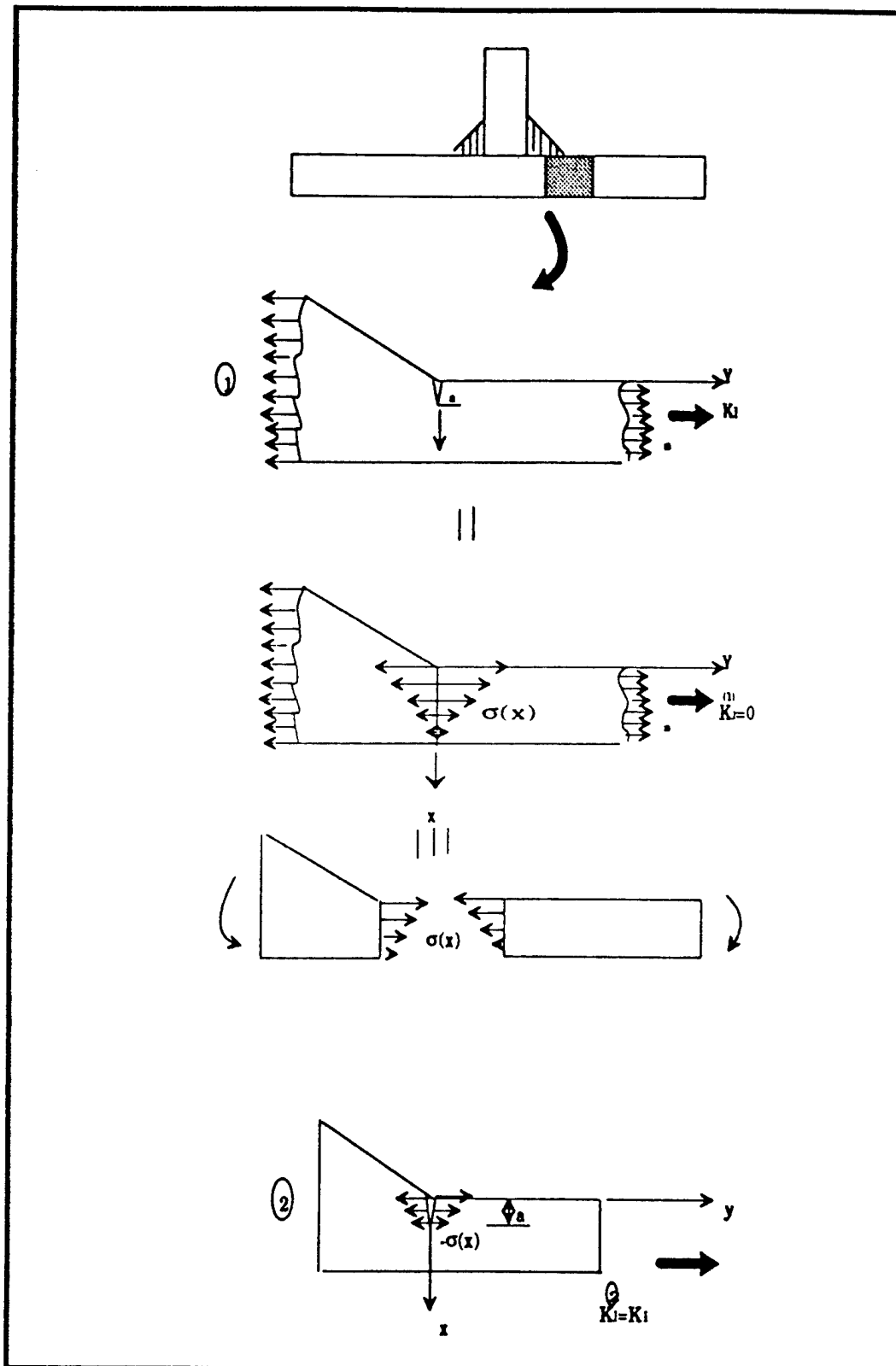
Fig. 3.13 Superposition of Stresses in a Welded Joint
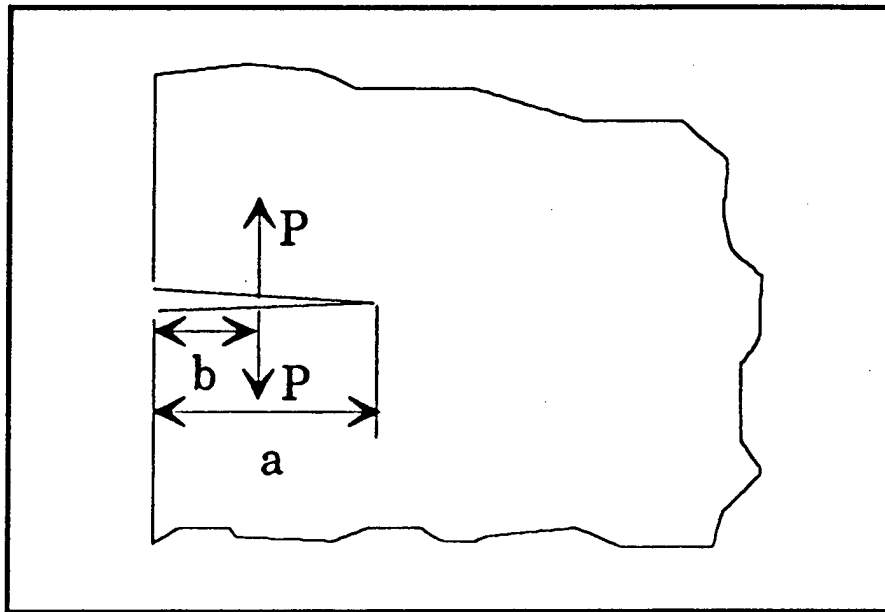
$$K_1 = \frac{2p}{\sqrt{\pi a}} \cdot \frac{a}{\sqrt{a^2 - b^2}} \cdot F(b/a)$$
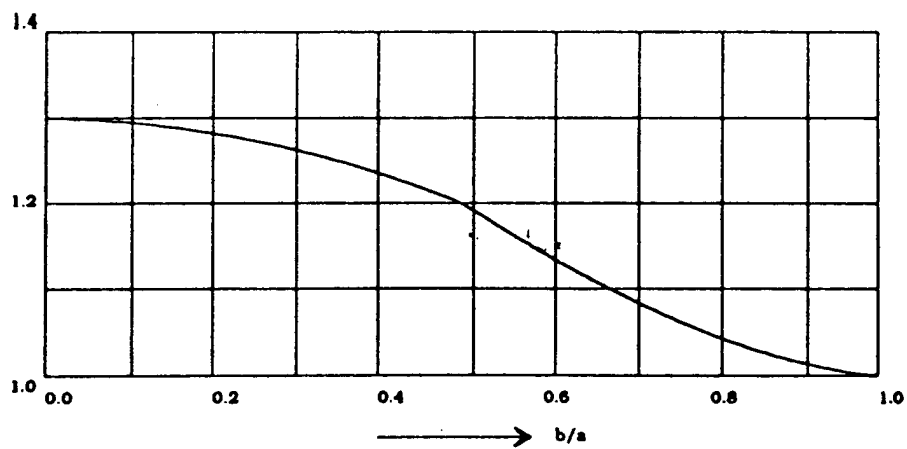
Fig. 3.14 Calculation of K-value by a pair of Splitting Forces applied to the Crack Surface

65
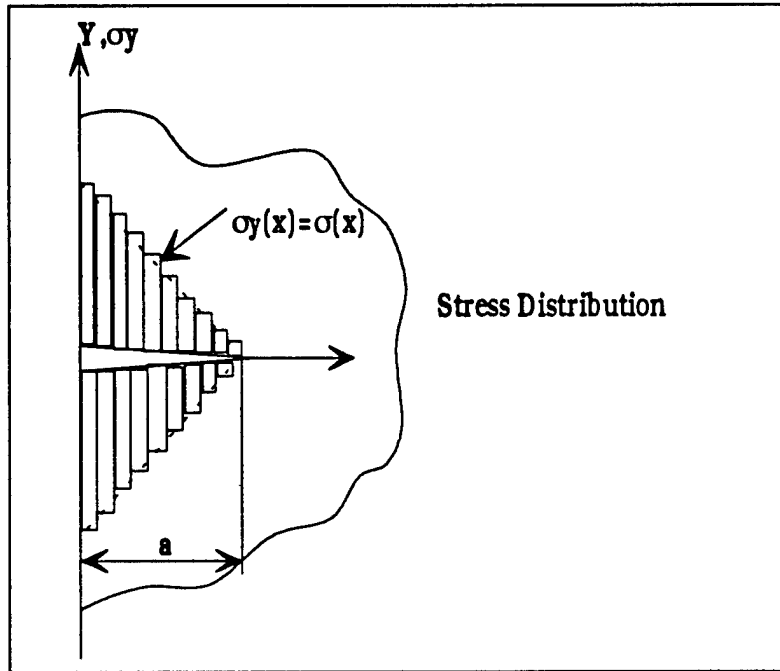
$$K_1 = \frac{2}{\pi} \sqrt{\pi a} \sum_{i=1}^{n} \left\{ \sigma_{b_i} F(\overline{b}_i / a) \bullet \arcsin(x / a)\Big|_{b_i}^{b_{i+1}} \right\}$$

$$\overline{b}_i = 1 / 2(b_i + b_{i+1})$$

Fig. 3.15 Discretized stress distribution

$$\{K_1\}_{\pm} = \frac{P}{\sqrt{\pi a}} \cdot \sqrt{\frac{a \pm b}{a \mp b}}$$
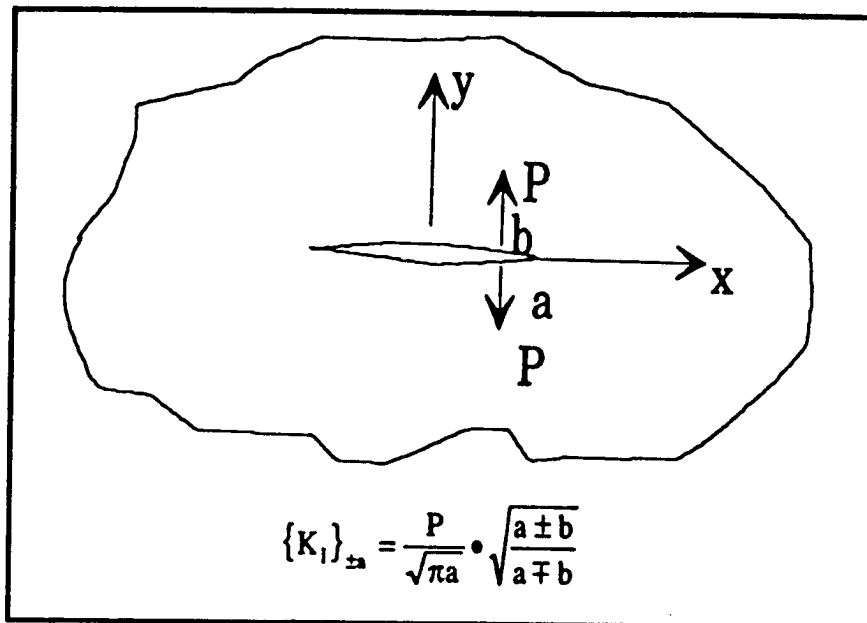
Fig 3.16 Two Pairs of Splitting Forces on a Through Crack in an Infinite Sheet

$$K_1 = \frac{2P}{\sqrt{\pi a}} \cdot \frac{a}{\sqrt{a^2 - b^2}}$$
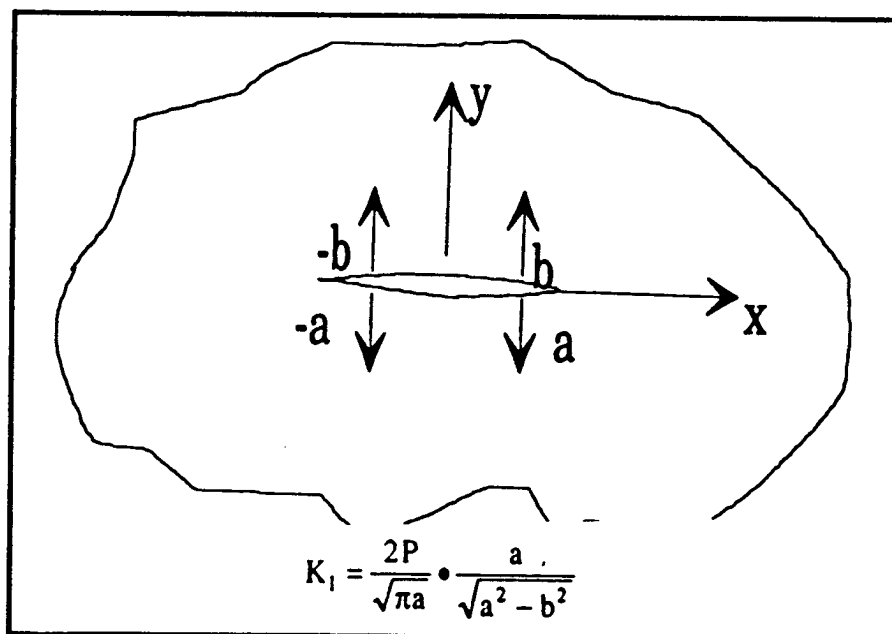
Fig. 3.17 One Pair of Splitting Forces on a Through Crack in an Infinite Sheet
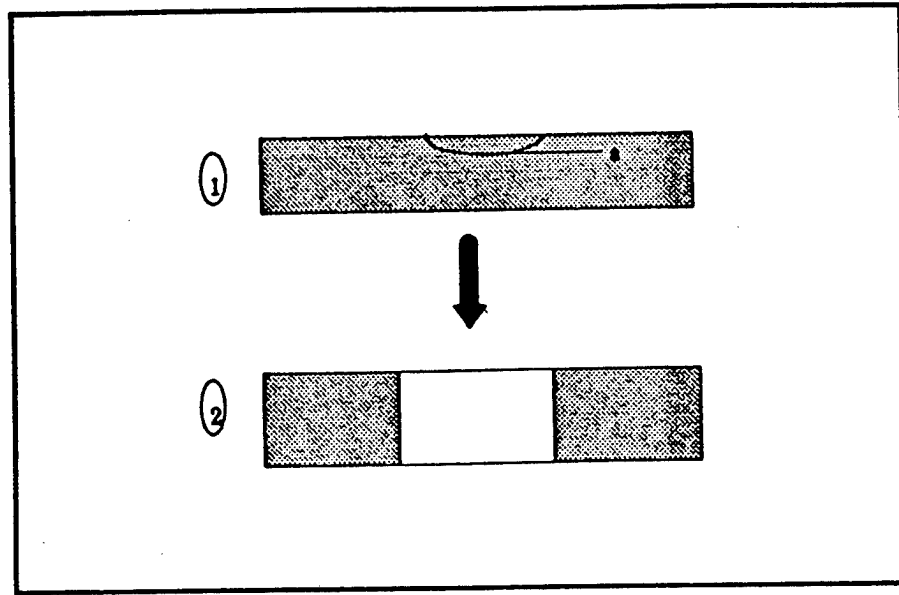
Fig. 3.18 Stages of Crack Growth
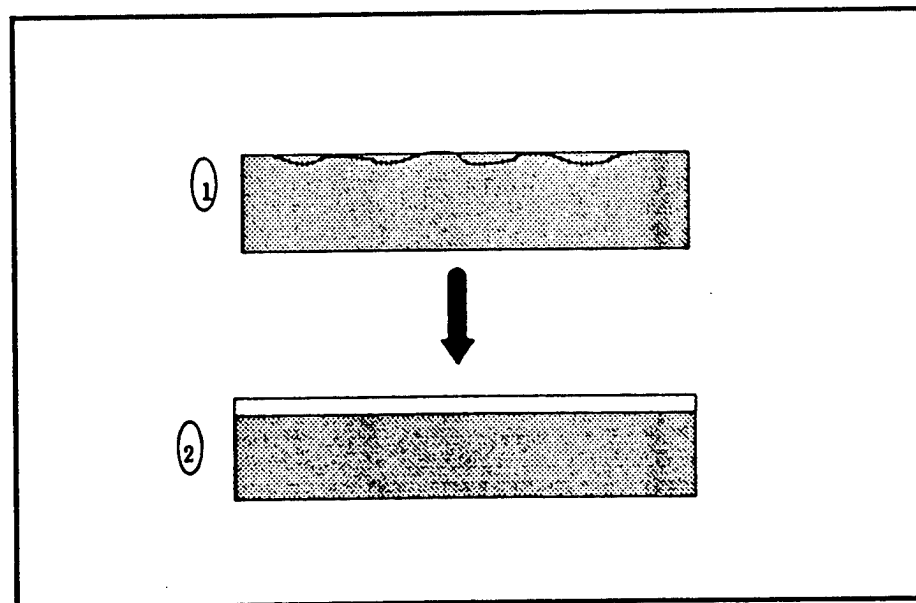
Fig. 3.19 Phases of Crack Growth in Stage 1
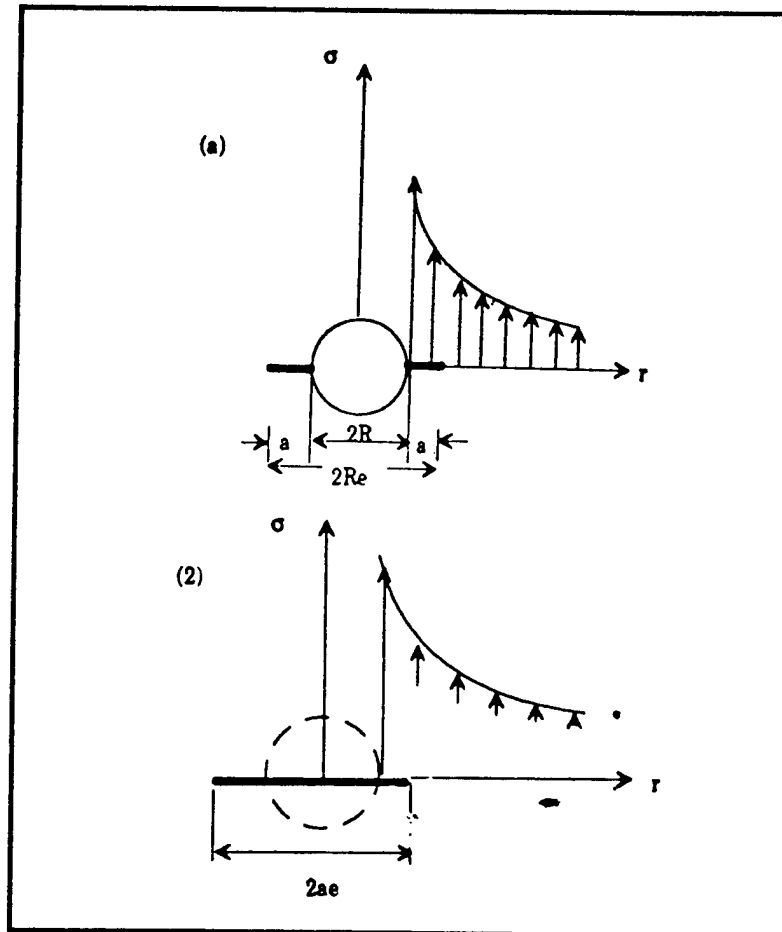
Fig 3.20 Penny-shaped Crack emanating from Spherical Cavity

Chapter 4

S-N Curve Development

4.1 Introduction

The conventional S-N fatigue design method based on the Miner's damage accumulation rule is applicable to tanker CSD with the S-N selections determined by fatigue experiments. More reliable prediction of the fatigue resistance of CSD may be achieved by testing real CSD that represent the actual condition of fabrication, loading and enviroment as far as possible. Due to the expense of these tests, small specimens test are conducted to deine the S-N relationship. However, numerical method can provide an complimentary approach to estimate the fatigue resistance of the structural details. In the following, such a methodology is presented.

In the following, a numerical method of the prediction of the fatigue behavior of CSD is presented which allows one to classify structural details with a few tests. This method includes the local notch approach for the estimation of the crack initiation phase, and the fracture mechanics for the crack propagation phase.

4.2 Development of General S-N Curves

The objective of the following development is to determine the $\Delta\sigma$ - Nt curve numerically.

The total fatigue life Nt of a structural detail is considered to be composed of the crack initiation phase Ni and the consequent crack propagation phase that is limited by the failure of the structure. (Fig. 4.1)

$$N_t = N_i + N_p \tag{4.1}$$
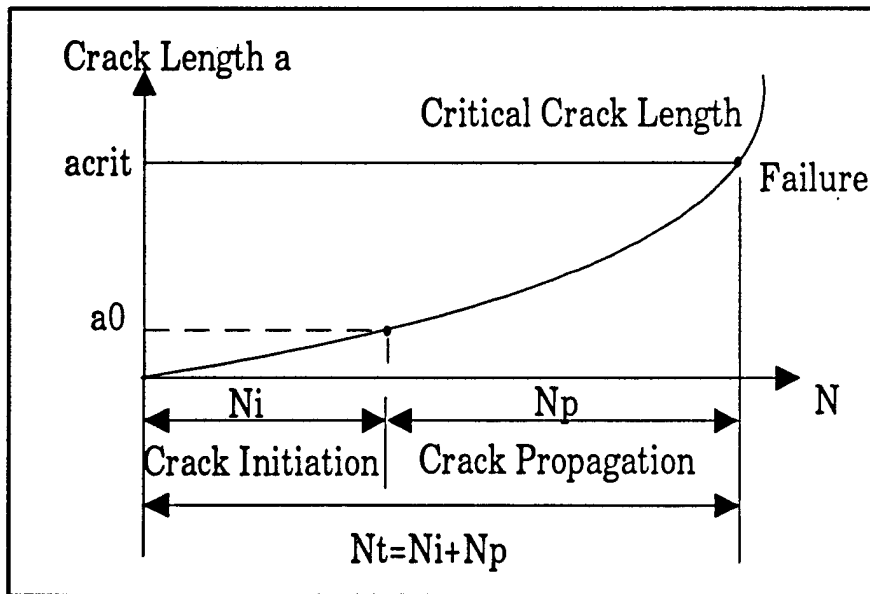
Fig. 4.1 Total Fatigue Life Nt

The crack initiation phase is described by the local notch approach and assumed to be limited by the formulation of the initial crack size ao. The crack initiation phase yields the part N_i of the total fatigue life N_t.

The residual number of the load cycles N_p is considered to be produced by crack propagation starting with the initial crack size ao. The crack growth is modeled with the Paris equation. The crack propagation phase is limited by the formulation of the critical crack size a$_{crit}$ which is determined by material property. It's usually recognized that the crack initiation can be neglected for welded structures. But it's still documented here in order to present a general approach.

4.2.1 Crack Initiation Phase

The local notch approach method is used for determining the crack initiation life Ni of a detail until a crack size ao is achieved.

It is assumed that the fatigue behavior of the material at a structural detail, where due to notch effects high local strains will form and the initiation of cracks is expected, can be represented by the fatigue behavior of small test specimen with an equivalent strain history.

For the case of a fatigue loading with the mean stress $\sigma_m = 0$ the material behavior can be described by the cyclic stress-strain curve $\sigma_a - \varepsilon_a$, the strain wholer curve $D_{mod} - N_i$, (Fig. 4.2). As a damage parameter in general, the factor :

$$D_{mod} = \sqrt{\sigma_a \varepsilon_a E} \qquad (4.2)$$

according to Smith, Watson, Topper [4.7]

The determination of the local stresses and strains at a fatigue detail is usually determined by the Neuber's rule, Fig.4.3

72

$$(\sigma_a \varepsilon_a)_{notch} = K_f^2 \Delta\sigma_{nom} \Delta\varepsilon_{nom} \qquad (4.3)$$

where K_f is the elastic notch factor

$$K_f = \frac{\Delta\sigma_{notch}}{\Delta\sigma_{nom}} \qquad (4.4)$$

determined by finite element analysis.
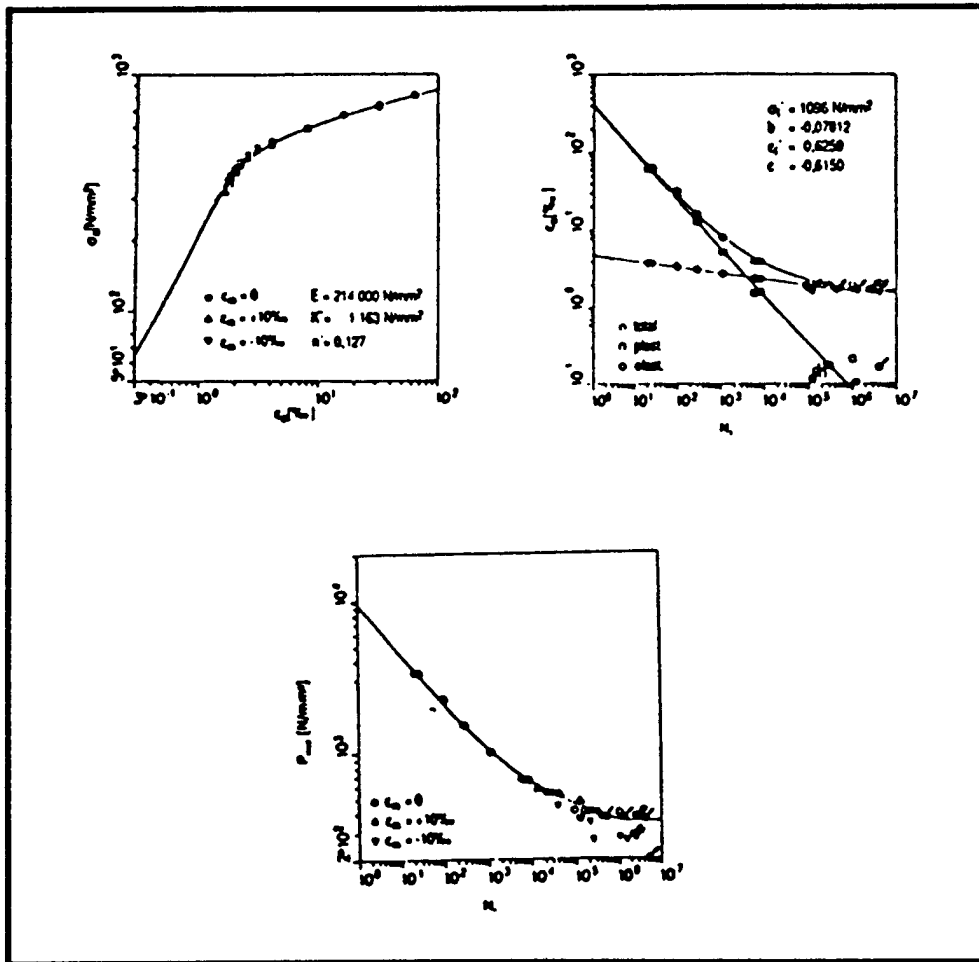
Fig. 4.2 Description of material Behavior

In using this equation $\Delta\sigma_{notch} - N_i$ curves can be produced for details with different elastic notch factor K_f.(Fig. 4.4)

73
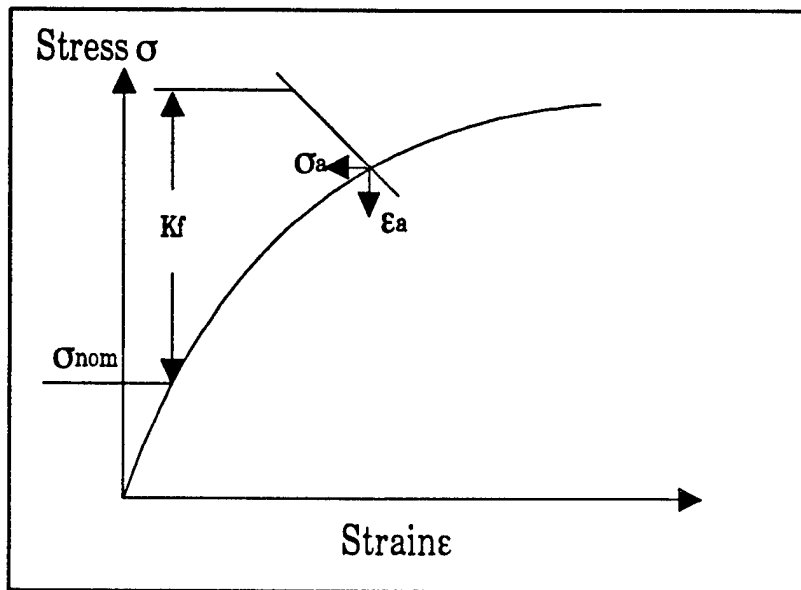
Fig. 4.3 Neuler Rule
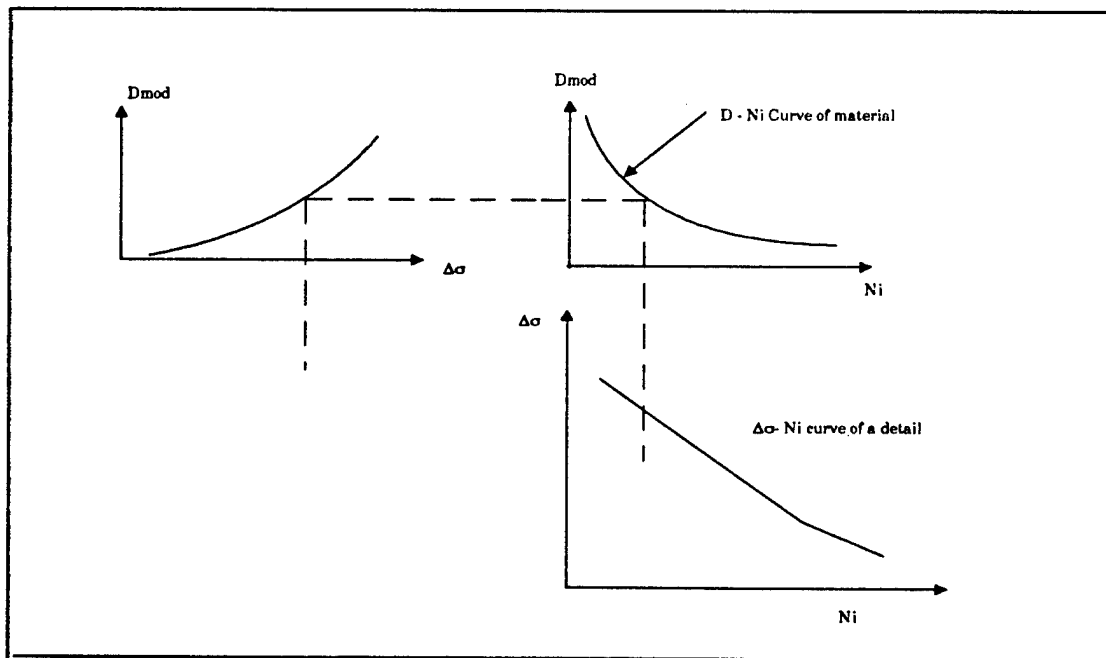
Fig 4.4 Determination of a Detail $\Delta\sigma - N_i$ Curve

4.2.2 Crack Propagation Phase

The fatigue life, N_p, after crack initiation is determined by linear fracture mechanics (Paris-equation). The residual life is determined as the crack propagates from the initial crack size, ai, to the critical size, a_{crit}, that cause failure (see Fig. 4.5).
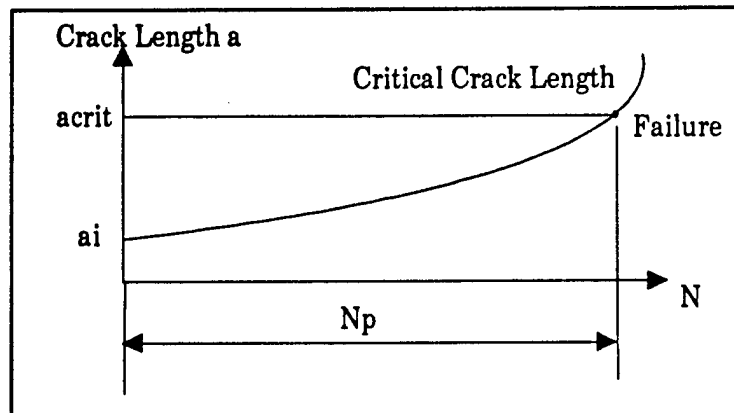
Fig. 4.5 Fatigue Life N_p

In linear elastic fracture mechanics, the behavior of a crack is characterized by the stress intensity factor, K. The evaluation of the stress intensity factors is presented in the previous chapter. From the knowledge of the range of K occurring at the crack tip, an estimate of the growth can be made.

The stress intensity factor for a classical center through-thickness crack in an infinite plate is given by :

$$K_0 = \Delta\sigma\sqrt{\pi a} \tag{4.5}$$

where a is the crack length, and $\Delta\sigma$ is the uniformly applied far field stress.

The stress intensity factor for a crack in a finite geometry can be written in the following general form:

$$K = FK_0 \tag{4.6}$$

where F is called the total correction factor and is a function of the crack length and dimensions of structural and crack geometry.

It is usual to assume that the growth of a crack is according to Paris' law, i.e :

$$da / dN = C(\Delta K)^m \tag{4.7}$$

where da/dN is the crack growth rate per cycle; ΔK is the range of stress intensity factor occurring at the crack tip, and C and m are material constants.

Substitution of Equations (4.5) and (4.6) into Equation (4.7) leads to :

$$da / dN = C(\Delta \sigma F \sqrt{\pi a})^m \tag{4.8}$$

Prediction of total number of cycles, N, required to grow the crack from an initial length of a_i to the final length of a_f can be obtained by directly integrating above Equation, or :

$$N = \frac{1}{C\pi^{m/2}} \int_{a_i}^{a_f} \frac{a^{-m/2}F^{-m}}{(\Delta \sigma)^m} da \tag{4.9}$$

The above integration can easily be carried out if the applied stress range $\Delta \sigma$ and the normalized stress intensity factor are constant. However, in general, the load the tanker structure experienced is not constant; and except for few crack geometry, is almost always a function of the crack length. These make the direct integration difficult.

Therefore, a numerical integration technique is normally used in predicting the total crack growth cycles, N.

4.3 Development of Cracked S-N Curves

As discussed earlier, the fracture mechanics analysis can be applied in the fatigue crack propagation analysis to provide insight into the crack growth of CSD. The conventional fracture mechanics approach presented in chapter 2 and 3 is somehow cumbersome to use. A strong incentive exists to simplify the approach to make it practicable to predict the remaining fatigue life of cracked CSD.

Based on Paris Equation, we can derive the following expression under the constant loading:

$$N_p = \frac{1}{C \bullet \Delta\sigma^m \pi^{m/2}} \int_{a_i}^{a_f} \frac{da}{a^{m/2} \bullet F^m} = \frac{I}{C_1 (\Delta\sigma)^m} \qquad (4.9)$$

where I is the following integral:

$$\int_{a_i}^{a_f} \frac{da}{a^{m/2} \bullet F^m} = I \qquad (4.10)$$

This yields further:

$$\Delta\sigma = \sqrt[m]{\frac{I}{C_1 \bullet N_p}} \qquad (4.11)$$

and

$$\log \Delta\sigma = -\frac{1}{m}\log N_p - \frac{1}{m}\log C_1 + \frac{1}{m}\log I \qquad (4.12)$$

77

$$\log \Delta\sigma = A \log N_f + B(a_i) \qquad (4.13)$$

This is the equation for cracked S-N curves. From the different initial crack size (the inspection size a_{insp}), equivalent S-N curves for cracked detail can be constructed. (See Fig. 4.6)
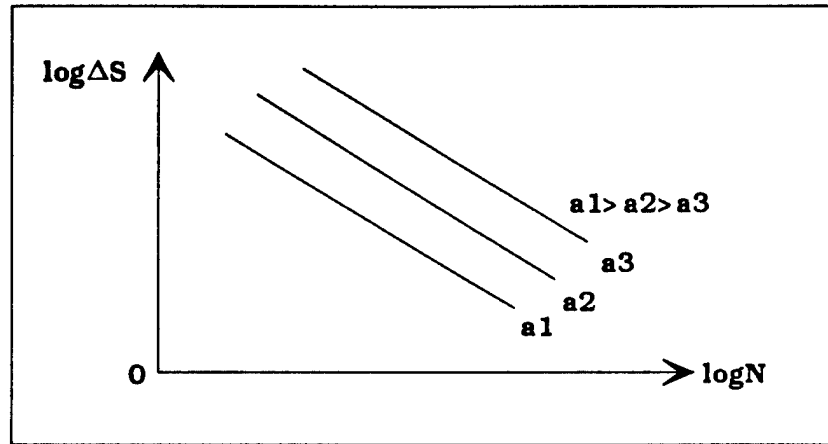
Fig 4.6 Equivalent Cracked S-N Curves

4.5 Numerical Example

This procedure is applied to determine the $\Delta\sigma - N_t$ numerical for the following two cases. The first case is the determination of the general S-N curve for non-welded details (e.g. CSD cutout edges). The second case is the determination of cracked S-N curves for welded details (e.g. CSD bracket toe).

4.5.1 Case 1: Finite-Width Plate with a Transverse Hole

This detail can approximate the cutout geometry in ship CSD. Fig 4.7 is the typical geometry and dimension of the test detail. Based on detailed finite element

analysis [4.9], the notch stress factor was determined (See Fig. 4.8). The material curve
for crack initiation was chosen from Fig. 4.2. The stress intensity factors for crack
propagation is determined by hybrid method and shown in Fig 4.9 The numerical
procedure presented early was carried out to determine the fatigue resistance (Fig 4.10).
The results was compared with the fatigue test results [4-2].
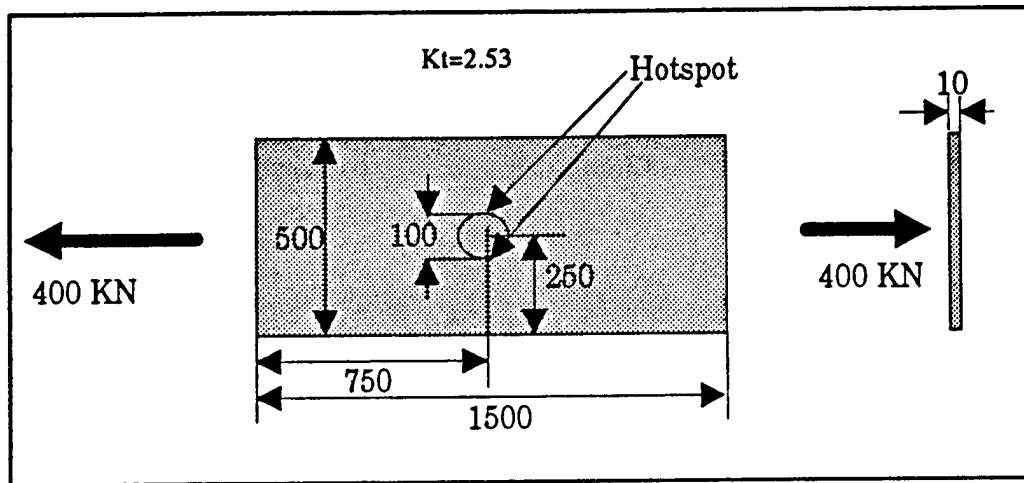
Fig 4.7 Dimensions of the Finite Width Plate with Transverse Hole under Axial Loading
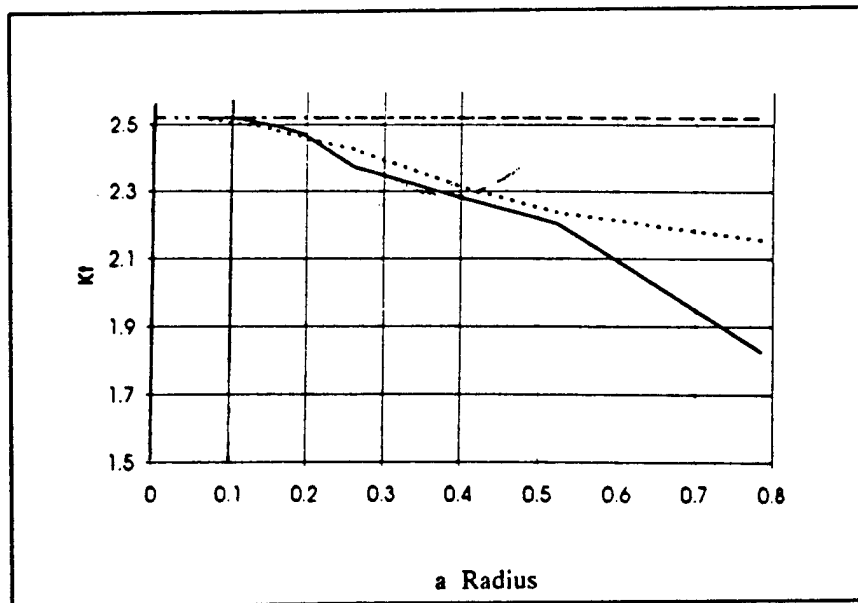
Fig 4.8 Notch Stress Factor determined by Finite Element Analysis
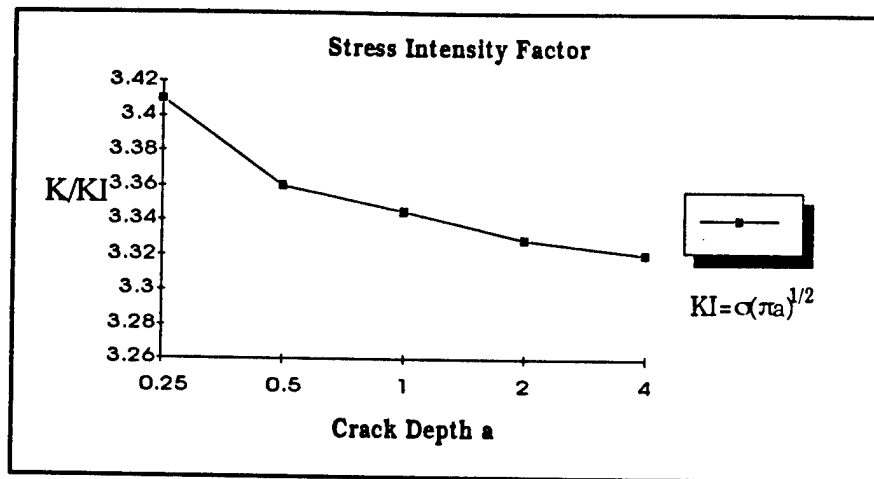
Fig 4.9 Stress Intensity Factor for Crack around the hole
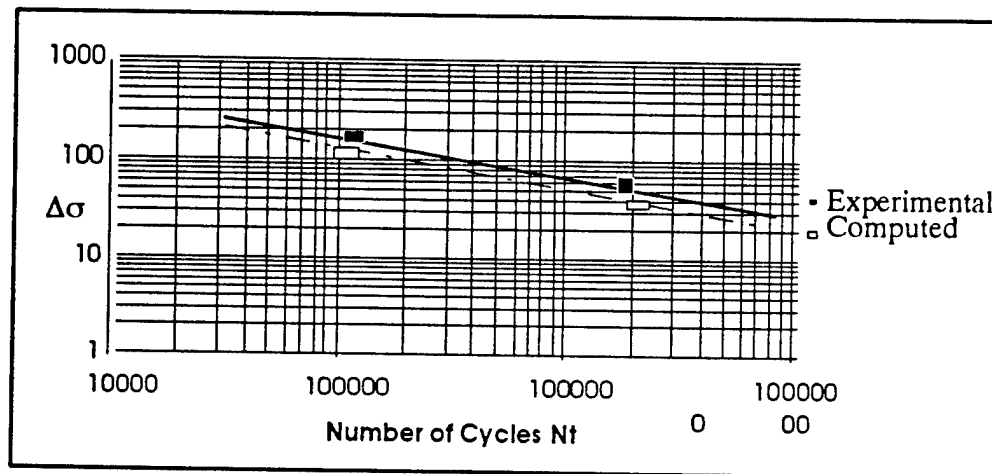
Fig 4.10 Numerical Fatigue Resistance and Experimental Fatigue Resistance

The solid sequences are the experimental point while the open sequence are the numerical resistance. It is seen that the results are comparable. The difference is about 3% between the experimental and numerical results.

The initial crack length, ai, that defines the crack initiation and propagation can be chosen to provide a good fit with the experimental data. This example is selected with ai=0.25 mm.

We can calculate the fraction for the crack initiation phase and propagation phase. The results are shown in Fig 4.11
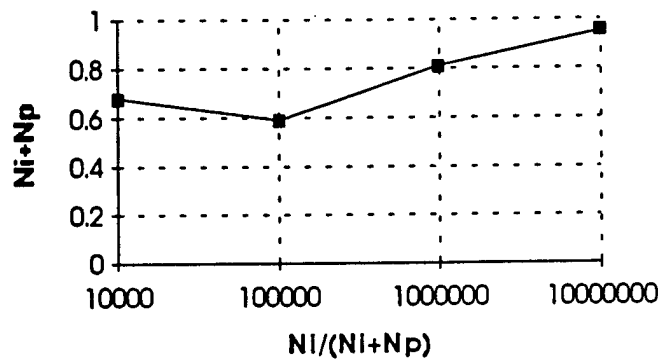
Fig. 4.11 Ratios of the Crack Initiation Phase and Crack Propagation Phase

Most of the fatigue life for this detail is from the crack initiation phase since it is a non-welded details. For general welded details, the crack propagation phase is dominant.

4.5.2 Case 2 Longitudinal Non Loading Carrying Joint

An analysis was performed for the fatigue specimen with a longitudinal non load carrying joint. The configuration is shown in Fig. 4.12. The dimensions for this specimen are given in Fig. 4.13. . It's assumed that the steel grade is A36. The analysis is performed for cracked S-N curves.
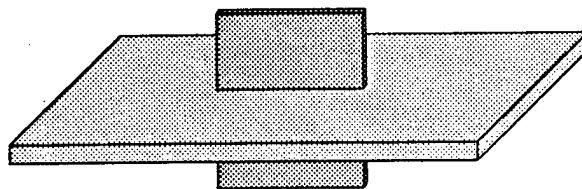
Fig 4.11 Configuration and Geometry of the Specimen

81
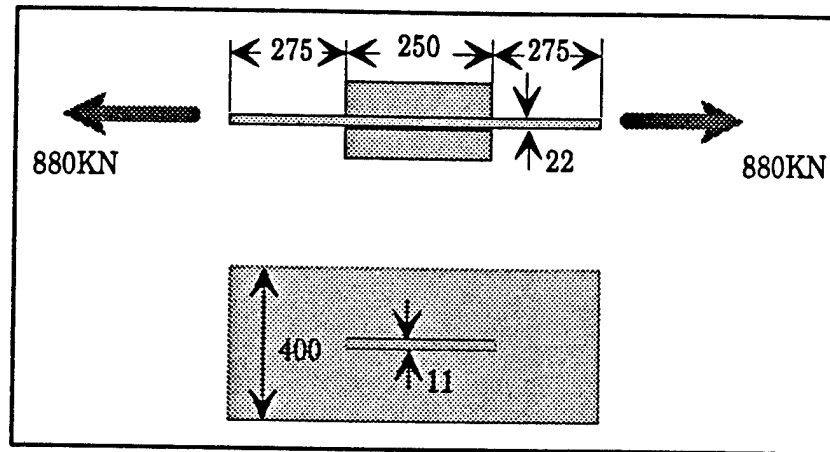
Fig. 4.13 Geometry and Dimensions for Longitudinal Non load carrying Joint
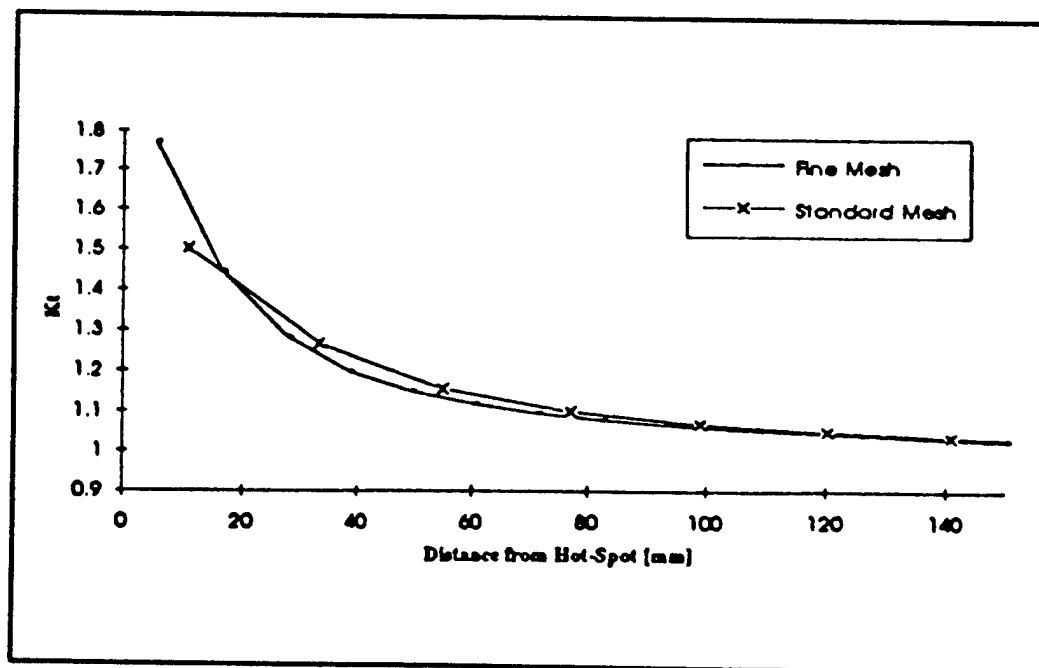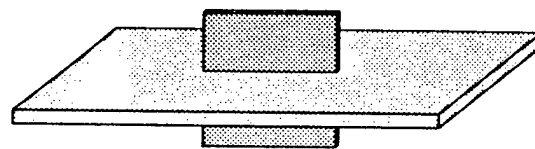
Fig 4.14 Stress Distribution along the Crack

82
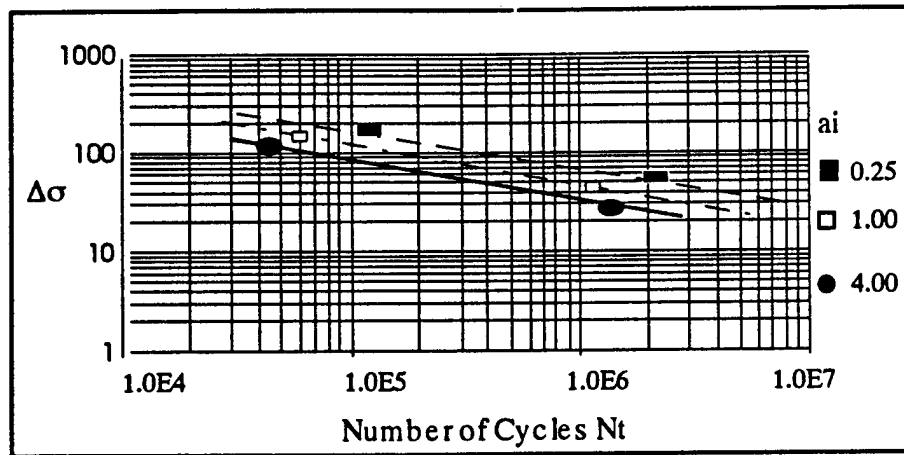
Fig 4.15 Equivalent S-N curves for non load carrying joint with initial crack

length ai = 0.25mm, 1mm, 4mm

The stress distribution was determined by finite element analysis and is shown in Fig 4.14. The stress intensity factor was computed based on the determined stress distribution and was plotted in Fig 4.12. Based on the stress intensity factors, the cracked S-N curves were constructed

The equivalent S-N curves are shown in Fig 4.15. The critical crack length was defined as a through thickness crack. Verification of the developed equivalent S-N curves will be discussed in Chapter 6.

4.6 Summary

This chapter presents a numerical procedure for S-N curve development for CSD. The proposed procedure is divided into two phases : 1) Crack initiation, and 2) crack propagation. In crack initiation phase, the local notch is applied for the estimation of the initial life. In crack propagation phase, fracture mechanics is used to determine the

propagation life. Based on the methodology for crack propagation, the equivalent S-N curves for cracked CSD have been constructed.

Two numerical example were developed to illustrate the methodology. It was found that the crack initiation stage is major part of the fatigue life for non-welded details. The propagation stage contains the major portion of fatigue life for welded details.

4.7 References

4.1 Rolf Schulte-Strathaus **Integrated Procedure for fatigue Life Evaluation of Critical Structural Details in Oil Tankers** Doctor of. Engineering Dissertation. Department of Naval Architecture & Offshore Engineering, University of California at Berkeley, December 1993 Berkeley, CA

4.2 G.Sedlacek, D. Grotmann, J.Gusgen, J.B.Jo and D.Dutta **Determination of the Fatigue Resistance of Steel Structures on the Basis of the "Combined Method".** Proceeding of 2nd International Offshore Mechanics and Polar Engineering Conference. San Franciso, CA

1992

4.3 Owen, D.R.J.; Fawkes, A.J. **Engineering Fracture Mechanics Numerical Methods and Applications, 1983**

4.4 Smith, K.N.; Watson, P., Topper, T.H. **A Stress-Strain Function for the Fatigue of Materials. Journal of Materials,** JIMLSA, Vol. 5 No. 4, Dec. 1970

4.5 Frederick Lawence, C-Y.Hou, Grzegorz Banas Draft Final Report **Reduction of S-N Curves for Ship Structural Details.** March 31, 1991 University of Illinois Urbana Champaign Campus. Urbana, IL

4.6 J.W.Fisher, R.J.Dexter, R.Roberts, B.T.Yen, G. Decorges, S.P. Pessiki, A.C. Nussbaumer, J.E. Tarquinio, G.R. Kober, M.L. Gentilcore, and S.M. Derrah. **Structural Failure Modes for Advanced Double-Hull : Fatigue and Fracture Failure Modes.** Technical Report, Lehigh University, Bethelehem, Pennsylvania, 1993. Final Report for Cooperative Agreement N00014-91-CA-0001 TDL 91-01 Phase I.3(a)

4.7 Alain C. Nussbaumer **Propagation of Very Long Fatigue Cracks in a Cellular Box Beam.** Ph.D Dissertation. Department of Civil Engineering, Lehigh University 1994

Chapter 5

The Fatigue Loading Process

5.1 Loading Process

In Chapter 4, the methodology of the numerical development of S-N curve for non-welded and welded CSD was presented. Meanwhile, there are a lot S-N experiment data available. The fatigue analysis can be performed based on S-N curves.

In this approach, the fatigue strength is expressed through the S-N relation which gives the number of stress cycles (N) with stress range ($\Delta\sigma$) necessary to cause failure. The S-N curves can be obtained from laboratory testing in which a specimen is subjected to cyclic loading until fracture. The new numerical development of S-N curves were documented in Chapter 4. However, most of the S-N curves are defined based on constant amplitude loading. The existing experimental based S-N curves are based on statistical analysis of experimental data. They are fitted with a linear or piece wise linear line to the $\log_{10}\Delta\sigma$ and $\log_{10}N$ data. The line is usually defined as the mean curve with a parallel shift to the left of two standard deviations of $\log_{10}N$ due to the data variance. The S-N curves are of the form:

$$\log_{10} N = \log_{10} a - 2\sigma_{\log_{10} N} - m \log_{10} \Delta S \qquad (5.1)$$

$$N\Delta S^{m} = C_{1} \qquad (5.2)$$

where: ΔS = stress range

N = number of cycles to failure

a = constant relating to the mean S-N curve

$\sigma log_{10}N$ = standard deviation of the $log_{10} N$

m = inverse slope of the S-N curve

$log_{10}C_1 = log_{10}a - 2\sigma log_{10}N$

Often a stress range threshold $\Delta\sigma_0$ is included in the S-N curve. For stress levels below this threshold, no damage is assumed to occur (and an infinite life is assumed).

It should be realized that the S-N approach, though still widely used in design applications, does not deal with any of the physical phenomena within the material. For example, it doesn't separate the crack initiation from the propagation stage, and only the total life to fracture is considered.

Tanker structures are subjected to environmental loading which are random in nature. Therefore, the wave induced stresses during the service time are of varying range. Most of S-N curves are derived considering constant stress range, the calculation of fatigue damage under stochastic loading is commonly performed by the Miner-Palmgren linear damage accumulation model.

In this model, it's assumed that the damage on structure per load cycle is constant at a given stress range and equal to :

$$D_j = \frac{1}{N(\Delta S_j)} \tag{5.3}$$

where $N(\Delta S_i)$ is the number of cycles to failure at stress range ΔS_i. The total damage accumulated in time, t, is obtained by summing the fraction of damage to the structure caused by each stress range and corresponding cycles :

$$D = \sum_{j=1}^{N(\tau)} \frac{1}{N(\Delta S_j)} \qquad (5.4)$$

where $N(\tau)$ is the total number of stress cycles at time τ.

The weakness of the preceding hypothesis is obvious. The most significant shortcoming of the Palmgren-Miner hypothesis is that it does not account for sequence effects; that is, it assumes that damage caused by a stress cycle is independent of where it occurs in the load history.

Based on S-N curve, the damage D is written as:

$$D = \sum_{j=1}^{N(\tau)} \frac{\Delta S_j^m}{C_1} \qquad (5.5)$$

The stress caused by wave loads vary with time and can be considered as a stochastic process. Since stress range is defined as the difference between maximum and minimum value of the stress process in a cycle, the stress range is considered as random variable. The sum is also a random variable. If $N(\tau)$ is sufficiently large and the stress are partially correlated, the uncertainty of the sum is small and can be replaced by its expected value. Thus the cumulative damage is written as:

$$D = \frac{1}{C_1} E[N(\tau)] E[\Delta S^m] \qquad (5.6)$$

For tankers, it is common practice to divide the whole travel routine into several seastates while the stress process for every seastate is referred as stationary Gaussian process and the stress range follows a Rayleigh distribution. The proceeding equation can thus written as:

$$E[N(\tau)] = \nu_0 \tau \qquad (5.7)$$

$$E[\Delta S^m] = (2\sqrt{2})^m \Gamma(1 + \frac{m}{2}) \sigma^m \qquad (5.8)$$

$$v_0 = \frac{1}{2\pi}\sqrt{\frac{\lambda_2}{\lambda_0}} \qquad (5.9)$$

$$\sigma = \sqrt{\lambda_0} \qquad (5.10)$$

where:

v_0 = mean rate of cycles of the stress process,

σ = standard deviation of the stress process, and

λ_i = i-th stress spectral moment.

The long-term variation of the travel routines can be approximated by a series of stationary short term sea states. In this case, the total damage can be obtained by Palmgren-Miner rule over all the sea states. It should be pointed out that load sequence was neglected here.

$$D = \frac{\tau}{C_1}\Omega \qquad (5.11)$$

$$\Omega = \frac{(2\sqrt{2})^m}{2\pi}\Gamma(1+\frac{m}{2})\sum_k\sum_j f_k P_j \lambda_{0_{kj}}^{(m-1)/2}\lambda_{2_{kj}}^{1/2} \qquad (5.12)$$

where:

f_k = fraction of time in the k-th sea state,

p_j = probability of occurrence of j-th main wave direction, and

$\lambda_{0_{ki}}, \lambda_{2_{kj}}$ = zero and second stress spectrum moment in k-th sea state and j-th direction.

It is found that the wave induced long-term stress range under the narrow-banded condition can be described as a Weibull distribution[5.5] :

$$F_{\Sigma}(\Delta S) = 1 - e^{-(\Delta S/A)^B} \qquad (5.13)$$

where A and B are the scale and shape distribution parameters in the Weibull stress range distribution function. Then :

$$E[\Delta S^m] = A^m\Gamma(1+\frac{m}{B}) \qquad (5.14)$$

The fatigue damage can be formulated as :

$$D = \gamma_0 \tau A^m (1 + \frac{m}{B})$$ (5.15)

5.2 Wide-Band Load Process

The foregoing discussion is based on the assumption of narrow banded stress process,. When the stress process is wide banded, the foregoing procedure gives a conservative estimation of the mean damage. In order to reduce the conservation of the narrow banded assumption, a damage correction factor p(m,f) should be found to actual S-N curve parameter, m, and spectral density distribution in frequency dominion f, which is defined as :

$$D_{wB} = \rho(m, f) D_{NB}$$ (5.16)

$$S_{wB}^m = \rho(m, f) S_{NB}^m$$ (5.17)

Based on Wirsching and Light 's study from Rain Flow Counting (RFC) method, an empirical approximation was suggested as following[5-2] :

$$\rho(m, f) = a(m) + [1 - a(m)](1 - \sqrt{1 - \alpha^2})^{b(m)}$$ (5.18)

where :

$$a(m) = 0.926 - 0.033m$$ (5.19)

$$b(m) = 1.587m - 2.323$$ (5.20)

However, analysis by Lutes [5-4] has shown that Wirsching's formula has its limitations.

When the regularity is known, a theoretical approximation to p(m,f) can be found. Jiao and Moan [5-5] proposed the approximate formula based on the combinations of

90

narrow-banded Gaussian process. [5-5]. Here, A new analytical formula for the correction factor is proposed.

According to Rice [5-10], the distribution of local maxim of a unit-variance wide-banded Gaussian process follows :

$$f(S) = \frac{\varepsilon}{\sqrt{2\pi}\sigma} \exp(-\frac{S^2}{2\sigma^2\varepsilon^2}) + \frac{S}{2\sigma^2}\sqrt{1-\varepsilon^2}[1 + erf(\frac{S}{\sqrt{2}\sigma}\frac{\sqrt{1-\varepsilon^2}}{\varepsilon})]\exp(-\frac{S^2}{2\sigma^2}) \qquad (5.21)$$

where :

erf( ) is error function. Bandwidth ranges varies from 0 to 1.

S is the peak stress,

ε is the bandwidth, and

σ is the variance of the stress process.

To find the cumulative damage, all local maxim above zero are counted. A stress cycle is defined as the load history between two consecutive load maxim with the range of the double numerical magnitude of the first peak amplitude. The number of stress cycles is therefore reduced because the stress reversals corresponding to local maxim below zero are ignored. However, larger weights are given to large stress ranges since all small stress reversals are counted as much larger ones. So this approach is regarded as conservative.

Fatigue damage under the above assumption and Miner's rule can be derived as:

$$D = \sum_{i=1}^{N}\frac{1}{N(S_i)} = \frac{1}{K}\sum_{i=1}^{N}S_i^m \qquad (5.22)$$

The expected damage

$$\overline{D} = \frac{1}{K}\left[\sum_{i=1}^{N}S_i^m\right] = \frac{N_0}{K}\overline{S^m} \qquad (5.23)$$

The stress range based on the local maxim is then 2S and

$$\overline{S^m} = \int_0^\infty (2S)^m f(S)ds \qquad (5.24)$$

Substituting Eq(5.21) into Eq(5.24), we have:

$$\overline{S^m} = \int_0^\infty (2S)^m \frac{\varepsilon}{\sqrt{2\pi}\sigma} \exp(-\frac{S^2}{2\sigma^2\varepsilon^2})dS$$

$$= (2\sqrt{2}\sigma)^m \frac{\varepsilon^{m+2}}{2\sigma^2\varepsilon^2}$$

$$+ \int_0^\infty (2S)^m \frac{S}{2\sigma^2}\sqrt{1-\varepsilon^2}[1+erf(\frac{S}{\sqrt{2}\sigma}\frac{\sqrt{1-\varepsilon^2}}{\varepsilon})]\exp(-\frac{S^2}{2\sigma^2})dS \qquad (5.25)$$

For the first term in Eq. (5.25), we used $\Gamma(n) = \int_0^\infty t^{n-1}e^{-t}dt$ and $t = \frac{S^2}{2\sigma^2\varepsilon^2}$, we

obtained:

$$\overline{S^m} = \int_0^\infty (2S)^m \frac{\varepsilon}{\sqrt{2\pi}\sigma} \exp(-\frac{S^2}{2\sigma^2\varepsilon^2})dS$$

$$= (2\sqrt{2}\sigma)^m \frac{\varepsilon^{m+2}}{2\sigma^2}\Gamma(\frac{m+1}{2}) \qquad (5.26)$$

For the second term of the Eq. (5.25), we defined

$$g(S) = [1+erf(\frac{S}{\sqrt{2}\sigma}\frac{\sqrt{1-\varepsilon^2}}{\varepsilon})] \qquad (5.27)$$

and :

$$\varphi(S) = \frac{S^{m+1}}{2\sigma^2}\sqrt{1-\varepsilon^2}\exp(-\frac{S^2}{2\sigma^2}) \qquad (5.28)$$

Using $\int_0^\infty g(x)\varphi(x)dx = g(x_m)\int_0^\infty \varphi(x)dx$, if $g(x)$ is a linear function and x_m is the

center of weight of $\int_0^\infty \varphi(x)dx$.

Since the function $\varphi(x)$ is nearly equal to zero after $S > 3\sigma$ and $g(x)$ can be

approximate as a linear function from S=0 to S=3σ. it is possible to deduce the second

term as:

$$\int_0^\infty \frac{(2S)^{m+1}}{2\sigma^2}\sqrt{1-\varepsilon^2}[1+erf(\frac{S}{\sqrt{2}\sigma}\frac{\sqrt{1-\varepsilon^2}}{\varepsilon})]\exp(-\frac{S^2}{2\sigma^2})dS$$

$$= \frac{\sqrt{1-\varepsilon^2}}{2}[1+erf(\frac{S_w}{\sqrt{2}\sigma}\frac{\sqrt{1-\varepsilon^2}}{\varepsilon})](2\sqrt{2})^m\Gamma(\frac{m+2}{2}) \qquad (5.29)$$

where S_w is the center of weight of $\int_0^\infty S^m \frac{S}{\sigma^2}\exp(-\frac{S^2}{2\sigma^2})dS$:

$$S_w = \frac{\int_0^\infty \frac{S^{m+1}}{\sigma^2}\exp(-\frac{S^2}{2\sigma^2})dS}{\int_0^\infty \frac{S^m}{\sigma^2}\exp(-\frac{S^2}{2\sigma^2})dS} = \sqrt{2}\,\frac{\Gamma(\frac{m+3}{2})}{\Gamma(\frac{m+2}{2})} \tag{5.30}$$

By letting $\beta = \text{erf}(\frac{S_w}{\sqrt{2}\sigma}\frac{\sqrt{1-\varepsilon^2}}{\varepsilon})$, we have:

$$\overline{S^m} = (2\sqrt{2}\sigma)^m[\frac{\varepsilon^{m+2}}{2\sqrt{\pi}}\Gamma(\frac{m+1}{2}) + \frac{1+\beta}{2}\sqrt{1-\varepsilon^2}\Gamma(\frac{m+2}{2})] \tag{5.31}$$

The average number of positive maxim in time period T is :

$$N_m = v_m T \int_0^\infty f(S)dS \tag{5.32}$$

$$= \frac{1+\alpha}{2\alpha}v_0 T \tag{5.33}$$

where:

$$\alpha = \sqrt{1-\varepsilon^2} \tag{5.34}$$

The expected damage is therefore

$$D_{WB} = \frac{N\overline{S^m}}{K} = \rho(m,f)D_{NB} \tag{5.35}$$

where $\rho(m,f)$ is :

$$\rho(m,f) = \frac{1+\alpha}{2}[\frac{\varepsilon^{m+1}}{2\sqrt{\pi}} \bullet \frac{\Gamma(\frac{m+1}{2})}{\Gamma(\frac{m+2}{2})} + \frac{1+\beta}{2}\sqrt{1-\varepsilon^2}] \tag{5.36}$$

5.3 Load Sequence

The traditional fatigue analysis based on S-N curves or Paris Erdogen Equation do not take into account so called interaction effects due to irregularity of loading, which is included in random loading while the tanker loading is a random process. In contrast to the constant-amplitude loading, the increment of fatigue growth depends in general not only on the present crack size and applied load, but also on the preceding load history. Load interaction or sequence effects have influence on the fatigue crack growth rate and, consequently, fatigue life.

One of the important interaction effects (recognized in the early 1960s) is the retardation in the fatigue growth following a sufficiently large tensile overload. (see Fig. 5.1). Crack retardation remains in effects for some period after the overloading. The number of cycles in the retarded growth has been shown to be related to the plastic zone size developed due to the overload. The larger the plastic zone generated by the overload, the longer the crack growth retardation remains in effect.
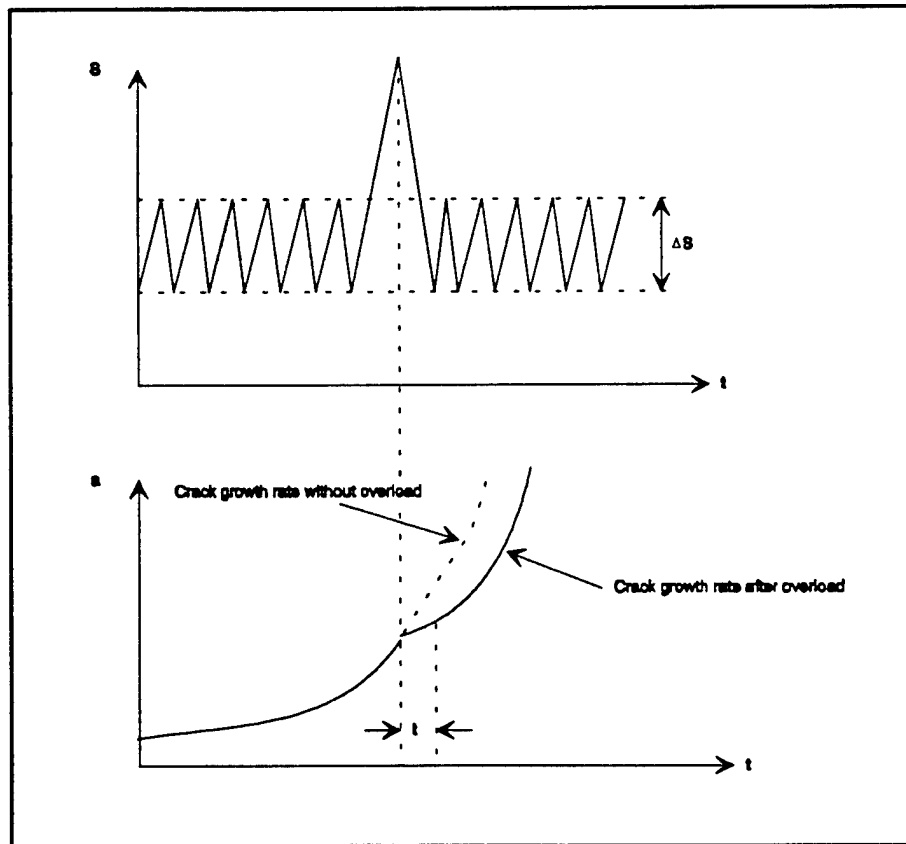
Fig. 5.1 Load Sequence during the Crack Propagation

Various model were proposed for the fatigue crack growth under the random loading such as Cycle-by-Cycle (Non interactive) Prediction, Crack Closure Model of Elber (Elber), Wheeler model (Wheeler) and so on. The above approach which is discussed in section 2.2 is based on the equivalent stress intensity factor concept for different sea state. In this approach, the root mean square (rms) value of the sea state was proposed for this purpose, i.e., $\Delta K = \Delta K_{rms}$. In this case, the fatigue crack growth equation is postulated in the form :

$$\frac{da}{dN} = C(\Delta K_{rms})^m \qquad (5.37)$$

Based on previous studies [5-2], the equivalent stress intensity factor approach can predict the reasonable results for fatigue crack growth under the random loading for different loading order or sequence. Fig 5.2 shows the typical results.
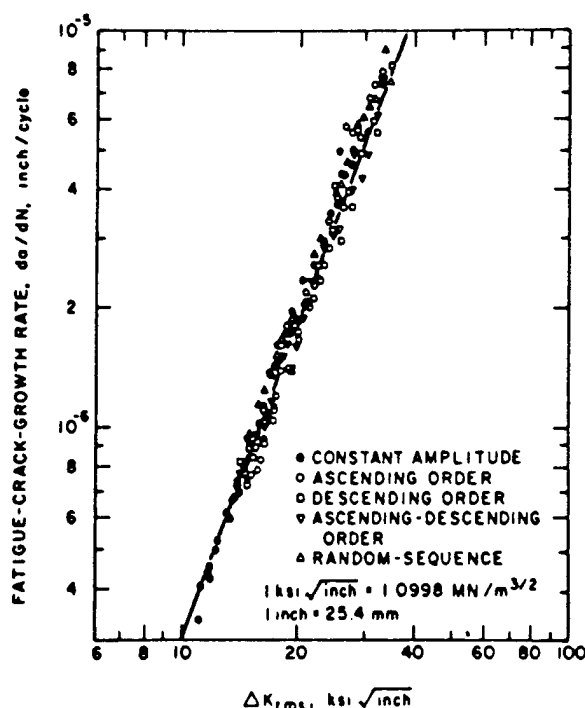
Fig 5.2 Crack Growth under different load sequence for the same RMS

95

Based on Fig. 5.2, we may conclude that the equivalent stress intensity factor approach for one sea state can predict the rational and reasonable fatigue crack growth or the load sequence can be neglected in this approach for one sea state.

The reason for the success of this approach is still unknown. It may be significant that the crack growth exponent is close to two for the materials used in the studies (making the RMS a particularly appropriate measure). The load block may also been short enough that sequence effects would be minimal [Schijve, et.al.,1970]. But the simplicity of the method and its success in the application of the specific sea state makes it attractive. But the lack of any physical basis for its validity admits the possibility that it may be inaccurate in the application of the tanker's whole travel routines.

In general, random loading are always divided into segments with stationary behavior in each segment. Sequenceless crack growth prediction is done by the RMS approach in each segment and summing over the relative amount of time spent in each type of segment. This is typical approach which is presented in section 5.1 to study the fatigue in oil tankers. It is highly probable, however, that the transition from one segment (sea state) to another can introduce crack growth sequence effects, especially if the transition involves a change in the overall magnitude of the load peaks. Veers, Winterstein, Nelson and Cornell [5-5] has conducted the simulation of the crack growth for this problem.

For oil tankers, Although the RMS approach can have the reasonable result for one sea state, the load sequence between different sea state is still a problem. To some extent, it's more important in the fatigue of tanker structure since tanker travel through different sea states during its service travel routine. It was obvious that Palmgren-Miner

96

Damage model or Paris-Erdogan Crack Growth Model can not take the load sequence into account since both of them have no memory effects. It's impossible to conduct the simulation for tanker structure. Thus, a new damage accumulation model was proposed for this purpose. The new model which is called "Henry Damage Model" was first introduced in early 1950s. [5-6]. The validity of this model is still unclear due to the lack of the sufficient experimental data.

5.3.1 Henry Damage Model

The accumulative damage theory proposed by Henry [5-6] is based on the concept that S-N curve is shifted as fatigue damage accumulates and that fatigue damage is defined as the ratio of the reduction in fatigue limit to the origin fatigue limit of the virgin material. That is :

$$\Delta = \frac{F_0 - F}{F_0} \tag{5.38}$$

where Δ = damage

F_0 = origin fatigue limit, and

F = fatigue limit after damage.

In the development of the Henry theory, it's assumed that the virgin S-N curve could be represented by the equation of an eqivlateral hyperbola referred to the stress axis and a line pass through F_0 parallel to the cycle axis as the asymptotes of the hyperbola. Then the equation assumed for S-N has the form

$$N = \frac{K_0}{S - F_0} \tag{5.39}$$

where N = number of cycles to failure at stress ed amplitude S

S = completely reversed amplitude of applied stress

K_0 = material constant, and

F_0 = original fatigue limit.

It's implied that no damage is occurred by operation at cyclic stress levels below the fatigue limit. Henry further assumed that the S-N curve after damage could be represented by the equation of equivalalateral hyperbola where

$$N_r = \frac{K}{S-F} \tag{5.40}$$

where Nr = number of sceinaring cycles to failure at stress amplitude S

S = completed reversed amplitude of the applied stress,

K = material constant, and

F = damage failure limit (reduced from Fo)

Based on experimental data, Henry further assented that it's approximately true that :

$$\frac{K}{K_0} = \frac{F}{F_0} \tag{5.41}$$

Based on the above assumption, the damage relationship proposed by Henry [5-6] was developed as follows: If n cycles of stress amplitude S are applied to a specimen, the remaining life Nr at that stress amplitude is given by :

$$N_r = N - n \tag{5.42}$$

where N is the total number of cycles required to procedure failure of the virgin material when subjected to stress amplitude S

Thus ;

$$N - n = \frac{K}{S-F} \tag{5.43}$$

$$1 - \frac{n}{N} = \frac{1}{N}(\frac{K}{S-F}) \tag{5.44}$$

$$1 - \frac{n}{N} = \frac{S-F_0}{K_0}(\frac{K}{S-F}) \tag{5.45}$$

or

$$1 - \frac{n}{N} = \frac{K}{K_0}\frac{S-F_0}{S-F} = \frac{F}{F_0}(\frac{S-F_0}{S-F}) \tag{5.46}$$

$$F = \frac{S(1-\frac{n}{N})}{(\frac{S-F_0}{F_0})+(1-\frac{n}{N})}$$

(5.47)

This equation is one useful form of the Henry theory. It gives an expression for the current value E of the fatigue limit after n cycles of stress amplitude S have been applied. If the total number of cycles to failure was originally N at stress level S and original fatigue limit was Fo. Then :

$$\Delta = \frac{F_0 - F}{F_0} = 1 - \frac{S(1-\frac{n}{N})}{(S-F_0)+F_0(1-\frac{n}{N})}$$

(5.48)

where Δ = damage fraction,

n = number of cycles applied at stress amplitude S,

N = number of cycles to failure,

Fo = original fatigue limit, and

So = applied stress amplitude.

5.3.2 Load Sequence between Different Sea States

The Henry theory can be extended to study the load sequence for different sea states. Based on the equivalent mean stress approach which was developed in section 2.2 and 2.3,the sequence of different stress levels in different sea states can be studied by applying F and Δ successively in the order of the applied stress levels for different sea states. In this sequence procedure, the value of Fo must be updated after the application of each equivalent stress amplitude for each sea state. Thus, a sequence of values for fatigue limit would be obtained, say Fo, F1, F2, ... where Fo is the original fatigue limit after applying n1 cycles of the equivalent stress level S1 for sea state 1, and so on.

5.4 Numerical Example:

In this section, a numerical example for wide banded loading process is conducted. The load sequence effects are not studied due to the time and data limitations.

The numerical comparision was made between Wirsching Formula (Eq. 5.18-5.20), Numerical Integration of Rice Formula (Eq. 5.21) and New proposed model (Eq. 5.36). The analysis was performed at m=3 with different irregularity factors, α, from 0 to 1 (Table 5.1).

The numerical comparision was shown in Fig. 5.4. The analysis was performed at m=3 with different irregularity factor (Table 5.1). It has been found that the new model (Eq. 5.36) is better than Wirsching formula when the irregularity factor is larger (Fig 5.4) It has been demonstrated that the new model is a good approximation while Wirsching formula (Eq. 5.18-5.21) is relative conservative.

Damage Correction Factor
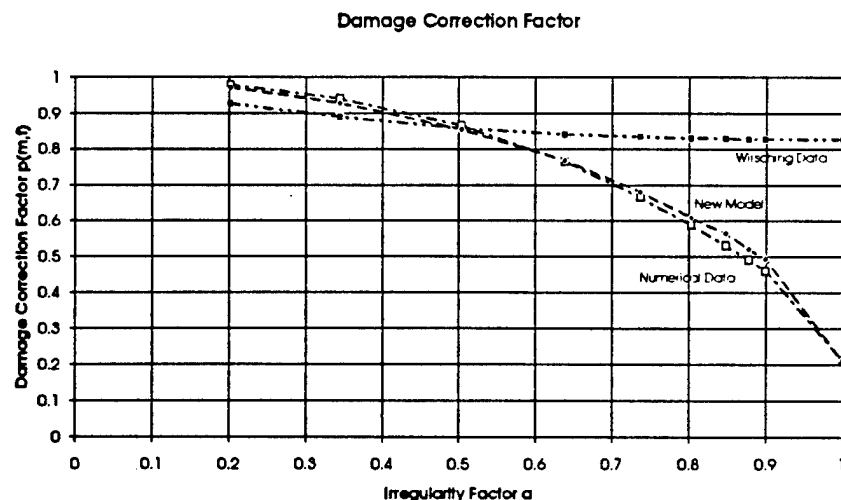
Fig 5.4 Numerical and Analytical Comparison

100

m	3	3	3	3	3	3	3	3	3	3
α	0.202	0.345	0.504	0.639	0.737	0.803	0.848	0.878	0.899	1.0

Table 5.1 Analysis Parameters

5.5 Summary and Conclusions

This chapter discussed the fatigue loading process. The general approximation of the wide-banded process was presented and tested by the numerical example. The loading sequence was discussed briefly. The Henry damage model was presented to describe the sequence fatigue damage. Due to the lack of the experimental data, this model is only an illustration. More detailed discussion about load sequence in crack propagation is beyond the scope of this work.

5.6 References

5.1 Miles, J.W. **On Structural Fatigue Under Random Loading.** Journal of Aeronautical Science 21 1954

5.2 S.T. Rolf, J.M. Barsom. **Fracture and Fatigue Control in Structures.** Printice Hall, 1977

5.3 Henry et **A Cumulative Fatigue Damage Model** ASME Proceeding 1954

5.4 P.S. Veers, S.R. Wintersein, D.V. Nelson, and C.A. Cornell. **Variable Amplitude Load Model for Fatigue Damage and Crack Growth.** In Symposium on Development of Fatigue Loading Spectra ASTM, Cincinnati, Ohio, April 1987

5.5 P.W.Wirsching, M.C.Light. **Fatigue under Wide Band Random Stresses.** Journal of Structural Division, ASCE 1980

5.6 D.Ritchie, P.A.J. Van Der Veer, and K.Smith. **Fatigue Crack Growth under Broad Band Stationary and Non-stationary Random Loading.** In Steel in Marine Structures, June 1987

5.8 Jiao **Fatigue Crack Growth under Random Loading with Inspection Updating.** Dr. Ing Dissertation. Dept. of Marine Structures, Norway Institue of Technology. Norway

5.9 R.Bell, O.Vosikovsky **Fatigue Life Prediction of Welded Joints for Offshore Structures Under Variable Amplitude Loading.** Journal of Offshore Mechanics and Artic Engineering May 1993

Chapter 6

Fitness for Purpose Analysis

6.1 Introduction

The objective of this project is to develop an engineering procedure to make fitness for purpose evaluations for cracked CSD in tankers. Based on the methodology developed in previous chapters, a general fitness for purpose procedure for cracked CSD has been developed as follows :

1) Determination of the long-term loading for the residual or extended life.

2) Identification of the specific CSD where cracks occur based on the previous experience and data-base or the fatigue life determined by the traditional S-N curves.

3) Inspection of these CSD to determine the appropriate initial crack size ao, to be used in remaining life analysis.

4) Determination of the fracture toughness value of the steel plate used in CSD under the study to find the critical crack length. The critical crack length is the length that a crack must reach before the crack can propagate for brittle fracture.

5) Select the equivalent S-N curves for the cracked CSD to evaluate the residual life based on long-term loading. (Fig 6.1)

103
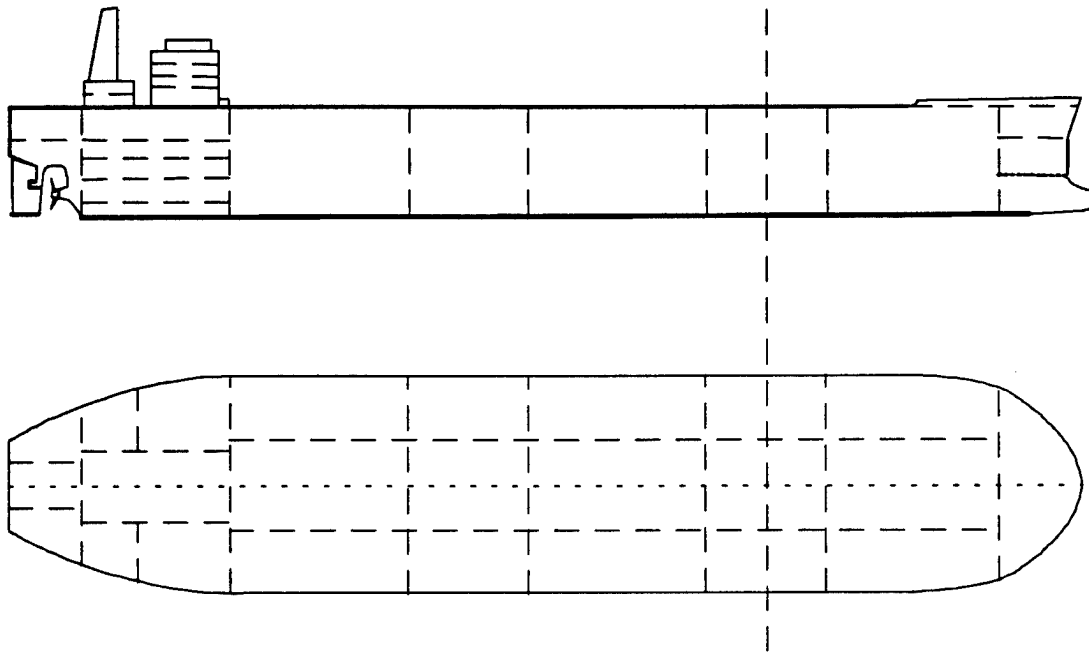
Fig 6.2 General arrangement for a 165,000 DWT tanker.

DWT	165,000
LOA	274.2m
LBP	262.1m
Breadth	52.7m
Depth	22.9m
Draft	17.4m
Construction	Single Hull

Table 6.1 Overall Dimensions for the 165,000 DWT Tanker

6) Based on the estimated residual life, the inspection and repair can be established for safe and reliable service.

Residual Life for Cracked CSD
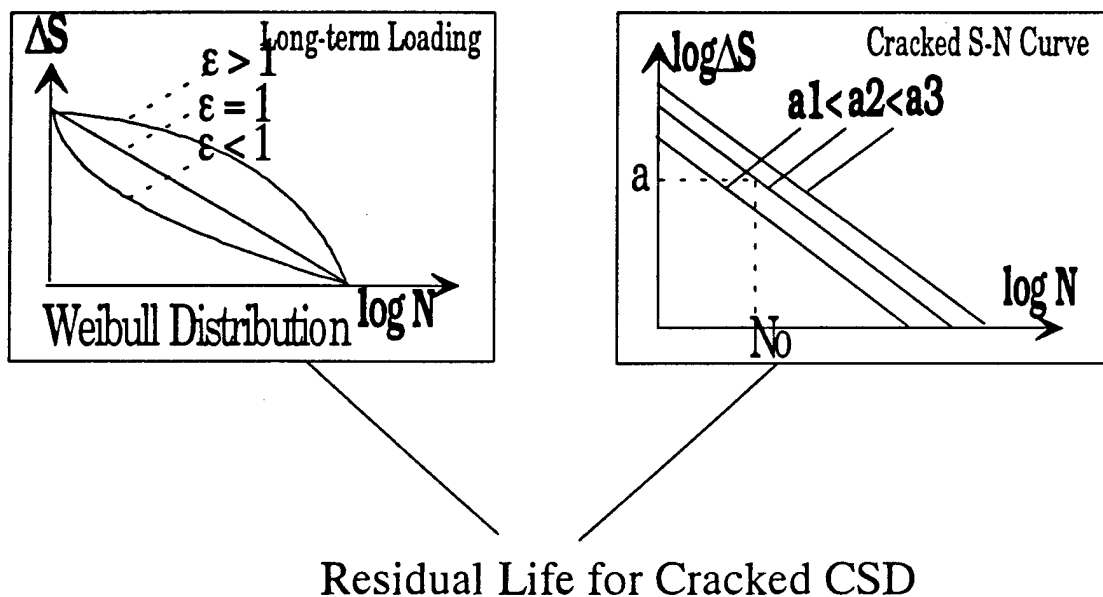
Fig 6.1 Remaining Life Estimation based on Fitness for Purpose Evaluation.

This chapter addresses in detail a fitness for purpose analysis for cracked CSD in a 165,000 DWT single-hull tanker.

6.2 165,000 DWT Tanker

The proposed analysis is performed for three details in 165,000 DWT single hull tanker which was studied in SMP I. The characteristics for this tanker are summarized in Table 6.1. The general arrangement is shown in Fig 6.2 and Fig 6.3 is the midsection.
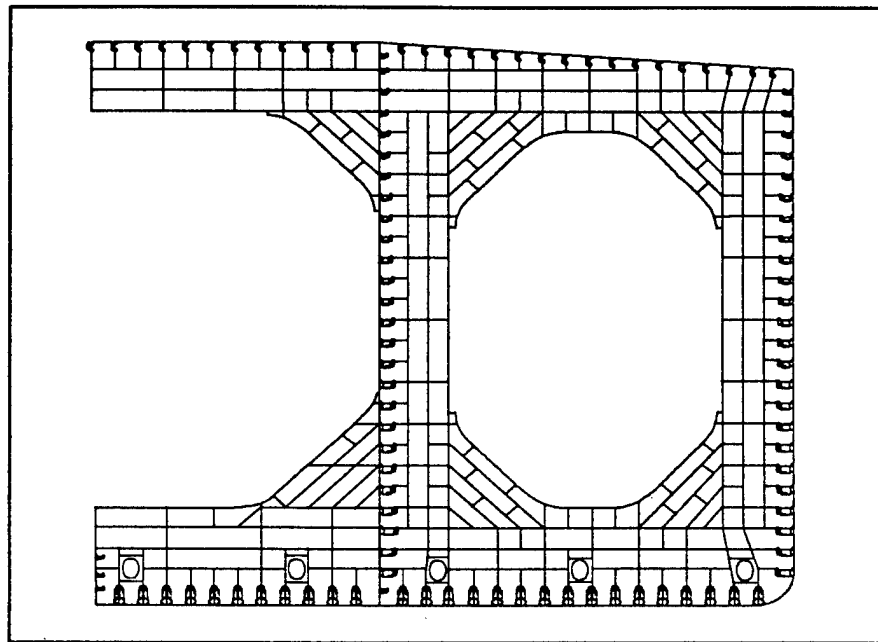
Fig 6.3 Midsection for a 165,000 DWT tanker

The ship operated almost exclusively on the TAPS trade route between California and Alaska. This route passes through the Madsen zones 6,7,13,14,22. Fig 6.4 shows these Marseden zones and some common courses and definitions. Information about this ship's maneuvering has been obtained from the operator. For the given trade route from California to Valdez and back in general no course changes due to bad weather are made. Speed is reduced only for the worst sea conditions. Table 6.3 summaries the information about the maneuvering philosophy.

The previous fatigue studies have been conducted in order to verify the SMP software [6.1]. The objective of this chapter is to perform the verification study of the fitness for purpose procedure developed in this project.

Harbour Time	6.26
Zone 6	2.46
Zone 7	1.75
Zone 13	1.80
Zone 14	1.48
Zone 22	1.25
Total	15
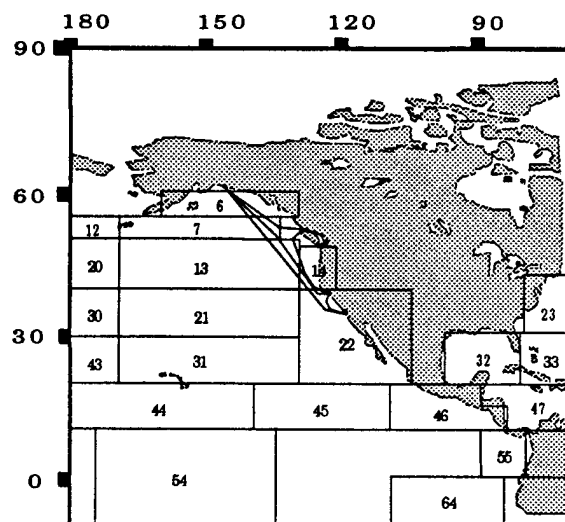
Table 6.2 Travel Route for a 165,000 DWT Tanker

Speed, Maneuvering:

LC 1: Laden	55 %
Steering Speed	2.06 m/s
Cruising Speed	7.90 m/s
LC2: Ballast	45 %
Steering Speed	2.06 m/s
Cruising Speed	8.23 m/s
Course Change for Hs:	12, 12, 12
Cruising Speed Change for Hs	9, 8, 9
Steering Speed Change for Hs	10, 9, 10

Table 6.3 Maneuvering Philosophy for 165,000 DWT Tanker

The proposed analysis is conducted based on the following steps.

1 - Definition of structural detail and crack location.

2 - Computation of the transfer function for the ship. The transfer functions are computed for the two load cases. Full load and Ballast and for several wave headings and speeds based on the proposed travel routines and sea environment.

3 - Determination of the stress vectors at the Hotspots from finite element analysis.

- Estimation of the long-term distribution of the stress range σ at a hotspot. This estimation is based on a specified travel routine for given Madsen zones and specified maneuvering philosophy.

4 - Determination of the initial crack size for given hotshot

5 - Determination of the critical crack size for given hot-spot based on material toughness or durability requirement.

6 - Determination of the stress intensity factors for given hot-spots at the specified CSD

7 - Construction of the equivalent S-N curves for the hot-spot in given CSD.

8 - Determination of the remaining fatigue life based on the long-term extreme stress range and constructed equivalent S-N curves.

The above procedure will be addressed in detail in the next sections.

6.3 Critical Structural Details

The critical structural details were selected based on the detailed fatigue data-base analysis. [6-1]. The sideshell longitudinal 32-36 (Fig 6.2) on tank 4 are selected as the analysis CSD. We selected one detail as the numerical example. The geometry configuration and dimension are shown in Fig 6.4

Fig 6.4 Configuration for Detail in Sideshell 32- 36.

Frame Spacing	5120 mm
Longitudinal Spacing	890 mm
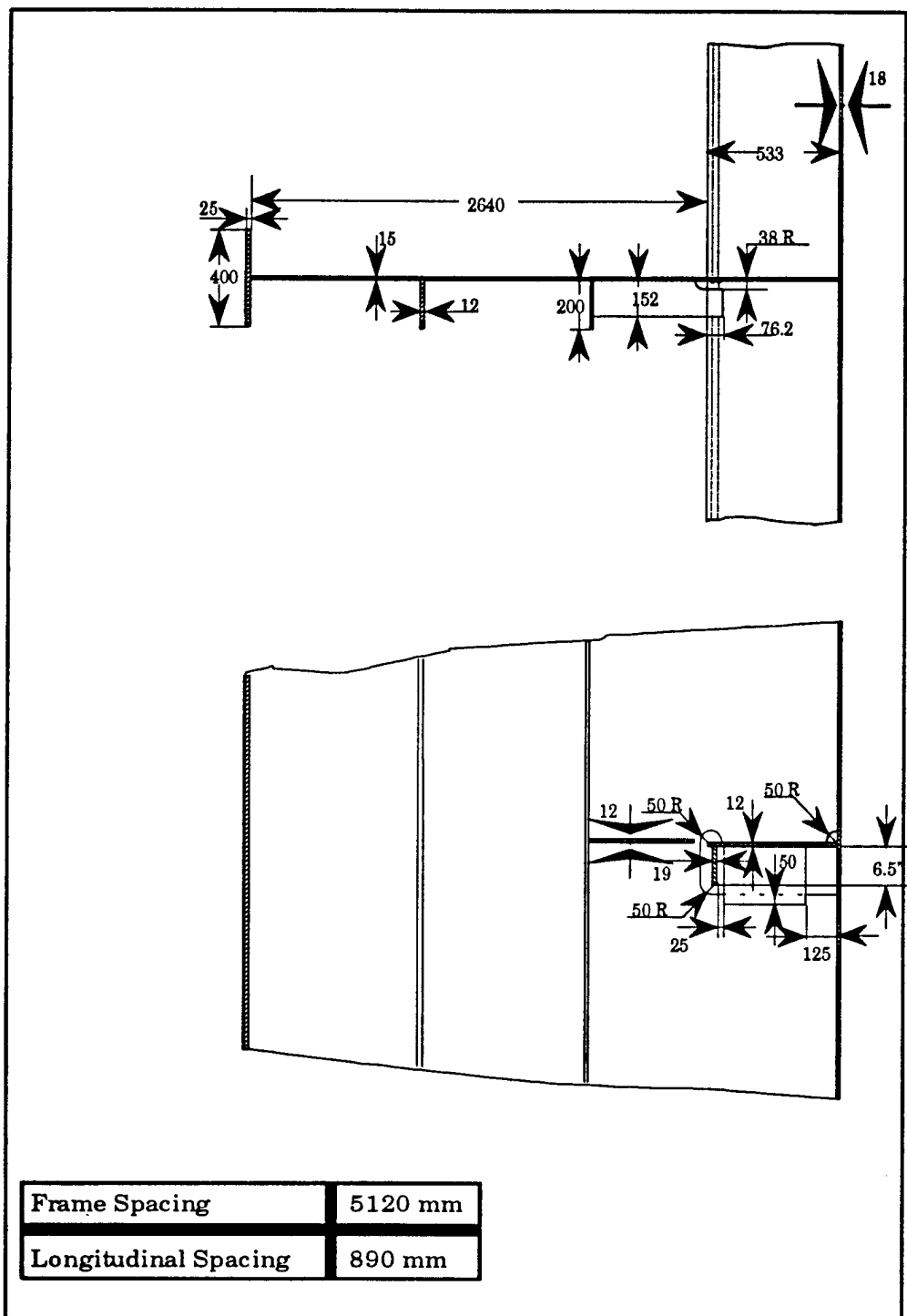
6.4 Transfer Function

The ship motion analysis based on strip theory [6-2] was performed to generate the transfer function for bending and hydrodynamic pressures in various headings. In addition, the accerlations generated by the ship motion were used to determine inner pressures. the detail analysis procedure and results are presented in [6-1]. Fig 6.5 shows the transfer function for bending under full load conditions.
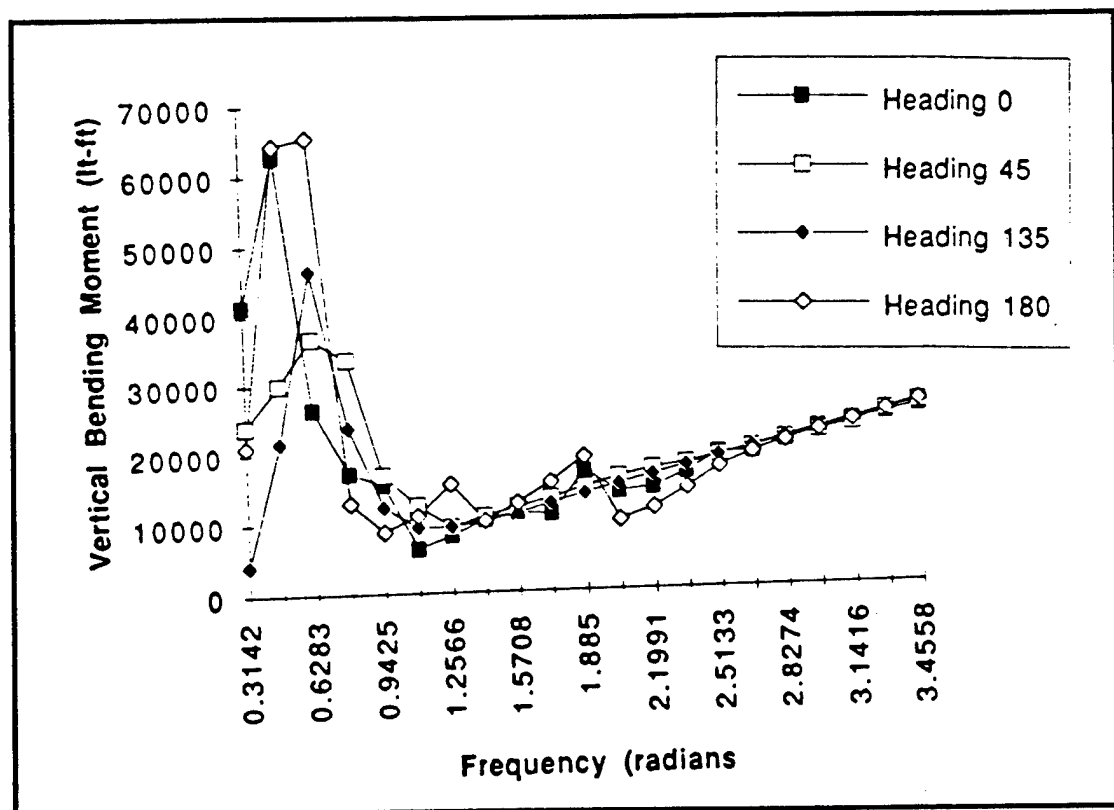
Fig 6.5 Transfer Function for Proposed 165,000 DWT Tanker

6.5 Stress Vectors

Based on the detail geometry shown in Figs 6.4, finite element models have been developed in previous SMP project. The finite element mesh and stress contours are shown in Fig 6.6 6.7a, and 6.7b. The stress vector for two unit load cases was computed and shown in Table 6.4.
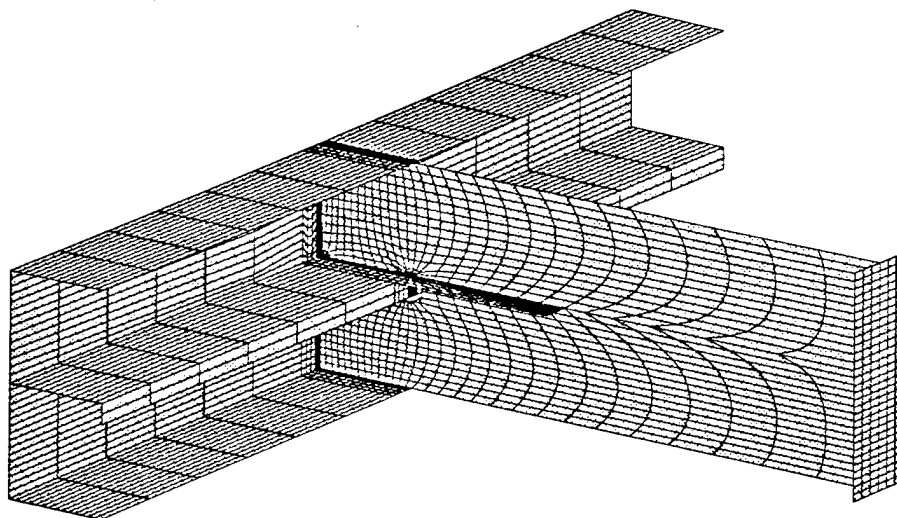
Fig 6.6 Finite Element Mesh for Proposed CSD

Detail	Stress Vectors	
	Axial	Pressure
Hotspot A	1.2	-280
Hotspot B	0.25	1030

Table 6.4 Stress Vectors for Proposed CSD
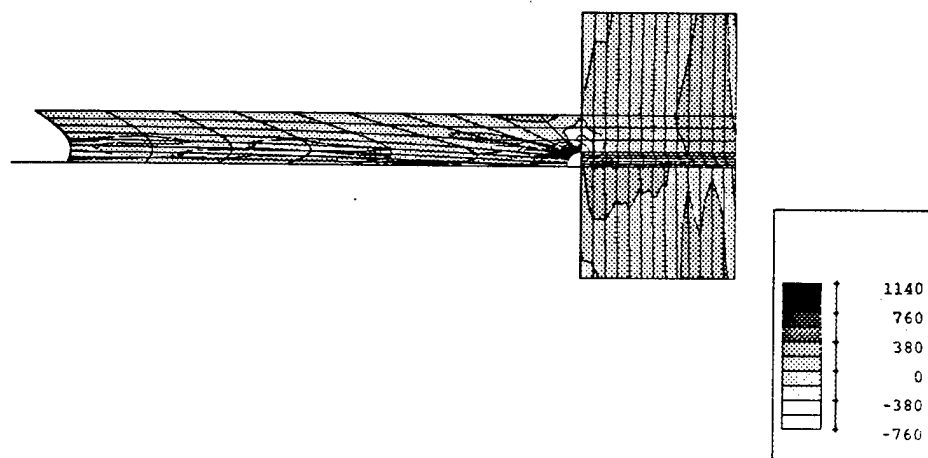
Fig 6.7a Stress Contour for CSD due to Unit Axial Force
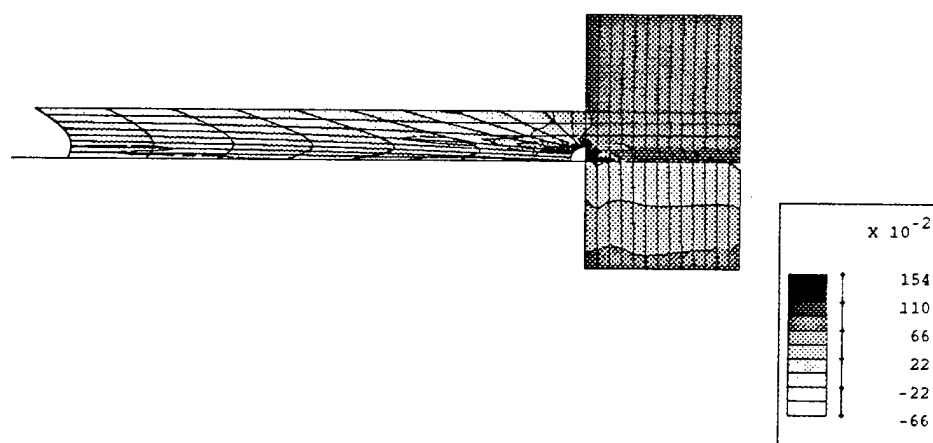
Fig 6.7b Stress Contour for CSD under Unit Pressure

6.6 Long-term Stress Range

The long-term stress range is one of the key issues for the fitness for purpose analysis. Assuming that the ship is a linear system, the total response in a seaway can be described by a super-position of the response to all regular wave componenets that constitute the irregular sea. Given the linearity, the ship response is a stationary, ergodic but not necessarily a narrow banded Gaussian process. The long-term stress range can be estimated.

6.6.1 Enviromental Modeling

For a specified sailing route, the relative time period within each Mardsen zone is estimated, and the frequency of the occurrence of difference of different sea state is

$$(H_s, T_z)_{lifetime} = \sum_{i=1}^{N} \mu_i (H_s, T_z)_i \qquad (6.1)$$

where $(Hs,Tz)i$ is the scatter diagram for the i-th Mardsen zone, mi the fraction of the lifetime which the ship is in Mardsen zone i and N the total number of zones passed by ship over its lifetime. For the proposed 165,000 DWT tanker, Table 6.5 shows the tme spent in port and in each of the Madsen zone.

	Time (Years)
Harbour Time	3.255
Marsden Zone	
6	1.7463
7	1.258
13	1.297
14	1.276
22	1.051
Residal Life	10

Table 6.5 Voyage Profile for Residual Life of 10 years.

For a specified short-term sea state (Hs,Tz), the wave spectrum under the assumption of stationarity is derived as:

$$S(w) = ABw^{-5}e^{-Bw^{-4}} \tag{6.2}$$

where

$$A = 0.25(H_s^{\frac{1}{3}})^2 \tag{6.3}$$

$$B = (0.817\frac{2\pi}{T_z})^4 \tag{6.4}$$

In order to account for the energy spreading in different directions for short crested sea. Short crested sea waves was described by a two-dimensional directional spectrum as follows:

$$S_\eta(w,\bar{\theta}) = S_\eta(w)w(\bar{\theta}) \tag{6.5}$$

where w(.) is the spreading function and the spreading angle from the main wave componenet direction.

6.6.2 Wave Response

A linear assumption for ship is made to evaluate the wave response. The transfer function modeling the response due to a sinusoidal wave with a unit amplitude for different frequencies is obtained from the strip theory. For the proposed 165,000 DWT tanker, it's shown in Fig 6.5. The estimated transfer function is however, only valid for a specified ship velocity V, wave heading angle and loading condition. For example, Fig 6.5 shows the full load condition for different speed with a frequency range.

For the fatigue or fitness for purpose analysis, it is the combined stress response effect on the investigated detail that is sought. The local stress response is a combined

effect of different load response as horizational and veritcal bending moments, external water pressure, and internal cargo inertia pressure.

Based on the linear model assumption, a combined local stress response transfer function for all the sepcified types of stress response can be obtained. The combined transfer function describes the combined directional stress response due to a unit wave excitation. This means that even a non-linear combination of the separate stress responses can be evaluated applying a linear frequency analysis by deriving the combined transfer function for the different response directly.

The response spectrum of the ship based on the linear model is directly given by the wave spectrum.

$$S_\sigma(w_e | h_s, t_z, v, \theta, l) = |H_\sigma(w_e | v, \theta, l)|^2 S_\eta(w_e | h_s, t_z, v, \theta) \qquad (6.6)$$

where we is the encoutered wave frequency and $|H_\sigma(w_e)|$ is the modulus of the transfer function.

6.6.3 Operational Philosophy

In severe states, it's common to change the speed and course of the ship in order to reduce the wave induced repsonse such as slamming and large roll motions. Therefore, the effects of the maneuvering should therefore be included in the response analysis.

The combined effect of course change (relative to the main wave heading direction) and speed reduction as a function of the significant wave height is modeled as

$$f_{V\theta | H_s}(v, \theta_0 | l, h_s, t_z) = f_{V | \theta H_s}(v | \theta_0, l, h_s, t_z) f_{\theta | H_s}(\theta_0 | l, h_s, t_z) \qquad (6.7)$$

116

where $f_{\theta|H_s}(\theta_0|1, h_s, t_z)$ defines the density function for course selection as a function of significant wave height, and the conditional density of speed. The detailed procedure was described in [6.1].

6.6.4 Short-term Response Statistics

Under the assumption of a stationary, zero mean Gaussian process within each seastate, the response process is also a stationary zero mean Gaussian process. For a narrow banded process, the peak is Rayleigh distributed

$$F_p(a) = 1 - \exp(-\frac{a^2}{2m_0}) \tag{6.8}$$

where mo is the spectral meonet of the zero order, which is equal to the mean square of the process. It should be emphased that the distribution is conditional on Hs,Tz,v,θ and L. The rate of peaks with each time period is approximated by the rate of zero crossings mo.

$$v_p \approx v_0 = \frac{1}{2\pi}\sqrt{\frac{m_2}{m_0}} \tag{6.9}$$

In fatigue analysis, the stress range distribution is twice the amplitude leading the following stress range distribution for narrow banded process

$$F_{\Delta S}(s) = 1 - \exp(-\frac{s^2}{8m_0}) \tag{6.10}$$

6.6.5 Long-term Response Statistics

The long-term peak distribution of the response effect over the lifetime is obtained by unconditioning the short term distribution

$$F_p(a) = \int\limits_{H_s} \int\limits_{T_z} \int\limits_{L} \int\limits_{\theta} \int\limits_{V} \bar{v}_{h_s, t_z, l, \theta, v} F_p(a|h_s, t_z, v, \theta, l) f_{V\theta}(v, \theta|l, h_s, t_z) x$$

$$f_{H_s T_z(h_s, t_z)} f_L(l) dv d\theta dl dt_z dh_s \tag{6.11}$$

117

$v_{h_s,t_z,l,\theta,v}$ is a weighing factor which expresses the relative rate of response peaks within each sea state. $f_{v\vartheta}(v,\theta|l,h_s,t_z)$ accounts for the effect of maneuvering in heavy weather with respect to sailing speed and relative heading angle. $f_L(l)$ is the discrete distribution of loading conditions and f_{HsTz} is the two-dimensional description of the sea state experienced by the ship over the lifetime.

The above equation is too complicated to be applicable in engineering problems. Therefore, an equivelent long-term Weibull distribution is calibrated to the simulated outcome of the Monte Carlo simulation outcome for equation.

The Weibull distribution for fatigue analysis is fitted to the long-term stress range distribution.

$$F_{Long\Delta S}(s) = 1 - exp(-(s/A)^B) \tag{6.12}$$

The fitting of the Weibull parameters are based on the 0.95 and 0.99 fractile values, which approximately divides the contribution to the fatigue damage $(E(S^m))$ into three areas of equal magnitude,

$$\ln A = \frac{k \ln a_{0.95} - \ln a_{0.99}}{k - 1} \quad ; \quad B = \frac{\ln(-\ln 0.99)}{\ln a_{0.95} - \ln A} \tag{6.13}$$

where

$$k = \frac{\ln(-\ln 0.95)}{\ln(-\ln 0.99)} \tag{6.14}$$

The expression for the m'th moment of the stress range is then further :

$$E[\sigma^m] = A^m \Gamma(1 + \frac{m}{B}) = \sigma_N^m (\ln N)^{-m/B} \Gamma(1 + \frac{m}{B}) \tag{6.15}$$

The average rate of stress cylces over the lifetime is found in the simulation procedure for the evaluation of the long-term response distribution :

$$v_0 = \frac{1}{N} \sum_{i=1}^{N} v_{hs,tz,l,\theta,v,i} \tag{6.16}$$

where v_0 is the rate of stress cycles for the specified short term condition i and N is the number of simulations used in evaluating the integral. The number of stress cyles the ship is exposed to its lifetime T_L is then

$$N_{peak} = v_0 \gamma_L T_L \qquad (6.17)$$

where γ_L models the fraction of the lifetime the ship is expected to be at sea.

Based on the above procedure, the Weibull parameters for the long-term stress range is computed under the transfer function and stress vectors which is presented in section 6.3 and 6.4. The computational results are in Table 6.6.

Detail	Parameter A	Parameter B	Zero Crossing Rate
Detail A	3.3416	0.7538	0.12041
Detail B	0.8234	0.7538	0.12038

Table 6.6 Long-term stress range for fitness for purpose analysis

6.8 Cracked S-N Curve

6.8.1 Stress Intensity Factor

In order to obtain S-N Curves for the critical structural details (CSD) using the procedure described in chapter 4, the stress intensity factors for these details have to be found. A way to compute the stress intensity factors for corresponding specimen is proposed based on the fatigue classification . Fig 6.8 is the general fatigue classification for CSD in tankers.

119
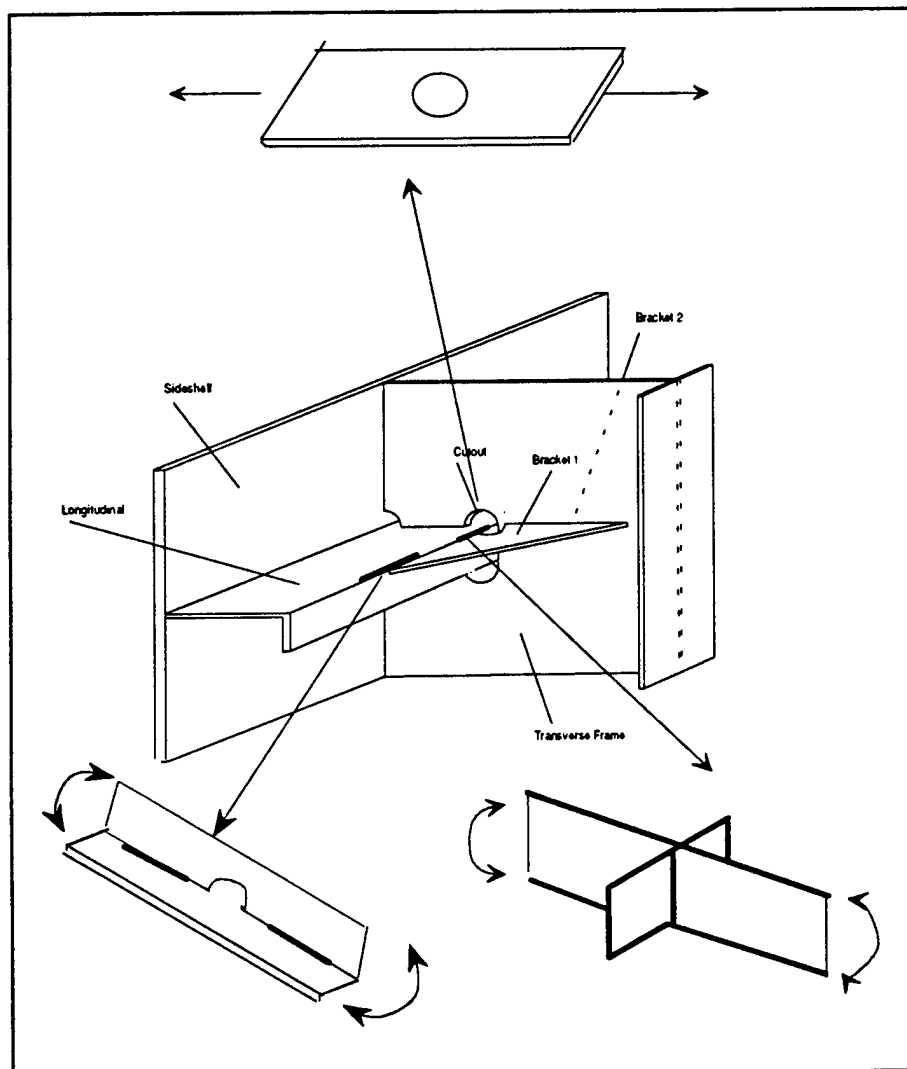
Fig 6.8 Fatigue Classification for CSD in Tankers.

Based on the fatigue classification in Fig 6.8, two stress intensity factors have to be computed in order to construct the equivalent S-N curves for the fitness for purpose analysis for the proposed detail. (Fig 6.9)
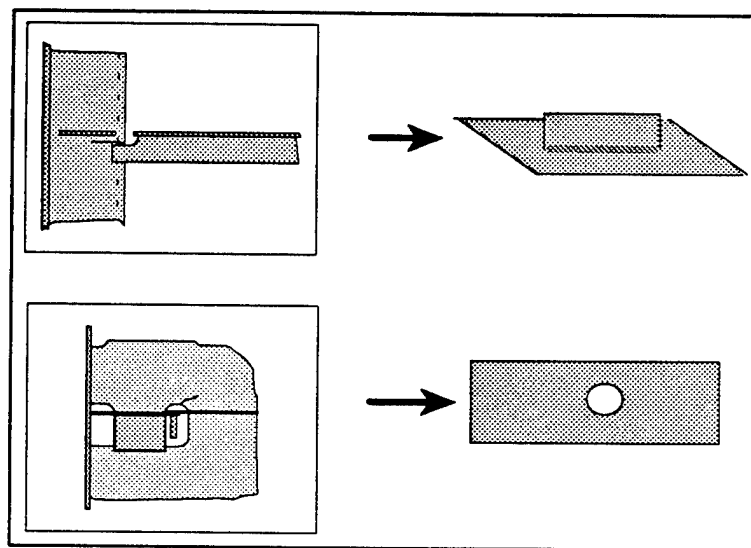
Fig 6.9 Proposed CSD and Corresponding Specimens

The FEA analysis for the corresponding specimen was conducted to determine the stress distribution around the crack. Fig 6.10 -6.14 is the stress distribution along the crack for the specimens. Based on the stress distribution, the stress intensity factors are computed for these specimens. It is assumed that these values are the approximate values for the stress intensity factors for the hotspots on proposed CSD.
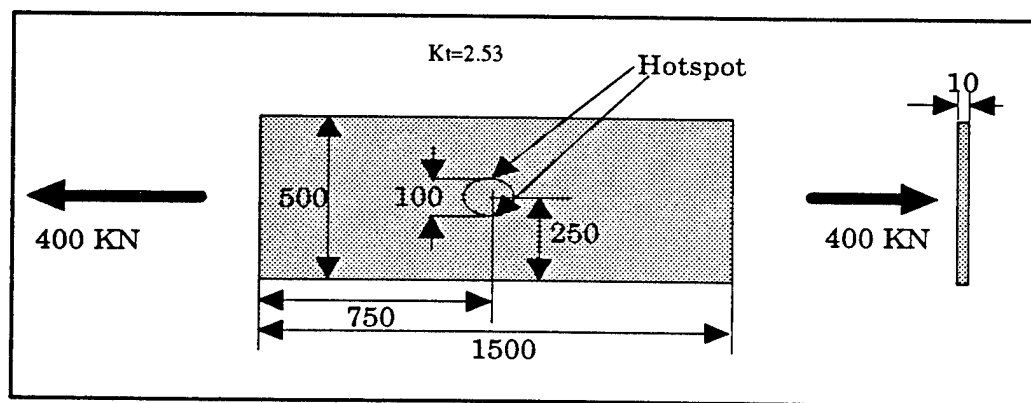
Fig. 6.10 Geometry and Dimension for Specimen A
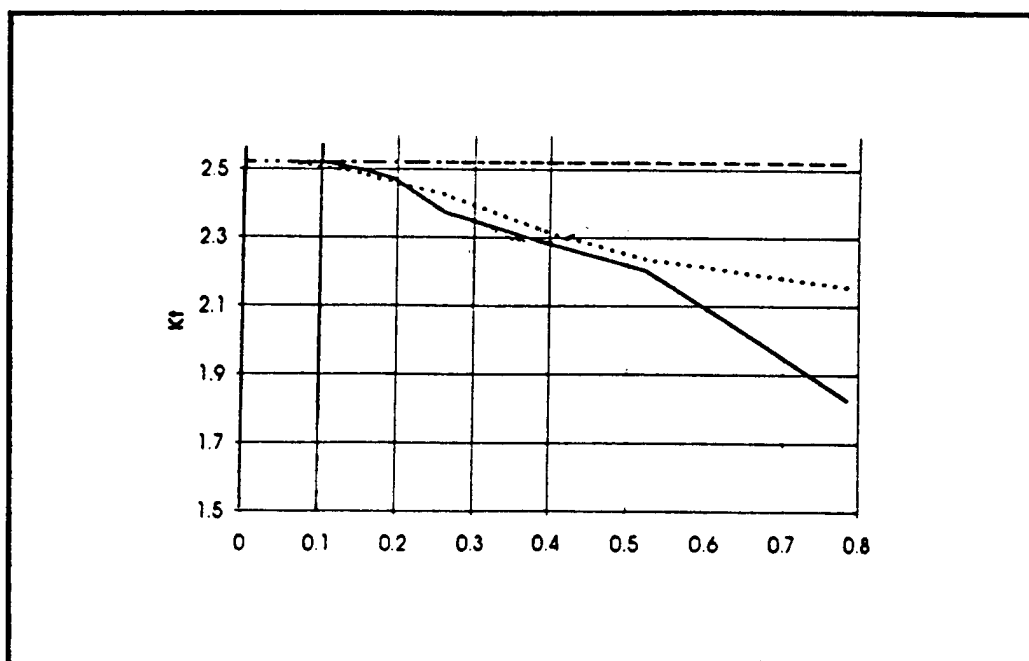
Fig 6.11 Stress Distribution for Specimen A
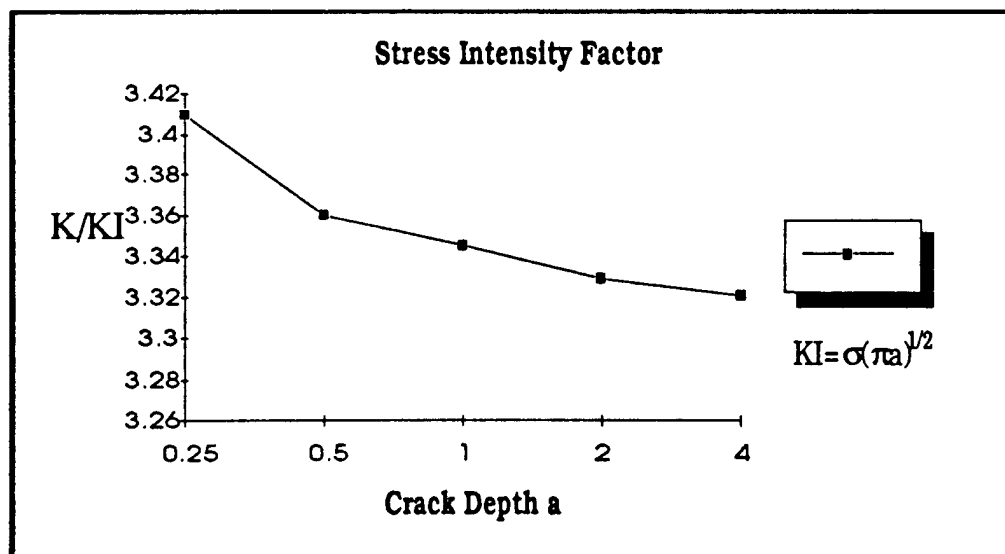
Fig. 6.12 Stress Intensity Factor for Specimen A

123
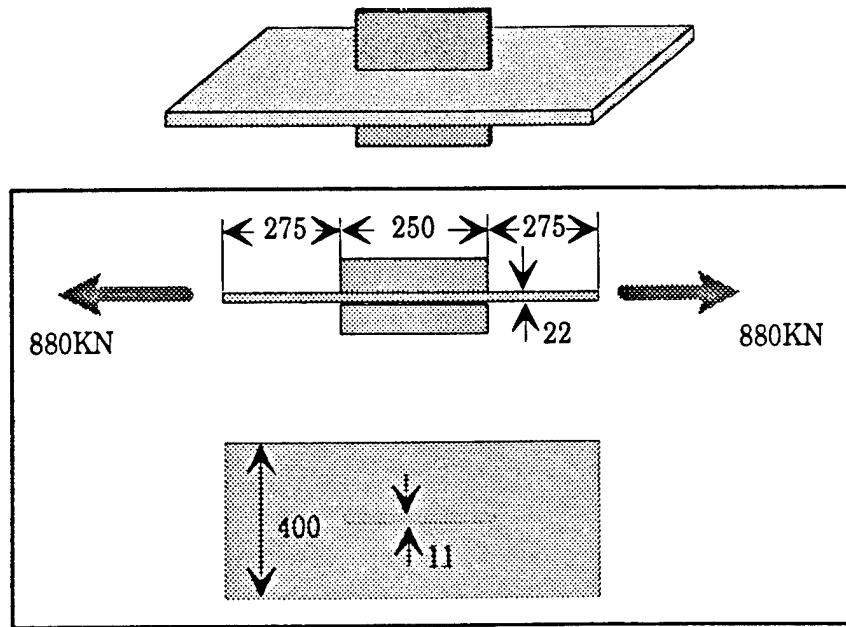
Fig. 6.13 Geometry and Dimension for Specimen B
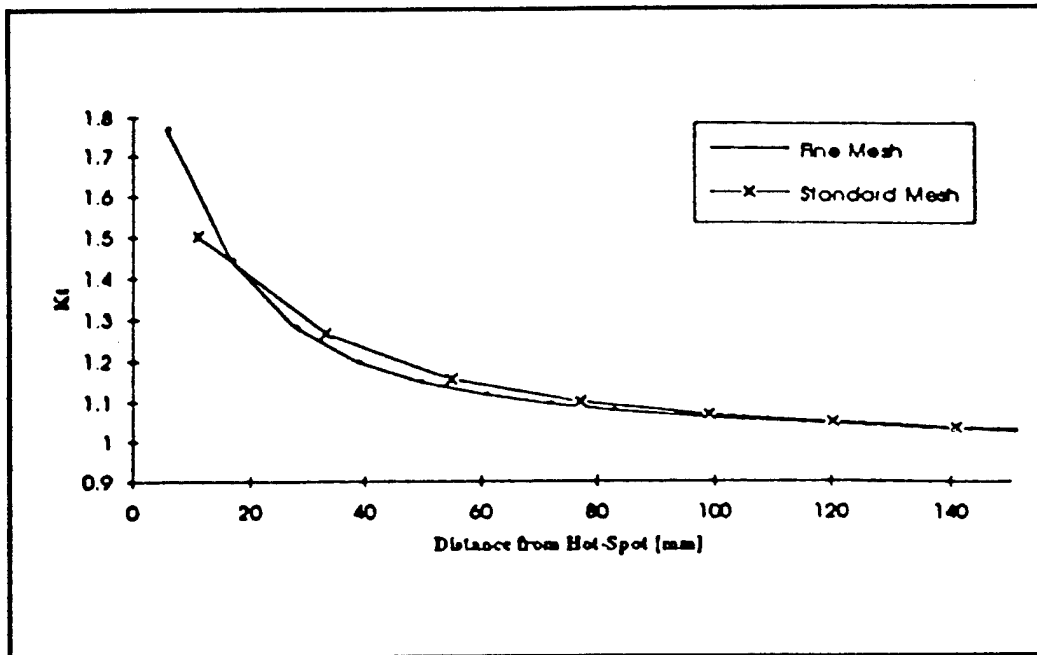
Fig 6.14 Stress Distribution for Specimen B

124

Stress Intensity Factor for Longitudinal Non load carrying Joint
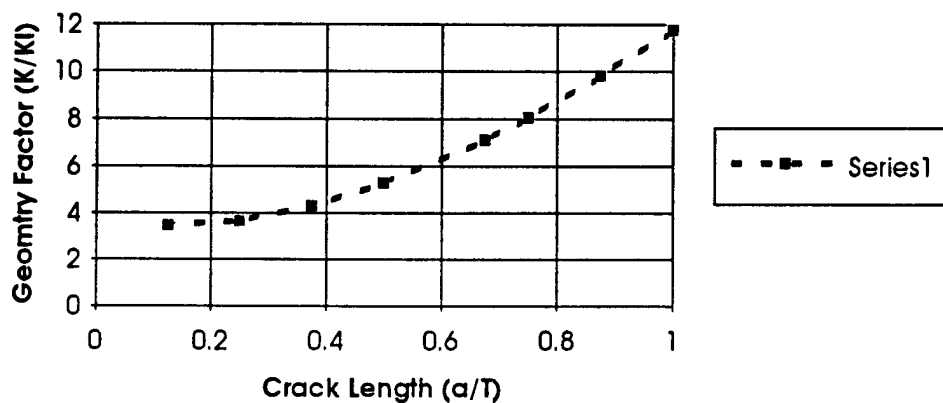
Fig 6.15 Stress Intensity Factor for Specimen B

6.8.2 Initial and Critical Crack Length

Inital crcak length and critical crack length are required to determine the equivalent S-N curves for cracked CSD. As discussed in chapter 2, the crack propagation is a two dimensional problem with crack depth and crack length. This leads to consideration for equivalent S-N curves. One is based on the crack depth while the other is based on crack length. Here, we used crack depth as the criteria to derive the equivalent S-N curve for the longitudinal non load carrying joint (Specimen B), and crack length as the criteria for the plate with a hole (Specimen A). We assume that the initial cracks are 0.25mm 0.5mm 1mm and 4mm. The critical crack length is 14mm which is the plate thickness.

6.8.3 S-N Curves for Cracked CSD

As we discussed early, the fracture mechanics analysis can be applied in the fatigue crack propagation analysis to provide insight into the crack growth and to set in-service inspection and repair program. A conventional fracture mechanics approach which is presented early is somehow cumbersome to use in inspection, maintenance and repair. Therefore, a strong intensive exists to simplify the approach to make it practicable to predict the remaining fatigue life of cracked detail.

Based on Paris Equation, we can derive the following expression under the constant loading:

$$N_p = \frac{1}{C \bullet \Delta\sigma^m \pi^{m/2}} \int_{a_i}^{a_f} \frac{da}{a^{m/2} \bullet F^m} = \frac{I}{C_1 (\Delta\sigma)^m} \tag{6.17}$$

where I is the following integral:

$$\int_{a_i}^{a_f} \frac{da}{a^{m/2} \bullet F^m} = I \tag{6.18}$$

This yields further:

$$\Delta\sigma = \sqrt[m]{\frac{I}{C_1 \bullet N_p}} \tag{6.19}$$

and

$$\log \Delta\sigma = -\frac{1}{m} \log N_p - \frac{1}{m} \log C_1 + \frac{1}{m} \log I$$

$$\log \Delta\sigma = A \log N_f + B(a_i) \tag{6.20}$$

which is the equation for cracked S-N curves. From the different initial crack size (the inspection size a_{insp}), the equivalent S-N curves for cracked detail was constructed. In this calcualtion, the material parameter m and C is selected as :

$$m = 3$$

$$C = \frac{1.315 \times 10^{-4}}{(895.4)^m} \tag{6.21}$$

Based on the following parameters and stress inetsnity factors which is calculated early, the equivalent S-N curves are constructed .
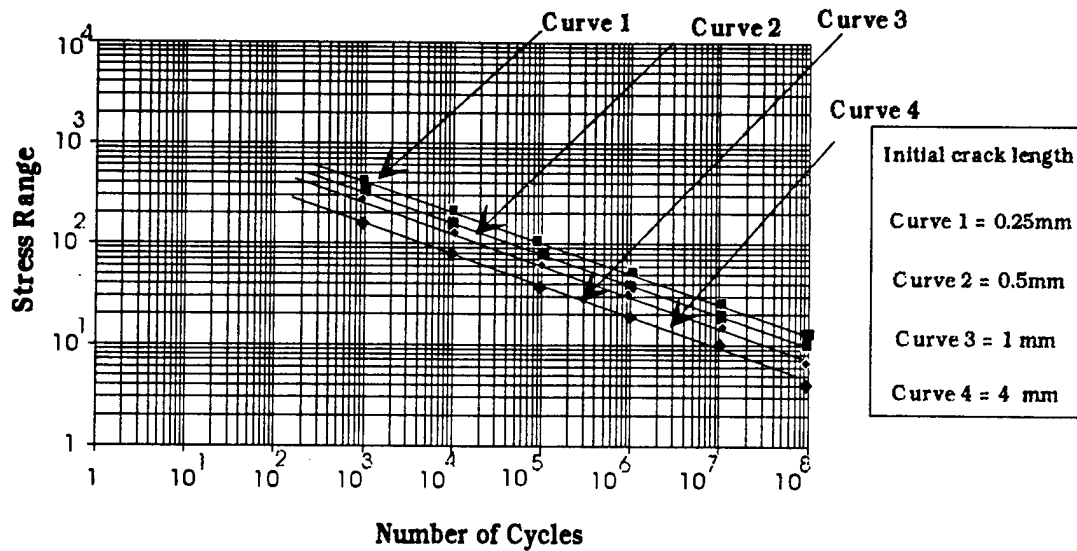
Fig 6.15 Equivalent S-N curves for Specimen A (Plate with a hole)
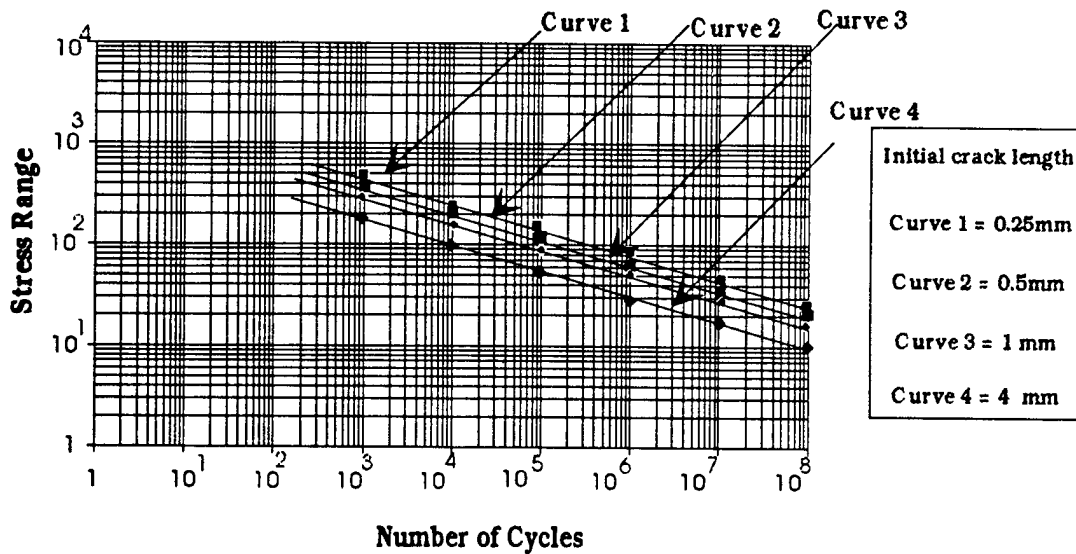
Fig 6.16 Equivalent S-N curves for Specimen B

127

Fig 6.16 and 6.17 is the equivalent S-N curves for a cracked longitudinal Joint and plate with a hole. It can be seen that curves for the plate with a hole is higher than that for longitudinal joint since the stress intensity factor for the plate is lower. If these curves are compared with the corresponding original fatigue S-N curves [6-6], we can see that these curves are much lower.

6.9 Remaining Life

The fatigue remaing life was computed by the updated fatigue evaluation software developed in SMP project.The uncertainties associated with cracked S-N curves are assumed to be the same as original S-N curves [6-1]. These are shown in Table 6.7. The S-N curves used in the analysis are the equivalent S-N curves developed in Fig. 6.16 and 6.17. The long-term stress range is from Table 6.6.

Frabrication and Assembly	1.2	0.2
SeaState Characterization	1.1	0.3
Wave Loads	0.8	0.2
Determination of Loads	0.9	0.3
SCF	1.0	0.3
	Median Bias	Cov Bias
Total	0.95	0.63

Table 6.7 Uncertainty Modeling in Fitness for Purpose Analysis

Fig 6.18-6.19 shows the probability of failure during the remaining 10 years with the initial crack depth 0.25mm,0.5mm,1mm and 2mm. It can be seen that the probability of failure for hotspot on sideshell longitudinal intersection with the initial crack size ao= 4mm is 88% which is very high if the critical crack ac=14 mm. That means that the propose detail not fit the purpose to extend another 10 years although the probability of failure for cutout is lower.

Another interesting point is that the probability of failure with the initial crack size ao =0.25 mm is 7% which is equivalent for results from traditional S-N analysis [6-1]. It may conclude that 0.25mm may be the good assumption for the initial crack size of weld details.

The probability of failure for cutout is lower. One reason may be due to the small long-term stress range. One may be due to its stress intensity factors.

The proposed analysis is based on the equivalent S-N approach which the residual life is determined by the cracked S-N curves. Thus, the uncertainty described here (Table 6.7) is the uncertainty modeling for long-term stress range while the fracture uncertainty is described through the uncertainty for equivalent S-N curves with standard deviation 0.3. It may not be enough for fracture behavior. The more rational modeling for fracture should be further developed to describe in detail about the uncertainty of critical crack, stress intensity factors and so on. This will be developed by probabilistic fracture mechanics and documented in subsequent report.
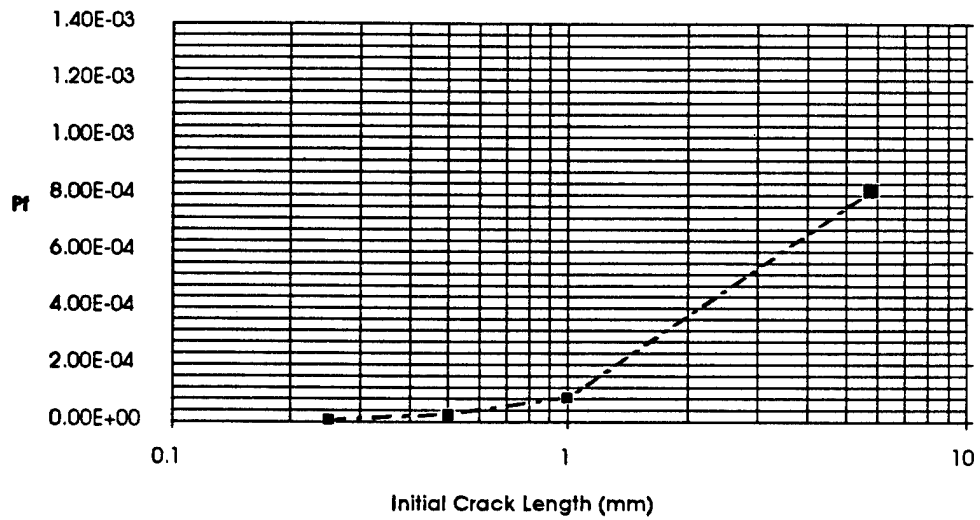
Fig 6.18 Probability of Failure During the Remaining 10 Years for Hot Spot around

Cutout
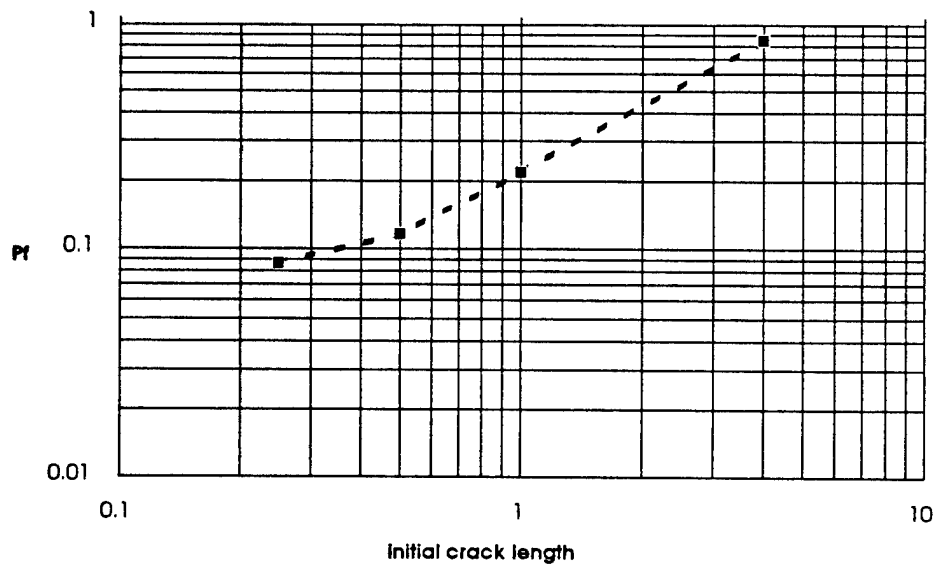
Fig 6.19 Probability of Failure during the Remaining 10 Years for Hotspot

on Sideshell Longitudinal Intersection

130

Based on the proposed analysis, several conclusions can be derived:

1) Equivalent S-N curves for cracked CSD are sensitive to the initial crack length while they are less sensitive for the critical crack length if it's well defined.

2) Equivalent S-N curve approach can provide rational results with enough accuracy.

3) In this study, the initial crack depth and through thickness crack depth are used to derive an equivalent S-N curve. It's well known that fatigue crack is two dimensional problem with crack depth and crack length. It may be more appropriate to derive S-N from crack length although the final critical crack length is hard to determine due to complex CSD in tankers.

4) Evaluation of stress intensity factors is the key issue for this approach. Hybrid method is developed to compute the stress intensity factors for general joints. In order to reduce the computation effects, the stress intensity factors are determined for corresponding fatigue specimens for general CSD. This may lead into some uncertainties. Meanwhile, load shedding is another issue which may result in some uncertainties. These issues will be addressed later.

6.10 Summary

The proposed fitness for purpose analysis has been conducted for the CSD in a 165,000 DWT tanker. It has shown that the proposed procedure can help naval architect make the evaluation about cracked CSD rapidly. The proposed fitness for purpose procedure is :

1 - Definition of structural detail and crack location.

131

2 - Computation of the transfer function for the ship. The transfer functions are computed for the two load cases. Full load and Ballast and for several wave headings and speeds based on the proposed travel routines and sea environment.

3 - Determination of the stress vectors at the Hotspots from finite element analysis.

- Estimation of the long-term distribution of the stress range σ at a hotspot. This estimation is based on a specified travel routine for given Madsen zones and specified maneuvering philosophy.

4 - Determination of the initial crack size for given hotshot

5 - Determination of the critical crack size for given hot-spot based on material toughness or durability requirement.

6 - Determination of the stress intensity factors for given hot-spots at the specified CSD

7 - Construction of the equivalent S-N curves for the hot-spot in given CSD.

8 - Determination of the remaining fatigue life based on the long-term extreme stress range and constructed equivalent S-N curves.

6.11 References

6.1 **Structural maintenance for New and Existing Ships**, Research Report SMP 1-1 through SMP 5-2. Dept. of Naval Architecture & Offshore Engineering, University of California at Berkeley, Berkeley, CA 94720. October, 1992

6.2 **Ship Structural Maintenance Project**, Research Report SMP II-1 through SMP II-3. Dept. of Naval Architecture & Offshore Engineering. October, 1993

6.3 Tao Xu & Robert, G Bea. Proposal for Joint Government-Industry Project **Evaluation of Fitness for Purpose of Cracked CSD in Tankers**. May 1993

6.4 Espen Cramer **Fatigue Reliability of Welded Joints in Tanker Structures**. Ph.D Dissertation. Department of Naval Architecture & Offshore Engineering, University of California at Berkeley, Berkeley, CA 1992

6.5 A.E.Mansour, **Ship Structure Reliability**. NA 240B Lecture Notes. Department of Naval Architecture & Offshore Engineering, University of California at Berkeley, Berkeley, CA 1990

6.6 A.E.Mansour, **A Notes for Extreme Wave Load and the Associated Probability of Failure**, Journal of Ship Research, 1986

6.7 R.G.Bea **Marine Structural Intergrity Program**. SHip Structure Committe Report, SSC-365

6.8 R.G.Bea **Reliability-Based Design Criteria for Coastal and Ocean Structures**, The Institute of Engineers, Australia, 1990

6.9 E.Nikolaidis, P. Kaplan, **Uncertainties in Stress Analysis on Marine Structures**, Ship Structure Committee Report, SSC-363

6.10 Anil Thayamballi, Y-K.Chen, Donald Liu, **Fracture Mechanics Based Assessment of Fatigue Reliability in Ship Structures**. Trans, SNAME 1984

6.11 **Guide for the Fatigue Strength Assessment of Tanker**, American Bureau of Shipping, New York, NY 1992.

6.12 **Definition and Validation of a Practical Rationally-Based Method for the Fatigue Analysis and Design of Ship Hulls**. Society of Naval Architects and Marine Engineers T&R Report No. R-41

6.13 Fatigue Reliability (a series of papers) ASCE Committee on Fatigue and Fracture Reliability, Journal of Structural Division 1982

6.14 Wirsching, P.H. and Chen, Y.N **Consideration of Probability-Based Fatigue Design for Marine Structures**, Proceeding of the Marine Structural Reliability Symposium, 1987

6.15 S.R. Winterstein, P. Friis-Hansen, **Fatigue Damage in the Sideshell of Ships**. Submitted to Journal of Marine Structures, 1992

Chapter 7

Conclusions

The purpose of this project to establish a general fitness for purpose analysis for cracked critical structural details (CSD) in tankers. Particular emphasis was paid to evaluation of the stress intensity factor and development of S-N curves for cracked CSD in tankers

The fitness for purpose procedure developed herein can provide a sufficient basis for naval architects to make rapid decision for maintenance and repair of the cracked CSD in tankers.

The S-N curve for cracked CSD is the key issue for the fitness for purpose analysis. The methodology for the development of cracked S-N curves provide high accuracy in application. But the determination of the input parameters such as final critical crack length, material toughness and stress intensity factors may lead to considerable uncertainties.

The stress intensity factor (SIF) evaluation is the key in fracture mechanics. The hybrid method is one of the most efficient methods to determine the SIF with high accuracy. It only employs one finite element analysis to determine the stress gradients. However, this method is still conservative due to the load shedding and complex due to requirements for FEA with extremely fine mesh.

The long-term fatigue loading may be one of the most important uncertainty resources for fatigue analysis and fitness for purpose analysis. A new model for wide-banded process can predict more accurate results than previous models. The load sequence effects on crack growth for large CSD is still unclear although it is widely believed that this effects is not important in comparision with other factors.

It can be concluded that there are three major uncertainties in fitness for purpose analysis. One is critical crack length, one is long-term fatigue loading, and one is stress intensity factors. The study of SIF for cracked CSD to calibrate the rational analytical formula including load shedding has been conducted during this project. This will documented in a subsequent report.

As we know, many factors related to the fatigue crack growth process are variable, indefinite, or unknown, leading to large uncertainties. As the result of the uncertainties, the durability of the considered tanker against fatigue is more likely to evaluate in a probabilistic sense. This will be addressed in a subsequent report.

Fitness for Purpose Evaluation of Critical Structural Details in Tankers

FRACTURE- A Computer Code for Fracture Mechanics Analysis of Crack Growth in Cracked Critical Structural Details in Tankers

Tao Xu
and
Professor Robert G. Bea

Department of Naval Architecture and Offshore Engineering
University of California, Berkeley

Preface

The one year Joint Industry Research Project **"Fitness for Purpose Evaluation of Cracked Critical Structural Details (CSD) in Tankers"** was initiated in 1993 by the Department of Naval Architecture & Offshore Engineering, University of California at Berkeley as an extension of the projects **"Structural Maintenance for New and Existing Ships"** and **"Ship Structural Maintenance"**. The objective of this project is to develop engineering guidelines and procedures to help ship repair engineers, port superintendents and surveyors make evaluations of the fitness for purpose of cracked Critical Structural Details (CSD) in tankers.

This project was made possible by the following sponsoring organizations:

-American Bureau of Shipping -Chevron Shipping Cooperation

-Mitsubishi Heavy Industries   -Newport News Shipbuilding & Dry Dock Co.

-Ship Structure Committee

This report documents the theoretical background with the computer program FRACTURE.

Table of Contents

List of Figures

Chapter 1

Introduction

Based on the previous studies and previous SMP I & II projects, fatigue cracks were usually located in internal structural details. The typical fatigue cracks in details are shown in Fig. 1.1

In general, fatigue cracks are occurred in CSD within two different categories. One is the structural cutout, another one is the joint. For these two different categories, the computation of the stress intensity factors is different in FRACTURE.

This report is divided into five chapters. Chapter 1 is the introduction. Chapter 2 documents the stress intensity factor's computation. Chapter 3 addresses the crack growth and fatigue life computation. Chapter 4 is the user's manual. Chapter 5 is the program versatility.

Fig. 1.1 Typical Fatigue Cracks in Critical Structural Details (CSD)
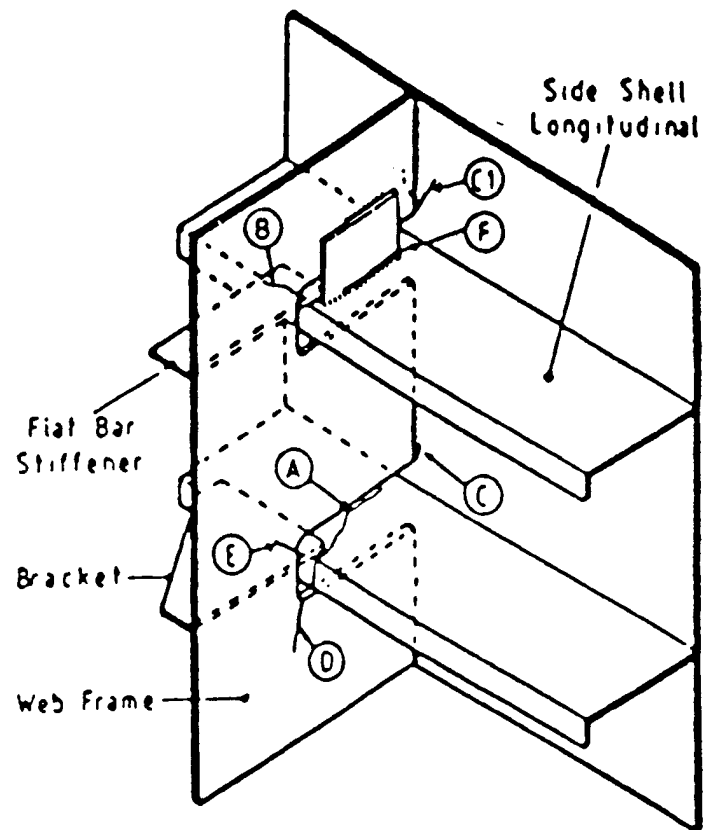
A   Longitudinal Stiffener Cracked.
B   Flat Bar Stiffener Cracked
C   Shell Plate to Web Weld Cracked
C1 C'Type Crack Extending into Shell Plate
D   Web Frame Cracked
E   Bracket Cracked
F   Lug Cracked (Typical Detail)

Chapter 2

Stress Intensity Factors

2.1 Stress Intensity Factors for Joints.

The method used in computing the stress intensity factor for joints in CSD is basically an influence function - and a superposition method. It employs available solutions for two- and three- dimensional crack problems. From these the influence of different factors affecting K are separated and used to "compose" and estimate of K in actual case. (1-8)

General Expression for K

The stress intensity factor can be expressed in a general form as

$$K = K_B F \tag{2.1}$$

where :

K_B = stress intensity factor pertaining to "standard case".

F = correction factor that modifies K_B to account for the actual configuration of the local geometry and crack geometry as compared to the standard case.

The standard case for 2-D is a through crack of length 2a in an infinite plate with a remote uniform tensile stress acting normal to the crack. (Fig. 2.1). The standard K solution is

$$K_{B2} = \sigma\sqrt{\pi a} \tag{2.2}$$

The standard 3-D case is an elliptical crack embedded in an infinite solid subjected to uniform tension (Fig. 2.2). The stress intensity factor along the boundary of the elliptical crack is (Mode I):

$$K_{B3} = \frac{\sigma\sqrt{\pi a}}{\varphi}(\frac{a^2}{c^2}\cos^2\varphi + \sin^2\varphi)^{0.25} \tag{2.3}$$

where φ is the complete elliptical integral and is given by:

$$\varphi = \int_0^{\pi/2}\left\{1 - (1 - \frac{a^2}{c^2})\sin^2\phi\right\}^{0.5} d\phi \tag{2.4}$$

It is shown that K_{B2} (relating to a straight curve front) differs from K_{B3} (relating to an elliptic, i.e. a curved crack front) by the expression

$$\frac{1}{\varphi}(\frac{a^2}{c^2}\cos^2\varphi + \sin^2\varphi)^{0.25} \tag{2.5}$$

which accounts for the effect of the crack shape (a/2c) and position (φ) on the crack front.

7

A practical joint case usually differs from a standard case due to

- boundary effects

- stress gradients

Boundary- or, finite-dimension-, effects are taken into account through correction factor, as illustrated in Fig. 2.3

The "two dimensional crack" of Fig. 2.3a differs from the standard case of Fig. 2.1, by a finite width, this is taken into account through F_W.

The "two-dimensional crack" case of Fig. 2.3b differs from the standard case of Fig. 2.1 due to finite thickness and the crack emanation from a free surface. These are accounted through factors F_T and F_S respectively.

The "three-dimensional crack" case of Fig. 2.3c differs from the basic case of Fig. 2.2 as the crack emanates from a free surface, and as the body has a finite width and finite thickness. These deviations from the basic case are accounted for through the factors F_S, F_W and F_T.

The "two-dimensional crack" case of Fig. 2.4 differs from the basic case of Fig. 1 by the sheet curvature. It's taken into account through F_C.

Stress concentration are synonymous with stress gradients. This stress condition is an important deviation from a basic case, and must be taken into account through a correction factor F_G.

Fatigue cracks may obtain various shapes (Fig. 2.3), e.g. the crack front may be straight or curved. The curvature (crack shape) is an important parameter influencing K. Thus, it is essential that this effects should be accounted for through a factor F_E. (elliptic

8

shape factor). The solution for the 3-D standard case of Fig. 2.2 includes the effect of crack

shape through expression $\frac{1}{\varphi}(\frac{a^2}{c^2}\cos^2\varphi + \sin^2\varphi)^{0.25}$. A curved crack front (a/2c > 0)

specializes to a straight one as a/2c -> 0. The φ (and F_E) -> 1, and accordingly the standard

stress intensity factors for the two- and three-dimensional case, these two can be unified

through the expression

$$K_B = \sigma\sqrt{\pi a}F_E \qquad (2.6)$$

The standard solutions are elastic. Local plasticity around the crack tip may occur,

however, and is in fact a prerequisite for fatigue cracking to occur. The effect of this

plasticity on K is normally insignificant. However, the effect can be generally be taken into

account through a plasticity correction factor F_P.

Implementing the above correction factors, F may generally be expressed as

$$F = F_s \bullet F_T \bullet F_W \bullet F_C \bullet F_G \bullet F_P \qquad (2.7)$$

or

$$F = F_B \bullet F_C \bullet F_G \bullet F_P \qquad (2.8)$$

i.e. $\quad F_B = F_S \bullet F_T \bullet F_W \qquad (2.9)$

Finally, K may be conveniently expressed as

$$K = \sigma\sqrt{\pi a} \bullet F \qquad (2.10)$$

In the above expressions

F_E = basic crack shape factor

F_B = boundary correction factor, encompassing the total boundary (i.e. free

surface) effect

9

Fs = front face correction factor, accounting for a free surface behind the crack front.

FT = back face or finite thickness correction factor, accounting for a free surface ahead the crack front.

Fw = finite width correction factor, accounting for a free surface ahead of the crack front.

Fc = cylindrical shell (i.e. curvature) correction factor

FG = stress gradient correction factor

FP = crack tip plasticity correction factor.

The basic crack shape factor - FE

This factor takes into account the effect of crack front curvature, i.e., crack shape. It stems from Irwin's solution for an elliptical flaw, embedded in an infinite elastic solid subject to uniform tension. Hence, the resulting FE for any position along the crack front, describe by angle ϕ to the major axis (Figs 2.2 ,2.5) is

$$\frac{1}{\phi}(\frac{a^2}{c^2}\cos^2\phi + \sin^2\phi)^{0.25} \tag{2.12}$$

This equation was derived on the basis of uniform tension across the crack surface while it may argued that gradients will modify the result, that is taken into account by the FG correction later described. Likewise, this equation was derived for a crack embedded in an infinite elastic solid. Hence, it may be expected that the free surfaces encountered in practical case (finite body) will influence FE. Thus, FE can be interpreted as a factor that accounts for the (elliptical) crack shape without encompassing the complete shape-effect, only these related to the standard case. Parts of these effects are included in the Fs-, FT- and FG- estimates, as these are functions of a/2c. Hence, FE is maintained in its original (i.e.

10

standard case) form for stress intensity estimates. The dependence of F_E on crack shape is shown in Fig. 2.6.

φ is the complete elliptical integral of the second kind, as given in

$$\varphi = \int_{0}^{\pi/2} \left\{ 1 - (1 - \frac{a^2}{c^2})\sin^2 \phi \right\}^{0.5} d\phi \tag{2.13}$$

A good approximation is obtained through the expression

$$\varphi = \left\{ 1 + 4.5945(a / 2c)^{1.65} \right\}^{0.5} \tag{2.14}$$

hence,

$$F_E = \left\{ 1 + 4.5945(a / 2c)^{1.65} \right\}^{-0.5} \tag{2.15}$$

The Front Free Surface Correction Factor - Fs

This factor accounts for a free surface at the "mouth" of the crack. (Fig. 2.3). Several expressions are proposed for the crack shape influence on Fs. A reasonable relation provides intermediate values is [6]

$$F_S = 1.122 - 0.18(a / 2c) \tag{2.16}$$

while the curved function in Fig. 2.8 provides upper bounds.

The Finite Thickness Correction Factor - F_T

This factor (also called "the back free surface correction factor") accounts for the effect of a finite plate thickness, i.e. a free surface ahead of the crack front (see Fig. 2.3). It depends on

- crack geometry (size, shape)

- bending conditions (free, restrained, during cracking)

- crack opening stress distribution

- position on crack front

Surface cracks are among the most common flaws in many structures. Consequently accurate stress intensity factors for such cracks are needed for reliable prediction of crack growth rates and fracture strengths. However, exact solutions are not available, but several solutions have been obtained by approximate methods and these solutions differ considerably. In [7] it was shown that the estimates compared varied by 6 per cent when a/2c > 0.3 and a/t < 0.5. Beyond these ranges deviations might exceed 100 per cent. More, deviations are particularly large for small (a/2c) - ratios.

Two of the closed-form expressions available for uniform tension loading are

$$F_T = \sqrt{\sec \frac{\pi a}{2t}} \qquad \text{when a/2c = 0} \qquad (2.17)$$

$$F_T = \sqrt{\frac{2t}{\pi a} \tan \frac{\pi a}{2t}} \qquad \text{when a/2c = 0} \qquad (2.18)$$

These are the forms most frequently cited in the literature, although in later years very often in modified versions, [8]. They pertain to the symmetrical crack cases presented in Fig. 9, case 1 and 2.

These two expressions are also applicable to non-symmetrical crack configurations where bending is prevented by imposed boundary conditions. Hence, the strips in Fig. 9, case 1' and 2', are comparable to those in case 1 and 2. At real ship structural details the roller supports might be provided by a web and /or stiffener.

F_T for an edge crack (a/2c =0, see Fig. 2.3) is quite sensitive to whether or not the section is permitted to bend as crack growth occurs. The bending tendency is natural for any strip in which crack growth is not symmetrical with respect to the strip centerline.

Bending amplifies the back surface correction - particularly at high values of a/t where more bending occurs. If the rollers on either strip of Fig. 2.9, case 1' and 2', are removed, the back surface correction must be modified, according to case 3.

It should be noted that the solution for case 3 is valid only when the displacement of the strip is free from constraint. In actual structures, any connected structural member is under constraints imposed by connections. When a crack occurs in a certain component, its compliance increases. The load and deformation are redistributed between members. (Load shedding which will be discussed later in this project). Thus, the boundary condition is not displacement-free but displacement-limited.

Other examples of displacement constrained strips with a single edge crack are given in case 4 and 5. The in-plane transverse displacement at infinity is restrained.

In case 4 the local in-plane transverse displacement near the cracked section is not restrained, while it is in case 5.

The F_T - expressions pertaining to the above cases are given as following [8,9]

-Case 1;

$$F_T = [1 - 0.025(a/b)^2 + 0.06(a/b)^4] \frac{1}{\sqrt{\cos \dfrac{\pi a}{2b}}} \qquad (2.19)$$

surface crack : b=t

subsurface crack : b=t/2

-Case 2;

$$F_T = \frac{(1 + 0.122 \cos^4 \dfrac{\pi a}{2b})}{1.122} \sqrt{\frac{2b}{\pi a} \tan \frac{\pi a}{2b}} \qquad (2.20)$$

Single crack : b=t

Double crack : b=t/2

-Case 3;

$$F_T = \left\{ \frac{0.752 + 2.02(a/b) + 0.37(1 - \sin \dfrac{\pi a}{2b})^3}{1.122 \cos \dfrac{\pi a}{2b}} \right\} \sqrt{\frac{2b}{\pi a} \tan \frac{\pi a}{2b}} \qquad (2.21)$$

b=t

-Case 4;

$$F_T = \left\{ \frac{1.122 - 0.561(a/b) + 0.085(a/b)^2 + 0.180(a/b)^3}{1.122\sqrt{1 - a/b}} \right\} \qquad (2.22)$$

b=t

-Case 5;

$$F_T = \sqrt{\frac{2b}{\pi a} \tan \frac{\pi a}{2b}} \qquad (2.23)$$

b=t

14

The above expressions are plotted in Fig. 2.10 which clearly shows the effect of displacement constraint.

Within the computer program, the user decides which of the case is closest to the actual case, and has the option to choose the appropriate F_T among the solutions for these cases.

For semi-elliptic surface cracks (a/2c >0), the net ligament on either side of the crack inhibits bending, and significantly limits the crack from sensing the upcoming free surface. Therefore, any amplifications due to bending effects are likely to be small or negligible, as long as the crack is small compared to the cross sectional area of the body. Hence the choice between bending and no bending depends on the structural details as well as how the crack is growing (i.e. the crack shape). Fatigue crack growth at welded cover plates, stiffeners, gusset plates and other common girder attachments in ship structure is rarely symmetrical. Yet, bending is usually limited by virtue of the girder web and/or the attachment itself. Thus, no bending corrections are considered to be most applicable in typical ship structures.

The F_T - estimates adopted here, for semi-elliptic surface cracks are shown in Fig. 2.11 [7]. These pertain to the deepest point on the crack front. (i.e. point A in Figure 7).

It should be pointed out that all F_T corrections mentioned are strictly valid only in cases of uniform tension stress.

The Finite width Correction Factor - F_w

This correction factor accounts for the effect of finite width on K for a through crack. It is analogous to F_T for a part-through crack when a/2c=0 and, hence, the same expressions are used to estimate F_w by merely replacing t with W (plate width).

15

The Curvature Correction Factor -Fc

This factor accounts for the effect of the curvature of cylindrical shell upon the flat plate solution for K for a through crack. It may be expressed as [10]

$$F_C = G_m + 2\frac{z}{t}G_b \tag{2.24}$$

where G_m = contribution due to membrane stresses

G_b = contribution due to secondary bending stresses (due to the cracking)

z = distance from shell "mid plane"

t = shell thickness

that is,

- On the outer surface : z=+t/2   ; $F_C = G_m + G_b$

- On the inner surface : z=-t/2   ; $F_C = G_m - G_b$

- On the shell mid plane :z =0   ; $F_C = G_m$

G_m and G_b are functions of a / $\sqrt{Rt}$ (fig. 2.12), where

2a = length of circumferential through crack (perpendicular to the cylinder axis)

R = radius of cylinder (tube)

In the computer program, F_C is set equal to its mean value, i.e. $F_C = G_m$.

The Stress Gradient Correction Factor - FG

This factor (also called " the geometry correction factor") accounts for non-uniform crack opening stresses. i.e. stress field gradients at the crack locus [1-4,7]. The gradients may be due to e.g. non-uniform applied stress (such as bending) or stress concentration caused by detail body. This stress gradient should not be confused with that which occurs

16

at the crack tip. F_G represents a more global condition which is not acknowledged by a strength of materials analysis.

F_G is conveniently derived from known solutions for K in the following manner. The solution of a crack stress field problem can be visualized as a two-step process [7,8], Fig. 2.13

1. The stress distribution problem is solved in a manner satisfying the boundary conditions (displacements, stresses) but with the crack considered absent.

2. To this stress field is superposed another stress field which cancels any stresses acting directly across the crack along the line of the crack.

Step 1 is a non-singular elasticity problem and can be solved by a FEM analysis. As the addition of a non-singular stress field ($\sigma(x)$, Step 1) does not affect the value of K (caused by -$\sigma(x)$, Step 2) the resulting K will be identical with that obtained from Step 2.

To evaluate K from Step 2, an influence (Green's) function method is employed. An influence function can be defined as

$$G_I(b,a) = \frac{1}{p} K_{IP}(b,a) \tag{2.25}$$

where K_{IP} = due to a load P at x = b

P   = load per unit sheet thickness / width

Hence, $G_I(b,a)$ is the K_I value arising from a unit force (per unit thickness/width) applied at abscissa x = b. $G_I(b,a)$ is independent of loading and depends merely on all the geometry parameters of the cracked body. If a solution for the stress intensity factor is

17

known for any particular load system, then this information is sufficient to determine the stress intensity factor for any other load system.

A pressure $p(x)$ applied on an infinitesimal surface $t($ or W $)$ dx results in an infinitesimal stress factor.

$$dK_I(x,a) = G_I(x,a) \bullet p(x)dx \qquad (2.26)$$

Thus, the K_I resulting from the total crack surface loading is

$$K_I = \int_0^a G_I(x,a) \bullet p(x)dx \qquad (2.27)$$

In the actual case $p(x) = -\sigma(x) =$ crack opening stresses (mode I). Hence, the stress distribution in step 1, although being a non-singular distribution, affects the strength of the singularity through this integral. The most significant general feature of G_I is the inverse square root singularity at the crack tip. This indicates that the stresses near the crack tip exerts a much greater influence on the strength of the singularity than the stresses far from it.

Values of K for intermediate crack sizes and the corresponding gradient correction factors can be computed by a simply repeating Step 2 for any desired crack size.

In a part- through crack case the computation of the stress gradient corrector F_G might be based on the following solution of the problem shown in fig. 2.14 [8]

$$K_I = \frac{2p}{\sqrt{\pi a}} \bullet \frac{1}{\sqrt{1-(b/a)^2}} \bullet F(b/a) \qquad (2.28)$$

18

Therefore the influence function in this case is

$$G_I = \frac{2}{\sqrt{\pi a}} \cdot \frac{1}{\sqrt{1 - (b/a)^2}} \cdot F(b/a) \qquad (2.29)$$

With the condition of $p(x) = \sigma(x)$, yields

$$K_I = \sqrt{\pi a} \cdot \frac{2}{\pi} \int_0^a \frac{\sigma(x)}{\sqrt{a^2 - x^2}} \cdot F(x/a) dx \qquad (2.30)$$

where $\sigma(x)$ can be obtained from a FEM analysis.

The stress distribution could be represented by a polynomial expression and could be integrated analytically. However it is more convenient to use a discretized stress distribution and the above equation then may be reformulated as

$$K_I \approx \sqrt{\pi a} \cdot \frac{2}{\pi} \sum_{i=1}^n \sigma_{b_i} \cdot F(\overline{b_i}/a) dx \int_{b_i}^{b_{i+1}} \frac{dx}{\sqrt{a^2 - b^2}} \qquad (2.31)$$

where σ_{bi} = stress in block no. "i"

$bi = 1/2(bi + bi_{+1})$

The integration is carried out over the block width, and the summation over the number of blocks. After factoring out the nominal stress σ, applied remotely from the crack, integration leads to

$$K_I = \sigma \sqrt{\pi a} \cdot \{ \frac{2}{\pi} \sum_{i=1}^n \frac{\sigma_{bi}}{\sigma} \cdot F(\overline{b_i}/a) dx [\arcsin \frac{x}{a}]_{b_i}^{b_{i+1}} \}$$

19

$$= \sigma \sqrt{\pi a} \cdot \{\frac{2}{\pi} \sum_{i=1}^{n} \frac{\sigma_{bi}}{\sigma} \cdot w_{bi}\}$$

$$= \sigma \sqrt{\pi a} \cdot F \tag{2.32}$$

where w_{bi} = weight of block no. "i".

In the underlying case of Fig. 2.15, i.e. an edge crack is a semi-infinite body, $F_T = F_E = 1.0$ according to the present terminology. Then F corresponds to $F_S \cdot F_G$ ($F_P := 1.0$), and hence, the stress gradient correction factor may isolated as

$$F_G = \frac{F}{F_S} \tag{2.33}$$

F_S depends on the stress distribution, and is equal to 1.122 for the case of uniform stresses acting over the whole area of an edge crack. A non-uniform stress-field with the stress peak at the surface accentuates the free surface effect, as indicated by the weight function in Fig. 2.14. Thus, by expressing the gradient factor as

$$F_G = \frac{F}{1.122} \tag{2.33}$$

the stress gradient effect on F_S is included in F_G. The resulting expression used in computing F_G in the case of an edge crack might then be written as

$$F_G = \frac{2}{1.122\pi} \sum_{i=1}^{n} \left\{ \frac{\sigma_{bi}}{\sigma} F(\overline{b}_i / a) \cdot [\arcsin \frac{b_{i+1}}{a} - \arcsin \frac{b_i}{a}] \right\} \tag{2.34}$$

The computation of F_G in the case of a through crack might be based on a solution of the problem in Fig. 2.16 [8],

20

$$K_I = \frac{2p}{\sqrt{\pi a}} \frac{a}{\sqrt{a^2 - b^2}} \qquad (2.35)$$

which is an exact solution in the case of symmetrically distributed opening stresses. A comparison of this Eqs. and part through thickness Equation shows that they differ by the factor F(b/a), which thus is a factor accounting for the free surface effect.

F_G for this case might be expressed as

$$F_G = \frac{2}{\pi} \sum_{i=1}^{n} \left\{ \frac{\sigma_{bi}}{\sigma} [\arcsin \frac{b_{i+1}}{a} - \arcsin \frac{b_i}{a}] \right\} \qquad (2.36)$$

with $b \in (0, +a)$

For more general case in Fig. 2.17 which is not symmetry in the stresses, i.e.

$$K_{I_a} = \frac{p}{\sqrt{\pi a}} \sqrt{\frac{a \pm b}{a \mp b}} \qquad (2.37)$$

This case yields the following expression for F_G :

$$(F_G)_{\pm a} = \frac{1}{\pi} \sum_{i=1}^{n} \left\{ \frac{\sigma_{bi}}{\sigma} [\arcsin \frac{b_{i+1}}{a} - \arcsin \frac{b_i}{a} \mp \sqrt{1 - (\frac{b_{i+1}}{a})^2} \pm \sqrt{1 - (\frac{b_i}{a})^2}] \right\} \qquad (2.38)$$

where $b \in (-a, +a)$

It should be noted that the F_G - estimate for a part-through crack is conservative when a/2c >0. The conservatism increase as the stress concentration and the crack front curvature increase.

The Plasticity Correction Factor - Fₚ

This correction factor accounts for the effect of crack tip plasticity on ΔK. Irwin suggested that the effect of small plastic zones corresponding to an apparent increase of the elastic crack length by an increment (r_P) equal to half the plastic zone size (R_P).

The plastic zone size may be written as [7]

$$R_p = \kappa \left(\frac{\Delta K}{\sigma_y}\right)^2 \tag{2.39}$$

where $\quad\quad \Delta K$ = stress intensity factor range

$\quad\quad\quad\quad \sigma_y$ = monotonic, uniaxial yield stress

$\quad\quad\quad\quad \kappa$ = coefficient depending on

$\quad\quad\quad\quad$ - type of loading, i.e. monotonic/ cyclic

$\quad\quad\quad\quad$ - stress state , i.e. plane stress/plane strain

Thus, the crack length correction is

$$r_p = \frac{\kappa}{2}\left(\frac{\Delta K}{\sigma_y}\right)^2 \tag{2.40}$$

ΔK might be expressed as

$$\Delta K = \Delta\sigma\sqrt{\pi a} \cdot F_1 \tag{2.41}$$

where $\quad\quad F_1$ = product of all correction factors except F_P

Taking plasticity into account, the corrected ΔK then is

$$\Delta K^* = \Delta\sigma\sqrt{\pi(a + r_p)} \cdot F_1$$

$$= \Delta\sigma\sqrt{\pi a}\sqrt{1+\frac{\kappa}{2a}(\frac{\Delta K}{\sigma_y})^2} \cdot F_1 \qquad (2.42)$$

Accordingly, the plasticity correction factor might be expressed as

$$F_p = \sqrt{1+\frac{\kappa}{2a}(\frac{\Delta K}{\sigma_y})^2} \cdot F_1 \qquad (2.43)$$

The plastic zone size coefficient κ is an input parameter to the program. Interesting values for κ are

$$\kappa = 1/24\pi \qquad ; \text{cyclic plane strain}$$

$$\kappa = 1/8\pi \qquad ; \text{cyclic plane stress}$$

F_p will usually be close to one for fatigue crack propagation under nominally elastic stresses. It is very often ignored in high-cycle fatigue situations. However, it should be noted that crack tip plasticity affects crack growth (and fatigue life) more than it affects ΔK. This is because ΔK is typically raised to the power 3 in the crack growth equation.

2.2 Stress Intensity Factor for Cutout

Stress intensity factor for cutout is relatively complicated. We use cavity (pore) model to approximate it. stress intensity factor for a penny-shaped crack (in an infinite solid) with normal stress distribution having circular symmetry [9]:

$$K = \frac{2}{\sqrt{\pi a}}\int_0^a \frac{\sigma(r)r}{\sqrt{a^2-r^2}}dr$$

$$\approx \sqrt{\pi a}\frac{2}{\pi}\frac{1}{a}\sum_{i=1}^n \sigma_{b_i}\int_{b_i}^{b_{i+1}} \frac{r}{\sqrt{a^2-r^2}}dr$$

23

$$\approx \sqrt{\pi a}\{\frac{2}{\pi}\frac{1}{a}\sum_{i=1}^{n}\frac{\sigma_{bi}}{\sigma}\left[-\sqrt{a^2-r^2}\right]_{b_i}^{b_{i+1}}\}$$

$$\sqrt{\pi a}\{\frac{2}{\pi}\frac{1}{a}\sum_{i=1}^{n}\frac{\sigma_{bi}}{\sigma}\left[\sqrt{a^2-b_i^2}-\sqrt{a^2-b_{i+1}^2}\right]\}$$

$$\approx \sigma\sqrt{\pi a}\cdot F_E\cdot F_G \qquad \text{(no boundaries)} \qquad (2.44)$$

Penny-shaped crack $\rightarrow a/2c = 0.5 \rightarrow$ $F_E = 2/\pi$

$$F_G = \frac{1}{a}\sum_{i=1}^{n}\left\{\frac{\sigma_{b_i}}{\sigma}(\sqrt{a^2-b_i^2}-\sqrt{a^2-b_{i+1}^2})\right\} \qquad (2.45)$$

Stress intensity factor for a penny-shaped crack emanating from a spherical cavity (pore)

$$K = \frac{2}{\sqrt{\pi a_e}}\int_R^{a_e}\frac{\sigma(r)\cdot r}{\sqrt{a_e^2-r^2}}dr \qquad (2.46)$$

where $2a_e$ = effectively crack length (Fig. 2.20)

$\sigma(r)$ = stress distribution at spherical cavity, i.e. [11]

$$\sigma(r) = [1+0.2237(\frac{R}{r})^3 + 0.8182(\frac{R}{r})^5]\sigma \qquad (2.47)$$

where σ = nominal stress at the cavity

Thus the crack-and-pore geometry (Fig. 2.20a) is treated as a penny-shaped crack with radius a_e (Fig. 2.20b) to approximate the crack cutout. Stress concentration effect due to the pore is accounted for employing the above equation in computing the block stresses.
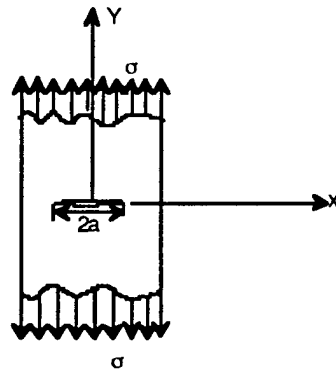
Fig. 2.1 Two-dimensional standard case : Through crack in an infinite

sheet subjected to uniform tension
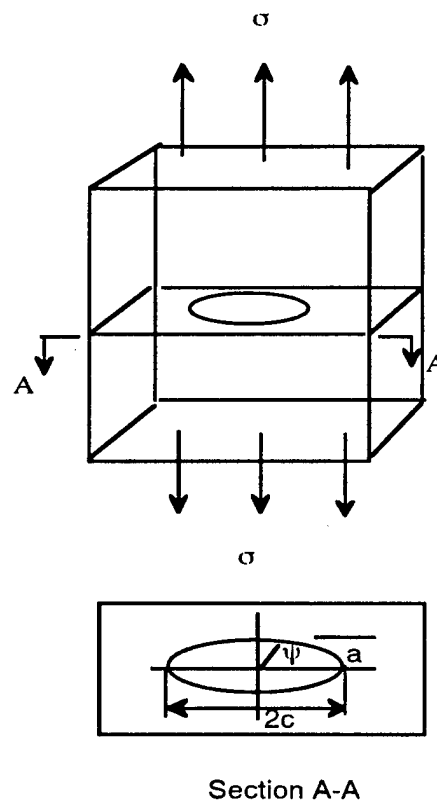
Section A-A

Fig. 2.2 Three-dimensional standard case : Embedded elliptical crack

in an infinite solid subjected to uniform tension.
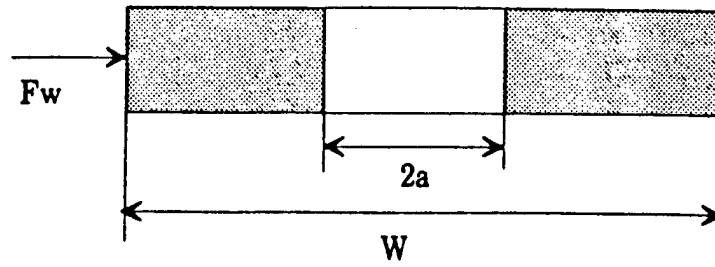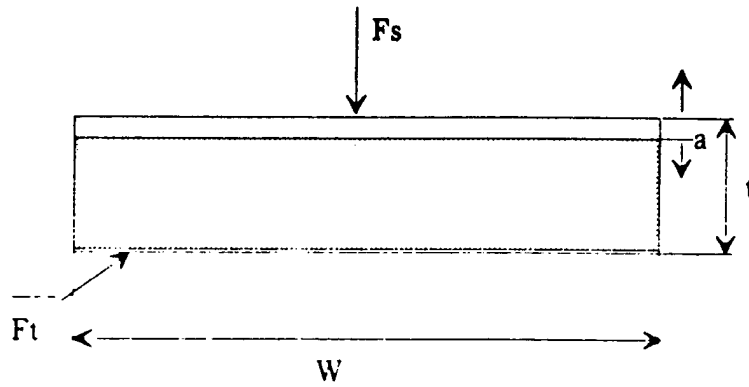
a) "Through" Crack

b) "Edge" Crack
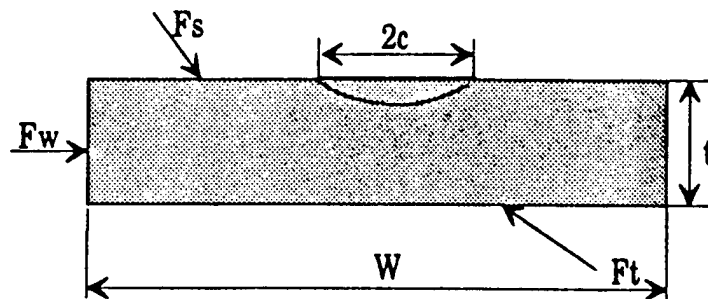
c) "Surface" crack

Fig. 2.3 Plate Cross-Section with various Crack Geometries.

Free Surface and Related Correction Factors
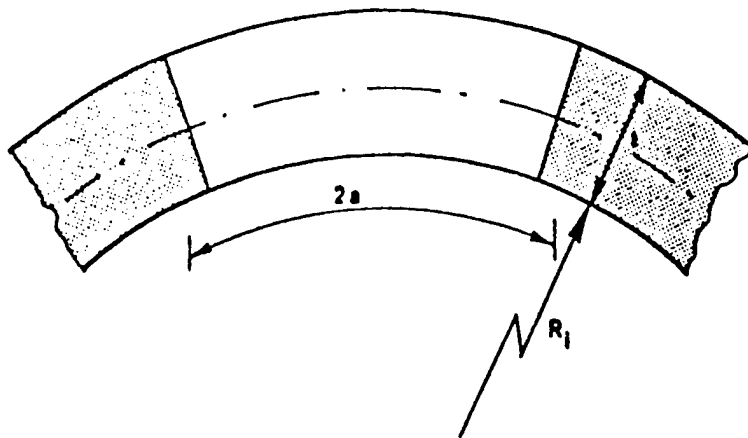
Fig. 2.4 Through Crack in a Curved Sheet
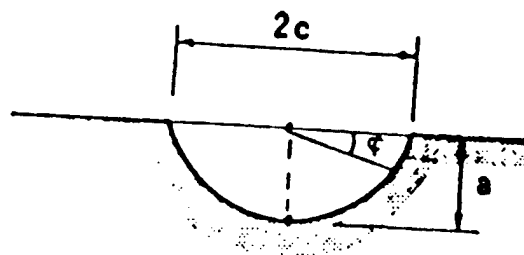
Fig. 2.5 Crack Front as Given by the Angle φ
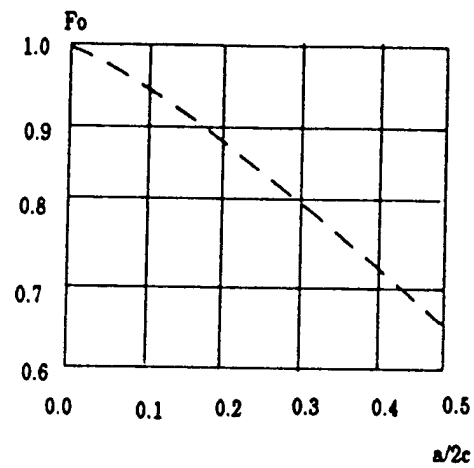
Fig. 2.6 The basic (elliptic) shape correction factor
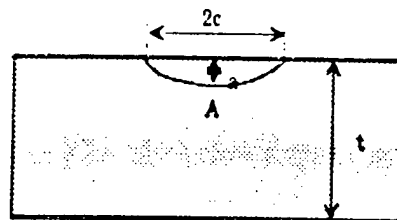
Fig. 2.7 Semi-elliptic Surface Crack

29
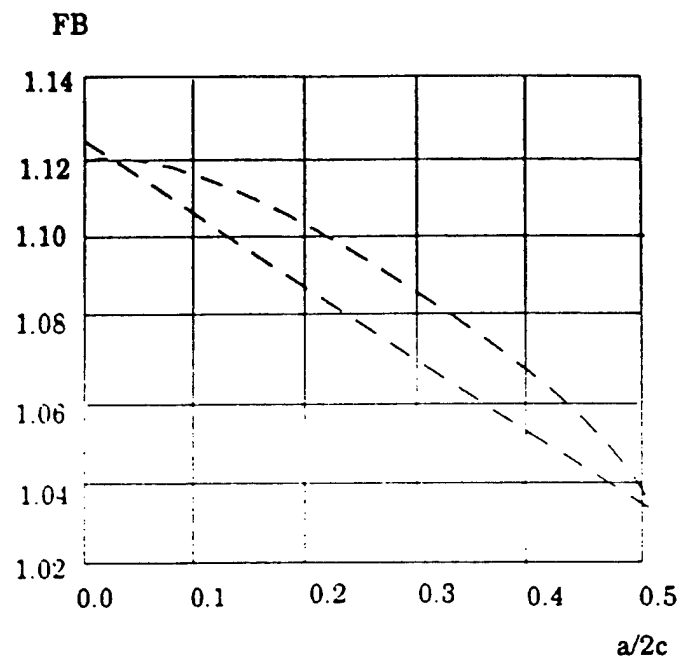
Fig. 2.8 The Front Free Surface Correction Factor
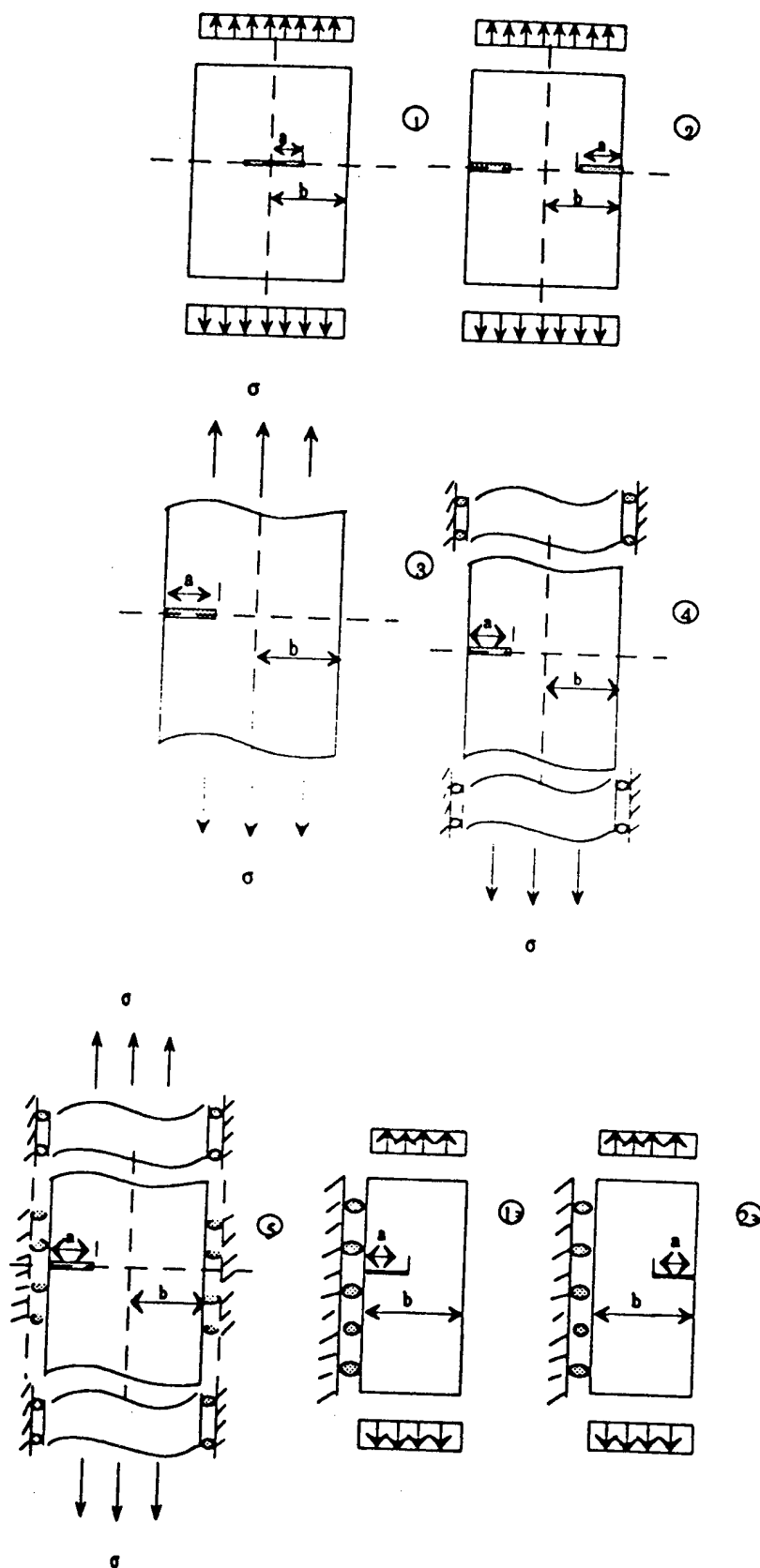
Fig. 2.9 various Cases of Cracking and Boundary Conditions
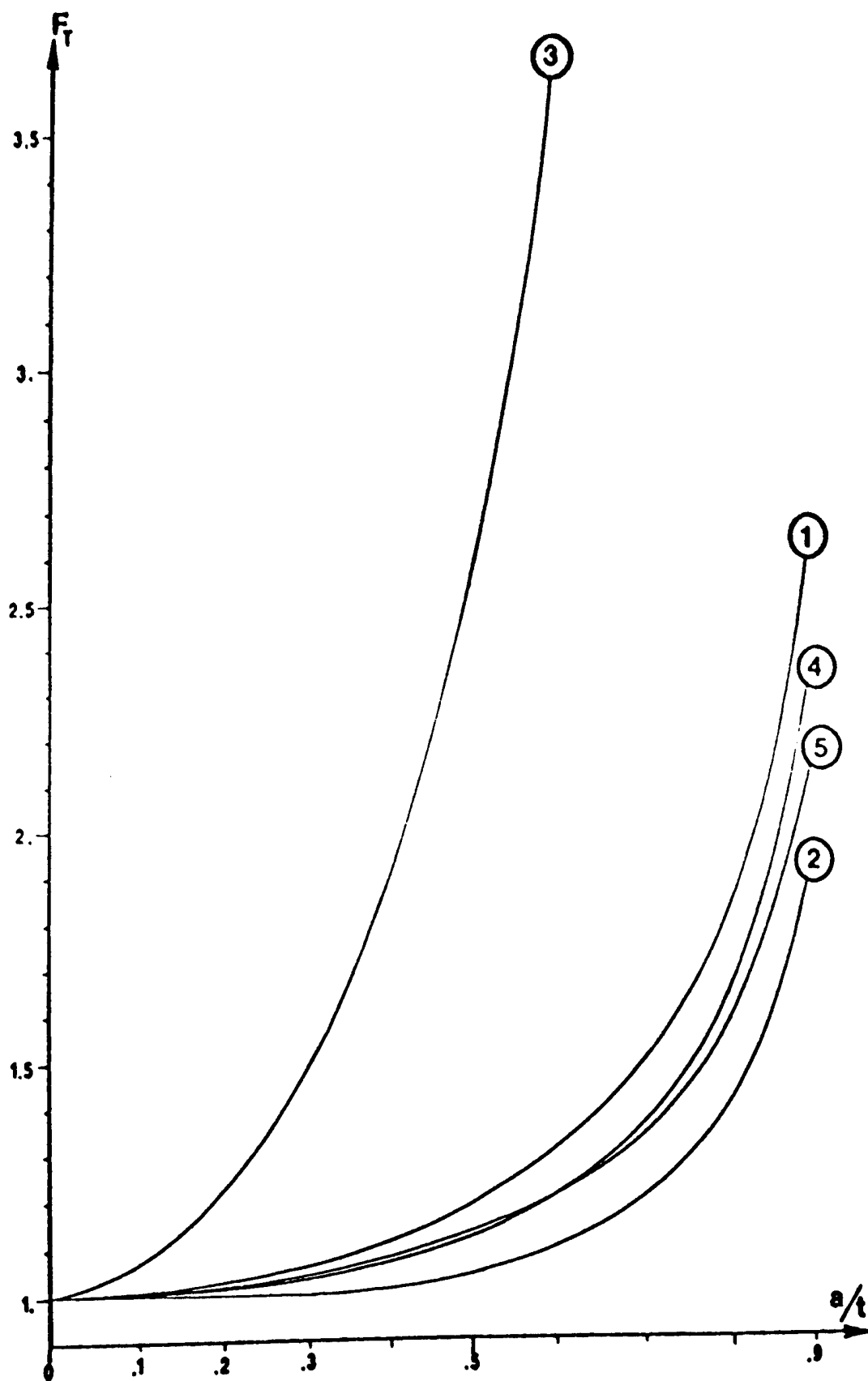
Fig. 2.10 The Finite Thickness Correction Factor Straight Crack Front (a/2c =0)
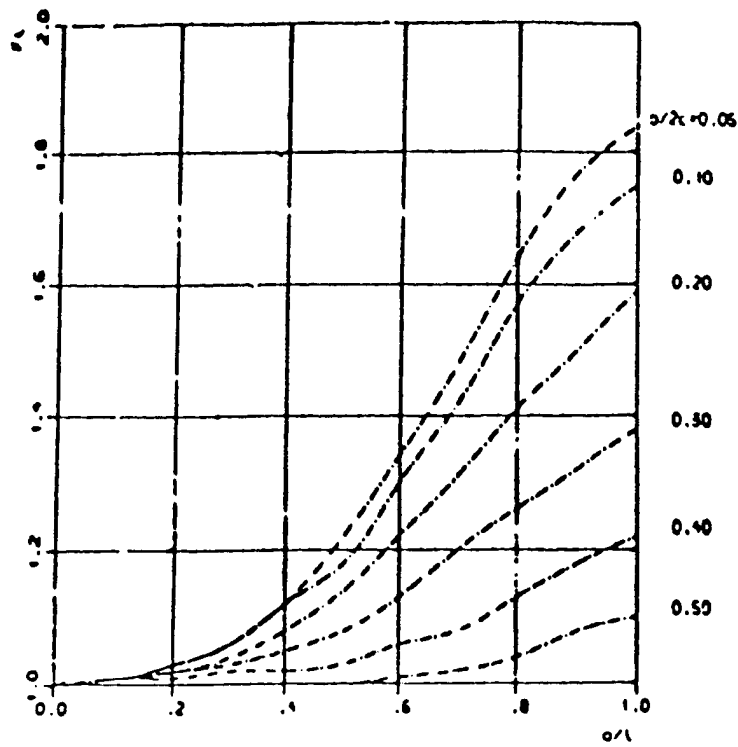
Fig. 2.10 The Finite Thickness Correction Factor Curved Crack Front (a/2c >0)
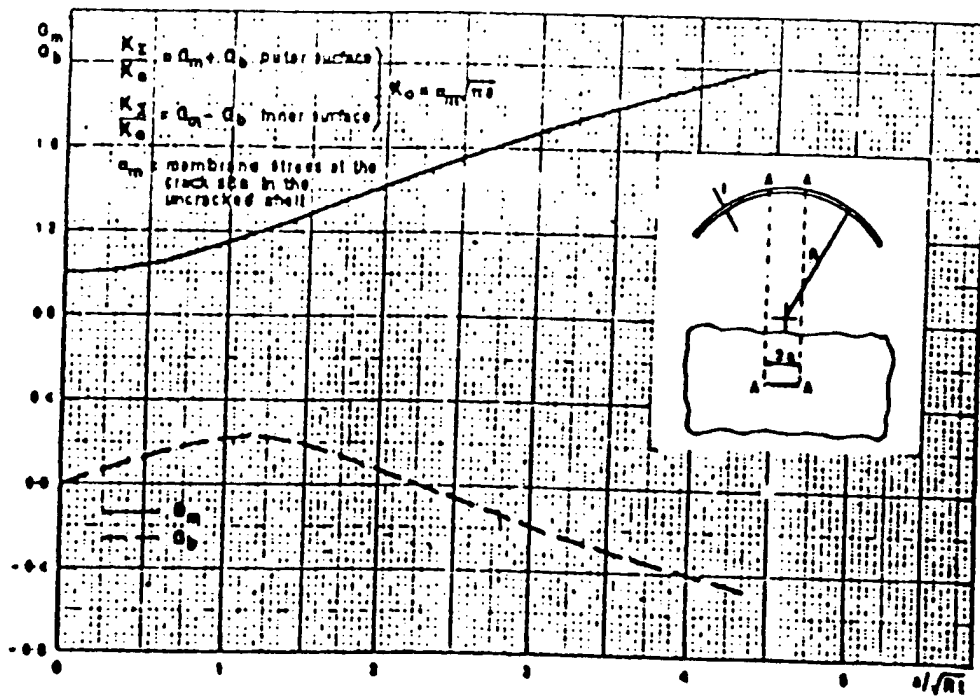
Fig.2.12 KJ for point A of a Circumferential Crack in a Cylindrical Shell Subjected to a Uniform Membrane Stress (10)
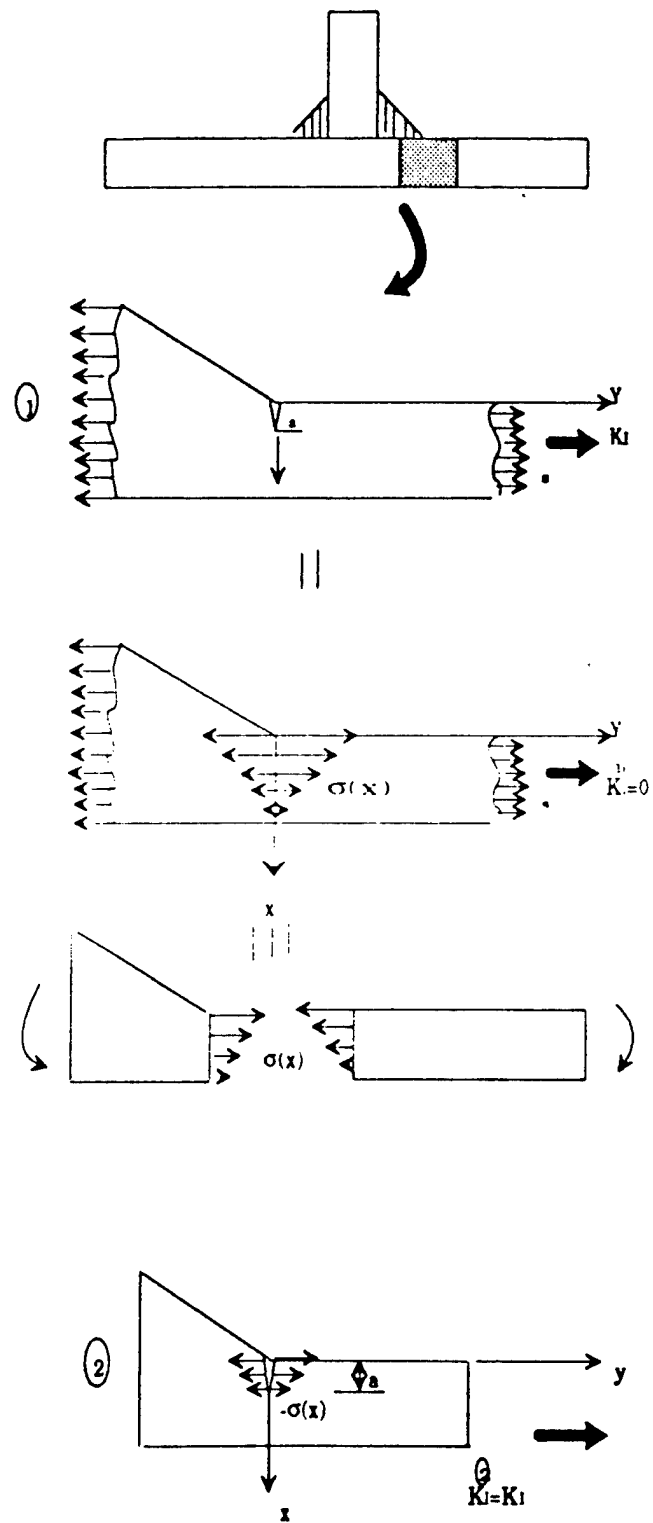
Fig. 2.13 Superposition of Stresses in a Welded Joint

34
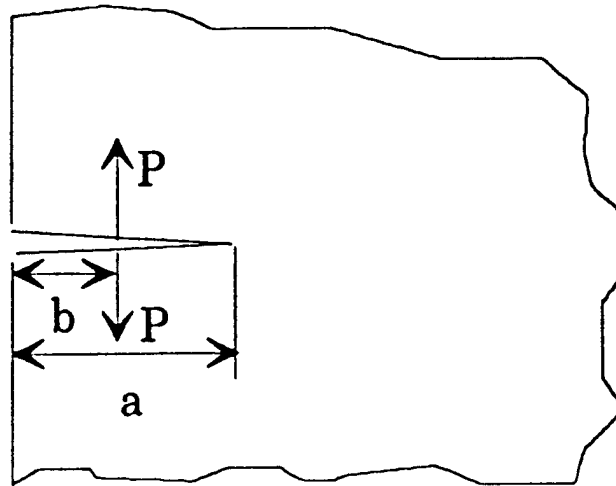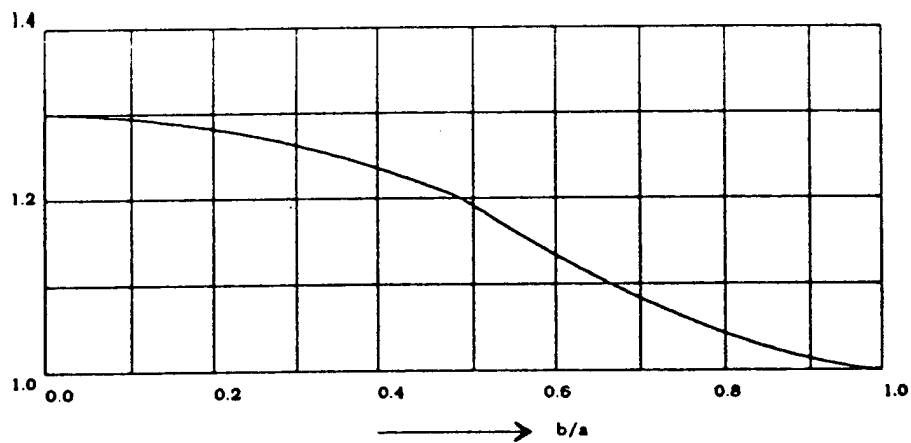
$$K_1 = \frac{2p}{\sqrt{\pi a}} \cdot \frac{a}{\sqrt{a^2 - b^2}} \cdot F(b/a)$$

Fig. 2.14 Calculation of K-value by a pair of Splitting Forces Applied to the Crack Surface

35
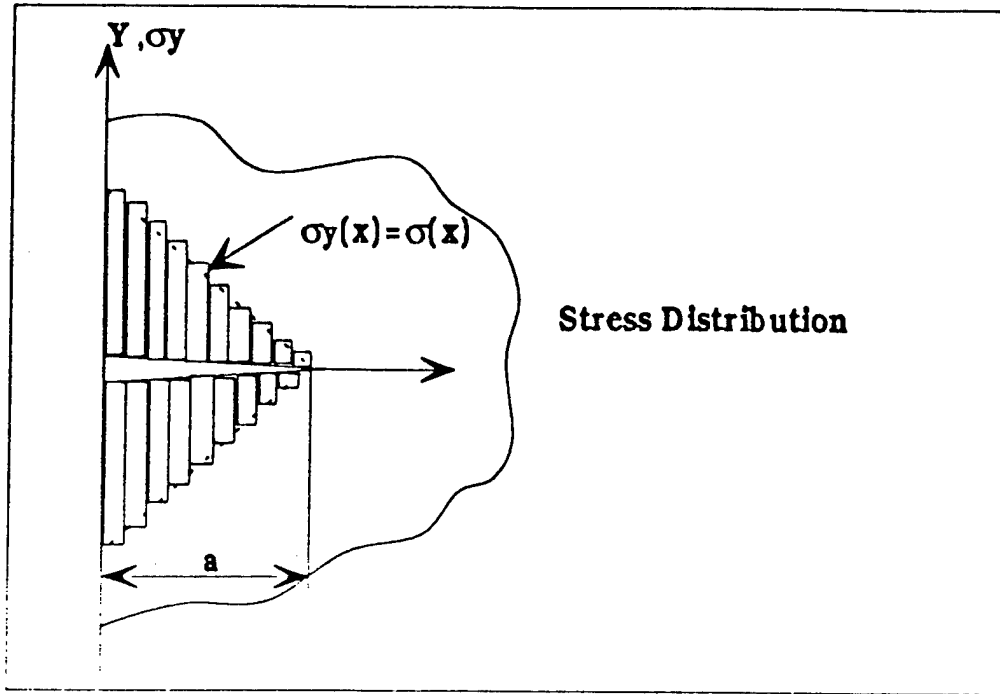
$$K_1 = \frac{2}{\pi}\sqrt{\pi a}\sum_{i=1}^{n}\left\{\sigma_{b_i}F(\bar{b}_i/a)\bullet \arcsin(x/a)|_{b_i}^{b_{i+1}}\right\}$$

$$\bar{b}_i = 1/2(b_i + b_{i+1})$$

Fig. 2.15 Discretized stress distribution
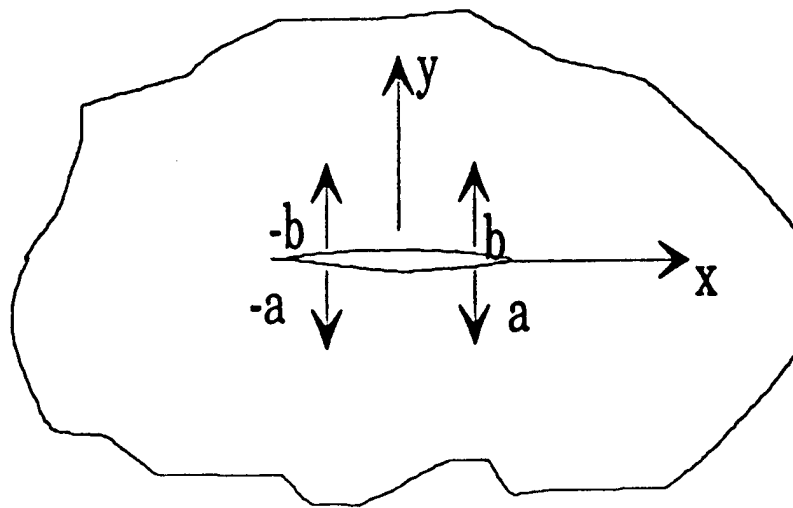
$$K_1 = \frac{2P}{\sqrt{\pi a}} \bullet \frac{a}{\sqrt{a^2 - b^2}}$$

Fig. 2.11 Two Pairs of Splitting Forces on a Through Crack in an Infinite Sheet
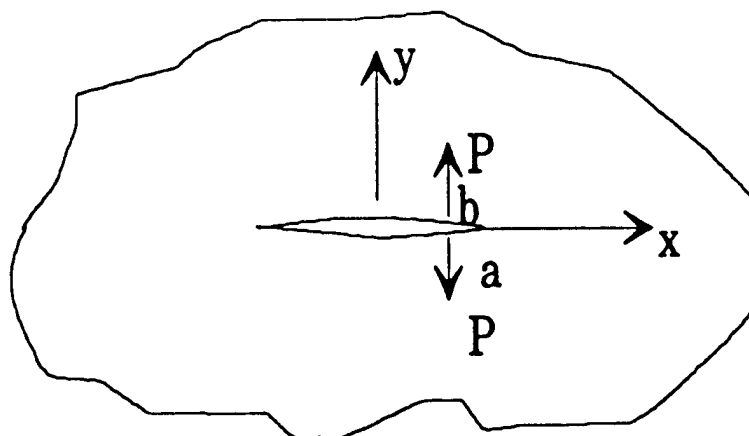
$$\{K_1\}_{\pm a} = \frac{P}{\sqrt{\pi a}} \bullet \sqrt{\frac{a \pm b}{a \mp b}}$$

Fig. 2.17 One Pair of Splitting Forces on a Through Crack in an Infinite Sheet

37
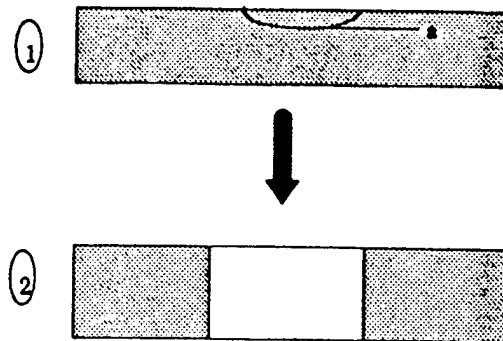
Fig. 2.18 Stages of Growth
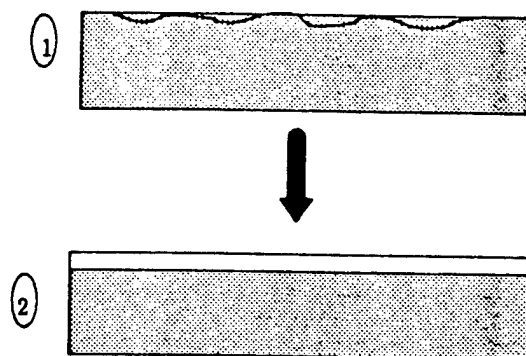
Fig. 2.19 Phases of Growth in Stage 1

38
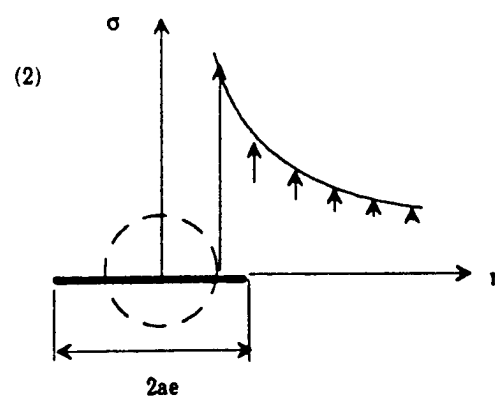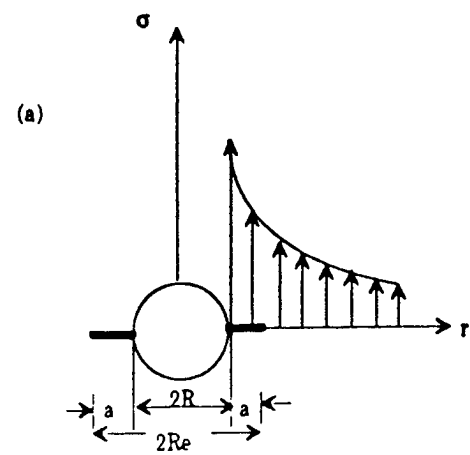
Fig. 2.21 Penny-shaped Crack emanating from Spherical Cavity

Chapter 3

Crack Growth and Fatigue Life

3.1 Crack Growth

In the computer program, Paris' equation is used to estimate the rate of growth. We can make various estimates concerning crack growth, e.g. the time or number of cycles required to grow a crack from one size to another.

$$N_{12} = \int_{a_1}^{a_2} \frac{da}{(da.dN)} \tag{3.1}$$

This is necessary for fitness for purpose evaluation when the structure is in service. E.g. a crack may be detected and reported through the in-service inspection program, and decisions have to be taken whether this crack should be stopped, or allowed to grow to a certain length. The program has the option for printout of a table of a vs N.

3.2 Fatigue Life

Fatigue initiation is neglected in the program.

Constant Amplitude Fatigue Life

The crack propagation part of the fatigue life may be expressed as

$$N_p = \int_{N_i}^{N_f} dN = \int_{a_i}^{a_f} \frac{da}{(da/dN)} \tag{3.2}$$

where $\qquad$ a_i = initial crack length (depth). Input to the program

$\qquad\qquad\quad$ a_f = final (critical) crack length (depth). Input, or computed in the program.

By inserting the relevant expression for crack growth rate, one can obtain an estimate of the fatigue crack propagation life. Thus by employing the Paris' equation one gets

$$N_p = \int_{a_i}^{a_f} \frac{da}{C(\Delta K)^m} \tag{3.3}$$

The computer program offers the option of superposing the effect of several (< 4) stress distributions. Hence, the following computation is conducted.

For Each Stress Distribution:

$$(K/\sigma)_j = \sqrt{\pi a} \bullet F_j \tag{3.4}$$

$$(K_{min})_j = (\sigma_{min})_j \bullet (K/\sigma)_j \tag{3.5}$$

$$(K_{max})_j = (\sigma_{max})_j \bullet (K/\sigma)_j \tag{3.6}$$

Superposition:

$$K_{min} = \sum_{j=1}^{n} (K_{min})_j \qquad\qquad ; n < 4$$

$$K_{max} = \sum_{j=1}^{n} (K_{max})_j \qquad\qquad ; n < 4 \qquad\qquad (3.7)$$

Effective Stress Intensity factor Range

If $K_{min} < 0$ then $K_{min} := f\, K_{min}$, where $f\,(0.\ -1.)$. The factor f is given as input, and offers the possibility to truncate the negative part of (ΔK).

$$\Delta K = K_{max} - K_{min} \qquad\qquad (3.8)$$

Number of cycles in crack growth stage j

$$N_j = \frac{1}{C} \int_{a_{i,j}}^{a_{f,j}} \frac{da}{(\Delta K)^m} \qquad\qquad (3.9)$$

The integral is evaluated numerically.

Fatigue Life

$$N = \sum_{j=1}^{k} N_j \qquad\qquad (3.10)$$

where   k = no. of crack growth stages.

Chapter 4

User's Manual

4.1 File or Terminal Input

Upon the startup of the Fracture Program the choice is requested whether to perform the input from a file or from the terminal. The following screen is shown:

If you want to read data from a file,   type 1

If you want to read data from the terminal, type 2

The program will only accept the integer values 1 or 2.

File Input

A standard file input is provided in Appendix which is the same format as the terminal input.

4.2 Material Data

This module has the purpose to specify the CSD's material data. The user is requested to input the following material data

Please enter the following material data:

1) Crack growth parameter C

2) Crack growth parameter m

3) Yield stress   [NN/m2]

4) Fracture Toughness   [MN/M**1.5]

Please enter the values

The user inputs the above four data in the column.

4.3 Geometry Data

This module has the purpose to read the CSD's geometry data. The following is shown on the screen:

Please enter the following geometry data :

1) **initial crack depth**   **[m]**

2) **Aspect ratio,   i.e.   A/2C**

3) **Plate thickness**   **[m]**

4) **Plate width**   **[m]**

Please enter the values:

The user is requested to input the data in the column

4.4 Stress Data

This module is supposed to read fatigue stress data. The following is shown on the screen:

Please enter the following stress data

1) **Nominal stress range [MN/m2]**

(Actual fatigue Loading)

2) **Stress ratio**

3) Nominal stress [MN/m2]

(For Stress Intensity Factor)

4) No. of elements in through thickness distribution

5) No. of elements in plate width stress distribution

This user is requested to enter the above data in column. It should be noted that the difference between the nominal stress range and nominal stress.

4.5 Stress Distribution

Based on the number of the elements which is inputted in the above module, the stress distribution along the crack is requested as following:

For the stress distribution along the crack depth:

Please enter N rows of stress data

1) Nominal stress in crack plane /through thickness distribution [MN/m2]

2) Corresponding distance from the plate surface [M]

please enter row 1

The user is requested to input the stress distribution along the crack depth here.

For the stress distribution along the crack length:

Please enter N rows of stress data

1) Nominal stress in crack plane /plate width distribution

2) corresponding distance from crack centerline [m]

Please enter row 1

The user is requested to input the stress distribution along the crack width here.

4.6 Compute Module

Several options are provided in fracture analysis. The following dialog is used to enter the choice:

Please choose the following 6 options:

1) Option 1

Continuous aspect ratio	**0**
Constant aspect ratio	**1**

2) Option 2

Crack growth from one surface only	**1**
Crack growth from both surface	**2**

3) Option 3

Printout of SIF	**1**
No printout	**0**

4) Option 4

One growth phase through thickness	**1**
Two growth phase through thickness	**2**

5) Option 5

Print A-N Relation	**1**
A-N Relation not printed	**0**

6) Option 6

Longitudinal Weld	**1**
Transverse Weld	**2**
Cutout	**0**

The user is to specify the above options to start the program.

Chapter 5

Program Versatility

5.1 Material

Steel, other metallic materials

Please note: Empirical crack shape relations in the existing version are only

related to steel. For other application, it need be modified.

5.2 Loading

- Constant amplitude

- Variable amplitude, bu equivalent stress range

- Nominal load for stress intensity factor   ,   axial

,   bending

,   mixed

5.3 Stress Distribution

- Several (< 4) stress distribution. might be input

- Loading stress

- Residual Stress (e.g. due to welding)

- Compressive stresses taken into account

5.4 Geometry

- Plated Joint

- Tubular Joint

5.5 Detail Geometry

- Welding joints

stiffener   ;   longitudinal

transverse   ;   ringer stiffeners

5.6 Crack Initiation Sites

- Weld toe

- Weld root

- Cavities (spherical, i.e. pore)

Please note this is the model for cutout.

5.7 Crack Type

- Surface crack

- Subsurface crack   ; $a/2c = const = (0.0 - 0.5)$

- Through crack

5.8 Crack Geometry

- Straight crack front   (a/2c = 0)

- Curved crack front   (a/2c > 0)

- Fixed shape (const a/2c) during growth

- Continuously varying shape during growth

- Crack growth from one or two plate surface.

5.9 Crack Growth Stage

- Two stages of growth (Fig. 2.18)

1) Growth as a part-through crack

2) Growth as a through crack

5.10 Failure Modes

- Yielding

- Fracture (Kmax=Kc)

- a_f = a_{final} as an input.

Fitness for Purpose Evaluation of Critical Structural Details in Tankers

Pro-IMR: A Computer Code for Probability-Based Inspection Planning

Tao Xu

and

Professor Robert G. Bea

Department of Naval Architecture and Offshore Engineering
University of California, Berkeley

Preface

The one year Joint Industry Research Project **"Fitness for Purpose Evaluation of Cracked Critical Structural Details (CSD) in Tankers"** was initiated in 1993 by the Department of Naval Architecture & Offshore Engineering, University of California at Berkeley as an extension of the projects **"Structural Maintenance for New and Existing Ships"** and **"Ship Structural Maintenance"**. The objective of this project is to develop engineering guidelines and procedures to help ship repair engineers, port superintendents and surveyors make evaluations of the fitness for purpose of cracked Critical Structural Details (CSD) in tankers.

This project was made possible by the following sponsoring organizations:

-American Bureau of Shipping **-Chevron Shipping Cooperation**

-Mitsubishi Heavy Industries **-Newport News Shipbuilding & Dry Dock Co.**

-U. S. Coast Guard

This report documents the background about the computer code "Pro-IMR"-A Computer Program for Probability-based Inspection Planning.

Chapter 1

1.1 Introduction

There is an increasing need today to evaluate the fatigue strength of hull structures along with the increasing use of new structural design, new material aimed at longer life and low cost. In order to achieve a longer service life for hull structures in the expectation of a ship service life of 15 to 20 years or even longer, Inspection, Maintenance and Repair (IMR) program is considered to be very important. Particularly when a ship is to be operated for a long period at high levels of safety and reliability, an IMR plan from the outset of ship design and construction is important. Unfournately, the field of IMR techniques is an area that lags significantly behind highly developed computer technology for fatigue analysis.

1.2 Scope

Fatigue damage is considered to be initiated in a structure when the smallest size measurable crack develops, whether or not it is detected. The fatigue process in a structure member consists of crack initiation, followed by crack propagation and the resulting member strength degradation. Periodic inspection of fatigue sensitive structures have been common practice in order to maintain the reliability of the structures at the desired pre specified level. If a fatigue crack is detected by inspection, the cracked detail is repaired or replaced.

This report presents documentation about the computer code Pro-IMR - A Computer Program for Probability-based IMR planning. In Pro-IMR, the inspection procedures are based on POD (probability of detection) curves, detail stress and inspection repair histories. The inspection intervals are intended to keep the reliability at predetermined design levels.

This report is divided into five chapters. Chapter 1 is the general introduction. Chapter 2 addresses the theory about the probability-based inspection planning. Chapter 3 is the user's manual. Chapter 4 is the numerical examples and Chapter 5 is the summary and conclusion.

Reference

1.1. *Structural Maintenance for New and Existing Ships*, Reports SMP 1-1 through 5-2, Department of Naval Architecture and Offshore Engineering, University of California at Berkeley, September 1992.

1.2 *Guide for the Fatigue Strength Assessment of Tanker*, American Bureau of Shipping, New York, NY 1992.

1.3 *Reliability-Based Maintenance for Fatigue Cracks in Tankers*. Report SMP III-3 , Department of Naval Architecture and Offshore Engineering, University of California at Berkeley, September 1994.

1.4. *Relation of Inspection Faindings to Fatigue Reliability* Ship Structure Committee Report SSC-355

1.5 *Fatigue handbook, Offshore Steel Structures*. A. Almar-Naess Tapir, 1985

1.7 *Fracture - A Computer Code for Fracture Mechanics Analysis of Cracked Critical Strcutural Details (CSD) in Tankers*. Report SMP III-4 , Department of Naval Architecture and Offshore Engineering, University of California at Berkeley, September 1994.

1.8 *Marine Structural Integrity Programs*. Ship Structure Committee Report SSC-365

Chapter 2

Inspection Planning

2.1 Introduction

In the previous chapter, the effect of periodic inspection on fatigue reliability was examined. This chapter present the procedure for the probability-based inspection planning for tanker structures so as to maintain the reliability at a predesign level through the lifetime. In order to simplify the procedure, several assumption was further made based on the model developed in the previous studies [2.2].

Section 2.2 discusses the POD (Probability of Detection) Curves. Section 2.3 describes the analytical models used and the various assumptions employed in this analysis. In section 2.4, analytical intepretation of inspection is given. Section 2.5 and 2.6 are associated with the determination of appropriate inspection intervals so that the structural reliability is kept at the desired level.

2.2 POD Function

The quality of the inspections are modeled through the probability of detecting an existing crack where the probability for crack detection depends on the size of the crack, the inspection method applied, and the experience of the inspection team. The inspection quality is commonly defined through the probability of crack detection (POD) curve, modeling the detection probability as a function of the size of the crack, $P(D|a)$.

Information concerning detectable lengths of cracks in marine industry is still a little although several research are being conducted now. [2.1,2.2] But the information in airframe industry has been available in the literature for some time. [2.3,2.4] It is concluded from both marine industry and airframe industry that several factors will influence the chances of detection, such as the capability and attitude of the inspector, the geometry of the structure, the environment in which the inspection is performed, and the location or orientation of the flaw as well as the size. It is also realized that no inspection procedure can provide a hundred percent assurance that all cracks larger than some prescribed, limited size will be detected.

The reset crack length after an inspection, ainsp which is the largest crack that can pass undetected through the inspection system, must be specified in terms of a high confidence that a given percentage of all cracks larger than ain will be found. Generally it requires 90 percent probability of detection with 95 percent confidence level.

As we discussed early, the capability of an inspection procedure is thus defined in terms as the probability of detection (POD) for all cracks of a given length, and is evaluated as the proportion of cracks that would be detected by the procedure when applied by professional inspectors to a population of structural details in specified environment. (Fig. 2.1)

6
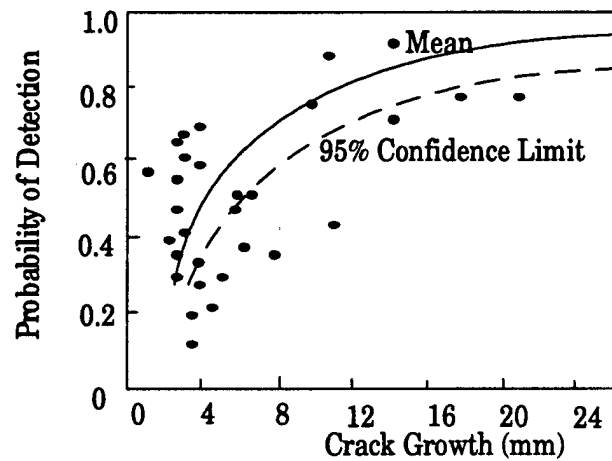
Fig 2.1 Example Application of Log Odds-Regression Analysis

As described previously, the detection probability for a given crack length involves considerable statistical variability. The distribution of detection probabilities at a given crack length is illustrated in Fig. 2.2. The curve connecting the average values of the detection probabilities for all crack lengths is defined as the POD(a) function. Hence, the POD(a) function is a function which passes through the mean of detection probabilities at each crack length. Consequently, many individual cracks will have detection probabilities below the POD(a) value.
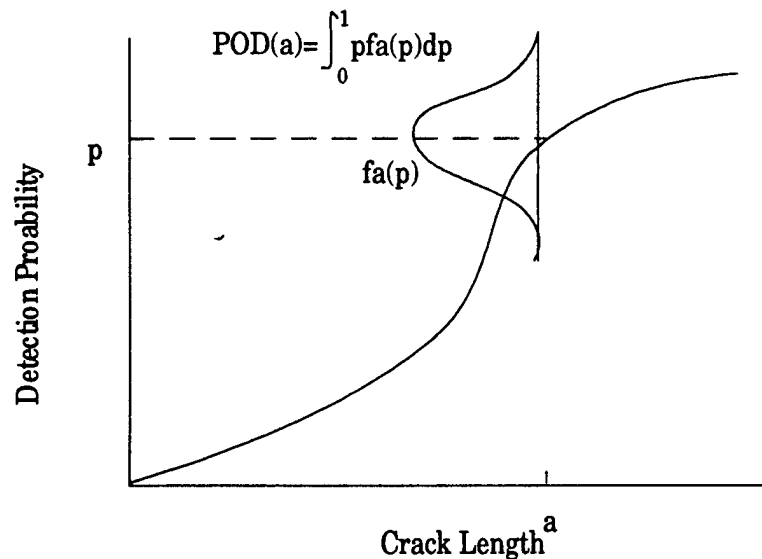
Fig 2.2 Probability Density Function of Crack Detection Proabilities at a Crack Length

7

The information on POD functions is needed in the reliability analysis of structures under scheduled inspection maintenance. It is also crucial for the determination of the inspection interval. To establish the POD function from experimental test results, a functional form should be assumed. The so-called log odds or log logistic model has been investigated extensively.

$$POD(a) = \{1 + \exp[-\frac{\pi}{3}(\frac{\ln a - \mu}{\sigma})]\}^{-1} \qquad 2.1$$

in which POD(a) is the probability of detecting crack size a, and μ and σ are parameters.

Let $a_{0.5}$ be the median crack detection capability, i.e., the crack length associated with a 50% detection probability, $POD(a_{0.5}) = 0.5$. Then, it follows from Eq. 2.1 that:

$$\mu = \ln a_{0.5} \qquad 2.2$$

in which ε is the crack length below which a crack can not be detected by the inspection. Again, α and β are constants, representing the bandwidth and central location of the POD function respectively.

Another POD function, referred to the Weibull function, has also been used:

$$POD(a) = 0 \qquad\qquad a < \varepsilon$$

$$= 1 - \exp[-(\frac{a-\varepsilon}{\beta})^{\alpha}] \qquad a > \varepsilon \qquad 2.3$$

As mentioned previously, the POD function is a unit step function at a_{insp} for an ideal inspection, i.e.,

$$POD(a) = 0 \qquad\qquad a < a_{insp}$$

$$= 1 \qquad\qquad a > a_{insp} \qquad 2.4$$

Such an ideal POD function can be obtained from exponential function by setting ε = a_{insp}, b ->o and a ->∞.

In the computer code Prob-IMR, the Weibull function was used.

8

2.3 Basic Assumptions

The following assumption are made for the purpose of this study:

1. In each structural memeber there is only one hotspot where a crack can initiate

2. All structural memebers are inspected immediately after initiation of service and at the time of each scheduled inspection. If a memeber is found not to be intact, the following action is taken:

   If a crack is detected in a member, that member is repaired and regains its initial strength charcateristics

   if a member is found to have failed, it is replaced by a new one

3. The entire inspection history of each member is considered to be known at the current inspection

4. For fatigue crack initiation, the time to crack initiation (TTCI) denoted by t is assumed to be a random variable with a density function following the Weibull distribution

$$f_c(t|\beta) = \frac{\alpha}{\beta} \bullet (\frac{t}{\beta})^{\alpha-1} \bullet \exp[-(\frac{t}{\beta})^{\alpha}] \qquad 2.5$$

The uncertainty in the TTCI is introduced by the scale parameter β. Hence, Eq. 2.5 indicates a Weibull density condition to a given value of β

$$F_c(t|\beta) = 1 - \exp[-(\frac{t}{\beta})^{\alpha}] \qquad 2.6$$

5. For fatigue propagation, fracture mechanics theory is used to determine the length of a propagating crack under random loading. It's assumed that the crack grows according to:

9

$$\frac{da}{dt} = C_1(\Delta K)^2 = C_1(S \bullet \sqrt{\pi a})^2 = ca \qquad 2.7$$

Integrating Eq. 2.7 from the initial crack length ao at the TTCI=tc up to the current crack length a(t-tc) at time t, the following result is obtained:

$$a(t - t_c \vert c) = a_0 \exp[c(t - t_c)] \qquad 2.8$$

The uncertainty in fatigue crack propagation is introduced by parameter c. There fore the crack length is conditional to a given value c.

6.   The probability of detecting a fatigue crack at lengtha at time of inspection is

$$D(a \vert d) = 1 - \exp[-d(a - a_0)] \qquad 2.9$$

The uncertainty is introduced by parameter d. Thus the probability dection function is conditional to a given value of d. The minimum detectable crack length is denoted by ao.

7.   If a crack is detected in a member at time of inspection, the crack length is assumed to be accurately measured.

8.   Failure of a member occurs when random stress exceeds the strength of the member for the first time. There are two cases :

Failure before the crack initiation

The failure rate is constant depending on the random stress on the hotspot as

$$h(t) = h_0 = \exp(r) \qquad 2.10$$

Failure after the crack initiation

The failure rate also depends on the crack size, on which the member's residual strength depends.

$$h(t) = \exp[q(t - t_c) + r] \qquad 2.11$$

For the sake of simplicity, parameters r and q are assumed to be deterministic.

the reliability of a member before crack initiation during the service (Ti , t) is denoted by U(t-Ti) and given by

$$U(t - T_l) = \exp\{-\int_{T_l}^t h(\tau)d\tau\} = \exp\{-\int_{T_l}^t h_0 d\tau\} \qquad 2.12$$

or

$$U(t - T_l) = \exp\{-(t - T_l) \bullet \exp(r)\} \qquad t < t_c \qquad 2.13$$

where T_l is the time of service initiation for the member under consideration;

this implies that member was repaired or replaced at the time of l-th inspection

The reliability of a member after crack initiation during the service period from

tc to t is denoted by V(t-tc) and given by

$$V(t - t_c) = \exp\{-\int_{t_c}^t h(\tau)d\tau\} = \exp\{-\int_{t_c}^t \exp[q(r - r_c) + r]d\tau\} \qquad 2.14$$

or

$$V(t - t_c) = \exp\{-\frac{1}{q}[\exp\{q(t - t_c) + r\} - \exp\{r\}]\} \qquad 2.15$$

9. The probability of detecting member failure at the time of inspection is equal to

    one if such a failure exists

10. No stress redistribution is considered in the structure

2.4 Inspection Event

At the time of j-th inspection, Tj, of the certain member (with the knowledge that this member was repaired or replaced immediately as a result of the l-th inspection performed at time T_l (l < j-1) or this member initiate service at T_l denoting the beginning of the service for the structure). The possible inspection events are:

1. $\{A: j,l\}$ = event that failure occurs during the timeinterval $[T_{j-1}, T_j]$

    This event consists of the two events

    $E_{1,j}$ = event that the member fails before the crack initiation

$E_{2,j}$ = event that the member fails after the crack initiation

2. $\{B_1(a_j) : j,l\}$ = event that the member is found not to have failed at the time of

the j-th inspection T_j and a crack of length a_j and a_j+da_j is detected in the member.

It's defined alternatively as $E_{3,j}$

3. $\{B_2:j,l\}$ = event that the member is found not have failed at the time of the j-th

inspection T_j and no crack is detected in the member.

$E_{4,j}$ = event that member does not fail in the time interval $[T_{j-1},T_j]$ and no crack

exists in the member at T_j

$E_{5,j}$ = event that member doesn't fail in the time interval $[T_{j-1},T_j]$ and a crack

Exists in the member which is not detected.

2.5 Event Probability

Event $E_{1,j}$

Event $E_{1,j}$ consists of two exclusive events, $E_{1,j}^a$ and $E_{1,j}^b$ which are defined as

1 $E_{1,j}^a$ = event that a crack initiates after T_j and the member fails before crack

initiation between $[T_{j-1},T_j]$. The probability $P_{1,j}^a$ is :

$$P_{1,j}^a = \{1 - F_c(T_j - T_l | \beta)\} \bullet \{U(T_j - T_l)\} \qquad \qquad 2.16$$

where $\{1-F_c(T_j-T_l|\beta\}$ is the probability that crack will initiate after T_j and $\{U(T_{j-1}-T_l)-$

$U(T_j-T_l)\}$ is the probability that the member will fail during $[T_{j-1},T_j]$. This is the

conditional probability given that a crack initiate after T_j.

2 $E_{1,j}^b$ = event that a crack iniates at some time instant t in the time interval $[T_{j-1},T_j]$

and the member fails before crack initiation sometime during the interval $[T_{j-1},t]$. The

probability $P_{1,j}^b$ of event $E_{1,j}^b$ is given by:

$$P_{1,j}^b = f_c(t - T_l | \beta)\} \bullet \{U(T_{j-1} - T_l) - U(t - T_l)\} \qquad \qquad 2.17$$

12

where $f_c(t-T_1|\beta)$ dt denotes the probability that a crack will initiate during the time interval $[t,t+dt]$ and $\{U(T_{j-1}-T_1)-U(t-T_1)\}$ denotes the probability that the member will fail during the interval $[T_{j-1},t]$.

The probability $P_{1,j}$ of the Evenet $E_{1,j}$ is given by:

$$P_{1,j} = P_{1,j}^a + P_{1,j}^b$$

$$= \{1 - F_c(T_j - T_1|\beta)\} \bullet \{U(T_{j-1} - T_1) - U(T_j - T_1)\}$$

$$+ \int_{T_{j-1}}^{T_j} f_c(t - T_1|\beta) \bullet \{U(T_{j-1} - T_1) - U(t - T_1)\}dt \qquad 2.18$$

Event $E_{2,j}$

Event $E_{2,j}$ consists of two events, $E_{2,j}^a$ and $E_{2,j}^b$ defined as:

1     $E_{2,j}^a$ = event that a crack initiates at some time instant t in the time interval $[T_i,T_{i+1}]$ (i=1,....,j-2) and the crack is not detected during all the subsequent inspections (from inspection at time T_{i+1} up to inspection at time T_{j-1} inclusive) and the member fails sometime during the time interval $[T_{j-1},T_j]$

The probability $P_{2,j}^a$ of event $E_{2,j}^a$ is given by:

$$P_{2,j}^a = \sum_{i=1}^{j-2} \int_{T_i}^{T_{i+1}} f_c(t - T_1|\beta) \bullet \{U(t - T_1) \bullet [V(T_{j-1} - t) - V(T_j - t)]$$

$$\bullet [\prod_{k=i+1}^{j-1} \{1 - D(a(T_k - t|c|d))\}]dt\} \qquad 2.19$$

where $f_c(t-T_1|\beta)$ denotes the probability that a crack will initiate during the time interval $[t,t+dt]$, $U(t-T_1)$ denotes the probability that the member will survive during the time interval $[T_{j-1},T_j]$ and $[V(T_{j-1} - t) - V(T_j - t)]$ denotes the nondetectable probability during $[T_i,T_{i+1}]$ (i=1,2,....,j-2].

Event $E_{3,j}$

$E_{3,j}$ = event that the member is found not to have failed at the time of the j-th inspection T_j and a crack of length between a_j and a_j+da_j is detected in the member.

The, the probability $p_{3,j}da_j$ of Event $E_{3,j}$ is given by

$$p_{3,j}da_j = p_{3,j}(a_j)da_j = f_c(t_c - T_1|\beta)dt_c \bullet U(t_c - T_1) \bullet V(T_j - t_c)$$

$$\bullet \left[\prod_{k=l+1}^{j-1} \{1 - \delta \bullet D(a(T_k - t_c|c)|d)\} \right] \bullet D(a_j|c|d) \qquad 2.20$$

where

$$t_c = T_j - \frac{1}{c}\ln(\frac{a_j}{a_0})$$

and $\qquad \delta = 1$ for $T_k > t_c$

$\qquad\qquad \delta = 0$ for $T_k < t_c$

$$dt_c = |\frac{dt_c}{da_j}|da_j = \frac{da_j}{(ca_j)}$$

and $f_c(t_c - T_1|\beta)dt_c$ denotes the probability that a crack will initiate during the time interval $[t_c, t_c + dt_c]$, $U(t_c - T_1)$ denotes the probability that a member will survive during the time interval $[T_1, t_c]$, $V(T_j - t_c)$ denotes the probability that a member will survive during the time interval $[t_c, T_j]$, $\{1 - \delta \bullet D(a(T_k - t_c|c)|d)\}$denotes the probability that a crack will not be detected at inspection T_k and $D(a_j|c)|d)$ denotes the probability that a crack will be detected at inspection T_j.

Event $E_{4,j}$

$E_{4,j}$ = event that member does not fail and no crack existis in member at time of inspection T_j.

The probability $P_{4,j}$ of event $E_{4,j}$ is given by:

$$P_{4,j} = \{1 - F_c(T_j - T_l|\beta)\} \bullet U(T_j - T_l)$$ 2.21

where $\{1-F_c(T_j-T_l|\beta)$ denotes the probability that a crack initiate after T_j and $U(T_j-T_l)$ denotes the probability that a member will survive the time interval $[T_l, T_j]$.

Event $E_{5,j}$

Event $E_{5,j}$ is defined as follows:

$E_{5,j}$=event that member does not fail, and a crack exists in the member which is not detected at the time of inspection T_j

The probability $P_{5,j}$ of event $E_{5,j}$ is given by:

$$P_{5,j}^a = \sum_{i=1}^{j-1} \int_{T_i}^{T_{i+1}} f_c(t - T_l|\beta) \bullet \{U(t - T_l) \bullet [V(T_j - t)]$$

$$\bullet [\prod_{k=i+1}^{j-1} \{1 - D(a(T_k - t|c)|d)\}]]dt\}$$ 2.22

where $f_c(t-T_l|\beta)dt$ denotes the probability that a crack will initiate during time interval $[t,t+dt]$, $U(t-T_l)$ denotes the probability that a member will survive during time interval $[T_l,t]$, $V(T_j-t)$ denotes the probability that a member will survive during time interval $[t,T_j]$ and $\{1-D(a(T_k-t|c)|d)\}$ denotes the probability that a crack will not detected at inspection T_k

Finally, the probabilities of events $\{A : j, 1\}$, $\{B_1(a_j) : j, 1\}$ and $\{B_2 : j,1\}$ are given by

$$P\{A:j,1\} = P_{1,j} + P_{2,j}$$

$$P\{B_1(a_j):j,1\} = P_{3,j}da_j$$

$$P\{B_2:j,1\} = P_{4,j} + P_{5,j}$$ 2.23

15

2.6 Reliability of Member after J-th Inspection

2.6.1 Member Repaired at J-th Inspection

It is assumed that members are repaired or replaced at the j-th inspection in case of event {A:j,l} or {B₁(aⱼ):j,l}. The reliability R(t*,Repair) of a member is given by the sum of the following two probabilities : a) the probability that a member will not fail during the time interval [Tⱼ , t*] and a crack will initiate after t* and b) the probability that a crack will initiate during time interval [Tⱼ, t*], but the member will not fail during the same time interval.

$$R(t^*: \text{Repair}) = \{1 - F_c(t^* - T_j | \beta)\} \bullet U(t^* - T_j)$$

$$+ \int_{T_j}^{t^*} f_c(t - T_j | \beta) \bullet U(t - T_j) \bullet V(t^* - t) dt \qquad 2.24$$

where {1-Fc(t*-Tⱼ|β)} denotes the probability that a crack will initiate after t*, U{t*-Tⱼ} denotes the probability that a member will survive time interval [Tⱼ,t*] denotes the probability that a member will survive time interval [Tⱼ,t*], fc(t-Tⱼ|β)dt denotes the probability that a crack will initiate during time interval [t,t+dt],U(t-Tⱼ) denotes the probability that a member will survive time interval [Tⱼ,t] and V(t*-t) denotes the probability that a member will survive during time interval [t,t*]

2.6.2 Members Not Repaired at j-th Inspection

It is known that members are not repaired at the j-th inspection in caes of event {B2:j,1}

The reliability R(t*: No repair) of a member is given by the sum of following three probabilities (written as Z) divided by $(P_{4,j}+P_{5,j})$ which represents the probability of event {B2:j,1}:

a   Probability that member will not fail during the time interval $[T_1,t^*]$ and crack will initiate after t*

b   Probability that a crack will initiate during time interval $[T_j,t^*]$, but member will not fail during time interval $[T_1,t^*]$

c   Probability that crack initiates at some time instant t during time interval $[T_i,T_{i+1}]$ (i=1,...,j-1) and this crack si not detected during all subsequent inspections (from inspection at time T_{i+1} to inspection at time T_j inclusive) and member will not fail during time interval $[T_1,t^*]$.

Hence,

$$R(t^*: \text{No Repair}) = \frac{Z}{P_{4,j}+P_{5,j}} \qquad\qquad 2.25$$

which:

$$Z = \{1 - F_c(t^*-T_1|\beta)\} \bullet U(t^*-T_1)$$

$$+ \int_{T_j}^{t^*} f_c(t-T_1|\beta) \bullet U(t-T_1) \bullet V(t^*-t)dt$$

$$+\sum_{i=1}^{j-1}\{\int_{T_i}^{T_{i+1}} f_c(t-T_i|\beta)\bullet U(t-T_i)\bullet V(t*-t)[\prod_{k=i+1}^{j}\{1-\delta D(a(T_k-t|c)|d)\}]dt\}$$

2.26

where $\{1-F_c(t*-T_i|\beta)\}$ denotes the probability that a crack will initiate after $t*$. $U(t*-T_i)$ denotes the probability that a member will survive time interval $[T_i,t*]$, $f_c(t-T_i|\beta)dt$ denotes the probability that a crack will initiate during time interval $[t,t+dt]$, $U(t-T_i)$ denotes the probability that a member will survive time interval $[T_i,t]$, $V(t*-t)$ denotes the probability that a member will survive time interval $[t,t*]$ and $\{1-D(a(T_k-t|c)|d)\}$ denotes the probability that a crack will not detected at inspection T_k. Note that $R(t*;No\ Repair)$ indicates the probability of event A that a member survives time interval $[T_j,t*]$ given event B that has not been replaced or repaired at the j-th inspection. There ,$P\{AB\}=P\{A\}P\{B|A\}$ where $P\{AB\}=Z$, $P\{A\}=P_{4,j}+P_{5,j}$ and $P\{B|A\}=R(t*;No\ Repair)$

2.7 Bayesian Analysis

2.7.1 Uncertain Parameters and Their Prior Density Function

In thsi study, β,d and c are considered as possible sources of the uncertainty. Initially, a uniform distribution is assumed for the three uncertain parameters having the following jointly uniform density function:

$$f^0(\beta,d,c)=\frac{1}{(\beta_{max}-\beta_{min})(d_{max}-d_{min})(c_{max}-c_{min})}=constant \qquad 2.27$$

where

$$\beta_{min}\leq\beta\leq\beta_{max}$$

$$d_{min}\leq d\leq d_{max}$$

$$c_{min}\leq c\leq c_{max} \qquad\qquad 2.28$$

18

2.7.2 Likihood Function as Result of J-th Inspection

The likelihood function LF_j for the entire structure as a result of the j-th inspection is expressed as follows:

$$LF_j = \prod_{m=1}^{M} LF_j^{(m)} \qquad 2.29$$

where $LF_j(m)$ is the likelihood function as a results of the j-th inspection for member m and M is the total number of members in the structure.

For a typical member m, assume that replacement due to failure or repair due to a detected crack occured at the time of inspections $T_{l1}, T_{l2}, ..., T_{lr}$ where r indicates the number of times the member has been repaired or replaced before the j-th inspection, and:

$$l_1 < l_2 < ... < l_r < j \qquad 2.30$$

It is pointed out that $l_1, l_2, ..., l_r$ are all known at the time of the j-th inspection since the whole inspection history of each member is considered to be known. It is also noted

$$l_r < j-1 \qquad 2.31$$

Then, the likelihood function as a result of the j-th inspection for member is given by

$$LF_j = P_m\{X : j, l_r\} \bullet \prod_{k=1}^{r} P_m\{Y : l_k, l_{k-1}\} \qquad 2.32$$

It is noted that $l_1, l_2, ..., l_r$ as well as r usually take certain values unique to each memeber.

In the above equation. X stands for either A or $B_1(a_j)$ or B_2 depending on the result of the j-th inspection for member m. Specifically, if at the time of the j-th inspection, member m is found to have failed, then X stands for $B_1(a_j)$ and if member is

19

found to have a crack of length between a_j and a_j+da_j, then X stands for $B_1(a_j)$ and if member is found intact, then X stands for B_2. Also, in the above equation, Y stands for either A or $B_1(a_{lk})$ depending on the result of the l_k-th inspection for member m. Specifically, if at the time of the l_k-th inspection, memebr m is found to have failed, then Y stands for A and if member m is found to have a crack of length between a_{lk} and $a_{lk}+da_{lk}$, then Y stands for $B_1(a_{lk})$. Finally, for the case where memeber m is found intact at all inspections prior to the j-th inspection, the product appearing in the above equation is equal to 1 and the above equation takes the form:

$$LF_j^{(m)} = P_m\{X:j,l_0\} \qquad\qquad 2.33$$

Note that l_0 denotes the time of initiation of service for the structure.

2.7.3 Poster Joint Density Function of Uncertain Parameters

The poster joint density function of the three uncertain parameters immediately after the j-th inspection is :

$$f^j(\beta,d,c) = \frac{LF_j f^0(\beta,d,c)}{\int_{\beta_{min}}^{\beta_{max}} \int_{d_{min}}^{d_{max}} \int_{c_{min}}^{c_{max}} (Numerator)d\beta d(d)dc} \qquad\qquad 2.34$$

2.7.4 Reliability of Entire Structure at Time t*

The reliability of the entire structure consisting of M members at time t* after the j-th inspection is denoted by and is given by:

$$\overline{R_M(t^*)} = \int_{\beta_{min}}^{\beta_{max}} \int_{d_{min}}^{d_{max}} \int_{c_{min}}^{c_{max}} R_M(t^*|\beta,d,c)d\beta d(d)dc \qquad\qquad 2.35$$

where:

$$\overline{R_M}(t^*|\beta,c,d) = \{\prod_{m=1}^{M_1} R_m(t^*: \text{Re pair})\}\{\prod_{m=1}^{M_2} R_m(t^*: \text{No Re pair})\} \qquad 2.36$$

where M_1 = number of members being repaired or replaced at the j-th inspection. M_2=number of members found intact at the j-th inspection and $M_1+M_2=M$ in the equation 2.36, $R_m(t^*:$ Repair) and $R_m(t^*:$ No Repair) are identical with the reliabilities $R(t^*:$ Repair) and $R(t^*:$ No Repair) defined in eqs 6.24 and 6.25 respectively. The subscript m is used to indicate that these reliabilities are associated with member m.

2.7.5 Time Tj+1 for (j+1)-th Inspection

If the reliability of the entire structure is specified to be not less than a value Rdesign, find t* such that

$$\overline{R_M}(t^*) = R_{design} \qquad 2.37$$

Then the time T_{j+1} of the (j+1)-th inspection is found as the minimum value of t* which satisfies the above equation.

2.8 Tanker Structures

2.8.1 Introduction

The structures considered in the section 2.2-2.6 consists of structural components subjected to the same level of stress intensity which is different from tanker structures. In this chapter, the tanker structures are assumed to consist of several classes of componenents to represent the stress intensity level in tankers: class Ai compoenents subjected to the highest stress level Ai, class Ai-1 compoenents subjected to the stress

level Ai-1 which is lower than Ai. Class Ai-2, Ai-3,......,A1 and so on where Ai>Ai-1>Ai-2>....>A1

2.8.2 Bayesian Analysis

The reliability of the group of structural components subjected to stress intensity level J at time t* after the j-th inspection is denoted by $\overline{R_{M,J}}(t^*)$ and is given by

$$\overline{R_{M,J}}(t^*) = \int_{\beta_{Jmin}}^{\beta_{Jmax}} \int_{d_{min}}^{d_{max}} \int_{c_{Jmin}}^{c_{Jmax}} R_{M,J}(t^*|\beta_J,d,c_J)f^J(\beta,d,c)d\beta_J d(d)dc_J \qquad 2.38$$

where J=Ai,Ai-1,...A1 and

$$\overline{R_{M,J}}(t^*|\beta_J,d,c_J) = \{\prod_{m=1}^{M_{1,J}} R_{mJ}(t^*:Re\,pair)\}\{\prod_{m=1}^{M_{2,J}} R_{mJ}(t^*:No\,Re\,pair)\} \quad 2.39$$

where M1,J=number of memebrs of group J being replaced or repaired at the j-th inspection, M2,J = number of members of group J found intact at the j-th inspection, and M1J+M2J = MJ = number of members in group J. The posterior joint density function of the three uncertain parameters of group J immediately after the j-th inspection is given by:

$$f_J^j(\beta_J,d,c_J) = \frac{LF_{jJ} \times f_J^0(\beta_J,d,c_J)}{\int_{\beta_{Jmin}}^{\beta_{Jmax}} \int_{d_{min}}^{d_{max}} \int_{c_{Jmin}}^{c_{Jmax}}(Numerator)d\beta_J d(d)dc_J} \qquad 2.40$$

therefore, the structural reliability of the entire structure can be estiamted as:

$$\overline{R_M}(t^*) = \prod_{J=i,i-1,....,1}\overline{R_{M,J}}(t^*) \qquad 2.41$$

Time TJ+1 of the (j+1)-th inspection can then be estiamted with the aid of Eq. 2.37

22

2.9 Summary and Conclusion

This chapter presents the procedure for the probability-based inspection planning so as to maintain the reliability at a prespecified design level throughout the life. For this purpose, a Bayesian approach is applied to treat the various certainties. The uncertainties considered in this chapter is a) fatigue crack initiation time, b) fatigue crack propagation rate and c) probability of crack detection. Assuming uniform prior density function for the unknown parameters for these uncertainties, the inspection results are used in accordance with Bayes Theorem to upgrade the prior density function. A general mathematical formulation is given where a detailed record of the entire inspection history, including repair and replacement records for each and every member, is available.

Reference

2.1. *Structural Maintenance for New and Existing Ships*, Reports SMP 1-1 through 5-2, Department of Naval Architecture and Offshore Engineering, University of California at Berkeley, September 1992.

2.2 *Reliability-Based Maintenance for Fatigue Cracks in Tankers*. Report SMP III-3 , Department of Naval Architecture and Offshore Engineering, University of California at Berkeley, September 1994.

2.3. *Relation of Inspection Faindings to Fatigue Reliability* Ship Structure Committee Report SSC-355

2.4 *Probability Concepts in Engineering Planning and Design* A.H-S Ang and W H. Tang Vol I (1974) Vol II (1984) John Wiley & Sons

2.5 *Methods of Reliability Model Updating Through Additional Events* .G. Jiao and T. Moan, Structural Safety 1990

2.6 *Marine Structural Integrity Programs*. Ship Structure Committee Report SSC-365

Chapter 3

User's Manual

3.1 Terminal Input

Upon the startup of the Pro-IMR Program, the choice is requested whether or not to perform the reliability. The following screen is shown:

Calculation of the reliability after all inspections ? Yes=1

The program only accept the integers 1 or 0. The loop will be quit by typing 0 which cause the program to terminate.

3.2 Main Module

This module has the purpose to specify the main data for the inspection procedure. The user is requested to input the following data

Number of time steps after each inspection

The program need information to divide the inspection interval into several time step so that the reliability can be calculated at each step to form the reliability curve during the interval.

Corresponding time step

For the reliability analysis during the inspection interval, this parameter need be specified in order to determine the step number.

Number of members (Max=1000)

This is required to input the total number of the details (or hotspots) to perform the reliability analysis. The maximum number should be less than 100.

Integration points (Max=11)

This is required for the integration. The maximum number for the code should be less than 11. Meanwhile, It should be pointed out that this number should be odd number.

Inspections (Max=15)

This is the total inspection numbers in the inspection history. The program can only accept the integer number which is less than 15.

3.3 Uncertain Module

This module requires the input for the uncertain parameter b, c, e.

Increments in b,c,e, respectively (Max=7)

These three numbers should be odd numbers and less than seven. It's the increments for the uncertain parameter b, c, e under certain range. b is the uncertainty in crack initiation time. c is the uncertainty in crack propagation. e is the uncertainty in probability of detecting a fatigue crack of length a at the time of inspection.

Member classes (Max=3)

The total inspected members can be divided in to certain groups with the same stress level. This is the input for the number of stress levels. It should be pointed out that the number which is larger than 3 may be out of the memory.

Minimum value of b for member class No. i

This requires the user to input the minimum value for the uncertain parameter b.

Maximum value of b for member class No. i

This requires the user to input the maximum value for the uncertain parameter b.
This two values can determine the uncertain range for parameter b.

Exponent in crack initiation distribution

The user is required to input the shape parameter for the initial crack distribution which is modeled as Weibull distribution

Crack length at initiation

Here, the initial crack length is required to be as an input.

Minimum value of c for member class No.i

This requires the user to input the minimum value for the uncertain parameter c for member class No. i since the POD may be different for different groups of members.

Maximum value of c for member class No. i

This requires the user to input the maximum value for the uncertain parameter c for member class No. i since the POD may be different for different groups of members.
This two values can determine the uncertain range for parameter c for member class i..

Exponent in crack initiation distribution

The user is required to input the shape parameter for the initial crack distribution which is modeled as Weibull distribution

Minimum value of d for member class No. i

This requires the user to input the minimum value for the uncertain parameter c for member class No. i since the crack growth parameters may be different for different groups of members.

Maximum value of d for member class No. i

This requires the user to input the maximum value for the uncertain parameter d for member class No. i since the crack growth parameters may be different for different groups of members.

This two values can determine the uncertain range for parameter c for member class i..

Minimum crack length to be detected

This is the minimum crack length which can be detected during the inspections.

Step size in crack length detection

This is crack increments in the crack detection da (see Chapter 2 for detail)

Crack length factor in member failure rate

This input specify the member's failure as a function as the crack length.

Member failure rate without corrosion and cracks

This input is the parameter for the failure rate without crack and corrosion. Usually, it's determined by the experience to be around 0.9

Corrosion factor in member failure rate for two years period.

This specifies the corrosion effects for the failure rate.

3.4 Inspection Module

This module input the data about inspection history.

Time instant for inspection No.j

This requires the input for the inspection time at the inspection interval. For example, inspection interval i is divided into 5 time steps. So the step 5 is the end of the

inspection interval i. The next inspection i+1 is usually assumed to be performed around 5 so that we can assume that the time instant for inspection i+1 is 4.9.

Number of inspected members

The user need specify the total of the inspected members.

Number of Members found failed

The user need specify the number of the failed members which is found during the inspection.

Number of Members with cracks..

It requires the number of the cracked members which is detected during inspection as the input here.

Member numbers inspected

This is the process which number the members which is inspected in a certain order. It requires an input array.

Members found failed

This is the process which number the members which is found to be failed during the inspection in a certain order. It requires an input array.

Members with cracks are detected

This is the process which number the members which is found to be cracked during the inspection in a certain order. It requires an input array.

Crack length measured in member ng(i).

For each crack member ng(i), the specified crack length for this member is required to be input here.

3.5 Summary and Conclusion

This chapter presents the user's manual for the computer program Pro-IMR. The input data will be illustrated in the numerical example in next chapter.

Chapter 4

Numerical Illustration

The numerical illustration was carried out to verify the validity and effectiveness of Bayesian analysis to determine inspection intervals and uncertain parameters. The example is from Reference 4.1 so that the program validity can be verified. It's assumed that the structure have 100 hotspots (Mt=100). Of the total, 20 are subjected to stress intensity level A, 30 to B and 50 to C.

The design life is 25 years and the desired minimum reliability level of the structure throughout its service life is 0.8 (Rdesign = 0.8).

Two uncertain parameter β and c are examined now. The true values of the uncertain parameters as well as their assumed ranges are shown in Table 4.1, along with the values of the deterministic parameters appearing in the problem.

Item	A	Model Value B	C
Design Life (years)		25	
Min Required Reliability Rdesign		0.8	
Stress Intensity Level	A	B	C
Stress	S	0.9S	0.8S
Stress Range	$\Delta\sigma$	$\Delta\sigma$	$\Delta\sigma$
Number of Structural Members M=100	20	30	50
Parameters in PDF of TTCI	2.0	2.0	2.0
α	30	45	65
β(Years) True Value Assumed Range	(20–40)	(35–55)	(55–75)
Parameter of Crack Propagation	2.0	2.0	2.0
b	0.6	0.486	0.384
C True Value	(0.4–0.8)	(0.286–0.686)	(0.184–0.584)
Assumed Range	10 (0.4)	10 (0.4)	10 (0.4)
Initial Crack Length a_0 mm (in)	0.01	0.01	0.01
	–7.5	–8.25	–9
Parameter in POD d	0.9	0.729	0.576
Parameter in Failure Rate r			
q			

Table 4.1 Parameter Values of Numerical Example [Ref. 4.1]

34

Before the updating analysis, the particular case where both uncertain parameters (β and c) assume their true value is conducted. The inspection schedule is in Table 4.2 while the corresponding structural reliability for the entire structure is plotted in Fig 4.1.

Inspection No.	Inspection Time
1	8.3
2	12.1
3	15.3
4	18.2
5	20.9
6	23.6

Table 4.2 Inspection Schedule for the True Value

The updating analysis is conducted later. The results are displayed in Table 4.3 which include the inspection schedule, number of failed members in each stress intensity level and number and length of detected cracks in each stress intensity level. The estimation of true β and c immediately after the sixth inspection is accomplished reasonable well for stress intensity level A. This is due to that 8 cracks were found during the first six inspections. However, the same did not apply to the stress intensity levels B and C since only 7 and 3 cracks were found respectively. The analysis results from Pro-IMR is nearly the same as the results in Shinozuka's study. (Ref. 4.1). The inspection schedule and reliability which is from the Pro-IMR analysis is plotted in Fig. 4.2.

Inspection No.	Inspection Time : T	No.of Failed Members	No. of Detected Cracks	Detected Crack Length (mm)
1	8.2	0	A[1], B[1]	A[132],B[55]
2	11.6	0	A[2]	A[11,213]
3	14.2	0	A[1]	A[82]
4	16.6	0	B[3], C[1]	B[160,168,70], C[178]
5	19.1	0	A[2],B[1]	A[57,255],B[138]
6	21.5	C[1] (a)	A[2],B[2],C[2]	A[132,98],B[63,365],C[131,165]
7	23.9	0	A[3], C[1]	A[35,752,42],C[74]

Stress Intensity Level : A, B and C   1 in = 25.4 mm

(a); Failure after crack initiation

(b); Failure before crack initiation

Table 4.3 Inspection Schedule and Results from Pro-IMR

Inspection Schedule for True Values (Ref. 4.1)
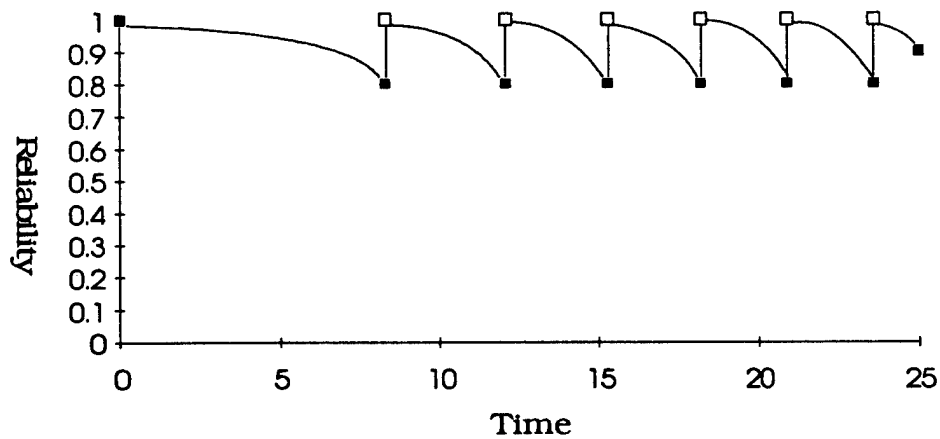
Fig 4.1 Inspection Schedule and Reliability for True β and c (Ref.4.1)

The average number of inspections required to maintain the specified reliability level for 25 years is equal to 6.8. This value should be compared with 6.0 which is the number of inspections when the true values of β and c are known.

Inpsection Schedule for Uncertain Parameters
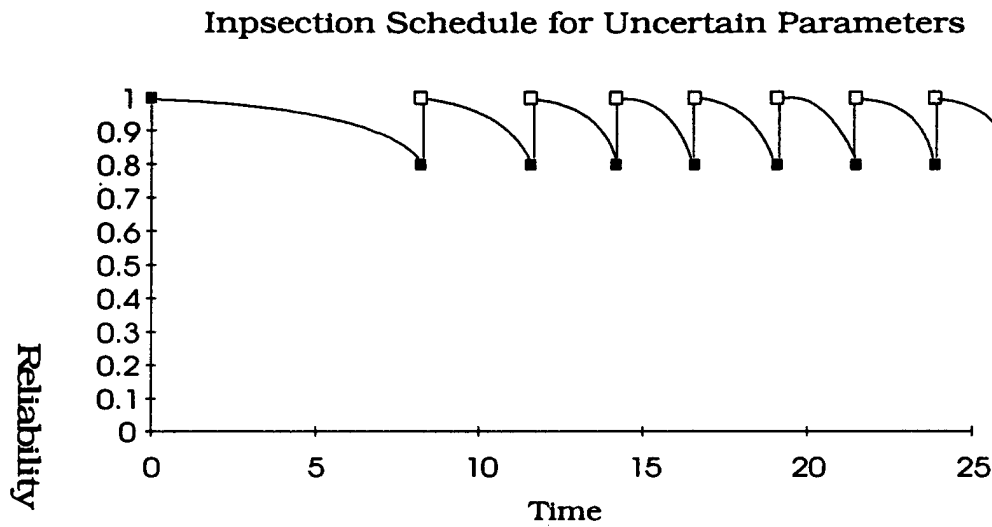
Fig 4.2 Inspection Schedule for Uncertain Parameter β and c

Reference

4.1 *Relation of Inspection Faindings to Fatigue Reliability* Ship Structure Committee Report SSC-355

4.2 *Probability Concepts in Engineering Planning and Design* A.H-S Ang and W H. Tang Vol I (1974) Vol II (1984) John Wiley & Sons

4.3 *Methods of Structural Safety* .H.O.Madsen, S.Krenk and N.C.Lind Prentice-Hall, Inc. 1986

4.4 *Reliability-Based Maintenance for Fatigue Cracks in Tankers* Report, SMP III-3 Department of Naval Architecture & Offshore Engineering, University of California at Berkeley Berkeley, CA 94720

Chapter 5

Conclusion

A general computer code for the probability-based inspection planning has been developed in this project. This report documents the technical background and user's manual for the code. The numerical example is presented to compare with the previous results. It has been shown that the proposed code is more efficient than the previous studies since there is no simulation there.

APPENDIX A

```
*documentation
* **************************************************************
* PURPOSE:      Calculation of the relation between the reliabi-
*               lity of the structure and the time between
*               inspections and subsequent repairs of cracks and
*               failed members.
*               The theory is given the the references below.
*
* USE: mnopti
*
*
*
* FLOW CHART:
*
*               /--> LIKELI -> PA,PB1,Pb2 -> U,V,FC,FFC,FD,CL,G,DTC
*       MNOPTI
*               \--> RELIAB -> REPAIR,NOREP -> PB2,V,FC,FFC,FD,Cl,G
*
* ROUTINES:     Functions: U,V,Fc,Ffc,Fd,Cl,G,Dtc
*               Subroutines: Pa,Pb1,Pb2,Repair,Norep,Reliab,Likeli
*
* REMARKS: Project SMP Phase III, 'Fitness for Purpose Evaluation for
*          Cracked Critical Structural Details in Tankers'
*
* REFERENCES:
*       'Structural Reliability under Bayesian Inspection'
*       Shinozuka, M.:
*       Chapter III in Ship Structure Committee Report 355, Dec. 1990
*
* PROGRAMMER:
*       Tao Xu
*       Department of Naval Architecture & Offshore Engineering
*       University of California at Berkeley
*       Berkeley, CA 94720
*
* DATE: 24. July 1994
*
*
* CORRECTED:
*
* **************************************************************
c
      program mnopti
c ------------------------------------
c COMMON
c ------------------------------------
      integer nt,nj,nb,nc,ne
      integer nm,mc(1000)
      double precision b0(3),b1(3),al(3)
      double precision ac(3),c0(3),cl(3),em(3)
      double precision e0(3),el(3),ad(3),da(3)
      double precision h0(3),p(3,30),q(3)
```

```fortran
      integer n
      double precision b,c,e
      common /struct/ nt,nj,nb,nc,ne
      common /mclass/ nm,mc
      common /initia/ b0,b1,al
      common /growth/ ac,c0,cl,em
      common /detect/ e0,el,ad,da
      common /failur/ h0,p,q
      common /bayesi/ n,b,c,e
c-------------------------------------
c  local variables
c-------------------------------------
      integer ni,j,i,k,nts,ib,ic,ie,mf,mg,imode,l
      integer mm(1000),nf(1000),ng(1000),inj(15000)
      double precision a(1000),hood(7,7,3),hoodl(7,7,7,3)
      double precision ts,r,dts,tsl,ti(15),avf,an(1000)
      double precision fi(11)
      imode=0
c Write introduction information to the screen
      write(*,1000)
1000  format(
     &'  ********************************************',/
     &'           RELIABILITY BASED INSPECTION PLANNING',/
     &'                     Version 1.1',/
     &'                 Last Updated Oct.2 1994',/,/
     &'                 Developed by Tao Xu',/
     &'        Dept.of Naval Architecture & Offshore Engineering',/
     &'            University of California at Berkeley',/
     &'                   Berkeley, CA 94720',//)
      write(*,606)
      read(5,*) imode
606   format(' Calculation of the reliability after all inspections ?',
     &         (YES=1) ')
c
c *******************************************************************
c *                                                                 *
c *                     INPUT OF MAIN DATA                          *
c *                                                                 *
c *  >>>>>>>>>> READ from file 'daoptins'  <<<<<<<<<<<<<<<<<<<<<     *
c *                                                                 *
c *  nts: number of time steps after each inspection                *
c *  dts: corresponding time step                                   *
c *  nt: number of members (max=1000)                               *
c *  ni:   - integration points (max=11)                            *
c *  nj:   - inspections (max=15)                                    *
c *  nb,nc,ne: - increments in b,c,e, respectively (max=7)          *
c *  nm:   - member classes (max=3)                                 *
c *  mc(i=1,nt): class for member No. i                             *
c *  fi(i=1,ni): Simpson integration coefficients                   *
c *  b0(i=1,nm): minimum value of b for member class No. i          *
c *  c0(- ):    -  / -     c    -  / -                               *
c *  e0(- ):    -  / -     e    -  / -                               *
c *  b1(- ): maximum value of b  -  / -                             *
c *  c1(- ):    -  / -     c    -  / -                               *
c *  e1(- ):    -  / -     e    -  / -                               *
c *  al(- ): exponent in crack initiation distribution              *
c *  ac(- ): crack length at initiation                             *
c *  em(- ): exponent        in        -  / -                       *
```

```
*     ad(- / - ): minimum crack length to be detected              *
*     da(- / - ): step size in crack length detection              *
*     h0(- / - ): member failure rate without corrosion and cracks *
*     p(- / - ,z): corrosion factor in member failure rate         *
*     q(- / - ): crack length factor in member failure rate        *
*                                                                   *
*********************************************************************
c
      open(unit=11,file='daoptins',status='old')
      write(*,*)
      write(*,*)    'number of time steps after each inspection:'
      read(5,*) nts
      write(*,*)
      write(*,*)    'corresponding time step:'
      read(5,*) dts
      write(*,*)
      write(*,*)    'number of members (max=1000):'
      read(5,*) nt
      write(*,*)
      write(*,*)    'integration points (max=11):'
      read(5,*) ni
      write(*,*)
      write(*,*)    'inspections (max=15):'
      read(5,*) nj
      write(*,*)
      write(*,*)    'increments in b,c,e, respectively (max=7):'
      read(5,*) nb,nc,ne
      write(*,*)
      write(*,*)    'member classes (max=3):'
      read(5,*) nm
      if (nm.gt.1) then
      read(5,*) (mc(i),i=1,nt)
      else
      do 4 i=1,nt
      mc(i)=1
    4 continue
      endif
c
***********************************************************************
c
c  nb,nc,ne and ni must be odd numbers
c
***********************************************************************
      if ((nb/2)*2.eq.nb) nb=nb+1
      if ((nc/2)*2.eq.nc) nc=nc+1
      if ((ne/2)*2.eq.ne) ne=ne+1
      if ((ni/2)*2.eq.ni) ni=ni+1
      if (ni.lt.3) ni=3
c
***********************************************************************
c
c  fi(i=1,ni): Simpson integration coefficients
c
***********************************************************************
      fi(1)=.33333333d0
      fi(ni)=.33333333d0
      do 14 i=2,ni-1
      fi(i)=.6666667d0
      if ((i/2)*2.eq.i) fi(i)=1.333333d0
   14 continue
```

```fortran
c*********************************************************************
      do 24 n=1,nm
      write(*,*)
      write(*,*)     'minimum value of b for member class No.i(i=1,nm):'
      read(5,*) b0(n)
c
      read(5,*) b0(n),b1(n),al(n),ac(n),c0(n),cl(n),em(n),
     &          e0(n),el(n),ad(n),da(n),q(n)
c
      write(*,*)     'maximum value of b for member class No.i(i=1,nm):'
      read(5,*) b1(n)
      write(*,*)     'exponent in crack initiation distribution'
      read(5,*) al(n)
      write(*,*)     'crack length at initiation'
      read(5,*) ac(n)
      write(*,*)     'minimum value of c for member class No.i(i=1,nm):'
      read(5,*) c0(n)
      write(*,*)     'maximum value of c for member class No.i(i=1,nm):'
      read(5,*) cl(n)
      write(*,*)     'exponent in crack initiation distribution:'
      read(5,*) em(n)
      write(*,*)     'minimum value of d for member class No.i(i=1,nm):'
      read(5,*) e0(n)
      write(*,*)     'maximum value of d for member class No.i(i=1,nm):'
      read(5,*) el(n)
      write(*,*)     'minimum crack length to be detected:'
      read(5,*) ad(n)
      write(*,*)     'step size in crack length detection:'
      read(5,*) da(n)
      write(*,*)     'crack length factor in member failure rate:'
      read(5,*) q(n)
      write(*,*)     'member failure rate without corrosion and cracks:'
      read(5,*) h0(n)
      do 20 l=1,20
c
      write(*,*)     'corrosion factor in member failure rate for two
     & years period'
      do 20 l=1,20
      read(5,*) p(n,l)
 20   continue
      if (ad(n).lt.ac(n)) ad(n)=ac(n)
 24   continue
c*********************************************************************
c
c >>>>>>>>>>>>>       Results are stored in file : 'results' <<<<<<<<<
c
c*********************************************************************
      open(unit=6,file='results',status='unknown')
      write(6,66) nts,dts,nt,ni,nj,nb,nc,ne,nm
 66   format(1x,'MAIN INPUT DATA:',//,' nts,dts,nt,ni,nj,nb,nc,ne,nm:',
     &          i3,f6.3,1x,7i3)
      if (nm.gt.1) write(6,626) (i,mc(i),i=1,nt)
 626  format(1x,/,' Member class for each member:',//,
     &          100(10(i4,'(',il,')'),/))
      do 904 n=1,nm
      write(6,76) n,b0(n),b1(n),al(n),ac(n),c0(n),cl(n),em(n),
     &          e0(n),el(n),ad(n),da(n),q(n),h0(n)
c
 76   format(1x,/,' Member class:',i3,/,
     &          ' b0,b1,al    :',3f9.5,/,
     &          ' ac,c0,cl    :',3f9.5,//,
```

```fortran
     &             '        em,e0,el,ad,da:',5f9.5,/,
     &             '        q,ho                  :',2f9.5)
c        do 902 l=0,9
c          write(6,765) h0(n,3*l+1),h0(n,3*l+2),h0(n,3*l+3)
c  765     format(1x,'       h0               :',3f9.5)
c  902   continue
        do 903 l=0,9
          write(6,77) p(n,3*l+1),p(n,3*l+2),p(n,3*l+3)
   77     format(1x,'       p                 :',3f9.5)
  903   continue
  904  continue
*******************************************************************
c
c    initialization of the arrays hood1 and inj
c    Note: if these arrays are stored after an inspection
c          a new run can begin at the next inspection,
c          provided these arrays reloaded.
c          (this facility is not included in the program now.)
c
*******************************************************************
        do 104 i=1,nb
        do 114 k=1,nc
        do 124 j=1,ne
        do 134 n=1,nm
          hood1(i,k,j,n)=1.d0
  134   continue
  124   continue
  114   continue
  104   continue
        do 304 i=1,nt
        do 314 j=1,nj
          inj(i+(j-1)*nt)=0
  314   continue
  304   continue

*******************************************************************
c
c    calculation of the reliability before the 1st inspection
c
*******************************************************************
        if (imode.eq.1) then
        j=0
        do 84 k=1,nts
          ts=dts*k
          call reliab(j,ti,inj,ni,fi,hood,ts,r,avf)
          write(6,*)
          write(6,6)  ts,j,r
          write(6,6)  ts,j,r
          write(6,16) avf
          write(6,16) avf
   84   continue
        endif
*******************************************************************
c
c    calculations for each inspection j=1,nj
c
*******************************************************************
```

```
      do 44 j=1,nj
      do 54 i=1,nt
      mm(i)=0
      nf(i)=0
      ng(i)=0
      a(i)=0.d0
54    continue
c
c*********************************************************************
*                                                                   *
*              INPUT OF INSPECTION DATA:                             *
*                                                                   *
* >>>>>>>>>>   READ from file 'daoptins'   <<<<<<<<<<<<<<<<<<<<<<    *
*                                                                   *
*            for current inspection No.j:                           *
*                                                                   *
*               ti(j): time instant for inspection No.j             *
*                  mi: number of inspected members                  *
*                  mf: number of members failed                     *
*                  mg: number of members with cracks                *
*        mm(i=1,mi): member numbers inspected                       *
*        nf(i=1,mf): members found failed                           *
*        ng(i=1,mg): members in with cracks are detected            *
*        an(i=1,mg): crack length measured in member ng(i)          *
*                                                                   *
*********************************************************************
c
c
      read(5,*) ti(j),mi,mf,mg
      write(*,*) 'time instant for inspection No.j:'
      read(5,*) ti(j)
      write(*,*) 'number of inspected members:'
      read(5,*) mi
      write(*,*) 'members found failed:'
      read(5,*) mf
      write(*,*) 'members in with cracks are detected:'
      read(5,*) mg
      write(*,*) 'crack length measured in member ng(i):'
      write(6,86) j,ti(j),mi,mf,mg
86    format(1x,//,' DATA FOR INSPECTION NO.',i3,':',//,
     &            ti(j),mi,mf,mg: ',f6.3,1x,3i4)
      if (mi.eq.nt) then
      do 404 i=1,mi
      mm(i)=i
404   continue
      else
      write(*,*) 'member numbers inspected:'
      read(5,*) (mm(i),i=1,mi)
      if (mi.lt.nt) write(6,616)  (mm(i),i=1,mi)
616   format(4x,'Member no. inspected:',//,100(4x,10i4,/))
      endif
      if (mf.gt.0) then
      write(*,*) 'members found failed:'
      read(5,*) (nf(i),i=1,mf)
      write(6,96) (nf(i),i=1,mf)
      endif
96    format(4x,'Failed member No.: ',100i3)
      if (mg.gt.0) then
      write(*,*) 'members in with cracks are detected,crack length
```

```fortran
      &   measured in member ng(i):'
          read(5,*) (ng(i),an(i),i=1,mg)
          write(6,106) (ng(i),an(i),i=1,mg)
          if (mg.gt.0) write(10,106)  (ng(i),an(i),i=1,mg)
      c
  106     format(4x,'Cracked member No. and corresponding crack lengths: '
      &           ,/,4x,100(i3,1x,f5.0))
      ************************************************************************
      *                                                                      *
      *  Lnj(m + (j-1)*nt) = 0 if not inspected,                             *
      *;                  = 1 if no failure or cracks                        *
      *                       are detected,                                  *
      *                     = 2 if a crack is detected,                      *
      *                     = 3 if failure was found.                        *
      *                                                                      *
      ************************************************************************
          do 414 i=1,mi
            inj(mm(i)+nt*(j-1))=1
  414     continue
          if (mf.gt.0)  then
            do 434 i=1,mf
            inj(nf(i)+(j-1)*nt)=3
  434       continue
          endif
          if (mg.gt.0) then
            do 444 i=1,mg
            inj(ng(i)+(j-1)*nt)=2
            a(ng(i))=an(i)
  444       continue
          endif
          write(6,46) j,ti(j)
  46      format(1x,//,' RESULTS AFTER INSPECTION NO.',i3,
      &       ' at time ',f6.3,' :',/)
          do 74 n=1,nm
          write(6,56) n
  56      format(1x,'Member class:',i3,/)
          write(6,36)
  36      format(1x,' ib ic ie   Posterior PDF')
      ************************************************************************
      c
      c  calculation of posterior probability density function
      c
      ************************************************************************
          write(6,806) j
  806     format(' Calculation of posterior pdf after inspection No.',
      &           i3)
          call likeli(j,ti,inj,a,ni,fi,hood,hood1)
          write(6,26) (((ib,ic,ie,hood(ib,ic,ie,n),ib=1,nb),ic=1,nc),
      &           ie=1,ne)
  26      format(1x,3i3,5x,d10.3)
  74      continue
      ************************************************************************
      c
      c  calculation of the reliability after the j-th inspection
      c
      ************************************************************************
          if (imode.ne.1.and.j.ne.nj)   goto 44
```

```
      do 64 k=1,nts
      tsl=dts*k
      ts=ti(j)+tsl
      call reliab(j,ti,inj,ni,fi,hood,ts,r,avf)
      write(6,*)
      write(6,6) tsl,j,r
      write(6,6) tsl,j,r
6     format(1x,'Reliability at time ',f6.3,' after inspection No.',
     &        i3,':  ',d9.3)
      write(6,16) avf
      write(6,16) avf
16    format(' Corresponding average number af failed members   :',
     &        d10.3)
64    continue
44    continue
      close(unit=6)
      close(unit=5)
      stop
      end
*documentation
*************************************************************************
* PURPOSE:        Calculation of the likelihood function for each      *
*                 member class.                                        *
*                 Equa. (3.29), (3.32), (3.33) and (3.40) in the       *
*                 reference below.                                     *
*                                                                      *
* USE:            Call likeli(J,Ti,Inj,A,Ni,Fi,Hood,Hoodl)            *
*                                                                      *
* INPUT ARGUMENTS:  J : current inspection no.                         *
*                 Ti(i): time for i-th inspection                      *
*              Inj(m+(J-1)*nt)): member status for member m out of nt members *
*                 A(m): crack length measured in member m at last      *
*                       inspection                                     *
*                 Ni : no. of integration points                       *
*                 Fi(i): Simpson integration coefficients              *
*                                                                      *
* I & O ARGUMENTS:                                                     *
*            Hoodl(ib,ic,ie,n) : Aux. function conditioned on b,c,e and n *
*                                                                      *
* OUTPUT ARGUMENTS:                                                    *
*            Hood(ib,ic,ie,n) : Posterior p.d.f conditioned on b,c,e and n *
*                                                                      *
* ROUTINES:       Subroutines: Pa, Pb1 and Pb2                         *
*                                                                      *
* REMARKS:                                                             *
*                                                                      *
* REFERENCES:                                                          *
*          'Structural Reliability under Bayesian Inspection'          *
*           Shinozuka, M.:                                             *
*           Chapter III in Ship Structure Committee Report 355, Dec. 1990 *
*                                                                      *
* PROGRAMMER:                                                          *
*           Tao Xu                                                     *
*           Department of Naval Architecture & Offshore Engineering    *
*           University of California at Berkeley                       *
*           Berkeley, CA 94720                                         *
*                                                                      *
```

```fortran
* DATE: 24. July 1994
*
* CORRECTED:
*
* *********************************************************************

      c

      subroutine likeli(j,ti,inj,a,ni,fi,hood,hoodl)

c------------------------------------------------------------
c COMMON
c------------------------------------------------------------
      integer nt,nj,nb,nc,ne
      integer nm,mc(1000)
      double precision b0(3),bl(3),al(3)
      double precision ac(3),c0(3),cl(3),em(3)
      double precision e0(3),el(3),ad(3),da(3)
      integer n
      double precision b,c,e
      common /struct/ nt,nj,nb,nc,ne
      common /mclass/ nm,mc
      common /initia/ b0,bl,al
      common /growth/ ac,c0,cl,em
      common /detect/ e0,el,ad,da
      common /bayesi/ n,b,c,e

c------------------------------------------------------------
c variables
c------------------------------------------------------------
      integer j,inj(*),ni
      double precision ti(*),a(*),fi(*)
      double precision hood(7,7,3),hoodl(7,7,3)

c------------------------------------------------------------
c local variables
c------------------------------------------------------------
      integer ib,ic,ie,k,l,m,i,in(1000)
      double precision h,hl,s,db,dc,de,sb,sc,se,p

c
      s=0.d0
      db=0.d0
      dc=0.d0
      de=0.d0
      if (nb.gt.1) db=(bl(n)-b0(n))/(nb-1.d0)
      if (nc.gt.1) dc=(cl(n)-c0(n))/(nc-1.d0)
      if (ne.gt.1) de=(el(n)-e0(n))/(ne-1.d0)
      do 4 ib=1,nb
      b=b0(n)+db*(ib-1.d0)
      sb=.66666667d0*db
      if ((ib/2)*2.eq.ib) sb=2.d0*sb
      if (ib.eq.1.or.ib.eq.nb) sb=.33333333d0*db
      if (nb.eq.1) sb=1.d0
      do 14 ic=1,nc
      c=c0(n)+dc*(ic-1.d0)
      sc=.66666667d0*dc
      if ((ic/2)*2.eq.ic) sc=2.d0*sc
      if (ic.eq.1.or.ic.eq.nc) sc=.33333333d0*dc
      if (nc.eq.1) sc=1.d0
      do 24 ie=1,ne
      e=e0(n)+de*(ie-1.d0)
```

```
      se=.66666667d0*de
      if ((ie/2)*2.eq.ie) se=2.d0*se
      if (ie.eq.1.or.ie.eq.ne) se=.33333333d0*de
      if(ne.eq.1) se=1.d0
      h=hoodl(ib,ic,ie,n)
      hl=h
      do 34 m=1,nt
        if (mc(m).ne.n) goto 34
        l=0
        do 44 i=1,j
        in(i)=0
        if (inj(m+(i-1)*nt).gt.0) in(i)=1
        if (inj(m+(i-1)*nt).gt.l.and.i.lt.j) l=i
44      continue
        k=inj(m+(j-1)*nt)
        if (k.eq.0) p=1.d0
        if (k.eq.1) call pb2(j,l,in,ti,ni,fi,p)
        if (k.eq.2) call pb1(j,l,in,ti,a(m),p)
        if (k.eq.3) call pa(j,l,in,ti,ni,fi,p)
        h=h*p
        if (k.ge.2) hl=hl*p
34      continue
      s=s+h*sb*sc*se
      hood(ib,ic,ie,n)=h
      hoodl(ib,ic,ie,n)=hl
24    continue
14    continue
4     continue
      s=1.d0/s
      do 104 ib=1,nb
      do 114 ic=1,nc
      do 124 ie=1,ne
      hood(ib,ic,ie,n)=hood(ib,ic,ie,n)*s
124   continue
114   continue
104   continue
      return
      end
```

*documentation
****
* PURPOSE: Calculation of the reliability of the system *
*   after the j-th inspection at time Ts.   *
*   Equa. (3.38), (3.39) and (3.41) in the reference *
*   below.   *
*   *
* USE: Call reliab(J,Ti,Inj,Ni,Fi,Hood,Ts,R,Avf)   *
*   *
* INPUT ARGUMENTS: J : current inspection no.   *
*   Ti(i) : time for i-th inspection   *
*   Inj(m+(J-1)*Nt): member status   *
*   Ni : no. of integration points   *
*   Fi(i): Simpson integration coefficients   *
*   N : current member class   *
*   Hood(ib,ic,ie,n) : Posterior function conditioned on b,c,e and n *
*   Ts : time instant (Ts > Ti(J))   *
*   Avf : average number of failed members at time Ts *
*   *
```

```
*  I & O ARGUMENTS:                                                      *
*                                                                        *
*  OUTPUT ARGUMENTS:  R : system reliability at t=Ts                     *
*                                                                        *
*  ROUTINES:       Subroutines: Repair, Norep                           *
*                                                                        *
*  REMARKS:                                                              *
*                                                                        *
*  REFERENCES:                                                           *
*     'Structural Reliability under Bayesian Inspection'                 *
*      Shinozuka, M.:                                                    *
*      Chapter III in Ship Structure Committee Report 355, Dec. 1990     *
*                                                                        *
*  PROGRAMER:                                                            *
*      Tao Xu                                                            *
*      Department of Naval Architecture & Offshore Engineering           *
*      University of California at Berkeley                              *
*      Berkeley, CA 94720                                                *
*                                                                        *
*  DATE: 24. July 1994                                                   *
*                                                                        *
*  CORRECTED:                                                            *
*                                                                        *
**************************************************************************
c
      subroutine reliab(j,ti,inj,ni,fi,hood,ts,r,avf)
c----------------------------------------------------
c COMMON
c----------------------------------------------------
      integer nt,nj,nb,nc,ne
      integer nm,mc(1000)
      double precision b0(3),b1(3),al(3)
      double precision ac(3),c0(3),c1(3),em(3)
      double precision e0(3),el(3),ad(3),da(3)
      integer n
      double precision b,c,e
      common /struct/ nt,nj,nb,nc,ne
      common /mclass/ nm,mc
      common /initia/ b0,b1,al
      common /growth/ ac,c0,c1,em
      common /detect/ e0,el,ad,da
      common /bayesi/ n,b,c,e
c----------------------------------------------------
c variables
c----------------------------------------------------
      integer j,inj(*),ni
      double precision ti(*),fi(*),hood(7,7,7,*),ts,r,avf
c----------------------------------------------------
c local variables
c----------------------------------------------------
      integer ib,ic,ie,k,l,m,i,in(1000)
      double precision h,rm,rn,db,dc,de,sb,sc,se,rnb,avm,f0
c
      r=1.d0
      avf=0.d0
      do 204 n=1,nm
```

```fortran
      db=0.d0
      dc=0.d0
      de=0.d0
      rnb=0.d0
      if (nb.gt.1) db=(b1(n)-b0(n))/(nb-1.d0)
      if (nc.gt.1) dc=(c1(n)-c0(n))/(nc-1.d0)
      if (ne.gt.1) de=(e1(n)-e0(n))/(ne-1.d0)
      if (j.eq.0) then
      f0=1.d0
      if (nb.gt.1) f0=f0*(b1(n)-b0(n))
      if (nc.gt.1) f0=f0*(c1(n)-c0(n))
      if (ne.gt.1) f0=f0*(e1(n)-e0(n))
      f0=1.d0/f0
      endif
      do 4 ib=1,nb
      b=b0(n)+db*(ib-1.d0)
      sb=.666667d0*db
      if ((ib/2)*2.eq.ib) sb=2.d0*sb
      if (ib.eq.1.or.ib.eq.nb) sb=.333333d0*db
      if (nb.eq.1) sb=1.d0
      do 14 ic=1,nc
      c=c0(n)+dc*(ic-1.d0)
      sc=.666667d0*dc
      if ((ic/2)*2.eq.ic) sc=2.d0*sc
      if (ic.eq.1.or.ic.eq.nc) sc=.333333d0*dc
      if (nc.eq.1) sc=1.d0
      do 24 ie=1,ne
      e=e0(n)+de*(ie-1.d0)
      se=.666667d0*de
      if ((ie/2)*2.eq.ie) se=2.d0*se
      if (ie.eq.1.or.ie.eq.ne) se=.333333d0*de
      if(ne.eq.1) se=1.d0
      if (j.eq.0) then
      h=f0*sb*sc*se
      else
      h=hood(ib,ic,ie,n)*sb*sc*se
      endif
      rn=1.d0
      avm=0.d0
      do 34 m=1,nt
      if (mc(m).ne.n) goto 34
      if (j.eq.0) then
      call repair(j,ti,ni,fi,ts,rm)
      else
      l=0
      do 44 i=1,j
      in(i)=0
      if (inj(m+(i-1)*nt).gt.0) in(i)=1
      if (inj(m+(i-1)*nt).gt.1) l=i
 44   continue
      k=inj(m+(j-1)*nt)
      if (k.gt.1) call repair(j,ti,ni,fi,ts,rm)
      if (k.le.1) call norep(j,l,in,ti,ni,fi,ts,rm)
      endif
      rn=rn*rm
      avm=avm+(1.d0-rm)
 34   continue
```

```fortran
            rnb=rnb+rn*h
            avf=avf+avm*h
   24       continue
   14     continue
    4   continue
        r=r*rnb
  204 continue
      return
      end
*documentation
*****************************************************
* PURPOSE:        Calculation of the probability of event (A:j,l),  *
*                 defined as the probability that the member is     *
*                 failed at the j-th inspection and assuming it     *
*                 was repaired after the l-th inspection.           *
*                 Equa. (3.11), (3.12), (3.13) and (3.23) in the    *
*                 reference below.                                  *
*                                                                   *
* USE:            Call pa(J,L,In,Ti,Ni,Fi,P)                        *
*                                                                   *
* INPUT ARGUMENTS:  J : current inspection no.                      *
*                   L : inspection no. at last repair               *
*                   In(i): 1 if i-th inspection performed for the member *
*                   Ti(i): time for i-th inspection                 *
*                   Ni : no. of integration points                 *
*                   Fi(i): Simpson integration coefficients         *
*                                                                   *
* I & O ARGUMENTS:  none                                            *
*                                                                   *
* OUTPUT ARGUMENTS: P : Probability of event (A:j,l)                *
*                                                                   *
* ROUTINES:        Functions: U,V,Fc,Ffc,Fd,Cl                      *
*                                                                   *
* REMARKS:                                                          *
*                                                                   *
* REFERENCES:                                                       *
*         'Structural Reliability under Bayesian Inspection'        *
*          Shinozuka, M.:                                           *
*          Chapter III in Ship Structure Committee Report 355, Dec. 1990 *
*                                                                   *
* PROGRAMMER:                                                       *
*          Tao Xu                                                   *
*          Department of Naval Architecture & Offshore Engineering  *
*          University of California at Berkeley                     *
*          Berkeley, CA 94720                                       *
*                                                                   *
* DATE: 24. July 1994                                               *
*                                                                   *
* CORRECTED:                                                        *
*                                                                   *
*****************************************************
c
      subroutine pa(j,l,in,ti,ni,fi,p)
c------------------------------------
c   variables
c------------------------------------
```

```fortran
      integer j,l,in(*),ni
      double precision ti(*),fi(*),p
c------------------------------------------------
c     functions
c------------------------------------------------
      double precision u,v,fc,ffc,fd,cl
c------------------------------------------------
c     local variables
c------------------------------------------------
      integer i,n,k
      double precision t,tl,tj,tjl,dt,ds,at,pl,p2,til
c
      tl=0.d0
      if (l.gt.0) tl=ti(l)
      tjl=0.d0
      if (j.gt.1) tjl=ti(j-1)-tl
      tj=ti(j)-tl
      pl=(1.d0-fc(tj))*(u(tjl)-u(tj))
      dt=(tj-tjl)/(ni-1.d0)
      do 4 n=1,ni
      t=tjl+dt*(n-1)
      pl=pl+ffc(t)*(u(tjl)-u(t))*fi(n)*dt
4     continue
      p2=0.d0
      if (l.lt.j-2) then
      til=tl
      do 14 i=l,j-2
      dt=(ti(i+1)-til)/(ni-1.d0)
      do 24 n=1,ni
      t=til-tl+dt*(n-1)
      ds=1.d0
      do 34 k=i+1,j-1
      at=cl(ti(k))-tl-t
      ds=ds*(1.d0-fd(at)*in(k))
34    continue
      p2=p2+ffc(t)*u(t)*(v(tjl,t)-v(tj,t))*ds*fi(n)*dt
24    continue
      til=ti(i+1)
14    continue
      endif
      dt=(tj-tjl)/(ni-1.d0)
      do 44 n=1,ni
      t=tjl+dt*(n-1)
      p2=p2+ffc(t)*u(t)*(1.d0-v(tj,t))*fi(n)*dt
44    continue
      p=pl+p2
      return
      end
*documentation
*********************************************************
* PURPOSE:       calculation of the probability of event (Bl:j,l), *
*                defined as the probability that the member has not*
*                failed at the j-th inspection but a crack of a    *
*                given length has been found. The member is assumed*
*                repaired after the l-th inspection.               *
*                Equa. (3.19), (3.20) and (3.23) in the reference  *
*                below.                                            *
```

```
*  USE:        Call pbl(J,L,In,Ti,A,P)                              *
*                                                                   *
*  INPUT ARGUMENTS:   J :  current inspection no.                   *
*                     L :  inspection no. at last repair            *
*                   In(*):  1 if i-th inspection performed for the member *
*                   Ti(*):  time for i-th inspection                *
*                     A :  measured crack length                    *
*                                                                   *
*  I & O ARGUMENTS:   none                                          *
*                                                                   *
*  OUTPUT ARGUMENTS:  P :  Probability of event (Bl:j,l)            *
*                                                                   *
*  ROUTINES:      Functions: U,V,Ffc,Fd,Cl,Dtc,G                    *
*                                                                   *
*  REMARKS:                                                      *
*                                                                   *
*  REFERENCES:                                                      *
*    'Structural Reliability under Bayesian Inspection'             *
*    Shinozuka, M.:                                                 *
*    Chapter III in Ship Structure Committee Report 355, Dec. 1990  *
*                                                                   *
*  PROGRAMMER:                                                      *
*    Tao Xu                                                         *
*    Department of Naval Architecture & Offshore Engineering        *
*    University of California at Berkeley                           *
*    Berkeley, CA 94720                                             *
*                                                                   *
*  DATE: 24. July 1994                                              *
*                                                                   *
*  CORRECTED:                                                       *
*  *****************************************************************
c
      subroutine pbl(j,l,in,ti,a,p)
c-------------------------------
c   variables
c-------------------------------
      integer j,l,in(*)
      double precision ti(*),a,p
c-------------------------------
c   functions
c-------------------------------
      double precision u,v,ffc,fd,cl,dtc,g
c-------------------------------
c   local variables
c-------------------------------
      integer k
      double precision t,tl,tj,tc,ds
c
      tl=0.d0
      if (l.gt.0) tl=ti(l)
      tj=ti(j)-tl
      tc=tj-g(a)
      if (tc.le.0.d0) then
      write(6,6) a
```

```
 6      format(' The crack length',f7.1,' corresponds to a',/,
     &  ' crack initiated BEFORE the member was put in use !',/,
     &  ' This is not possible and this result is omitted in',//,
     &  ' the calculation of the posterior function. However,'//
     &  ' the member will still be assumed repaired.',/)
        p=1.d0
        else
        ds=1.d0
        do 4 k=l+1,j-1
        t=ti(k)-tl-tc
        if (t.gt.0.d0) ds=ds*(1-fd(cl(t))*in(k))
 4      continue
        p=ffc(tc)*u(tc)*v(tj,tc)*ds*fd(a)*dtc(a)
        endif
        return
        end
*documentation
*****************************************************************
* PURPOSE:        Calculation of the probability of event {B2:j,l},  *
*                 defined as the probability that the member has not*
*                 failed at the j-th inspection and no cracks have  *
*                 been found. The member is assumed repaired after  *
*                 the l-th inspection.                              *
*                 Equa. (3.21), (3.22) and (3.23) in the reference  *
*                 below.                                            *
*                                                                   *
* USE:            Call pb2(J,L,In,Ti,Ni,Fi,P)                       *
*                                                                   *
* INPUT ARGUMENTS:  J : current inspection no.                      *
*                   L : inspection no. at last repair               *
*                  In(*): 1 if i-th inspection performed for the member *
*                  Ti(*): time for i-th inspection                  *
*                  Ni : no. of integration points                   *
*                  Fi(*): Simpson integration coefficients          *
*                                                                   *
* I & O ARGUMENTS:  none                                            *
*                                                                   *
* OUTPUT ARGUMENTS: P : Probability of event {B2:j,l}               *
*                                                                   *
* ROUTINES:        Functions: U,V,Fc,Ffc,Fd,Cl                     *
*                                                                   *
* REMARKS:                                                          *
*                                                                   *
* REFERENCES:                                                       *
*     'Structural Reliability under Bayesian Inspection'           *
*     Shinozuka, M.:                                                *
*     Chapter III in Ship Structure Committee Report 355, Dec. 1990 *
*                                                                   *
* PROGRAMMER:                                                       *
*     Tao Xu                                                        *
*     Department of Naval Architecture & Offshore Engineering      *
*     University of California at Berkeley                          *
*     Berkeley, CA 94720                                            *
*                                                                   *
* DATE: 24. July 1994                                               *
*                                                                   *
*                                                                   *
```

```
*  CORRECTED:
*
*  ******************************************************

      c     subroutine pb2(j,l,in,ti,ni,fi,p)

      c-----------------------------------
      c     variables
      c-----------------------------------
            integer j,l,in(*),ni
            double precision ti(*),fi(*),a,p

      c     functions
      c-----------------------------------
            double precision u,v,fc,ffc,fd,cl

      c-----------------------------------
      c     local variables
      c-----------------------------------
            integer k,i,n
            double precision t,tl,tj,dt,ds,at,p4,p5,til

      c
            tl=0.d0
            if (l.gt.0) tl=ti(l)
            tj=ti(j)-tl
            p4=(1.d0-fc(tj))*u(tj)
            p5=0.d0
            til=tl
            do 4 i=l,j-1
            dt=(ti(i+1)-til)/(ni-1.d0)
            do 14 n=1,ni
            t=til-tl+dt*(n-1.d0)
            ds=1.d0
            do 24 k=i+1,j
            at=cl(ti(k)-tl-t)
            ds=ds*(1.d0-fd(at)*in(k))
      24    continue
            p5=p5+ffc(t)*u(t)*v(tj,t)*ds*fi(n)*dt
      14    continue
            til=ti(i+1)
      4     continue
            p=p4+p5
            return
            end

*documentation
******************************************************
*  PURPOSE:          Calculation of the reliability for a member not   *
*                    repaired at the j-th inspection.                  *
*                    Equa. (3.25) and (3.26) in the reference below    *
*                                                                      *
*  USE:              Call norep(J,L,In,Ti,Ni,Fi,Ts,R)                  *
*                                                                      *
*  INPUT ARGUMENTS:  J  : current inspection no.                       *
*                    L  : inspection no at last repair                 *
*                    In(*): 1 if i-th inspection performed for the member *
*                    Ti(*): time at i-th integration                   *
```

```
*        Ni : no. of integration points                              *
*        Fi(*): Simpsom integration coefficients                     *
*        Ts : current time > Ti(J)                                   *
*                                                                    *
* I & O ARGUMENTS:  none                                             *
*                                                                    *
* OUTPUT ARGUMENTS:  R : Reliability R(Ts,no repair or replacement)  *
*                                                                    *
* ROUTINES:      Functions: U,V,Fc,Ffc,Fd,Cl. Subroutine: PB2       *
*                                                                    *
* REMARKS:                                                           *
*                                                                    *
* REFERENCES:                                                        *
*      'Structural Reliability under Bayesian Inspection'            *
*       Shinozuka, M.:                                               *
*       Chapter III in Ship Structure Committee Report 355, Dec. 1990 *
*                                                                    *
* PROGRAMMER:                                                        *
*       Tao Xu                                                       *
*       Department of Naval Architecture & Offshore Engineering      *
*       University of California at Berkeley                         *
*       Berkeley, CA 94720                                           *
*                                                                    *
* DATE: 24. July 1994                                               *
*                                                                    *
* CORRECTED:                                                         *
*                                                                    *
*********************************************************************
c
      subroutine norep(j,l,in,ti,ni,fi,ts,r)
c----------------------------------
c   variables
c----------------------------------
      integer j,l,in(*),ni
      double precision ti(*),fi(*),ts,r
c----------------------------------
c   functions
c----------------------------------
      double precision u,v,fc,ffc,fd,cl
c----------------------------------
c   local variables
c----------------------------------
      integer n,i,k
      double precision t,tl,tj,dt,tsl,z,ds,at,p,til
c
      tl=0.d0
      if (l.gt.0) tl=ti(l)
     +sl=ts-tl
      z=(1.d0-fc(tsl))*u(tsl)
      tj=ti(j)-tl
      dt=(tsl-tj)/(ni-1.d0)
      do 4 n=1,ni
      t=tj+dt*(n-1.d0)
      z=z+ffc(t)*u(t)*v(tsl,t)*fi(n)*dt
    4 continue
      til=tl
```

```
        do 14 i=1,j-1
        dt=(ti(i+1)-til)/(ni-1.d0)
        do 24 n=1,ni
        t=til-tl+dt*(n-1.d0)
        ds=1.d0
        do 34 k=i+1,j
        at=cl(ti(k)-tl-t)
        ds=ds*(1.d0-fd(at)*in(k))
 34     continue
        z=z+ffc(t)*u(t)*v(tsl,t)*ds*fi(n)*dt
 24     continue
        til=ti(i+1)
 14     continue
        call pb2(j,l,in,ti,ni,fi,p)
        r=z/p
        return
        end
```

```
*documentation
******************************************************
* PURPOSE:           Calculation of the reliability of a member repai- *
*                    red at the j-th inspection.                       *
*                    Equa. (3.24) in the reference below               *
*                                                                      *
* USE:          Call repair(J,Ti,Ni,Fi,Ts,R)                          *
*                                                                      *
* INPUT ARGUMENTS:  J : current inspection no.                         *
*                   Ti(*): time at i-th inspection                     *
*                   Ni : no. of integration points                     *
*                   Fi(*): Simpson integration points                  *
*                   Ts : current time > Ti(J)                          *
*                                                                      *
* I & O ARGUMENTS:   none                                              *
*                                                                      *
* OUTPUT ARGUMENTS: R : Reliability R(Ts,repair or replacement)        *
*                                                                      *
* ROUTINES:         Functions: U,V,Fc,Ffc                             *
*                                                                      *
* REMARKS:                                                             *
*                                                                      *
* REFERENCES:                                                          *
*     'Structural Reliability under Bayesian Inspection'               *
*      Shinozuka, M.:                                                  *
*      Chapter III in Ship Structure Committee Report 355, Dec. 1990   *
*                                                                      *
* PROGRAMMER:                                                          *
*      Tao Xu                                                          *
*      Department of Naval Architecture & Offshore Engineering         *
*      University of California at Berkeley                            *
*      Berkeley, CA 94720                                              *
*                                                                      *
* DATE: 24. July 1994                                                  *
*                                                                      *
* CORRECTED:                                                           *
******************************************************
```

```fortran
c
      subroutine repair(j,ti,ni,fi,ts,r)
c-----------------------------------------------------
c   variables
c-----------------------------------------------------
      integer j,ni
      double precision ti(*),fi(*),r,ts
c-----------------------------------------------------
c   functions
c-----------------------------------------------------
      double precision u,v,fc,ffc
c-----------------------------------------------------
c   local variables
c-----------------------------------------------------
      integer n
      double precision t,tj,dt
c
      tj=0.d0
      if (j.gt.0) tj=ti(j)
      r=(1.d0-fc(ts-tj))*u(ts-tj)
      dt=(ts-tj)/(ni-1.d0)
      do 4 n=1,ni
      t=dt*(n-1)
      r=r+ffc(t)*u(t)*v(ts-tj,t)*fi(n)*dt
    4 continue
      return
      end
*documentation
**********************************************************************
* PURPOSE:      Calculation of the probability that a crack has      *
*                 initiated at time T after last repair              *
*                                                                    *
* USE:          fc(T)                                                *
*                                                                    *
* INPUT ARGUMENT:  T : time T                                        *
*                                                                    *
* ROUTINES:                                                          *
*                                                                    *
* REMARKS: Can be replaced by any other distribution function.      *
*          (NB: the Function Ffc must be changed accordingly.)       *
*                                                                    *
* REFERENCES:                                                        *
*     'Structural Reliability under Bayesian Inspection'             *
*     Shinozuka, M.:                                                 *
*     Chapter III in Ship Structure Committee Report 355, Dec. 1990  *
*                                                                    *
* PROGRAMMER:                                                        *
*     Tao Xu                                                         *
*     Department of Naval Architecture & Offshore Engineering        *
*     University of California at Berkeley                           *
*     Berkeley, CA 94720                                             *
*                                                                    *
* DATE: 24. July 1994                                                *
*                                                                    *
* CORRECTED:                                                         *
*                                                                    *
```

```
******************************************************************************
c
c     double precision function fc(t)
c
c     ----------------------------------
c COMMON
c     ----------------------------------
      double precision b0(3),b1(3),al(3)
      integer n
      double precision b,c,e
      common /initia/ b0,b1,al
      common /bayesi/ n,b,c,e
c     ----------------------------------
c     variables
c     ----------------------------------
      double precision t
      fc=1.d0-dexp(-(t/b)**al(n))
      return
      end

*documentation
******************************************************************************
* PURPOSE:          Calculation of the probability that a crack will    *
*                   initiate at time T after last repair                *
*                                                                       *
* USE:        ffc(T)                                                    *
*                                                                       *
* INPUT ARGUMENT:   T : time T                                          *
*                                                                       *
* ROUTINES:                                                             *
*                                                                       *
* REMARKS: Can be replaced by any other density function.               *
*          (NB: the Function Fc must be changed accordingly.)           *
*                                                                       *
* REFERENCES:                                                           *
*       'Structural Reliability under Bayesian Inspection'              *
*       Shinozuka, M.:                                                  *
*       Chapter III in Ship Structure Committee Report 355, Dec. 1990   *
*                                                                       *
* PROGRAMMER:                                                           *
*       Tao Xu                                                          *
*       Department of Naval Architecture & Offshore Engineering         *
*       University of California at Berkeley                            *
*       Berkeley, CA 94720                                              *
*                                                                       *
* DATE: 24. July 1994                                                   *
*                                                                       *
* CORRECTED:                                                            *
*                                                                       *
******************************************************************************
c
c     double precision function ffc(t)
c
c     ----------------------------------
c COMMON
c     ----------------------------------
      double precision b0(3),b1(3),al(3)
      integer n
      double precision b,c,e
```

```fortran
      common /initia/ b0,b1,al
      common /bayesi/ n,b,c,e
c-------
c     variables
c-------
      double precision t
      ffc=al(n)/b*(t/b)**(al(n)-1.d0)*dexp(-(t/b)**al(n))
      return
      end
*documentation
*********************************************************************
* PURPOSE:        Calculation of the probability that a crack of   *
*                 length A will be detected.                        *
*                                                                  *
* USE:       fd(A)                                                  *
*                                                                  *
* INPUT ARGUMENT:   A : crack length A                             *
*                                                                  *
* ROUTINES:                                                        *
*                                                                  *
* REMARKS: Can be replaced by any other distribution function.    *
*                                                                  *
* REFERENCES:                                                      *
*       'Structural Reliability under Bayesian Inspection'         *
*       Shinozuka, M.:                                             *
*       Chapter III in Ship Structure Committee Report 355, Dec. 1990 *
*                                                                  *
* PROGRAMMER:                                                      *
*       Tao Xu                                                     *
*       Department of Naval Architecture & Offshore Engineering   *
*       University of California at Berkeley                       *
*       Berkeley, CA 94720                                         *
*                                                                  *
* DATE: 24. July 1994                                             *
*                                                                  *
* CORRECTED:                                                       *
*                                                                  *
*********************************************************************
c
      double precision function fd(a)
c-------
c COMMON
c-------
      double precision e0(3),e1(3),ad(3),da(3)
      integer n
      double precision b,c,e
      common /detect/ e0,e1,ad,da
      common /bayesi/ n,b,c,e
c-------
c     variables
c-------
      double precision a,aux
      aux=e*(a-ad(n))
      if (aux.lt.0.d0) then
      fd=0.d0
      else
```

```fortran
      fd=1.d0
      if (aux.lt.100.d0) fd=1.d0-dexp(-aux)
      endif
      return
      end
*documentation
************************************************************
*  PURPOSE:          Calculation of the time T to reach a crack length  *
*                    A after crack initiation.                          *
*                                                                       *
*  USE:          g(A)                                                   *
*                                                                       *
*  INPUT ARGUMENT:   A : crack length                                   *
*                                                                       *
*  ROUTINES:                                                            *
*                                                                       *
*  REMARKS: Can be replaced by any other function.                      *
*           (NB: Functions Dtc and Cl must be changed accordingly.)     *
*                                                                       *
*  REFERENCES:                                                          *
*     'Structural Reliability under Bayesian Inspection'                *
*      Shinozuka, M.:                                                   *
*      Chapter III in Ship Structure Committee Report 355, Dec. 1990    *
*                                                                       *
*  PROGRAMMER:                                                          *
*     Tao Xu                                                            *
*     Department of Naval Architecture & Offshore Engineering           *
*     University of California at Berkeley                              *
*     Berkeley, CA 94720                                                *
*                                                                       *
*  DATE: 24. July 1994                                                  *
*                                                                       *
*  CORRECTED:                                                           *
*                                                                       *
************************************************************
c
c     double precision function g(a)
c
c ----------------------------
c COMMON
c ----------------------------
      double precision ac(3),c0(3),cl(3),em(3)
      integer n
      double precision b,c,e
      common /growth/ ac,c0,cl,em
      common /bayesi/ n,b,c,e
c ----------------------------
c     variables
c ----------------------------
      double precision a,auy
      if (em(n).eq.2.d0) then
      g=dlog(a/ac(n))/c
      else
      auy=1.d0-.5d0*em(n)
      g=-1.d0/(auy*c)*(1.d0-(a/ac(n))**auy)
      endif
      return
```

```
      end
*documentation
*********************************************************************
* PURPOSE:        Calculation of the time increment dT correspond-  *
*                 ing to the uncertaincy in crack length detection. *
*                                                                   *
* USE:        dtc(A)                                                 *
*                                                                   *
* INPUT ARGUMENT:   A : crack length A                              *
*                                                                   *
* ROUTINES:                                                          *
*                                                                   *
* REMARKS: Can be replaced by any other function.                   *
*          (NB: Functions G and Cl must be changed accordingly.)    *
*                                                                   *
* REFERENCES:                                                        *
*    'Structural Reliability under Bayesian Inspection'             *
*    Shinozuka, M.:                                                 *
*    Chapter III in Ship Structure Committee Report 355, Dec. 1990  *
*                                                                   *
* PROGRAMMER:                                                        *
*    Tao Xu                                                          *
*    Department of Naval Architecture & Offshore Engineering        *
*    University of California at Berkeley                           *
*    Berkeley, CA 94720                                              *
*                                                                   *
* DATE: 24. July 1994                                               *
*                                                                   *
* CORRECTED:                                                         *
*                                                                   *
*********************************************************************
c
      double precision function dtc(a)
c
c     -----------------------------------
c COMMON
c     -----------------------------------
      double precision ac(3),c0(3),cl(3),em(3)
      double precision e0(3),el(3),ad(3),da(3)
      integer n
      double precision b,c,e
      common /growth/ ac,c0,cl,em
      common /detect/ e0,el,ad,da
      common /bayesi/ n,b,c,e
c     -----------------------------------
c     variables
c     -----------------------------------
      double precision a
      dtc=da(n)/(c*ac(n)*(a/ac(n))**(em(n)*.5d0))
      return
      end
*documentation
*********************************************************************
* PURPOSE:        Calculation of the reliability of a member with-  *
*                 out crack at time T after last repair.            *
*                                                                   *
* USE:        u(T)                                                  *
```

```
*  INPUT ARGUMENT:    T : time T
*
*  ROUTINES:
*
*  REMARKS: Can be replaced by any other function.
*
*  REFERENCES:
*     'Structural Reliability under Bayesian Inspection'
*     Shinozuka, M.:
*     Chapter III in Ship Structure Committee Report 355, Dec. 1990
*
*  PROGRAMMER:
*     Tao Xu
*     Department of Naval Architecture & Offshore Engineering
*     University of California at Berkeley
*     Berkeley, CA 94720
*
*  DATE: 24. July 1994
*
*  CORRECTED:
*
*****************************************************************
c
      double precision function u(t)
c
c ---------------------------------------
c COMMON
c ---------------------------------------
      double precision h0(3),p(3,30),q(3)
      integer n
      double precision b,c,d
      common /failur/ h0,p,q
      common /bayesi/ n,b,c,d
c
c ---------------------------------------
c  variables
c ---------------------------------------
      double precision t
      integer l,m
      u=0.d0
      if (p(n,1).eq.0.d0) then
      u=dexp(-h0(n)*t)
      else
      m=t/2
      do 3 l=1,m
      u=u+1/p(n,1)*(dexp(p(n,1)*2*l)-dexp(p(n,1)*2*(l-1)))
   3  continue
      u=dexp(-h0(n)*((u+1/p(n,m+1)*(dexp(p(n,m+1)*t)-
     &                             dexp(p(n,m+1)*2*m)))))
      endif
      return
      end


*documentation
*****************************************************************
*  PURPOSE:          Calculation of the reliability of a member with  *
```

```
*
*                a crack at time T after last repair.
*
*   USE:         v(T,Tc)
*
*   INPUT ARGUMENT:    T : time T
*                      Tc: time at crack initiation (Tc<T)
*
*   ROUTINES:
*
*   REMARKS: Can be replaced by any other function.
*
*   REFERENCES:
*        'Structural Reliability under Bayesian Inspection'
*        Shinozuka, M.:
*        Chapter III in Ship Structure Committee Report 355, Dec. 1990
*
*   PROGRAMMER:
*        Tao Xu
*        Department of Naval Architecture & Offshore Engineering
*        University of California at Berkeley
*        Berkeley, CA 94720
*
*   DATE: 24. July 1994
*
*   CORRECTED:
*
*****************************************************************************
c
      double precision function v(t,tc)
c-----------------------------------------------------------------
c COMMON
c-----------------------------------------------------------------
      double precision ac(3),c0(3),c1(3),em(3)
      double precision h0(3),p(3,30),q(3)
      integer n
      double precision b,c,d
      common /growth/ ac,c0,c1,em
      common /failur/ h0,p,q
      common /bayesi/ n,b,c,d
c-----------------------------------------------------------------
c variables
c-----------------------------------------------------------------
      double precision t,tc,aux,auy,auz,ax,ay,az
      integer ll,mzz,ss
      ss=tc/2+1
      mzz=t/2.d0
      aux=0.d0
      if (em(n).eq.2.d0) then
      do 4 ll=ss+1,mzz
      ax=q(n)*(2.d0*ll-tc)
      ay=q(n)*(2.d0*(ll-1)-tc)
      aux=aux+dexp(p(n,ll)*tc)*(dexp(ax)-dexp(ay))
    4 continue
      aux=aux+dexp(p(n,ss)*tc)*(dexp(q(n)*(2.d0*ss-tc))-1.d0)
      aux=aux+dexp(p(n,mzz+1)*tc)*(dexp(q(n)*(t-tc))-
     &                            dexp(q(n)*(2.d0*mzz-tc)))
```

```
      else
      auy=.5d0*em(n)-1.d0
      auz=1.d0-auy*(2*em(n))*c
      if (auz.gt.0.d0) then
      auz=-q(n)/auy/c
      do 5 ll=ss+1,mzz
      ax=auy*(2.d0*ll-tc)*c
      ay=auy*(2.d0*(ll-1)-tc)*c
      aux=aux+dexp(p(n,ll)*tc)*((1.d0-ax)**auz-(1.d0-ay)**auz)
5     continue
      az=auy*2.d0*mzz*c
      aux=aux+dexp(p(n,ss)*tc)*((1.d0-auy*(2.d0*ss-tc)*c)**auz-1.d0)
      aux=aux+dexp(p(n,mzz+1)*tc)*((1.d0-auy*(t-tc)*c)**auz-
     &    (1.d0-az)**auz)
      else
      aux=101.d0
      endif
      endif
      v=0.d0
      aux=aux*h0(n)/q(n)
      if (aux.lt.100.d0) v=dexp(-aux)
      return
      end


*documentation
*******************************************************************
*  PURPOSE:        Calculation of the crack length at time T after *
*                  crack initiation.                               *
*                                                                  *
*  USE:       cl(T)                                                *
*                                                                  *
*  INPUT ARGUMENT:   T : time T                                    *
*                                                                  *
*  ROUTINES:                                                       *
*                                                                  *
*  REMARKS: Can be replaced by any other function.                 *
*           (NB: Functions Dtc and G must be changed accordingly.) *
*                                                                  *
*  REFERENCES:                                                     *
*     'Structural Reliability under Bayesian Inspection'           *
*     Shinozuka, M.:                                               *
*     Chapter III in Ship Structure Committee Report 355, Dec. 1990*
*                                                                  *
*  PROGRAMMER:                                                     *
*     Tao Xu                                                       *
*     Department of Naval Architecture & Offshore Engineering      *
*     University of California at Berkeley                         *
*     Berkeley, CA 94720                                           *
*                                                                  *
*  DATE: 24. July 1994                                             *
*                                                                  *
*  CORRECTED:                                                      *
*                                                                  *
*******************************************************************
c
      double precision function cl(t)
```

```
c --------------------------------------------------
c COMMON
c --------------------------------------------------
      double precision ac(3),c0(3),c1(3),em(3)
      integer n
      double precision b,c,e
      common /growth/ ac,c0,c1,em
      common /bayesi/ n,b,c,e
c --------------------------------------------------
c   variables
c --------------------------------------------------
      double precision t,auy,aux
      if (em(n).eq.2.d0) then
      c1=ac(n)*dexp(c*t)
      else
      auy=1.d0-.5d0*em(n)
      aux=1.d0+auy*c*t
      if (aux.le.0.d0)  then
        c1=10000*ac(n)
      else
        c1=ac(n)*aux**(1.d0/auy)
      endif
      endif
      return
      end
```

PROJECT TECHNICAL COMMITTEE MEMBERS

The following persons were members of the committee that represented the Ship Structure Committee to the Contractor as resident subject matter experts. As such they performed technical review of the initial proposals to select the contractor, advised the contractor in cognizant matters pertaining to the contract of which the agencies were aware, performed technical review of the work in progress and edited the final report.

Chairman

Paul Cojeen   U. S. Coast Guard

Members

LT Robert Holzman   U. S. Coast Guard

Fred Seibold   Maritime Administration

Dr. Walter MacLean   U. S. Merchant Marine Academy

Chao Lin   Maritime Administration

Dr. Y-k Chen   American Bureau of Shipping

William Siekierka   Naval Sea Systems Command,
                                      Contracting Officer's
                                      Technical Representative

Dr. Robert Sielski   National Academy of Science,
                                      Marine Board Liaison

CDR Steve Sharpe   U.S. Coast Guard, Executive Director
                                      Ship Structure Committee

COMMITTEE ON MARINE STRUCTURES

Commission on Engineering and Technical Systems

National Academy of Sciences - National Research Council

The **COMMITTEE ON MARINE STRUCTURES** has technical cognizance over the interagency Ship Structure Committee's research program.

Dr. John Landes, *Chairman*, University of Tennessee, Knoxville, TN

Mr. Howard M. Bunch, University of Michigan, Ann Arbor, MI

Dr. Dale G. Karr, University of Michigan, Ann Arbor, MI

Mr. Andrew Kendrick, NKF Services, Montreal, Quebec

Dr. John Niedzwecki, Texas A & M University, College Station, TX

Dr. Alan Pense, NAE, Lehigh University, Bethlehem, PA

Dr. Barbara A. Shaw, Pennsylvania State University, University Park, PA

Dr. Robert Sielski, National Research Council, Washington, DC

CDR Stephen E. Sharpe, Ship Structure Committee, Washington, DC

DESIGN WORK GROUP

Dr. John Niedzwecki, *Chairman*, Texas A&M University, College Station, TX

Dr. Bilal Ayyub, University of Maryland, College Park, MD

Mr. Ovide J. Davis, Pascagoula, MS

Mr. Andy Davidson, NASSCO, San Diego, CA

Dr. Maria Celia Ximenes, Chevron Shipping Co., San Francisco, CA

Mr. Jeffrey Geiger, Bath Iron Works, Bath, ME

Mr. Hugh Rynn, Sea-Land Services, Elizabeth, NJ

MATERIALS WORK GROUP

Dr. Barbara A. Shaw, *Chairman*, Pennsylvania State University, University Park, PA

Dr. David P. Edmonds, Edison Welding Institute, Columbus, OH

Dr. John F. McIntyre, Advanced Polymer Sciences, Avon, OH

Dr. Harold S. Reemsnyder, Bethlehem Steel Corp., Bethlehem, PA

Dr. Bruce R. Somers, Lehigh University, Bethlehem, PA

RECENT SHIP STRUCTURE COMMITTEE PUBLICATIONS

<u>Ship Structure Committee Publications - A Special Bibliography</u> This bibliography of SSC reports may be downloaded from the internet at "http://www.dot.gov/dotinfo/uscg/hqmc/dn/ssc/171-dex.htm".

SSC-394   <u>Strength Assessment of Pitted Plate Panels</u> J. Daidola, J. Parente, I. Orisamolu, K.t. Ma 1997

SSC-393   <u>Evaluation of Ductile Fracture Models</u> R. Dexter, M. Gentilcore 1997

SSC-392   <u>Probability Based Ship Design Implementation of Design Guidelines</u> A. Mansour, P. Wirsching, G. White, B. Ayyub 1996

SSC-391   <u>Evaluation of Marine Structures Education in North America</u> R. Yagle 1996

SSC-390   <u>Corrosion Control of Inter-hull Structures</u> M. Kikuta, M. Shimko, D. Slavin 1996

SSC-389   <u>Inspection of Marine Structures</u> L. Demsetz, R. Cario, P. Schulte-Strathaus, R. Bea 1996

SSC-388   <u>Ship Structural Integrity Information System-Phase II</u> W. Dry, R. Schulte-Strathaus, R. Bea 1997

SSC-387   <u>Guideline for Evaluation of Finite Elements and Results</u> R.I. Basu, K.J. Kirkhope, J. Srinivasan 1996

SSC-386   <u>Ship's Maintenance Project</u> R. Bea, E. Cramer, R. Schulte-Strathaus, R. Mayoss, K. Gallion, K. Ma, R. Holzman, L. Demsetz 1995

SSC-385   <u>Hydrodynamic Impact on Displacement Ship Hulls - An Assessment of the State of the Art</u> J. Daidola, V. Mishkevich 1995

SSC-384   <u>Post-Yield Strength of Icebreaking Ship Structural Members</u> C. DesRochers, J. Crocker, R. Kumar, D. Brennan, B. Dick, S. Lantos 1995

SSC-383   <u>Optimum Weld-Metal Strength for High Strength Steel Structures</u> R. Dexter and M. Ferrell 1995

SSC-382   <u>Reliability of Design Criteria for Stiffened Plate Panels</u> by D. Ghose and N. Nappi 1995

SSC-381   <u>Residual Strength of Damaged Marine Structures</u> by C. Wiernicki, D.